frontiers | Research Topics

Epithelial-mesenchymal transition (EMT) as a therapeutic target in cancer

Edited by
Tao Sun, Guojun Sheng, Weilong Zhong and Dingzhi Huang

Published in
Frontiers in Oncology
Frontiers in Pharmacology

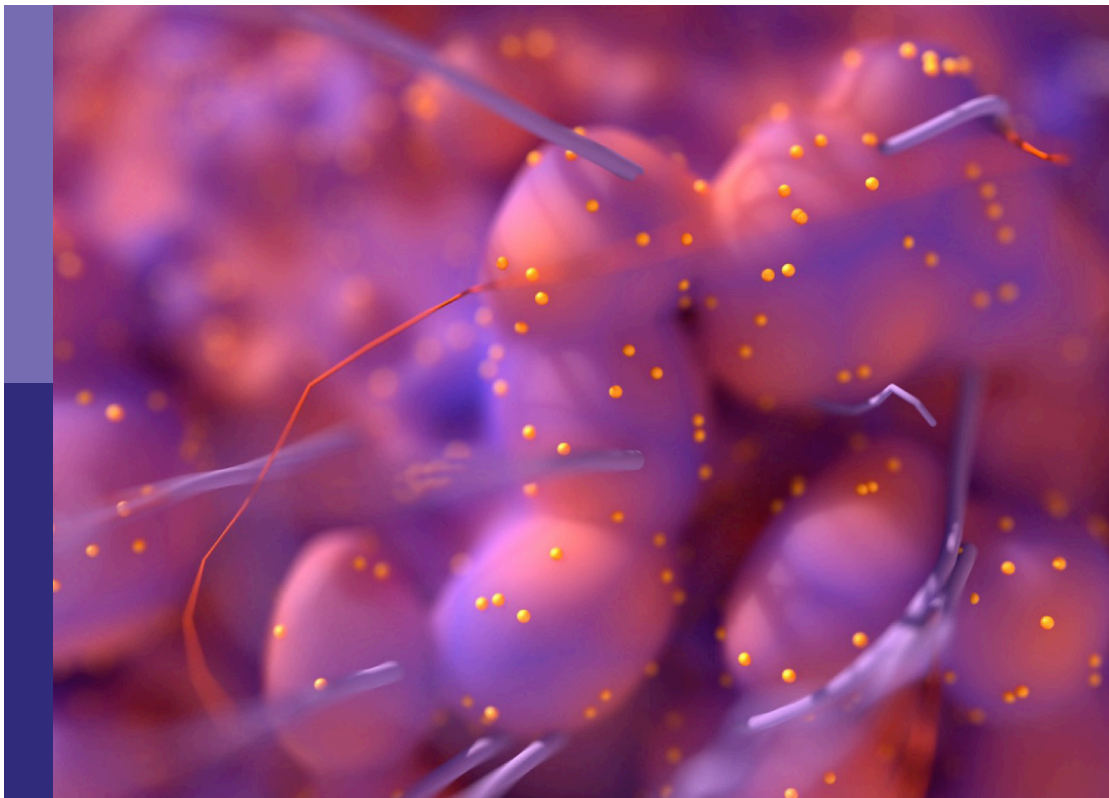

FRONTIERS EBOOK COPYRIGHT STATEMENT

The copyright in the text of individual articles in this ebook is the property of their respective authors or their respective institutions or funders. The copyright in graphics and images within each article may be subject to copyright of other parties. In both cases this is subject to a license granted to Frontiers.

The compilation of articles constituting this ebook is the property of Frontiers.

Each article within this ebook, and the ebook itself, are published under the most recent version of the Creative Commons CC-BY licence. The version current at the date of publication of this ebook is CC-BY 4.0. If the CC-BY licence is updated, the licence granted by Frontiers is automatically updated to the new version.

When exercising any right under the CC-BY licence, Frontiers must be attributed as the original publisher of the article or ebook, as applicable.

Authors have the responsibility of ensuring that any graphics or other materials which are the property of others may be included in the CC-BY licence, but this should be checked before relying on the CC-BY licence to reproduce those materials. Any copyright notices relating to those materials must be complied with.

Copyright and source acknowledgement notices may not be removed and must be displayed in any copy, derivative work or partial copy which includes the elements in question.

All copyright, and all rights therein, are protected by national and international copyright laws. The above represents a summary only. For further information please read Frontiers' Conditions for Website Use and Copyright Statement, and the applicable CC-BY licence.

ISSN 1664-8714
ISBN 978-2-83251-634-8
DOI 10.3389/978-2-83251-634-8

About Frontiers

Frontiers is more than just an open access publisher of scholarly articles: it is a pioneering approach to the world of academia, radically improving the way scholarly research is managed. The grand vision of Frontiers is a world where all people have an equal opportunity to seek, share and generate knowledge. Frontiers provides immediate and permanent online open access to all its publications, but this alone is not enough to realize our grand goals.

Frontiers journal series

The Frontiers journal series is a multi-tier and interdisciplinary set of open-access, online journals, promising a paradigm shift from the current review, selection and dissemination processes in academic publishing. All Frontiers journals are driven by researchers for researchers; therefore, they constitute a service to the scholarly community. At the same time, the *Frontiers journal series* operates on a revolutionary invention, the tiered publishing system, initially addressing specific communities of scholars, and gradually climbing up to broader public understanding, thus serving the interests of the lay society, too.

Dedication to quality

Each Frontiers article is a landmark of the highest quality, thanks to genuinely collaborative interactions between authors and review editors, who include some of the world's best academicians. Research must be certified by peers before entering a stream of knowledge that may eventually reach the public - and shape society; therefore, Frontiers only applies the most rigorous and unbiased reviews. Frontiers revolutionizes research publishing by freely delivering the most outstanding research, evaluated with no bias from both the academic and social point of view. By applying the most advanced information technologies, Frontiers is catapulting scholarly publishing into a new generation.

What are Frontiers Research Topics?

Frontiers Research Topics are very popular trademarks of the *Frontiers journals series*: they are collections of at least ten articles, all centered on a particular subject. With their unique mix of varied contributions from Original Research to Review Articles, Frontiers Research Topics unify the most influential researchers, the latest key findings and historical advances in a hot research area.

Find out more on how to host your own Frontiers Research Topic or contribute to one as an author by contacting the Frontiers editorial office: frontiersin.org/about/contact

Epithelial-mesenchymal transition (EMT) as a therapeutic target in cancer

Topic editors

Tao Sun — Nankai University, China
Guojun Sheng — Kumamoto University, Japan
Weilong Zhong — Tianjin Medical University General Hospital, China
Dingzhi Huang — Tianjin Medical University Cancer Institute and Hospital, China

Citation

Sun, T., Sheng, G., Zhong, W., Huang, D., eds. (2023). *Epithelial-mesenchymal transition (EMT) as a therapeutic target in cancer*. Lausanne: Frontiers Media SA. doi: 10.3389/978-2-83251-634-8

Table of contents

frontiers | Frontiers in Oncology

TYPE Editorial
PUBLISHED 25 January 2023
DOI 10.3389/fonc.2023.1121416

Check for updates

OPEN ACCESS

EDITED AND REVIEWED BY
Olivier Feron,
Université catholique de Louvain, Belgium

*CORRESPONDENCE
Tao Sun
tao.sun@nankai.edu.cn

SPECIALTY SECTION
This article was submitted to Pharmacology of Anti-Cancer Drugs, a section of the journal Frontiers in Oncology

RECEIVED 11 December 2022
ACCEPTED 09 January 2023
PUBLISHED 25 January 2023

CITATION
Zhong W and Sun T (2023) Editorial: Epithelial-mesenchymal transition (EMT) as a therapeutic target in cancer. *Front. Oncol.* 13:1121416. doi: 10.3389/fonc.2023.1121416

COPYRIGHT
© 2023 Zhong and Sun. This is an open-access article distributed under the terms of the Creative Commons Attribution License (CC BY). The use, distribution or reproduction in other forums is permitted, provided the original author(s) and the copyright owner(s) are credited and that the original publication in this journal is cited, in accordance with accepted academic practice. No use, distribution or reproduction is permitted which does not comply with these terms.

Editorial: Epithelial-mesenchymal transition (EMT) as a therapeutic target in cancer

Weilong Zhong [1] and Tao Sun [2*]

[1]Department of Gastroenterology and Hepatology, General Hospital, Tianjin Institute of Digestive Diseases, Tianjin Key Laboratory of Digestive Diseases, Tianjin Medical University, Tianjin, China, [2]State Key Laboratory of Medicinal Chemical Biology and College of Pharmacy, Nankai University, Tianjin, China

KEYWORDS

epithelial-mesenchymal transition, metastasis, drug target, tumor therapy, Traditional Chinese medicine (TCM)

Editorial on the Research Topic
Epithelial-mesenchymal transition (EMT) as a therapeutic target in cancer

Tumor local invasion and metastases are the main factors leading to death of patients, and their occurrence depends on the malignant evolution of tumor cells (1). Epithelial–mesenchymal transition (EMT) is a major theory used to explain malignant progression. The phenomenon of EMT, first observed in the formation of embryonic gastrum and neural crest, is a precise regulatory mechanism of cell population differentiation. In cancer, EMT is closely associated with tumor metastasis but is also related to the maintenance of cancer stem cells (2). The occurrence of EMT requires specific biological signals, the generation of which being in part dependent on microenvironmental conditions. In particular, local tumor microenvironment stress induces the production of stress molecules, which in turn induces the expression of transcription factors prone to support EMT (3). The occurrence of EMT can enhance the invasiveness, anti-apoptotic ability, and drug resistance of tumor cells (4). Therefore, inhibition of EMT can be an important direction for the development of antitumor drugs.

In this research, Jiang et al. analyzed the latest research advancements in the contribution of exosomes to the regulation of the EMT process in tumor cells. Moreover, the author summarized the potential and challenges of using exosomes as a tool for cancer treatment.

Wang et al. focused on the role of TGF-β1 in autophagy and apoptosis in breast cancer. Their results showed that TGF-β1 promotes autophagy and inhibits the apoptosis of breast cancer cells by inhibiting the expression of TP63. This study provides a potential marker for the prognosis of breast cancer and a potential target for the treatment of breast cancer.

Zheng et al. identified multiple oncogenic genes (e.g., midkine [MDK]) associated with tumor metastasis. Their study found that IFN-γ treatment can induce the activation of the EMT process in a variety of cancer cell lines and even promote tumor metastasis. Furthermore, MDK is a common response target for IFN-γ in these cell lines. Ultimately, they suggested that targeted inhibition of MDK can eliminate IFN-γ-induced metastatic cancer from all sources. The combined use of MDK may expand the use of IFN-γ in cancer and improve the clinical efficacy of IFN-γ therapy.

Song et al. analyzed and reported the research trends and hotspots of glioma stem cells (GSCs) in the world in recent years through bibliometrics. The authors analyzed the most cited articles. Their results showed that "epithelial–mesenchymal transition" and "immunotherapy" have

become new focus issues. Geographically, the United States is a leader in the field of GSC research. The focus of GSC research has gradually shifted from basic cell biology to clinical problem solving.

The field of cancer metabolism has evolved from a simple Warburg effect model to an understanding of the complexity of tumor metabolism, but some key issues still need to be addressed in the future. In the past few decades, the development and application of new technologies have not only revealed the heterogeneity and plasticity of tumors but also identified new metabolic pathways to sustain tumor growth. Yang et al. reported that ginseng nanoparticles inhibit EMT in lung cancer cells by inhibiting pentose phosphate pathway activity. We describe the typical characteristics of GDNP and the possible underlying mechanisms of GDNP's antitumor activity. Our study showed that GDNPs induced the downregulation of thymidine phosphorylase (TP) expression, which led to the inhibition of the pentose phosphate pathway and lung cancer cell metastasis. As a new and promising anticancer drug, nanomaterials are worthy of further study.

Circulating tumor cells (CTCs) are tumor cells that shed from the primary site or metastasis and enter the bloodstream during tumor formation and progression. The formation of CTCs runs through the whole process of tumor development. The CTC test may represent an important new type of "liquid biopsy." The number and type of CTCs are helpful in the differential diagnosis of early hepatic malignancies. Li Hua et al. systematically reviewed the clinical application of CTCs in hepatocellular carcinoma (HCC). The authors suggested that EMT plays a crucial role in distant metastasis. EMT also contributes to the powerful aggressiveness of CTCs. CTCs can also provide complete cell biology information, making CTCs one of the most promising targets for liquid biopsies. The clinical application of CTCs in HCC has a broad prospect.

Chen et al. reported that puerarin inhibits oxaliplatin (OXA)-induced EMT by targeting carbonic anhydrase (CA) XII. This study evaluated the anticancer effects of puerarin combined with OXA *in vitro* and *in vivo*. The author found that puerarin can reverse the resistance of platinum anticancer drugs and enhance the antitumor effect of OXA on breast cancer. Mechanistic studies suggested that CA XII is a potential target of puerarin. Puerarin has potential as an adjuvant chemotherapy drug and may be one of the "drug and food homologous" molecules in patients with breast cancer.

Zhang et al. investigated the expression of ZEB1 in three cases of hepatocellular sarcoma (HCS). Liu et al. found that during the malignant evolution of HCS, cancer cells acquire the mesenchymal phenotype and lose epithelial properties through the dynamic process of EMT. EMT-related transcription factor ZEB1 is highly expressed in sarcoma components. The high expression of ZEB1 in the HCS nucleus may be the key factor promoting EMT.

Cui et al. analyzed a novel EMT-related gene signature of predictive value for the survival outcomes in lung adenocarcinoma. They believe that the risk model based on E-signature is superior to the risk model reported in the literature. In patients with LUAD, E-signature risk scores are associated with stages T, N, M, and TNM. Their study explored an innovative EMT-based prognostic signature that may serve as a potential target for personalized and precision medicine.

Overall, EMT is an important cancer cell phenotype leading to tumor metastasis and drug resistance (5). Inhibitors of this cellular process can be used as chemotherapy or targeted therapeutic agents to provide clinical strategies for improving the efficacy of cancer therapy. Although many preclinical models have shown that EMT is involved in tumor metastasis, translating EMT into clinical application remains difficult. Targeting EMT is considered a new therapeutic direction to overcome cancer drug resistance. This topic includes some studies on the biological characteristics of EMT in tumor cells and its multilevel regulatory mechanisms. In addition, the relationship between EMT and cancer metastasis and the use of EMT as a potential therapeutic target were reported. In the personalized medicine of patients with cancer, EMT may serve as a useful therapeutic target to identify and intervene with disease-related EMT regulators, which is expected to promote the development of precision medicine and bring about technological changes in disease diagnosis and treatment.

Author contributions

All authors listed have made a substantial, direct, and intellectual contribution to the work and approved it for publication.

Conflict of interest

The authors declare that the research was conducted in the absence of any commercial or financial relationships that could be construed as a potential conflict of interest.

Publisher's note

All claims expressed in this article are solely those of the authors and do not necessarily represent those of their affiliated organizations, or those of the publisher, the editors and the reviewers. Any product that may be evaluated in this article, or claim that may be made by its manufacturer, is not guaranteed or endorsed by the publisher.

References

1. Brabletz T, Kalluri R, Nieto MA, Weinberg RA. EMT in cancer. *Nat Rev Cancer* (2018) 18(2):128–34.

2. Heerboth S, Housman G, Leary M, Longacre M, Byler S, Lapinska K, et al. EMT and tumor metastasis. *Clin Trans Med* (2015) 4(1):1–13.

3. Tiwari N, Gheldof A, Tatari M, Christofori G. EMT as the ultimate survival mechanism of cancer cells. In: *Seminars in cancer biology*. (Elsevier:Academic Press) (2012) 22(3).

4. Shibue T, Weinberg RA. EMT, CSCs, and drug resistance: the mechanistic link and clinical implications. *Nat Rev Clin Oncol* (2017) 14(10):611–29.

5. Pan G, Liu Y, Shang L, Zhou F, Yang S. EMT-associated microRNAs and their roles in cancer stemness and drug resistance. *Cancer Commun* (2021) 41(3):199–217.

frontiers in Oncology

REVIEW
published: 14 March 2022
doi: 10.3389/fonc.2022.864980

Exosomes Regulate the Epithelial–Mesenchymal Transition in Cancer

Jingwen Jiang†, *Jiayu Li*†, *Xiumei Zhou*, *Xueqin Zhao*, *Biao Huang** and *Yuan Qin**

College of Life Sciences and Medicine, Zhejiang Sci-Tech University, Hangzhou, China

Exosomes are important mediators of intercellular communication and participate in complex biological processes by transferring a variety of bioactive molecules between cells. Epithelial–mesenchymal transition (EMT) is a process in which the cell phenotype changes from epithelioid to mesenchymal-like. EMT is also an important process for cancer cells by which they acquire invasive and metastatic capabilities, which aggravates the degree of tumor malignancy. Numerous studies have demonstrated that exosomes encapsulate various components, such as microRNAs and proteins, and transfer information between tumor cells or between tumor cells and the tumor microenvironment, thereby regulating the EMT process. Exosomes can also be used for cancer diagnosis and treatment or as a drug delivery platform. Thus, they can be used as a therapeutic tool to control the occurrence of EMT and affect cancer progression. In this review, we summarize the latest research advancements in the regulation of the EMT process in tumor cells by the contents of exosomes. Furthermore, we discuss the potential and challenges of using exosomes as a tool for cancer treatment.

Keywords: cancer, epithelial–mesenchymal transition, exosome, tumor metastasis, contents in exosomes

OPEN ACCESS

Edited by:
Weilong Zhong,
Tianjin Medical University General Hospital, China

Reviewed by:
Fan Yang,
Shanghai JiaoTong University, China
Huijuan Liu,
Tianjin International Joint Academy of Biomedicine, China
Jing Meng,
Nankai University, China

****Correspondence:***
Yuan Qin
qinyuan@zstu.edu.cn
Biao Huang
jswxhb@163.com

†*These authors have contributed equally to this work*

Specialty section:
This article was submitted to Pharmacology of Anti-Cancer Drugs, a section of the journal Frontiers in Oncology

Received: *29 January 2022*
Accepted: *21 February 2022*
Published: *14 March 2022*

Citation:
Jiang J, Li J, Zhou X, Zhao X, Huang B and Qin Y (2022) Exosomes Regulate the Epithelial–Mesenchymal Transition in Cancer. Front. Oncol. 12:864980. doi: 10.3389/fonc.2022.864980

INTRODUCTION

Malignant tumors are complicated structures composed of cancer cells and tumor stromal cells, such as fibroblasts, immune cells, and epithelial cells. These tumor stromal cells continuously release a variety of cytokines and active substances, which directly or indirectly affect the tumor microenvironment (TME), thereby affecting the tumor cells themselves and the nearby normal cells. Tumor-derived exosomes (TDEs) are one of the tools for the interchange of substances between tumor cells and the TME. The main physiological role of TDEs is to mediate cell–cell communication by transferring small RNAs, such as microRNAs (miRNAs) (1), long noncoding RNAs (lncRNAs) (2), proteins (3), DNAs, and messenger RNAs (mRNAs) (4).

Metastasis significantly increases cancer malignancy. Before metastasis, a pre-metastasis niche (PMN) is established in the target organ, providing a suitable microenvironment to support the colonization of metastatic tumor cells (5). A large number of studies have shown that TDEs are involved in the formation of PMNs by inducing vascular permeability and angiogenesis, activating fibroblasts, and promoting inflammation (6–9). TDEs also mediate intercellular communication and play an essential role in epithelial–mesenchymal transition (EMT). EMT is a reversible process in which cell morphology transforms from the epithelial state into the mesenchymal state; it is a key process before tumor cells migrate and invade. During EMT, E-cadherin expression in tumor cells is

decreased, resulting in decreased adhesion and loss of apical polarity and basal anchoring, which enable tumor cells to easily leave the primary lesion and migrate to other organs (10). TDEs carry metabolites and signaling molecules from donor organs and are taken up by target organ cells through endocytosis. These contents activate intracellular EMT-related signaling pathways and promote the occurrence of EMT (1, 11–13).

In this review, we summarize the effects of different exosome contents on tumor cell metastasis, particularly EMT, and describe the related molecular mechanisms. Furthermore, we present the current research progress in the treatment of cancer with exosomes and discuss the prospects and potential challenges of using exosomes as therapeutic tools for cancer treatment.

EXOSOMES

Exosomes are extracellular vesicles (EVs) with a lipid bilayer (30–100 nm in diameter) that arise from the luminal membranes of multivesicular bodies (MVBs) and are released into the extracellular matrix after MVBs fuse with the cell membrane (14). Exosomes are produced by many cell types, including T cells (15), B cells (16), epithelial cells (17), and tumor cells (18). In 1987, Johnstone et al. (19) first isolated these extracellular vesicles from an *in vitro* culture of sheep reticulocytes and named them "exosomes". However, exosomes were largely ignored because they were initially considered cellular "garbage bags". In 1996, exosomes were found to play a role in antigen presentation during T-cell responses restricted by B lymphocyte-induced antigen-specific MHC class II (20). Since then, exosomes have begun to be appreciated for their active function in intercellular communication.

Exosomes contain a variety of bioactive molecules, some of which are related to their physiological functions. For example, some proteins are involved in exosome biogenesis (TSG101, flotillin, and Alix), MVB transformation, and exosome release. Tetraspanins (CD9, CD63, CD81, and CD82) and heat shock proteins (Hsp90 and Hsp70) are involved in exosome transport and membrane fusion with target cells (21–23). Some of these proteins have been used as markers for exosome detection (TSG101, Hsp70, and CD63).

TDE-mediated long-distance intercellular communication plays a key role in cancer occurrence and development. Increasing evidence indicates that TDEs regulate the TME and promote cancer cell proliferation, angiogenesis, EMT generation, and PMN formation (3, 7, 24, 25). However, not all news about TDEs is negative. Recently, the modification of exosomes as a cancer treatment tool has become a hot research topic. In addition to investigating the use of exosomes for cancer diagnosis and prognostic analysis (26), researchers examined the use of exosomes for EMT reversal and drug delivery (27, 28). Notably, animal cells are not the only cells that produce exosomes. Plant cells also produce similar extracellular vesicles, called plant exosome-like nanovesicles (PELNVs), which have received increasing attention as natural drug delivery nanoplatforms (29).

EMT IN CANCER CELLS

In the 1970s, Hay first observed the EMT process during embryonic development and proposed the concept of EMT (30). Subsequently, the roles of EMT in embryonic development, gastrulation, organ development, and maturation were discovered one after another (31). EMT is a process in which cell morphology changes from the epithelial state to the mesenchymal state. This process also occurs in cancer cells.

EMT is usually accompanied by tumor occurrence, invasion, metastasis, and resistance to therapy. Recent studies have shown that EMT occurs in different cellular states and is not a binary process (32–35). In monolayer cultures, epithelial cells are polygonal in shape with apical polarity and are closely connected to each other into sheets. In contrast, mesenchymal cells are spindle-shaped, lose the polarity of the apical group, and loosely adhere to the extracellular matrix. Hence, mesenchymal cells have better mobility and invasion ability than epithelial cells, and tumor cells are more prone to vascular infiltration and metastasis after EMT.

Figure 1 presents an overview of the EMT process. Epithelial cells are connected by tight junctions and adhesion junctions. Molecules involved in establishing the epithelial cell state also play an essential role in maintaining cell polarity. When the expression of genes involved in maintaining the cell state is changed in epithelial cells, their cellular properties are gradually lost and they gradually acquire mesenchymal properties.

EMT is a reversible process, in contrast to mesenchymal–epithelial transition (MET), but it is not a bipolar process; that is, the cells are either in the epithelial or mesenchymal state. E-cadherin is a membrane protein that increases cell–cell adhesion, and its high expression is a marker of epithelial cells. However, mesenchymal cells often lack E-cadherin and express vimentin and N-cadherin (36, 37). Studies have demonstrated co-expression of E-cadherin, N-cadherin, and vimentin in some cells during EMT, indicating that these cells are between the epithelial and mesenchymal states (called hybrid E/M cells) (38–40). This phenomenon proves that EMT (or MET) is not a binary process; it occurs gradually, and cells with different phenotypes can transform into one another.

EMT is widely considered as a key process in the generation of cancer stem cells (CSCs). EMT occurs after non-CSCs are stimulated by EMT-inducing signals, which induce the expression of cell stemness markers CD133 and CD44. As a result, these cells gain self-renewal capability, the invasion–metastasis cascade is activated, tumor metastasis is promoted *in vivo*, and even drug resistance develops (41–44). Exosomes often act as "accomplices" in this process by facilitating the communication between cells and the extracellular matrix to complete the EMT process and convert more non-CSCs to CSCs, accelerating the progression of cancer deterioration (13, 45).

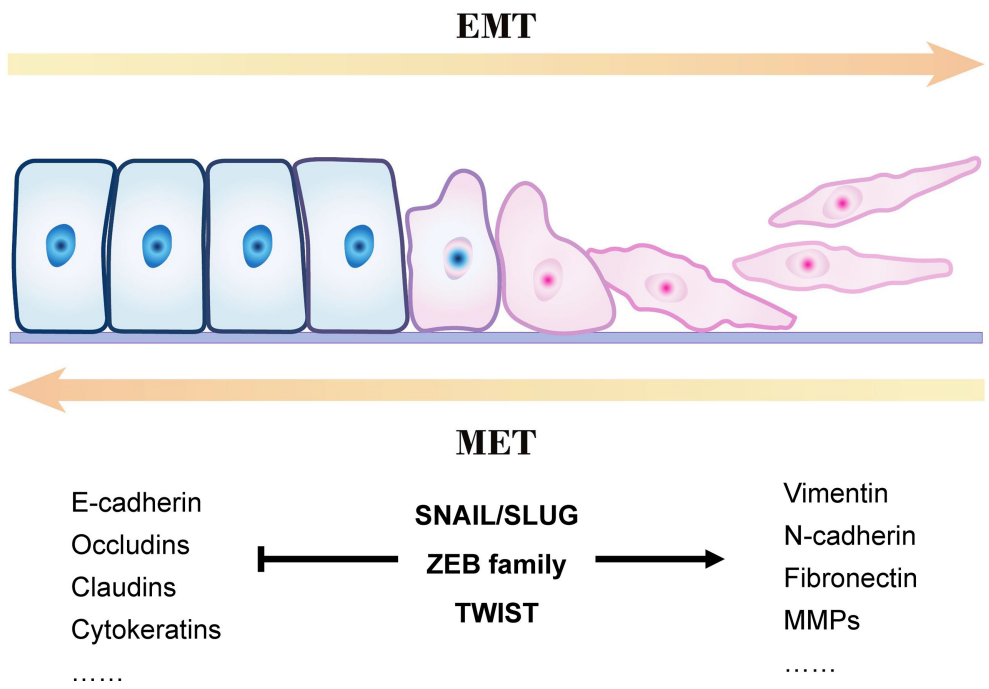

FIGURE 1 | Outline of a typical epithelial–mesenchymal transition (EMT) program.

EXOSOMES CARRY EMT-RELATED ACTIVE MOLECULES

The various bioactive molecules carried by exosomes have different regulatory effects on the EMT process in cancer and different underlying mechanisms. In this section, we describe the four main types of molecules carried by exosomes, namely, proteins, microRNAs (miRNAs), long non-coding RNAs (lncRNAs), and circular RNAs (circRNAs), and discuss those that have been studied the most (**Figure 2**). However, the active

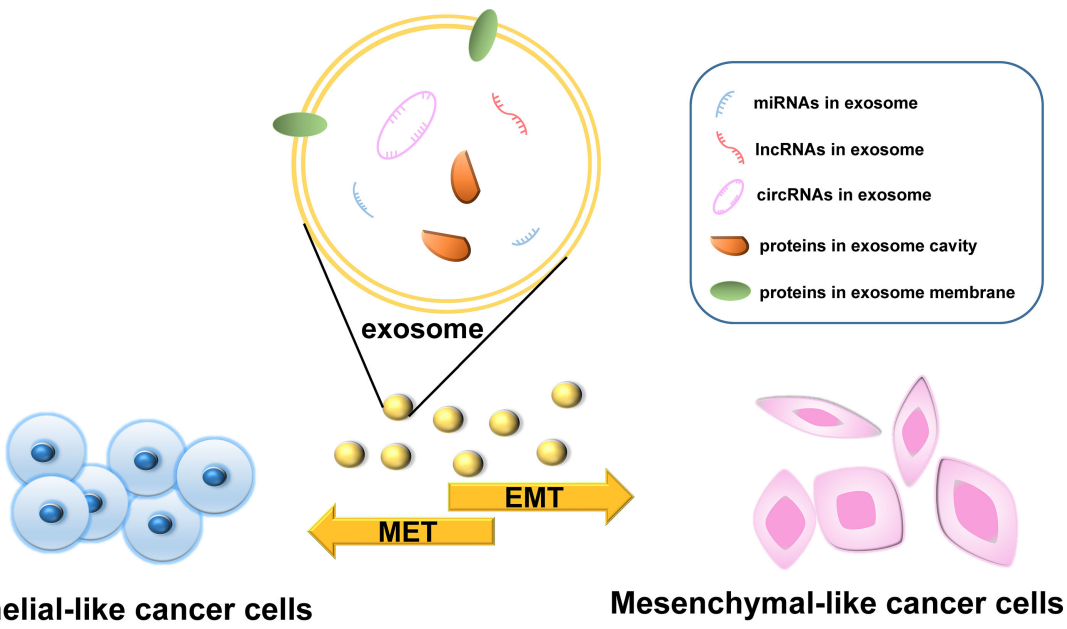

FIGURE 2 | The effects of molecules carried by exosomes on epithelial–mesenchymal transition (EMT).

components in exosomes are not limited to the biomolecules listed here; other components need to be further studied.

Exosomal Proteins and Peptides

Exosomes contain various proteins and peptides, some of which are enclosed in the exosome cavity or membrane (**Table 1**).

Transcription factors (TFs) can be bind specific gene sequences to control the expression of target genes. Members of the zinc finger transcription factor Snail superfamily often "travel" between cells in exosomes. Cancer-associated fibroblast (CAF)-derived exosomes carry Snail1 to inhibit E-cadherin expression and thus induce the occurrence of EMT in A549 lung cancer cells (46). SLUG and SOX2 are significantly upregulated in exosomes secreted from thyroid CSCs and can initiate EMT programming in recipient cells (2). In addition to members of the Snail superfamily, other common TFs are found in exosomes, serving as a "bridge" for tumor cells to interact with the TME. For example, under hypoxic conditions, paclitaxel-resistant breast cancer (PR-BC) cells upregulate the expression of HSP gp96. Then, the overexpressed HSP gp96 and hypoxia-inducible factor (HIF-1) are transported to paclitaxel-sensitive breast cancer (PS-BC) cells through exosomes to degrade p53, increase PS-BC resistance, and accelerate EMT (47). In nasopharyngeal carcinoma (NPC) cells, hypoxic exosomes carry MMP-13, which significantly upregulates the expression of vimentin in recipient cells and reduces the level of E-cadherin, thereby promoting the EMT of NPC cells and enhancing their migratory and invasive abilities (48).

The exosomal cavity also contains proteins and TFs. A previous study confirmed that CAF-derived exosomes can promote EMT in non-invasive bladder cancer cells and transform these cells into an aggressive phenotype by secreting IL-6 (3). A small protein, MAP17, is transferred between subsets of tumor cells by TDEs to promote the horizontal transmission of metastasis and EMT (49). Ji et al. (50) found that exosomal integrin beta-like 1 (ITGBL1) from primary tumors can convert fibroblasts in distal organs into CAFs by combining with TNFAIP3 and activating the NF-κB signaling pathway, thereby promoting the formation of PMNs and EMT. As previously mentioned, TFs participate in the information exchange between tumor cells and the TME through exosomes. This, however, is not a privilege of TFs. Breast cancer cells overexpress survivin (member of the inhibitor of apoptosis protein family) and secrete it into the extracellular environment through exosomes. CAFs then internalize the exosomes, upregulate the expression of SOD1, and transform into myofibroblasts, which in turn promote breast cancer cell proliferation, EMT, and stem cell formation (53).

Some proteins are present in the exosomal membrane. Prostate-specific G-protein coupled receptor (PSGR) is overexpressed in prostate cancer (PC) cells and can spread to surrounding cells along with TDEs, thereby mediating the enrichment of mRNA in exosomes in EMT-related pathways and facilitating the migration, invasion, stem cell differentiation, and EMT of PC cells and normal prostate epithelial cells (51). Proteins located in the exosomal membrane play a role in determining the target organs for metastasis during tumor migration and EMT. For example, exosomal integrins $\alpha_6\beta_4$ and $\alpha_6\beta_1$ target lung metastasis, whereas exosomal integrin $\alpha_V\beta_5$ is associated with liver metastasis (52).

Moreover, peptides with a smaller molecular weight than that of proteins can also be delivered to target cancer cells. Exosomes modified to secrete tumor necrosis factor-related apoptosis-inducing ligand (TRAIL) have remarkable efficacy in inducing cancer cell apoptosis (54). Survivin has anti-apoptotic effects in many types of cancers. Exosomes that transfer mutated survivin (T34A) can promote apoptosis in pancreatic cancer (55). In the presence of antigen-presenting cells, dendritic cell-derived exosomes load different types of peptide antigens (e.g., major histocompatibility complex class I and class II) and then stimulate T cells to participate in the anti-tumor response (56). However, the regulation of EMT in tumor cells by peptides carried by exosomes has rarely been reported. However, there is a reasonable prospect that more advances in this research field can be made in the near future.

Exosomal MiRNAs

MiRNAs, noncoding RNAs that contain 20–24 nucleotides, are the most widely studied molecules in exosomes (**Table 2**).

TABLE 1 | The effects of proteins carried by exosomes on EMT.

Proteins	Cancer Type	Effect	Reference
Snail1	Lung cancer	Inhibit E-cadherin expression, induce the occurrence of EMT.	(46)
HSP gp96, HIF-1	Breast cancer	Degrade p53, increases therapy resistance and accelerate EMT.	(47)
MMP-13	NPC	Upregulate vimentin, down-regulate E-cadherin, promote EMT.	(48)
IL-6	Bladder cancer	Increase pSTAT3 and pAKT level, activate the STAT3 signaling pathway, promote EMT.	(3)
MAP-17	Breast cancer	Interact with NUMB protein, activate the Notch signaling pathway, increase secretion of extracellular vesicles, promote the horizontal transmission and metastasis of EMT.	(49)
ITGBL1	CRC	Combine to TNFAIP3 and activate the NF-κB signaling pathway, convert fibroblasts into CAFs, promote the formation of PMN and the generation of EMT.	(50)
PSGR	PC	mediate the enrichment of mRNA in exosomes in EMT-related pathways to facilitate EMT.	(51)
Intergrin($\alpha_6\beta_4$, $\alpha_6\beta_1$, $\alpha_V\beta_5$,etc)		Determine the target organs of exosomes.	(52)

TABLE 2 | The effects of miRNAs carried by exosomes on EMT.

miRNAs	Cancer Type	Effect	Reference
miR-92a-3p	HCC	inhibit the expression of the tumor-suppressor gene PTEN, activate the Akt/Snail signaling pathway, facilitates the occurrence of EMT.	(57)
	CRC	activate the Wnt/β-catenin signaling pathway, inhibit mitochondrial apoptosis by inhibiting FBXW7 and MOAP1, helping CRC cells to obtain stemness and promote EMT.	(12)
miR-181d-5p	Breast cancer	Reduce CDX2 expression, inhibit the expression of HOXA5, thereby promoting EMT.	(11)
miR-375-3p	Colon cancer	promote E-cadherin expression, downregulate the expression of vimentin, inhibit EMT, and promote MET	(58)
miR-34a-5p	CSCC	Binding to AXL, reduce the activity of β-catenin, inhibit EMT.	(59)
miR-253p, miR-130b-3p, miR-425-5p, miR-934	CRC	Target macrophages, downregulate PTEN expression, activate the PI3K/Akt signaling pathway to induce the M2 polarization of TAMs. M2-polarized TAMs enhance EMT, secrete BLC to induce PMN formation and promote CRC liver metastasis.	(8, 60)

They cannot be translated into proteins, but they regulate gene expression at the post-transcriptional and translational levels by binding to mRNA. Under the protection of exosomes, exosomal miRNAs can avoid digestion by ribonucleases and are more stable. Thus, they can safely reach the target organ through the systemic circulation (61). However, different exosomal miRNAs have opposite effects, namely, promotion or inhibition of the tumor EMT process.

Exosomal miR-92a-3p is highly expressed in hepatocellular carcinoma (HCC) and colorectal cancer (CRC) (12, 57). In HCC, exosomal miR-92a-3p inhibits the expression of the tumor suppressor gene PTEN, activates the Akt/Snail signaling pathway, and facilitates EMT and metastasis (57). In CRC, the increased expression of miR-92a-3p activates the Wnt/β-catenin signaling pathway and inhibits mitochondrial apoptosis by inhibiting FBXW7 and MOAP1, thereby helping CRC cells obtain stemness and promote EMT and metastasis (12). Exosomal miR-181d-5p targets the transcription factor CDX2 in breast cancer, thereby inhibiting the expression of HOXA5 and promoting cancer cell proliferation, invasion, metastasis, and EMT (11).

The expression of some miRNAs in exosomes negatively correlates with the degree of EMT. Tumor-derived exosomal miR-375-3p promotes E-cadherin expression, downregulates vimentin expression, inhibits EMT, and promotes MET (58, 62). In addition, miR-34a-5p expression is reduced in CAF-derived exosomes and can be transferred to oral squamous cell cancer (CSCC) cells by exosomes from fibroblasts. However, following miR-34a-5p overexpression in CAFs, exosomal miR-34a-5p can reduce the activity of β-catenin by binding to its downstream target AXL, thereby inhibiting EMT in CSCC cells (59).

Exosomal miRNAs can also "incite" macrophages as accomplices in EMT. There are two subtypes of tumor-associated macrophages (TAMs): M1 and M2. The pro-tumorigenic M2 subtype can restrain T-cell function and promote tumor immune escape (63, 64). Exosomes from CRC cells transport miR-253p, miR-130b-3p, miR-425-5p, and miR-934 to macrophages. These miRNAs downregulate PTEN expression and activate the PI3K/Akt signaling pathway to induce the M2 polarization of TAMs. M2-polarized TAMs enhance EMT (60) and secrete B lymphocyte chemoattractant (BLC) to induce PMN formation and promote CRC liver metastasis (8).

Exosomal LncRNAs

LncRNAs, belonging to the noncoding RNA family, are also commonly present in exosomes (**Table 3**). In contrast to miRNAs, lncRNAs are more than 200 kb in length, less conserved across species, and have higher tissue-specificity (70).

In CRC, CAF-derived LINC00659 directly binds to the tumor suppressor miR-342-3p in cancer cells, enhances the expression of ANXA2, which is involved in the EMT process, and promotes the development of CRC (65). LncRNA RPPH1 can also induce EMT in CRC cells. It binds to TUBB3 to prevent ubiquitination and induces EMT by affecting the TME (66). In gastric cancer (GC) cells, the exosomal lncRNA HOTTIP activates its target HMGA1, causing GC cells to undergo EMT and acquire cisplatin resistance (67). In pancreatic ductal adenocarcinoma (PADC), exosomal lncRNA-Sox2ot competitively binds to the miR-200

TABLE 3 | The effects of lncRNAs carried by exosomes on EMT.

LncRNAs	Cancer Type	Effect	Reference
LINC00659	CRC	Bind to tumor suppressor miR-342-3p, enhance the ANXA2 expression, promote cancer development.	(65)
LncRNA RPPH1	CRC	Influence the occurrence of EMT induced by the tumor microenvironment	(66)
HOTTIP	GC	Activate HMGA1, cause the GC cells to undergo the EMT process and acquire cisplatin resistance.	(67)
LncRNA-Sox2ot	PADC	Regulates Sox2 expression and promotes PADC metastasis, invasion and EMT	(68)
MALAT1, linc-ROR	Thyroid cancer	Secreted by CSC, induce non-cancer thyroid cells to produce EMT	(2)
LINC00960, LINC02470	Bladder cancer	upregulate the β-catenin signaling pathway, the Notch signaling pathway, and the Smad2/3 signaling pathway, activate EMT process and promote deterioration.	(69)

family, affecting Sox2 expression and resulting in changes in PADC metastasis, invasion, and EMT (68).

LncRNAs also act in a hierarchical order. Hardin et al. (2) found that exosomes secreted by thyroid CSCs can carry lncRNA MALAT1 and linc-ROR as "infection factors" and induce EMT in non-cancerous thyroid cells. Highly malignant bladder cancer cells transmit LINC00960 and LINC02470 to early bladder cancer cells through exosomes, thereby inducing further deterioration and activating the EMT process by upregulating the β-catenin, Notch, and Smad2/3 signaling pathways (69).

Exosomal CirRNAs

CircRNAs act as competing endogenous RNAs (ceRNAs) in many tumors by capturing miRNAs (71). Similar to other noncoding RNAs, exosomal circRNAs can also play different roles in different tumor cells (**Table 4**).

In PC, exosomal circ_0001359 activates the TGF-β signaling pathway by capturing miR-582-3p and promoting EMT in RWPE-1 cells (72). CircRNAs also play a significant role in EMT in bladder cancer. In urothelial carcinoma of the bladder (UCB), the expression of exosomal circPRMT5 is upregulated to capture miR-30c, regulate the Snail1/E-cadherin signaling pathway, and promote EMT in UCB cells (73). In papillary thyroid carcinoma (PTC), exosomal circ007293 inhibits the activity of miR-653-5p by trapping miR-653-5p, thereby upregulating the expression of paired box 6 in PTC cells and accelerating the EMT of tumor cells (74). Exosomes can also deliver circNRIP1, promote GC metastasis *via* EMT, and upregulate EMT markers in GC cells (71). circRNAs affect the progression of non-small cell lung carcinoma (NSCLC) *via* multiple pathways. For example, exosomal circFARSA secreted by NSCLC cells induces the polarization of macrophages toward the M2 phenotype, thereby promoting EMT (75). Exosomal circPTPRA can stimulate mir-96-5P to inhibit metastasis and EMT in NSCLC cells (76). In addition, Circ-CPA4 can affect the migration and EMT of NSCLC cells by targeting the let-7 miRNA/PD-L1 axis (77). Thus, circRNAs can function not only as oncogenes but also as tumor suppressors.

EXOSOMES AS A THERAPEUTIC TOOL FOR EMT

Exosomes can transport contents between cells and protect them from degradation, making them more suitable for material delivery than liposomes (78). In a study by SS et al. (79), miR-381-3p mimics were encapsulated in ADMSC-exosomes using electroporation. Scratch assays and cell invasion experiments showed that the ADMSC-exosomes wrapped with miR-381-3p could target the Wnt signaling pathway and EMT transcription factors. This reduced the metastatic and invasive abilities of the TNBC cells. TDEs can also be used as vectors for tumor therapy. In a previous study, TDEs were loaded with miR-375 mimics as vectors and delivered to cancer cells. miR-375-loaded exosomes reduced the migratory and invasive abilities of SW480 and HT-29 CRC cells by reversing EMT (58). siRNA protected by exosomes can also be used for cancer therapy. In head and neck cancer, transfection of FaDu cells with the exosome/TRPP2 siRNA complex increased the expression of E-cadherin and decreased the expression levels of vimentin and N-cadherin, thereby suppressing FaDu cell invasion and metastasis (80).

The behavior of exosomes from different sources can provide new insights into cancer treatment. Exosomes derived from bone marrow mesenchymal stem cells promote tumor development. Exosomes may regulate tumor characteristics by activating the sonic hedgehog signaling pathway. The study of bone marrow mesenchymal stem cell-derived exosomes that activate the Sonic Hedgehog signaling pathway to regulate tumor invasion and metastasis will contribute to revealing tumor pathogenesis and possible therapeutic approaches (81, 82). In addition, a study has shown that CSC-derived exosomes preserve the biological characteristics of CSCs, promoting the proliferation and migration of human umbilical cord mesenchymal stem cells and vascular endothelial cells, and enhancing the resistance of tumor cells to chemotherapy by promoting the expression of tumor-related drug resistance genes. It is possible to discover potential targets for tumor therapy by studying the correlation between tumor stem cell-derived exosomes and drug resistance genes (83, 84). Exosomes as vectors cannot only be used for cancer treatment but also for overcoming drug resistance. LT et al. (78) encapsulated miR-128-3p in FHC cell-derived exosomes and delivered it to oxaliplatin-resistant cells. The inhibited expression of drug transporters reduced the efflux of oxaliplatin and alleviated chemotherapy resistance in colorectal cancer cells. Moreover, oxaliplatin-induced EMT was inhibited by the overexpression of miR-218-3p.

Although the majority of tumor treatment studies have used exosomes to inhibit EMT, a number of studies have attempted to inhibit the production of exosomes and regulate the anti-tumor effects of EMT. TF et al. (85) used cetuximab to prevent the production of exosome vesicles and reduce exosome secretion to induce EMT in oral cancer cells.

TABLE 4 | The effects of circRNAs carried by exosomes on EMT.

CircRNAs	Cancer Type	Effect	Reference
circ_0001359	PC	Capture miR-582-3p to activate the TGF-β signaling pathway, promote EMT.	(72)
circPRMT5	UCB	capture miR-30c, regulate the Snail1/E-cadherin signaling pathway, promote EMT.	(73)
circ007293	PTC	inhibit the activity of miR-653-5p to upregulate the expression of paired box 6, accelerate EMT	(74)
circNRIP1	GC	Promotes GC metastasis and upregulates EMT markers in GC cells	(71)
circFARSA	NSCLC	induce polarization of macrophages toward the M2 phenotype, thereby promoting EMT.	(75)
circPTPRA	NSCLC	stimulate mir-96-5P to inhibit metastasis and EMT	(76)
circ-CPA4	NSCLC	Targeting the let-7 miRNA/PD-L1 axis to modulate the mobility and EMT of NSCLC cells	(77)

In addition to human exosomes, which can be used to treat diseases, plant exosomes can also function in humans across races. In animal experiments, PELNVs secreted by ginger inhibited the expression of the secreted protein hemagglutinin, promoted wound healing, reduced the level of cyclin D1 mRNA in a mouse model of colon cancer, and inhibited the occurrence and development of CRC (86).

CHALLENGES AND PROSPECTS

In this review, we summarize the latest research advancements in the regulation of the EMT process in tumor cells by the contents of exosomes. However, several outstanding issues remain. There are many challenges in this research field. In terms of mechanistic research, the analysis of exosome components is incomplete, and the biogenesis of exosomes and the principle of content screening are unclear. Considering that cancer is a highly heterogeneous disease, the mechanism underlying the different effects of exosomes on EMT in different cancers is still unknown.

The exploration space for research on exosomes as a tool for cancer treatment is broad. At present, the treatment of cancer with exosomes is limited to the laboratory level and has not been applied in clinical practice. In addition, efficient and high-purity exosome isolation technology is lacking, which poses certain difficulties for the detection of cancer-related indicators using exosomes in research and clinical treatment. The relationship between different cell-derived exosomes and their therapeutic effects on EMT is still unknown. Elucidating this problem will help to formulate more effective treatment options. Researchers are also working on the accurate remolding of exosomes. Existing research has indicated that exosomes can be organ-targeted. Whether this feature can accurately regulate cancer progression, including EMT, remains unknown.

Although the treatment of cancer with PELNVs is receiving increased attention, we still have a limited understanding of the process of PELNV internalization by animal cells. Compared with exosomes derived from animals, PELNVs are slightly inferior because of their low toxicity and immunogenicity, which are some of the problems to be solved. Thus, there are many gaps in research on the regulation of EMT by exosomes in cancer. Nevertheless, this research field is promising.

In this review, we summarize the latest research advances in the regulation of the EMT process in tumor cells by the contents of exosomes. Furthermore, we discuss the potential and challenges of using exosomes as a tool for cancer treatment. Determining the mechanisms underlying EMT regulation by exosomes will contribute to designing new therapeutics that target exosome-mediated tumor metastasis and chemoresistance. We hope that our review will help researchers comprehend the relationship between exosomes and EMT and conduct further investigations in this area.

AUTHOR CONTRIBUTIONS

JJ and JL have equally contributed to this project. YQ, JJ, and JL have contributed to information interpretation, editing and critical revision of the manuscript. XMZ and XQZ were responsible for drawing the pictures. YQ and BH contributed to study design and critical revision of the manuscript. All authors contributed to the article and approved the submitted version.

FUNDING

Major Science and technology projects in Xiaoshan (Project Number: 2020207). Scientific Research Foundation of Zhejiang Sci-Tech University (Project Number: 21042102-Y). Key Research and Development Project of Hangzhou (Project Number:202004A23).

REFERENCES

1. Lin Q, Zhou CR, Bai MJ, Zhu D, Chen JW, Wang HF, et al. Exosome-Mediated miRNA Delivery Promotes Liver Cancer EMT and Metastasis. *Am J Transl Res* (2020) 12(3):1080–95.
2. Hardin H, Helein H, Meyer K, Robertson S, Zhang R, Zhong W, et al. Thyroid Cancer Stem-Like Cell Exosomes: Regulation of EMT *via* Transfer of lncRNAs. *Lab Invest* (2018) 98(9):1133–42. doi: 10.1038/s41374-018-0065-0
3. Goulet CR, Champagne A, Bernard G, Vandal D, Chabaud S, Pouliot F, et al. Cancer-Associated Fibroblasts Induce Epithelial-Mesenchymal Transition of Bladder Cancer Cells Through Paracrine IL-6 Signalling. *BMC Cancer* (2019) 19(1):137. doi: 10.1186/s12885-019-5353-6
4. Valadi H, Ekstrom K, Bossios A, Sjostrand M, Lee JJ, Lotvall JO. Exosome-Mediated Transfer of mRNAs and microRNAs Is a Novel Mechanism of Genetic Exchange Between Cells. *Nat Cell Biol* (2007) 9(6):654–9. doi: 10.1038/ncb1596
5. Kaplan RN, Riba RD, Zacharoulis S, Bramley AH, Vincent L, Costa C, et al. VEGFR1-Positive Haematopoietic Bone Marrow Progenitors Initiate the Pre-Metastatic Niche. *Nature* (2005) 438(7069):820–7. doi: 10.1038/nature04186
6. Costa-Silva B, Aiello NM, Ocean AJ, Singh S, Zhang H, Thakur BK, et al. Pancreatic Cancer Exosomes Initiate Pre-Metastatic Niche Formation in the Liver. *Nat Cell Biol* (2015) 17(6):816–26. doi: 10.1038/ncb3169
7. Zeng Z, Li Y, Pan Y, Lan X, Song F, Sun J, et al. Cancer-Derived Exosomal miR-25-3p Promotes Pre-Metastatic Niche Formation by Inducing Vascular Permeability and Angiogenesis. *Nat Commun* (2018) 9(1):5395. doi: 10.1038/s41467-018-07810-w
8. Zhao S, Mi Y, Guan B, Zheng B, Wei P, Gu Y, et al. Tumor-Derived Exosomal miR-934 Induces Macrophage M2 Polarization to Promote Liver Metastasis of Colorectal Cancer. *J Hematol Oncol* (2020) 13(1):156. doi: 10.1186/s13045-020-00991-2
9. Kong J, Tian H, Zhang F, Zhang Z, Li J, Liu X, et al. Extracellular Vesicles of Carcinoma-Associated Fibroblasts Creates a Pre-Metastatic Niche in the Lung Through Activating Fibroblasts. *Mol Cancer* (2019) 18(1):175. doi: 10.1186/s12943-019-1101-4
10. Pastushenko I, Blanpain C. EMT Transition States During Tumor Progression and Metastasis. *Trends Cell Biol* (2019) 29(3):212–26. doi: 10.1016/j.tcb.2018.12.001
11. Wang H, Wei H, Wang J, Li L, Chen A, Li Z. MicroRNA-181d-5p-Containing Exosomes Derived From CAFs Promote EMT by Regulating CDX2/HOXA5 in Breast Cancer. *Mol Ther Nucleic Acids* (2020) 19:654–67. doi: 10.1016/j.omtn.2019.11.024
12. Hu JL, Wang W, Lan XL, Zeng ZC, Liang YS, Yan YR, et al. CAFs Secreted Exosomes Promote Metastasis and Chemotherapy Resistance by Enhancing

Cell Stemness and Epithelial-Mesenchymal Transition in Colorectal Cancer. *Mol Cancer* (2019) 18(1):91. doi: 10.1186/s12943-019-1019-x
13. Wang L, Yang G, Zhao D, Wang J, Bai Y, Peng Q, et al. CD103-Positive CSC Exosome Promotes EMT of Clear Cell Renal Cell Carcinoma: Role of Remote MiR-19b-3p. *Mol Cancer* (2019) 18(1):86. doi: 10.1186/s12943-019-0997-z
14. Kim H, Lee S, Shin E, Seong KM, Jin YW, Youn H, et al. The Emerging Roles of Exosomes as EMT Regulators in Cancer. *Cells* (2020) 9(4):861. doi: 10.3390/cells9040861
15. Cortes-Troncoso J, Jang SI, Perez P, Hidalgo J, Ikeuchi T, Greenwell-Wild T, et al. T Cell Exosome-Derived miR-142-3p Impairs Glandular Cell Function in Sjogren's Syndrome. *JCI Insight* (2020) 5(9):e133497. doi: 10.1172/jci.insight.133497
16. Benjamins JA, Nedelkoska L, Touil H, Stemmer PM, Carruthers NJ, Jena BP, et al. Exosome-Enriched Fractions From MS B Cells Induce Oligodendrocyte Death. *Neurol Neuroimmunol Neuroinflamm* (2019) 6(3):e550. doi: 10.1212/NXI.0000000000000550
17. Hadley EE, Sheller-Miller S, Saade G, Salomon C, Mesiano S, Taylor RN, et al. Amnion Epithelial Cell-Derived Exosomes Induce Inflammatory Changes in Uterine Cells. *Am J Obstet Gynecol* (2018) 219(5):478 e1–478 e21. doi: 10.1016/j.ajog.2018.08.021
18. Yuan X, Qian N, Ling S, Li Y, Sun W, Li J, et al. Breast Cancer Exosomes Contribute to Pre-Metastatic Niche Formation and Promote Bone Metastasis of Tumor Cells. *Theranostics* (2021) 11(3):1429–45. doi: 10.7150/thno.45351
19. Johnstone RM, Adam M, Hammond JR, Orr L, Turbide C. Vesicle Formation During Reticulocyte Maturation. Association of Plasma Membrane Activities With Released Vesicles (Exosomes). *J Biol Chem* (1987) 262(19):9412–20. doi: 10.1016/S0021-9258(18)48095-7
20. Raposo G, Nijman HW, Stoorvogel W, Liejendekker R, Harding CV, Melief CJ, et al. B Lymphocytes Secrete Antigen-Presenting Vesicles. *J Exp Med* (1996) 183(3):1161–72. doi: 10.1084/jem.183.3.1161
21. Conde-Vancells J, Rodriguez-Suarez E, Embade N, Gil D, Matthiesen R, Valle M, et al. Characterization and Comprehensive Proteome Profiling of Exosomes Secreted by Hepatocytes. *J Proteome Res* (2008) 7(12):5157–66. doi: 10.1021/pr8004887
22. Maia J, Caja S, Strano Moraes MC, Couto N, Costa-Silva B. Exosome-Based Cell-Cell Communication in the Tumor Microenvironment. *Front Cell Dev Biol* (2018) 6:18. doi: 10.3389/fcell.2018.00018
23. Mashouri L, Yousefi H, Aref AR, Ahadi AM, Molaei F, Alahari SK. Exosomes: Composition, Biogenesis, and Mechanisms in Cancer Metastasis and Drug Resistance. *Mol Cancer* (2019) 18(1):75. doi: 10.1186/s12943-019-0991-5
24. Shang A, Gu C, Wang W, Wang X, Sun J, Zeng B, et al. Exosomal circPACRGL Promotes Progression of Colorectal Cancer *via* the miR-142-3p/miR-506-3p- TGF-Beta1 Axis. *Mol Cancer* (2020) 19(1):117. doi: 10.1186/s12943-020-01235-0
25. Wu XG, Zhou CF, Zhang YM, Yan RM, Wei WF, Chen XJ, et al. Cancer-Derived Exosomal miR-221-3p Promotes Angiogenesis by Targeting THBS2 in Cervical Squamous Cell Carcinoma. *Angiogenesis* (2019) 22(3):397–410. doi: 10.1007/s10456-019-09665-1
26. Qu Z, Wu J, Wu J, Ji A, Qiang G, Jiang Y, et al. Exosomal miR-665 as a Novel Minimally Invasive Biomarker for Hepatocellular Carcinoma Diagnosis and Prognosis. *Oncotarget* (2017) 8(46):80666–78. doi: 10.18632/oncotarget.20881
27. Yao Y, Chen R, Wang G, Zhang Y, Liu F. Exosomes Derived From Mesenchymal Stem Cells Reverse EMT *via* TGF-Beta1/Smad Pathway and Promote Repair of Damaged Endometrium. *Stem Cell Res Ther* (2019) 10 (1):225. doi: 10.1186/s13287-019-1332-8
28. Yong T, Zhang X, Bie N, Zhang H, Zhang X, Li F, et al. Tumor Exosome-Based Nanoparticles Are Efficient Drug Carriers for Chemotherapy. *Nat Commun* (2019) 10(1):3838. doi: 10.1038/s41467-019-11718-4
29. Dad HA, Gu TW, Zhu AQ, Huang LQ, Peng LH. Plant Exosome-Like Nanovesicles: Emerging Therapeutics and Drug Delivery Nanoplatforms. *Mol Ther* (2021) 29(1):13–31. doi: 10.1016/j.ymthe.2020.11.030
30. Stoker M, Perryman M. An Epithelial Scatter Factor Released by Embryo Fibroblasts. *J Cell Sci* (1985) 77:209–23. doi: 10.1242/jcs.77.1.209
31. Ribatti D, Tamma R, Annese T. Epithelial-Mesenchymal Transition in Cancer: A Historical Overview. *Transl Oncol* (2020) 13(6):100773. doi: 10.1016/j.tranon.2020.100773
32. Liang ZH, Pan YC, Lin SS, Qiu ZY, Zhang Z. LncRNA MALAT1 Promotes Wound Healing *via* Regulating miR-141-3p/ZNF217 Axis. *Regener Ther* (2020) 15:202–9. doi: 10.1016/j.reth.2020.09.006
33. Lavin DP, Tiwari VK. Unresolved Complexity in the Gene Regulatory Network Underlying EMT. *Front Oncol* (2020) 10:554. doi: 10.3389/fonc.2020.00554
34. Jiang Y, Zhan H. Communication Between EMT and PD-L1 Signaling: New Insights Into Tumor Immune Evasion. *Cancer Lett* (2020) 468:72–81. doi: 10.1016/j.canlet.2019.10.013
35. Marconi GD, Fonticoli L, Rajan TS, Pierdomenico SD, Trubiani O, Pizzicannella J, et al. Epithelial-Mesenchymal Transition (EMT): The Type-2 EMT in Wound Healing, Tissue Regeneration and Organ Fibrosis. *Cells* (2021) 10(7):1587. doi: 10.3390/cells10071587
36. Nakajima S, Doi R, Toyoda E, Tsuji S, Wada M, Koizumi M, et al. N-Cadherin Expression and Epithelial-Mesenchymal Transition in Pancreatic Carcinoma. *Clin Cancer Res* (2004) 10(12 Pt 1):4125–33. doi: 10.1158/1078-0432.CCR-0578-03
37. Loh C-Y, Chai J, Tang T, Wong W, Sethi G, Shanmugam M, et al. The E-Cadherin and N-Cadherin Switch in Epithelial-To-Mesenchymal Transition: Signaling, Therapeutic Implications, and Challenges. *Cells* (2019) 8(10):1118. doi: 10.3390/cells8101118
38. Jolly MK, Somarelli JA, Sheth M, Biddle A, Tripathi SC, Armstrong AJ, et al. Hybrid Epithelial/Mesenchymal Phenotypes Promote Metastasis and Therapy Resistance Across Carcinomas. *Pharmacol Ther* (2019) 194:161–84. doi: 10.1016/j.pharmthera.2018.09.007
39. Jolly MK, Boareto M, Huang B, Jia D, Lu M, Ben-Jacob E, et al. Implications of the Hybrid Epithelial/Mesenchymal Phenotype in Metastasis. *Front Oncol* (2015) 5:155. doi: 10.3389/fonc.2015.00155
40. Huang RY, Wong MK, Tan TZ, Kuay KT, Ng AH, Chung VY, et al. An EMT Spectrum Defines an Anoikis-Resistant and Spheroidogenic Intermediate Mesenchymal State That Is Sensitive to E-Cadherin Restoration by a Src-Kinase Inhibitor, Saracatinib (AZD0530). *Cell Death Dis* (2013) 4:e915. doi: 10.1038/cddis.2013.442
41. Mani SA, Guo W, Liao MJ, Eaton EN, Ayyanan A, Zhou AY, et al. The Epithelial-Mesenchymal Transition Generates Cells With Properties of Stem Cells. *Cell* (2008) 133(4):704–15. doi: 10.1016/j.cell.2008.03.027
42. Paolillo M, Colombo R, Serra M, Belvisi L, Papetti A, Ciusani E, et al. Stem-Like Cancer Cells in a Dynamic 3D Culture System: A Model to Study Metastatic Cell Adhesion and Anti-Cancer Drugs. *Cells* (2019) 8(11):1434. doi: 10.3390/cells8111434
43. Zhou P, Li B, Liu F, Zhang M, Wang Q, Liu Y, et al. The Epithelial to Mesenchymal Transition (EMT) and Cancer Stem Cells: Implication for Treatment Resistance in Pancreatic Cancer. *Mol Cancer* (2017) 16(1):52. doi: 10.1186/s12943-017-0624-9
44. Steinbichler TB, Dudas J, Skvortsov S, Ganswindt U, Riechelmann H, Skvortsova II. : Therapy Resistance Mediated by Exosomes. *Mol Cancer* (2019) 18(1):58. doi: 10.1186/s12943-019-0970-x
45. Shibue T, Weinberg RA. EMT, CSCs, and Drug Resistance: The Mechanistic Link and Clinical Implications. *Nat Rev Clin Oncol* (2017) 14(10):611–29. doi: 10.1038/nrclinonc.2017.44
46. You J, Li M, Cao LM, Gu QH, Deng PB, Tan Y, et al. Snail1-Dependent Cancer-Associated Fibroblasts Induce Epithelial-Mesenchymal Transition in Lung Cancer Cells *via* Exosomes. *QJM* (2019) 112(8):581–90. doi: 10.1093/qjmed/hcz093
47. Tian T, Han J, Huang J, Li S, Pang H. Hypoxia-Induced Intracellular and Extracellular Heat Shock Protein Gp96 Increases Paclitaxel-Resistance and Facilitates Immune Evasion in Breast Cancer. *Front Oncol* (2021) 11:784777. doi: 10.3389/fonc.2021.784777
48. Shan Y, You B, Shi S, Shi W, Zhang Z, Zhang Q, et al. Hypoxia-Induced Matrix Metalloproteinase-13 Expression in Exosomes From Nasopharyngeal Carcinoma Enhances Metastases. *Cell Death Dis* (2018) 9(3):382. doi: 10.1038/s41419-018-0425-0
49. Garcia-Heredia JM, Otero-Albiol D, Perez M, Perez-Castejon E, Munoz-Galvan S, Carnero A. Breast Tumor Cells Promotes the Horizontal Propagation of EMT, Stemness, and Metastasis by Transferring the MAP17 Protein Between Subsets of Neoplastic Cells. *Oncogenesis* (2020) 9(10):96. doi: 10.1038/s41389-020-00280-0
50. Ji Q, Zhou L, Sui H, Yang L, Wu X, Song Q, et al. Primary Tumors Release ITGBL1-Rich Extracellular Vesicles to Promote Distal Metastatic Tumor Growth Through Fibroblast-Niche Formation. *Nat Commun* (2020) 11 (1):1211. doi: 10.1038/s41467-020-14869-x

51. Li Y, Li Q, Li D, Gu J, Qian D, Qin X, et al. Exosome Carrying PSGR Promotes Stemness and Epithelial-Mesenchymal Transition of Low Aggressive Prostate Cancer Cells. *Life Sci* (2021) 264:118638. doi: 10.1016/j.lfs.2020.118638
52. Hoshino A, Costa-Silva B, Shen TL, Rodrigues G, Hashimoto A, Tesic Mark M, et al. Tumour Exosome Integrins Determine Organotropic Metastasis. *Nature* (2015) 527(7578):329–35. doi: 10.1038/nature15756
53. Li K, Liu T, Chen J, Ni H, Li W. Survivin in Breast Cancer-Derived Exosomes Activates Fibroblasts by Up-Regulating SOD1, Whose Feedback Promotes Cancer Proliferation and Metastasis. *J Biol Chem* (2020) 295(40):13737–52. doi: 10.1074/jbc.RA120.013805
54. Rivoltini L, Chiodoni C, Squarcina P, Tortoreto M, Villa A, Vergani B, et al. TNF-Related Apoptosis-Inducing Ligand (TRAIL)-Armed Exosomes Deliver Proapoptotic Signals to Tumor Site. *Clin Cancer Res* (2016) 22(14):3499–512. doi: 10.1158/1078-0432.CCR-15-2170
55. Aspe JR, Wall NR. Survivin-T34A: Molecular Mechanism and Therapeutic Potential. *OncoTargets Ther* (2010) 3:247–54. doi: 10.2147/OTT.S15293
56. Xu Z, Zeng S, Gong Z, Yan Y. Exosome-Based Immunotherapy: A Promising Approach for Cancer Treatment. *Mol Cancer* (2020) 19(1):160. doi: 10.1186/s12943-020-01278-3
57. Yang B, Feng X, Liu H, Tong R, Wu J, Li C, et al. High-Metastatic Cancer Cells Derived Exosomal miR92a-3p Promotes Epithelial-Mesenchymal Transition and Metastasis of Low-Metastatic Cancer Cells by Regulating PTEN/Akt Pathway in Hepatocellular Carcinoma. *Oncogene* (2020) 39(42):6529–43. doi: 10.1038/s41388-020-01450-5
58. Rezaei R, Baghaei K, Amani D, Piccin A, Hashemi SM, Asadzadeh Aghdaei H, et al. Exosome-Mediated Delivery of Functionally Active miRNA-375-3p Mimic Regulate Epithelial Mesenchymal Transition (EMT) of Colon Cancer Cells. *Life Sci* (2021) 269:119035. doi: 10.1016/j.lfs.2021.119035
59. Li YY, Tao YW, Gao S, Li P, Zheng JM, Zhang SE, et al. Cancer-Associated Fibroblasts Contribute to Oral Cancer Cells Proliferation and Metastasis *via* Exosome-Mediated Paracrine miR-34a-5p. *EBioMedicine* (2018) 36:209–20. doi: 10.1016/j.ebiom.2018.09.006
60. Wang D, Wang X, Si M, Yang J, Sun S, Wu H, et al. Exosome-Encapsulated miRNAs Contribute to CXCL12/CXCR4-Induced Liver Metastasis of Colorectal Cancer by Enhancing M2 Polarization of Macrophages. *Cancer Lett* (2020) 474:36–52. doi: 10.1016/j.canlet.2020.01.005
61. Ge Q, Zhou Y, Lu J, Bai Y, Xie X, Lu Z. miRNA in Plasma Exosome is Stable Under Different Storage Conditions. *Molecules* (2014) 19(2):1568–75. doi: 10.3390/molecules19021568
62. Selth LA, Das R, Townley SL, Coutinho I, Hanson AR, Centenera MM, et al. A ZEB1-miR-375-YAP1 Pathway Regulates Epithelial Plasticity in Prostate Cancer. *Oncogene* (2017) 36(1):24–34. doi: 10.1038/onc.2016.185
63. Arteaga-Blanco LA, Mojoli A, Monteiro RQ, Sandim V, Menna-Barreto RFS, Pereira-Dutra FS, et al. Characterization and Internalization of Small Extracellular Vesicles Released by Human Primary Macrophages Derived From Circulating Monocytes. *PloS One* (2020) 15(8):e0237795. doi: 10.1371/journal.pone.0237795
64. Cheng L, Wang Y, Huang L. Exosomes From M1-Polarized Macrophages Potentiate the Cancer Vaccine by Creating a Pro-Inflammatory Microenvironment in the Lymph Node. *Mol Ther* (2017) 25(7):1665–75. doi: 10.1016/j.ymthe.2017.02.007
65. Zhou L, Li J, Tang Y, Yang M. Exosomal LncRNA LINC00659 Transferred From Cancer-Associated Fibroblasts Promotes Colorectal Cancer Cell Progression *via* miR-342-3p/ANXA2 Axis. *J Transl Med* (2021) 19(1):8. doi: 10.1186/s12967-020-02648-7
66. Liang ZX, Liu HS, Wang FW, Xiong L, Zhou C, Hu T, et al. LncRNA RPPH1 Promotes Colorectal Cancer Metastasis by Interacting With TUBB3 and by Promoting Exosomes-Mediated Macrophage M2 Polarization. *Cell Death Dis* (2019) 10(11):829. doi: 10.1038/s41419-019-2077-0
67. Wang J, Lv B, Su Y, Wang X, Bu J, Yao L. Exosome-Mediated Transfer of lncRNA HOTTIP Promotes Cisplatin Resistance in Gastric Cancer Cells by Regulating HMGA1/miR-218 Axis. *Onco Targets Ther* (2019) 12:11325–38. doi: 10.2147/OTT.S231846
68. Li Z, Jiang P, Li J, Peng M, Zhao X, Zhang X, et al. Tumor-Derived Exosomal lnc-Sox2ot Promotes EMT and Stemness by Acting as a ceRNA in Pancreatic Ductal Adenocarcinoma. *Oncogene* (2018) 37(28):3822–38. doi: 10.1038/s41388-018-0237-9
69. Huang CS, Ho JY, Chiang JH, Yu CP, Yu DS. Exosome-Derived LINC00960 and LINC02470 Promote the Epithelial-Mesenchymal Transition and Aggressiveness of Bladder Cancer Cells. *Cells* (2020) 9(6):1419. doi: 10.3390/cells9061419
70. Wu P, Cai J, Chen Q, Han B, Meng X, Li Y, et al. Lnc-TALC Promotes O(6)-Methylguanine-DNA Methyltransferase Expression *via* Regulating the C-Met Pathway by Competitively Binding With miR-20b-3p. *Nat Commun* (2019) 10(1):2045. doi: 10.1038/s41467-019-10025-2
71. Zhang X, Wang S, Wang H, Cao J, Huang X, Chen Z, et al. Circular RNA Circnrip1 Acts as a microRNA-149-5p Sponge to Promote Gastric Cancer Progression *via* the AKT1/mTOR Pathway. *Mol Cancer* (2019) 18(1):20. doi: 10.1186/s12943-018-0935-5
72. Chen J, Rong N, Liu M, Xu C, Guo J. The Exosome-Circ_0001359 Derived From Cigarette Smoke Exposed-Prostate Stromal Cells Promotes Epithelial Cells Collagen Deposition and Primary Ciliogenesis. *Toxicol Appl Pharmacol* (2022) 435:115850. doi: 10.1016/j.taap.2021.115850
73. Chen X, Chen RX, Wei WS, Li YH, Feng ZH, Tan L, et al. PRMT5 Circular RNA Promotes Metastasis of Urothelial Carcinoma of the Bladder Through Sponging miR-30c to Induce Epithelial-Mesenchymal Transition. *Clin Cancer Res* (2018) 24(24):6319–30. doi: 10.1158/1078-0432.CCR-18-1270
74. Lin Q, Qi Q, Hou S, Chen Z, Jiang N, Zhang L, et al. Exosomal Circular RNA Hsa_Circ_007293 Promotes Proliferation, Migration, Invasion, and Epithelial-Mesenchymal Transition of Papillary Thyroid Carcinoma Cells Through Regulation of the microRNA-653-5p/Paired Box 6 Axis. *Bioengineered* (2021) 12(2):10136–49. doi: 10.1080/21655979.2021.2000745
75. Chen T, Liu Y, Li C, Xu C, Ding C, Chen J, et al. Tumor-Derived Exosomal circFARSA Mediates M2 Macrophage Polarization *via* the PTEN/PI3K/AKT Pathway to Promote Non-Small Cell Lung Cancer Metastasis. *Cancer Treat Res Commun* (2021) 28:100412. doi: 10.1016/j.ctarc.2021.100412
76. Wei S, Zheng Y, Jiang Y, Li X, Geng J, Shen Y, et al. The circRNA circPTPRA Suppresses Epithelial-Mesenchymal Transitioning and Metastasis of NSCLC Cells by Sponging miR-96-5p. *EBioMedicine* (2019) 44:182–93. doi: 10.1016/j.ebiom.2019.05.032
77. Hong W, Xue M, Jiang J, Zhang Y, Gao X. Circular RNA Circ-CPA4/let-7 miRNA/PD-L1 Axis Regulates Cell Growth, Stemness, Drug Resistance and Immune Evasion in Non-Small Cell Lung Cancer (NSCLC). *J Exp Clin Cancer Res* (2020) 39(1):149. doi: 10.1186/s13046-020-01648-1
78. Dong W, Dai ZH, Liu FC, Guo XG, Ge CM, Ding J, et al. The RNA-Binding Protein RBM3 Promotes Cell Proliferation in Hepatocellular Carcinoma by Regulating Circular RNA SCD-circRNA 2 Production. *EBioMedicine* (2019) 45:155–67. doi: 10.1016/j.ebiom.2019.06.030
79. Shojaei S, Hashemi SM, Ghanbarian H, Sharifi K, Salehi M, Mohammadi-Yeganeh S. Delivery of miR-381-3p Mimic by Mesenchymal Stem Cell-Derived Exosomes Inhibits Triple Negative Breast Cancer Aggressiveness; an *In Vitro* Study. *Stem Cell Rev Rep* (2021) 17(3):1027–38. doi: 10.1007/s12015-020-10089-4
80. Wang YH, Liu CL, Chiu WC, Twu YC, Liao YJ. HMGCS2 Mediates Ketone Production and Regulates the Proliferation and Metastasis of Hepatocellular Carcinoma. *Cancers (Basel)* (2019) 11(12):1876. doi: 10.3390/cancers11121876
81. Zhao G, Li H, Guo Q, Zhou A, Wang X, Li P, et al. Exosomal Sonic Hedgehog Derived From Cancer-Associated Fibroblasts Promotes Proliferation and Migration of Esophageal Squamous Cell Carcinoma. *Cancer Med* (2020) 9(7):2500–13. doi: 10.1002/cam4.2873
82. Li L, Zhao J, Zhang Q, Tao Y, Shen C, Li R, et al. Cancer Cell-Derived Exosomes Promote HCC Tumorigenesis Through Hedgehog Pathway. *Front Oncol* (2021) 11:756205. doi: 10.3389/fonc.2021.756205
83. Gimple RC, Bhargava S, Dixit D, Rich JN. Glioblastoma Stem Cells: Lessons From the Tumor Hierarchy in a Lethal Cancer. *Genes Dev* (2019) 33(11-12):591–609. doi: 10.1101/gad.324301.119
84. Au Yeung CL, Co NN, Tsuruga T, Yeung TL, Kwan SY, Leung CS, et al. Exosomal Transfer of Stroma-Derived miR21 Confers Paclitaxel Resistance in Ovarian Cancer Cells Through Targeting APAF1. *Nat Commun* (2016) 7:11150. doi: 10.1038/ncomms11150
85. Fujiwara T, Eguchi T, Sogawa C, Ono K, Murakami J, Ibaragi S, et al. Carcinogenic Epithelial-Mesenchymal Transition Initiated by Oral Cancer Exosomes Is Inhibited by Anti-EGFR Antibody Cetuximab. *Oral Oncol* (2018) 86:251–7. doi: 10.1016/j.oraloncology.2018.09.030
86. Zhang M, Viennois E, Prasad M, Zhang Y, Wang L, Zhang Z, et al. Edible Ginger-Derived Nanoparticles: A Novel Therapeutic Approach for the

Prevention and Treatment of Inflammatory Bowel Disease and Colitis-Associated Cancer. *Biomaterials* (2016) 101:321–40. doi: 10.1016/j.biomaterials.2016.06.018

Conflict of Interest: The authors declare that the research was conducted in the absence of any commercial or financial relationships that could be construed as a potential conflict of interest.

Publisher's Note: All claims expressed in this article are solely those of the authors and do not necessarily represent those of their affiliated organizations, or those of the publisher, the editors and the reviewers. Any product that may be evaluated in this article, or claim that may be made by its manufacturer, is not guaranteed or endorsed by the publisher.

Copyright © 2022 Jiang, Li, Zhou, Zhao, Huang and Qin. This is an open-access article distributed under the terms of the Creative Commons Attribution License (CC BY). The use, distribution or reproduction in other forums is permitted, provided the original author(s) and the copyright owner(s) are credited and that the original publication in this journal is cited, in accordance with accepted academic practice. No use, distribution or reproduction is permitted which does not comply with these terms.

frontiers | Frontiers in Oncology

ORIGINAL RESEARCH
published: 11 April 2022
doi: 10.3389/fonc.2022.865067

TGF-β1 Promotes Autophagy and Inhibits Apoptosis in Breast Cancer by Targeting TP63

Yichao Wang[1†], Hongsheng Lu[1†], Zhongrong Wang[2], Yueguo Li[3] and Xiaoying Chen[1*]*

[1] Department of Clinical Laboratory Medicine, Taizhou Central Hospital (Taizhou Univesity Hospital), Taizhou, China, [2] Key Laboratory of Brain-Like Neuromorphic Devices and Systems of Hebei Province College of Electron and Information Engineering, Hebei University, Baoding, China, [3] Department of Clinical Laboratory, Tianjin's Clinical Research Center for Cancer, Key Laboratory of Cancer Prevention and Therapy, National Clinical Research Center for Cancer, Tianjin Medical University Cancer Institute and Hospital, Tianjin, China

OPEN ACCESS

Edited by:
Tao Sun,
Nankai University, China

Reviewed by:
Hongjun Fei,
Shanghai Jiao Tong University, China
Antonio Ieni,
University of Messina, Italy

***Correspondence:**
Yueguo Li
yli08@tmu.edu.cn
Xiaoying Chen
xiaoying950927@163.com

[†]These authors have contributed equally to this work

Specialty section:
This article was submitted to Pharmacology of Anti-Cancer Drugs, a section of the journal Frontiers in Oncology

Received: *31 January 2022*
Accepted: *02 March 2022*
Published: *11 April 2022*

Citation:
Wang Y, Lu H, Wang Z, Li Y and Chen X (2022) TGF-β1 Promotes Autophagy and Inhibits Apoptosis in Breast Cancer by Targeting TP63. Front. Oncol. 12:865067. doi: 10.3389/fonc.2022.865067

Background: Breast cancer (BC) is a prevalent female cancer, which has high morbidity and mortality. However, the pathogenesis of BC has not been fully elucidated. Studies have shown that TGF-β1 plays an important role in regulating the balance between autophagy and apoptosis of tumor. We aim to clarify the specific mechanism of autophagy and apoptosis in breast cancer maintaining the tumor microenvironment.

Methods: The clinical characteristics of 850 BC patients were retrieved from the TCGA database. Differentially expressed autophagy-related genes (DEARGs) between tumor and normal tissues were obtained by the Wilcox test. Through Cox proportional hazard regression analysis, the prognostic risk model was constructed and verified by the ROC curve. We used MDC staining, colony formation assay, CCK-8, flow cytometric analysis to confirm the importance of TGF-β1 on the autophagy and apoptosis of breast cancer cells. Furthermore, western blot was performed to determine the relative expression of protein. The Kaplan-Meier Plotter database was utilized to identify the prognostic value of TP63.

Results: We successfully constructed a prognostic risk model of breast cancer and screened out an autophagy-related prognostic gene -TP63. We predicted that TGF-β1 and TP63 have a binding site in the JASPAR database as expected. Additionally, TGF-β1 promoted autophagy and inhibited apoptosis of breast cancer cells by inhibiting the expression of TP63.

Conclusion: Our study demonstrated that the molecular mechanism of TGF-β/TP63 signaling in regulating autophagy and apoptosis of breast cancer and provided a potential prognostic marker in breast cancer.

Keywords: autophagy-related genes, TGF-β1, TP63, autophagy, apoptosis, breast cancer

INTRODUCTION

Breast cancer (BC) is a common female cancer worldwide. In 2019, there were approximately 268,600 new cases of invasive breast cancer among American women, of which 41,760 women will die from the disease (1). For women, breast cancer alone accounting for 30% of female cancers (2). Breast cancer is also the most ordinary cancer among Chinese women during the last two decades. For instance, breast cancer cases in China accounted for 12.2% of newly diagnosed breast cancers worldwide and 9.6% of global breast cancer deaths, respectively (3). The common causes of breast cancer death are invasion, metastasis, and recurrence (4, 5). However, the mechanism of breast cancer occurrence and development is still unclear after years of research and extensive progress.

Autophagy can achieve cell renewal by degrading macromolecules in cells, which is conducive to maintaining the stability of the cell's internal environment and improving cell viability (6, 7). In most cases, autophagy is considered to inhibit the occurrence of early tumors and promote the development of formed tumors (8). Apoptosis is a physiological form of programmed cell death that removes damaged cells orderly and effectively, which affects the occurrence and development of tumors. Studies have supposed that autophagy and apoptosis are related to the occurrence and development of breast cancer (9–11) and that autophagy and apoptosis play an important regulatory role in the tumor microenvironment (12–14). One of the hallmarks of cancer is that the disorder of apoptosis mechanism (15). The cytoprotective function of autophagy is achieved through negative regulation of apoptosis in many cases, and the apoptotic signal plays a role in inhibiting autophagy in turn (16). Thereby, it is worth exploring the molecular mechanism about the occurrence and development of breast cancer through regulating autophagy and apoptosis.

Transforming growth factor-β (transforming growth factor-β, TGF-β) as a key factor modulates the transformation of endothelial cells (17), which plays a dual role in promoting and inhibiting the occurrence of tumors. In the early stages of carcinogenesis, TGF-β inhibits tumorigenesis mainly by inhibiting cell growth. However, when the growth inhibitory effect of TGF-β is broken by tumor cells, TGF-β will promote the progression and metastasis of advanced tumors. TGF-β1 takes part in various cellular processes such as cell growth, differentiation, and immunity, which is necessary for regulating the tumor microenvironment (18). Studies have shown that TGF-β can induce or inhibit autophagy (19–21) and apoptosis (22) to affect the occurrence and development of tumor cells. TGF-β1, TGF-β2, and TGF-β3 are three subtypes of mammals, among which TGF-β1 shows the strongest activity. This article explores the role of TGF-β1 in the occurrence and development of breast cancer.

As a transcription factor, TP63 has a conservative basic domain structure, which belongs to the p53 transcription factor family. Compared with p53 and p73, TP63 has different functions, although they have high amino acid similarity (23). TP63 is located on chromosome 3q27-29 and consisted of 15 exons distributed over 220 kilobases. Due to two different promoters (P1 and P2), two types of proteins are produced: TAp63 and ΔNp63. TAp63 contains the N-terminal transactivation (TA) domain, and ΔNp63 is the N-terminal truncated isoform without the TA domain (24). Studies have found that TP63 is a downstream effector of the TGF-β pathway and plays an important role in primary breast cancer (25).

Based on bioinformatics analysis, this study first constructed a prognostic risk model successfully and screened the prognostic gene TP63 as one of the autophagy-related genes (ARGs) in breast cancer. We explored the interaction and effects between TGF-β1 and TP63 in breast cancer on autophagy and apoptosis. Clarifying the importance of TGF-β1 and TP63 in breast cancer cells may provide a theoretical basis and a new idea for breast cancer treatment in the future.

MATERIALS AND METHODS

Data Collection

Corresponding clinical data and mRNA expression profiles of breast cancer patients are obtained from the TCGA database (https://portal.gdc.cancer.gov/). A total of 232 autophagy-related genes were extracted from the human autophagy database (HADb, http://autophagy.lu/Clusters/index.html).

Analysis of ARGs

Wilcox test was used to obtain differentially expressed autophagy-related genes (DEARGs) between tumor and normal tissues. ARGs with at least two-fold change in expression level and the P value of less than 0.05 were screened out. These ARGs were deemed to be differentially expressed autophagy-related genes. Gene function enrichment analysis of DEARGs was used Gene Ontology (GO) and Kyoto Encyclopedia of Genes and Genomes (KEGG) analysis, p and q values less than 0.05 will be considered statistically significant.

Construction of Prognostic Model Related to ARGs

After integrating the expression value of each specific gene, multivariate Cox regression analysis was used to weight the regression coefficients to successfully construct a risk score formula for each patient. Based on the risk score formula, breast cancer patients can be divided into low-risk groups and high-risk groups, and the cutoff point is the median risk score. The Kaplan-Meier method was used to assess the survival difference between the two groups. Eventually, ROC curve verified the accuracy of the prediction model. Data was divided into two groups based on clinicopathological characteristics such as age, tumor stage, tumor size, and lymph node metastasis. Age was divided into two groups for those age greater than or equal to 65 and less than 65 years old. The group of Stage was divided into Stage I & II and Stage III &IV. Tumor size for T1-2 belongs to one group, and T3-4 are another group. The group of lymph node status were divided into two groups: N0 and N1-3.

Cells and Reagents

MDA-MB-231 and MCF-7 cells were obtained from the cell bank of Taizhou University in June 2020, and were preserved in the laboratory of Taizhou University. MDA-MB-231 and MCF-7 cells were cultivated in DMEM and MEM medium (Gibco, CA, USA) with 10% fetal bovine serum (Gibco, CA, USA), and placed at 37°C with 5% CO_2. All cells used in this study were tested for absence of mycoplasma contamination and the authenticity of the cells was determined by short tandem repeat analysis through PCR following the instructions of ATCC in July 2020.

MDC Staining

MDA-MB-231 and MCF-7 cells were grown in 24-well plates and cultivated at 37°C with 5% CO_2. TGF-β1 intervention treatment was performed for 24h before staining (Solarbio, Beijing, China). After washing 3 times, the cells were incubated in the dark at room temperature for 45 min. Under a fluorescent microscope, the cells were immediately observed and photographed.

Colony Formation Assay

MDA-MB-231 and MCF7 cells (1000 cells/well) were seeded into 6-well plates and cultivated in DMEM and MEM medium treated with TGF-β1 for 10 days. The cells were fixed with 4% polymethanol for 20 minutes and stained with 0.1% crystal violet (Solarbio, Beijing, China) at room temperature. Count and image cell colonies instantly.

CCK-8 Assay

MDA-MB-231 and MCF-7 cells were cultivated in 96-well plates and under the conditions of 37°C and 5% CO2. On the second day, different concentrations of TGF-β1 protein (5, 10ng/ml) were added for intervention. Finally, the cell counting kit (Solarbio, Beijing, China) was used to measure the absorbance of OD_{450} at different times (24, 48 and 72h). CCK-8 (10μL) was added to each well and we should pay attention to operate in the dark during the whole process. After incubating at 37°C for 2 h, the absorbance at 450 nm was detected with a microplate reader.

Annexin V-FITC/PI Flow Cytometric Analysis

The apoptotic cells were counted with Annexin V-FITC apoptosis detection kit (Solarbio, Beijing, China). After TGF-β1 treatment for 24 hours, cells were collected with 0.25% trypsin without EDTA and washed twice with pre-cooled PBS. Then, the cells were resuspended in 500μL of 1x binding buffer and transferred to a sterile flow cytometer glass tube. The cell suspension was incubated with 5μL Annexin V-FITC and propidium iodide (PI) solution for 15 min in dark conditions at room temperature. The cell apoptosis rates were detected by a flow cytometer (Beckman Coulter Inc, CA, USA) within 1 h.

Western Blot

The total protein was extracted with RIPA lysis buffer (Solarbio, Beijing, China) containing protease inhibitors and phosphatase inhibitors. Then, the total protein was quantified with the BCA protein analysis kit (Solarbio, Beijing, China). The protein was separated by sodium dodecyl sulphate polyacrylamide gel electrophoresis (SDS-PAGE) and then transferred to PVDF membrane. Block the membrane in TBST buffer with 5% milk for 90 minutes, and incubate at 4°C overnight with anti-TP63 (Santa cruz, dilution 1:200), anti-P62/SQSTM1 (Abnova, dilution 1:1000), anti-Beclin1 (ABclonal, dilution 1:1000), anti-Bax (BOSTER, dilution 1:1000), anti-Bcl-2 (ABclonal, dilution 1:1000) and anti-GAPDH (ABclonal, dilution 1:40000) primary antibodies. Next, the secondary antibody (EarthOx, dilution 1:40000) labeled with horseradish peroxidase (HRP) was used for 2 hours at room temperature. A chemiluminescence imaging system (Amersham Imager 680, GE, USA) was used to detect the band intensity. The results were normalized to GAPDH, and Image J (National Institute of Mental Health, Bethesda, USA) was applied for band density analysis.

Statistical Analysis

Use SPSS26.0 and R3.6.3 software for statistical analysis. The log-rank test was used for comparison. Established a Cox proportional hazards model by Multivariate analysis. Kaplan-Meier Plotter was used to draw survival curves. Student's t-test and one-way ANOVA were used to analyze the statistical differences between the two groups and multiple groups, respectively. The experiment was repeated at least three times. $P<0.05$ was considered statistically significant.

RESULTS

Screening of DEARGs

The detailed workflow for the construction of the prognostic risk model was presented in **Figure S1**. There are 1085 cases of clinical data were collected from the TCGA database (https://portal.gdc.cancer.gov/). Finally, a total of 850 cases of primary breast cancer with follow-up time of more than 1 month and a complete gene expression profile were included for follow-up analysis. We extracted the expression value of 232 ARGs. According to the criteria of $p<0.05$ and $\log_2$(fold change)>1, we lastly obtained 17 up-regulated DEARGs and 13 down-regulated DEARGs (**Figures 1A, B**). The box plot showed the expression patterns of 30 DEARGs between tumor and normal tissues (**Figure 1C**).

Functional Enrichment of DEARGs

The functional enrichment analysis of 30 differentially expressed ARGs provides a biological understanding of these genes. It can be seen from GO and KEGG analysis that DEARGs are mainly involved in autophagy, apoptosis signaling pathway, ERBB2 signaling pathway, etc. (**Figures 1D–F**).

Construction and Verification of the BC Prognostic Risk Model

In order to analyze the role of ARGs in the prognosis of breast cancer, we first screened the ARGs that are significantly related to the prognosis of breast cancer. Using univariate Cox regression analysis, a total of 4 autophagy-related genes (EIF4EBP1, IFNG, NRG1, TP63) were significantly correlated with overall survival (OS) of breast cancer (**Table 1**). Multivariate Cox regression analysis

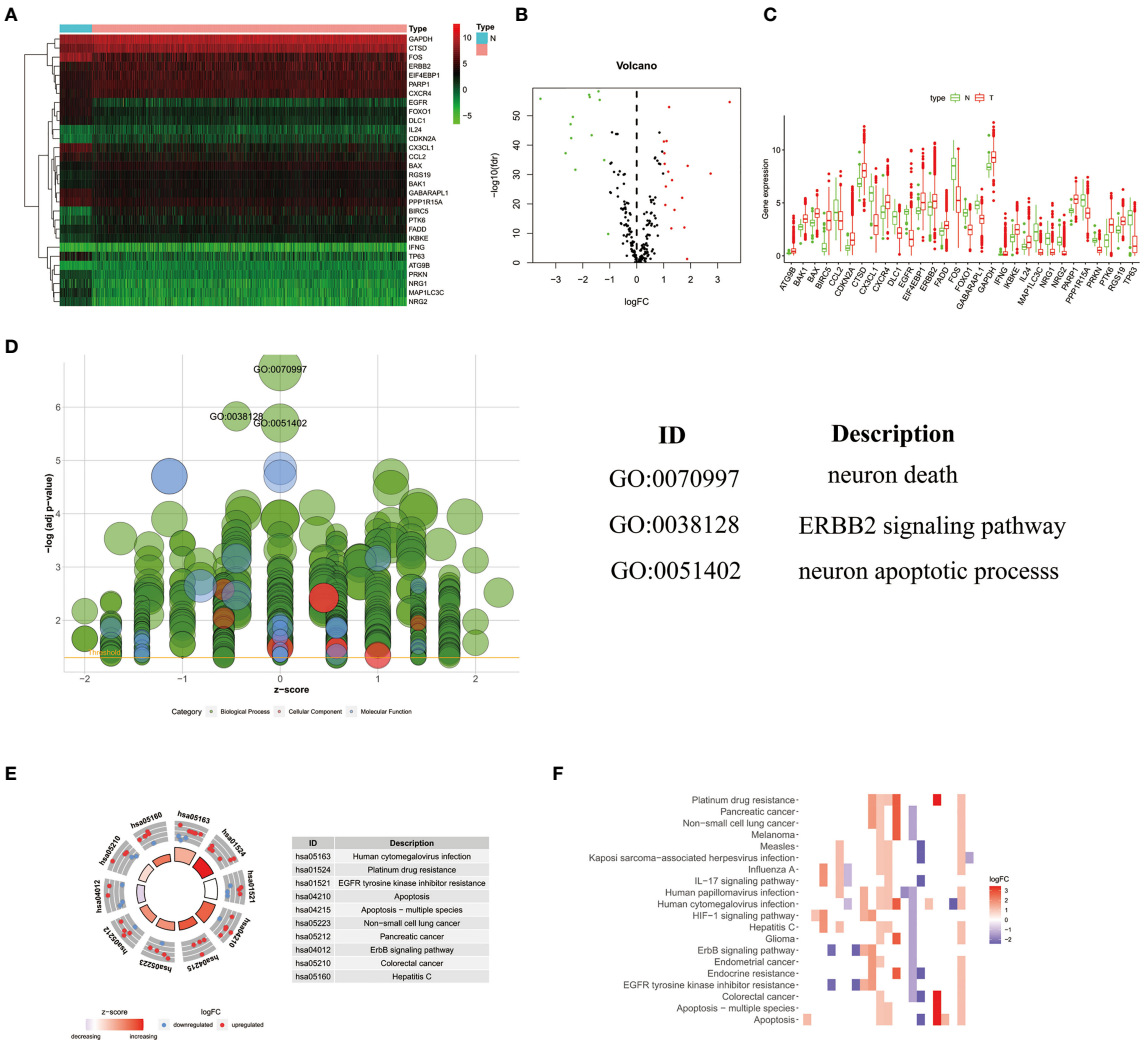

FIGURE 1 | The heatmap **(A)** and volcano map **(B)** showed 30 differentially expressed autophagy-related genes in breast cancer tissues. Red represented high expression level, green represented low expression level, and black represented no significant difference. **(C)**The box plot showed the expression patterns of 30 differentially expressed ARGs. Red dots indicated tumor tissues, and green dots indicated normal tissues. **(D)** GO analysis showed the biological processes, cellular components, and molecular functions involved in ARGs; the green, pink, and blue bubbles represented biological processes, cellular components, and molecular functions, respectively. **(E, F)** The potential enrichment pathways of ARGs in breast cancer were obtained by KEGG analysis.

TABLE 1 | Univariate cox regression analysis identified 4 ARGs related to the BC risks.

Genes	HR	95% CI	p value
EIF4EBP1	1.224	1.051-1.426	0.009
IFNG	0.601	0.386-0.934	0.024
NRG1	0.642	0.418-0.985	0.042
TP63	0.795	0.658-0.959	0.017

showed that a total of 3 genes (EIF4EBP1, IFNG, TP63) were significantly related to the prognosis (**Table 2**). The results showed the distribution of ARGs signals in the TCGA data set (**Figure 2A**), the risk score of different groups of patients (**Figure 2B**), and the heatmap of the included ARGs expression profile (**Figure 2C**). The K-M survival curve revealed the different survival time between the high-risk group and the low-risk group, verifying the performance of the prognostic model in predicting OS in BC patients. We observed that the survival time of the low-risk group was significantly higher than the high-risk group (**Figure 2D**), and there was a significant difference between the two groups(P<0.05). After adjusting the clinicopathological characteristics such as age,

TABLE 2 | Multivariate cox regression analysis identified 3 ARGs that are independent factors for BC risks.

Genes	Co-efficient	HR	95% CI	p value
EIF4EBP1	0.191	1.211	1.039-1.412	0.015
IFNG	0.565	0.568	0.367-0.880	0.011
TP63	0.197	0.821	0.680-0.992	0.041

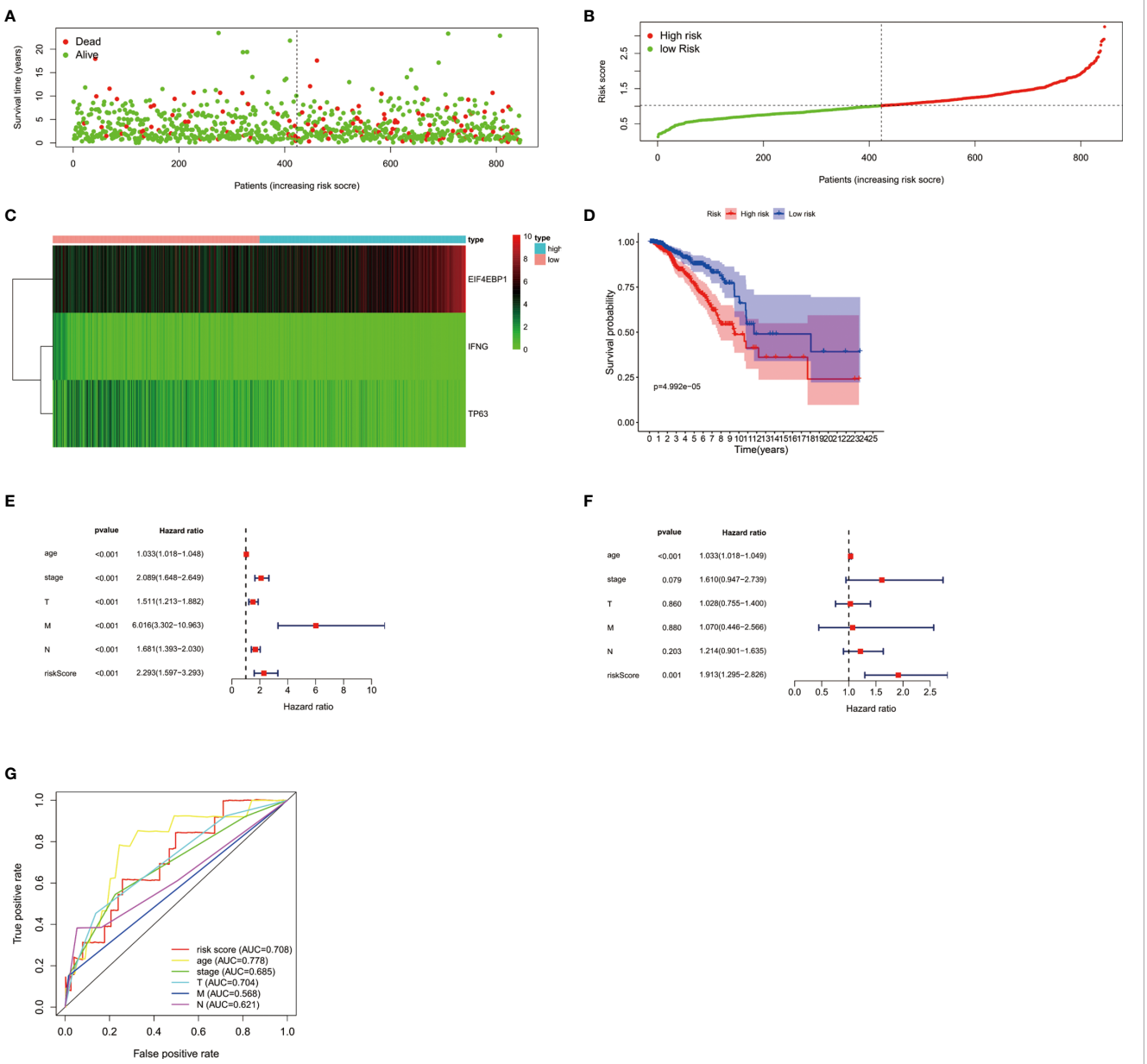

FIGURE 2 | **(A)** The distribution of prognostic indicators in different groups of breast cancer patients. **(B)** The distribution of risk score in different groups of breast cancer patients. **(C)** Heatmap of the expression profile of DEARGs. **(D)** Survival curves of breast cancer patients in the high and low risk groups. The forest plots showed univariate Cox regression analysis **(E)** and multivariate Cox regression analysis **(F)** in breast cancer. **(G)** The survival-dependent receiver operating characteristic (ROC) curve confirmed the prognostic significance of risk score based on ARGs.

tumor stage, tumor size, and lymph node metastasis, univariate analysis (HR=2.293, 95%CI, 1.597~3.393; P<0.001; **Figure 2E**) and multivariate analysis (HR= 1.913, 95% CI, 1.295~2.826; P=0.001; **Figure 2F**) indicated that the risk value is an independent prognostic indicator for breast cancer patients. The AUC value for 5 years of risk score is 0.708, which is significantly higher than tumor stage (0.685), metastasis status (0.568), and lymph node status (0.621), which indicated that the prognostic risk index based on ARGs had certain potential in survival prediction (**Figure 2G**).

Clinical Correlation Analysis of TP63

The clinical significance of TP63 in breast cancer was evaluated by analyzing the correlation between the expression of TP63 and clinical parameters. These parameters demonstrated that TP63 was significantly related to patient's age (**Figure 3A**), lymph node metastasis (**Figure 3B**), TNM stage (**Figure 3C**), and tumor size (**Figure 3D**).

TGF-β1 Promoted Autophagy in Breast Cancer by Targeting TP63

As shown in **Figure 4A**, the JASPAR database (http://jaspar.genereg.net/) predicted that TP63 was located as a transcription factor on the TGF-β1 promoter sequence, and there was a potential binding site between them. In order to illuminate the correlation between TGF-β1 and TP63, we detected the expression level of TP63 in breast cancer cells with TGF-β1 induced. We clearly observed that TGF-β1 inhibits TP63 in breast cancer cells (**Figure 4B**).

MDC staining was performed on MDA-MB-231 and MCF-7 cells to directly observe the autophagosomes. The results confirmed that TGF-β1 is related to the degree of autophagy. We can find that the two kinds of cells treated with TGF-β1 (5ng/ml, 10ng/ml) showed stronger fluorescent spots (**Figure 4C**) by MDC staining, that is, highly autophagy is activated in treated cells. Moreover, TGF-β1 inhibited P62 and TP63 protein levels in MDA-MB-231 (**Figure 4D**) and MCF-7 cells (**Figure 4E**), and increased Beclin1 protein levels. It is obvious that TGF-β1 enhanced the autophagy level in breast cancer cells by inhibiting TP63.

TGF-β1 Inhibited Apoptosis in Breast Cancer by Targeting TP63

In order to further explore the relationship between TGF-β1 and the ability of proliferation in breast cancer cells, TGF-β1 protein (5,

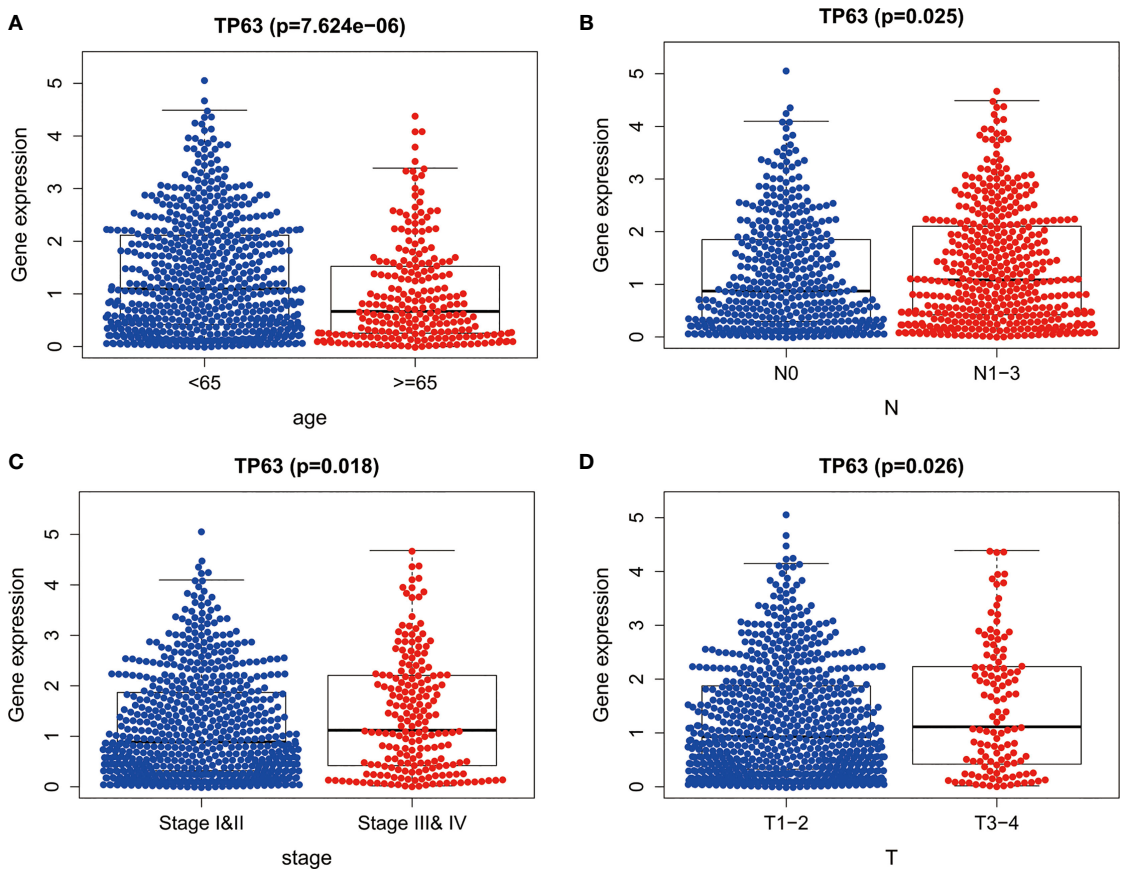

FIGURE 3 | The expression of TP63 between different clinical features of breast cancer. The P values of **(A)** age, **(B)** lymph node metastasis, **(C)** TNM stage and **(D)** tumor size between the two groups were all less than 0.05.

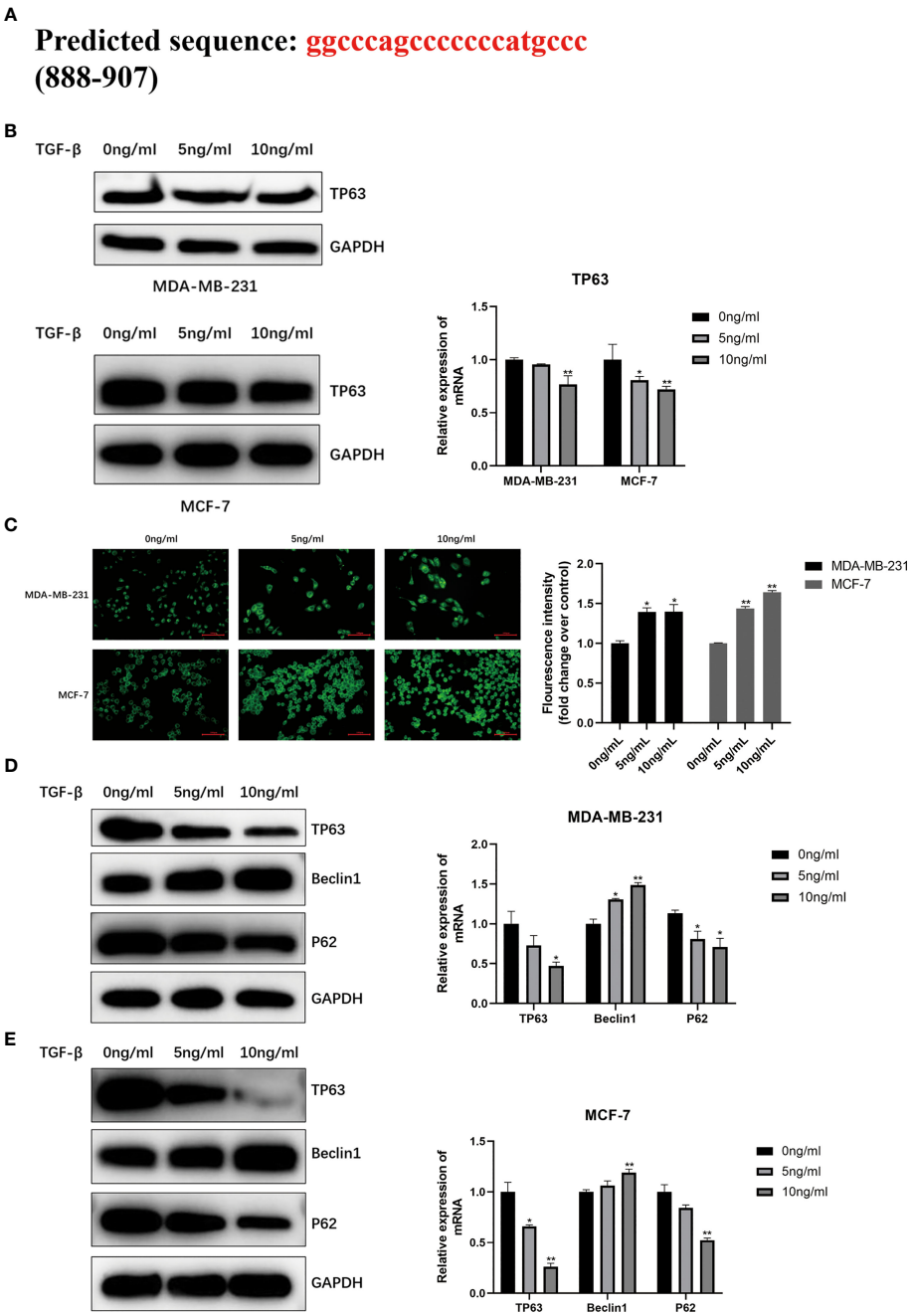

FIGURE 4 | **(A)** Predicted the TGF-β1 target TP63 potentially by using JASPAR database (http://jaspar.genereg.net/) and verified the TGF-β1 is negatively correlated with TP63 **(B)**. MDC staining was used to analyze autophagy **(C)**. When MDA-MB-231 cells and MCF-7 cells were induced by TGF-β1 for 24 hours, MDC staining was performed in the dark and observed under a fluorescence microscope immediately. Fluorescence intensity was quantified by ImageJ and shown as mean ± SD. The expression level of the autophagy-related proteins and TP63 in MDA-MB-231 cells **(D)** and MCF-7 cells **(E)** with TGF-β1 induced. GAPDH was used as an internal control. Quantitative analysis of TP63, Beclin1, and P62 are expressed as the mean ± SD (*$p < 0.05$, **$p < 0.01$).

10ng/ml) was acted on MDA-MB-231 and MCF-7 cells respectively. Compared with the control group, we observed that the number of cell colonies with TGF-β1 treatment was much smaller (**Figure 5A**). The cell proliferation abilities after 24, 48, 72h induced by TGF-β1 were tested by the CCK-8 method. As shown in **Figure 5**, TGF-β1 inhibited the proliferation of MDA-MB-231 (**Figure 5B**) and MCF-7 (**Figure 5C**) cells in a concentration and time-dependent manner.

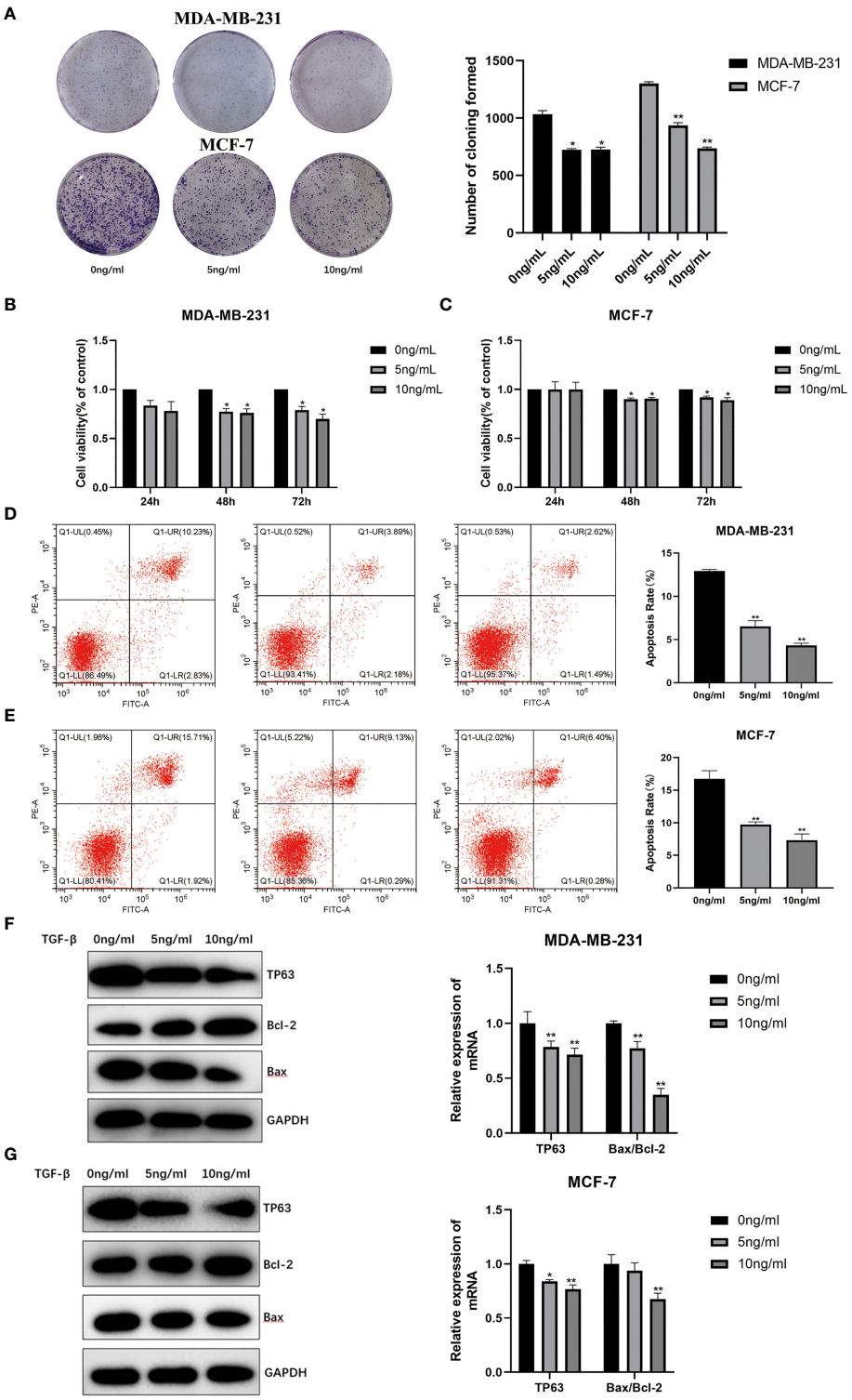

FIGURE 5 | **(A)** Proliferation ability of MDA-MB-231 and MCF-7 induced by TGF-β1 by plate cloning experiment. The effect of TGF-β1 on the proliferation of MDA-MB-231 cells **(B)** and MCF-7 **(C)** cells were analyzed by CCK-8 (*$p < 0.05$, **$p < 0.01$). Analysis of the effect of TGF-β1 on the apoptosis of MDA-MB-231 cells **(D)** and MCF-7 **(E)** cells by Annexin V-FITC/PI stain flow cytometry (*$p < 0.05$, **$p < 0.01$). The expression level of the apoptosis and TP63 proteins in MDR-MB-231 cells **(F)** and MCF-7 **(G)** cells with TGF-β1 induced. GAPDH was used as an internal control. Quantitative analysis of TP63, Bcl-2 and Bax are expressed as the mean ± SD. *, **$p < 0.01$ vs. control group.

The Annexin V-FITC/PI flow cytometric analysis was used to detect the apoptosis rates of MDA-MB-231 and MCF-7 cells with TGF-β1 treatment. The apoptotic rates of MDA-MB-231 cells (**Figure 5D**) with TGF-β1 treated in each group were (12.93 ± 0.18) %, (6.54 ± 0.66) %, (4.31 ± 0.28) %, and the apoptosis rates of MCF-7 cells (**Figure 5E**) with TGF-β1 treated in each group were (16.8 ± 1.23) %, (9.72 ± 0.42) %, (7.35 ± 0.94) %, respectively. From the results, we can find that the apoptosis rates of MDA-MB-231 and MCF-7 cells were inhibited by TGF-β1 ($p<0.05$). In terms of WB results, the expression level of TP63 and Bax were decreased, while the expression level of Bcl-2 gradually was increased with the increasing of TGF-β1 (**Figures 5F, G**). The results supposed that TGF-β1 can inhibit the ability of cell apoptosis by inhibiting TP63.

Prognostic Value of TP63 in Breast Cancer

Based on the Kaplan-Meier Plotter database (http://www.kmplot.com/analysis/), the prognostic potential of TP63 in breast cancer was explored. A total of 397 untreated breast cancer (BC) patients were included in the analysis. The results showed that the expression level of TP63 in breast cancer was positively correlated with the overall survival (OS) of patients [HR=0.41 (0.23-0.72), p=0.0013] (**Figure 6**). According to the different clinicopathological characteristics in the Kaplan-Meier Plotter database, the relationship between TP63 and the prognosis in breast cancer was explored. As shown in **Table 3**, it can be seen that TP63 is related to ER, HER2, subtype, Grade stage, and TP53 status in breast cancer patients, and the difference is statistically significant.

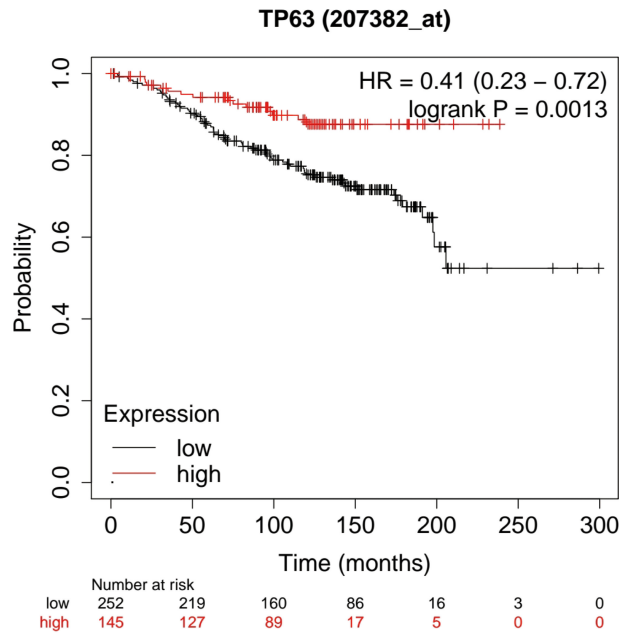

FIGURE 6 | Kaplan-Meier analysis was used to determine the prognostic role of TP63 in breast cancer. The prognostic potential of TP63 expression in breast cancer ($p < 0.05$).

DISCUSSION

Although the treatment for breast cancer has made great progress in cancer research, it is still a major health problem that plagues all mankind. In China and even all over the world, breast cancer is a common cancer among women and its morbidity and mortality are increasing gradually (26–29). Recently, it has been reported that autophagy is related to breast cancer invasion and metastasis (30), and even drug resistance (31, 32). Interestingly, there are numerous studies have found that autophagy can be considered as a new target for breast cancer treatment, but more in-depth researchs are still needed to clarify the specific mechanism of autophagy in the development of breast cancer. Breast cancer is a kind of highly heterogeneous type of cancer with high invasion and metastasis ability. The current standard systemic therapies (hormonal, cytotoxicity, and HER2 targeted therapy) are not suitable for every patient (33). Therefore, it is very necessary to find new targets for the treatment of breast cancer. The 5exploration of ARGs may provide a more adequate theoretical basis for breast cancer prognosis prediction and treatment.

From the current study, we firstly screened out prognostic-related ARGs based on the clinical information of 1085 breast cancer in the TCGA data by bioinformatics analysis. Using multivariate Cox regression analysis, we confirmed three ARGs (EIF4EBP1, IFNG, and TP63). These ARGs have shown a strong ability in the prognosis of breast cancer or other malignant tumors. EIF4EBP1 is a direct target of mTOR and a key effector of protein synthesis. Loss of EIF4EBP1 is associated with poor overall survival in patients with head and neck squamous cell carcinomas (HNSCC) (34). Also, EIF4EBP1 frequently increased in breast cancer, which is considered to be an indicator of poor prognosis and resistance to endocrine therapy (35). SK Ganapathi et al. reported that the expression level of IFNG in peripheral blood mononuclear cells (PBMCs) of patients with recurrent colorectal cancer (CRC) was significantly lower (36). It is reported that TP63 can predict the progression and survival of bladder cancer, kidney cancer, low-grade glioma, and skin cancer (37, 38). We successfully constructed a breast cancer prognostic risk model based on ARGs which can effectively evaluate the prognosis of breast cancer patients.

Based on the literature (39–41) and the clinical correlation analysis, we eventually screened out an autophagy-related gene-TP63. Adorno M et al. have reported that TGF-β1 promoted the invasion and metastasis of breast cancer by inhibiting the expression of TP63 (42). It has been reported that TGF-β may play an important role in the progression of breast cancer through ΔNp63 or inducing/inhibiting autophagy, and TGF-β-regulated miRNA network is crucial for regulating the expression of ΔNp63 in breast cancer progression (25, 43, 44). In addition, we predicted a binding site between TGF-β1 and TP63 by JASPAR database. WB results verified that TGF-β1 can inhibit the expression of TP63, and there were negatively correlated between TGF-β1 and TP63. This result was consistent with the previous research. The balance between autophagy and apoptosis is closely related to the tumor microenvironment (45–47). However, studies in regulating autophagy and apoptosis in

TABLE 3 | Correlation between TP63 expression and different clinical pathological factors by Kaplan-Meier plotter.

Clinicopathological characters	OS (Overall Survival)		
	N	HR	p value
Total	397	0.41(0.23-0.72)	0.0013
ER			
positive	259	0.25(0.1-0.58)	0.00049
negative	96	0.54(0.22-1.34)	0.18
unknown	42	–	–
HER2			
Positive	57	2.03(0.66-6.2)	0.21
negative	340	0.44(0.26-0.75)	0.0021
Intrinsic subtype			
basal	58	0.44(0.13-1.53)	0.18
luminal A	225	0.36(0.16-0.8)	0.0095
luminal B	95	0.26(0.07-0.88)	0.02
$HER2^+$	19	–	–
Grade			
1	95	0.32(0.08-1.25)	0.085
2	176	0.33(0.17-0.66)	0.00091
3	121	1.83(0.91-3.65)	0.084
unknown	5	–	–
TP53 status			
mutated	29	0.25(0.05-1.29)	0.073
wild type	111	0.2(0.06-0.65)	0.003
unknown	257	–	–

breast cancer about TGF-β1 and TP63 have not been reported in word. Therefore, the effects of TGF-β1 and TP63 on autophagy and apoptosis in breast cancer cells were explored in this study.

Chen Liang et al. demonstrated that TGF-β1 induced autophagic flux in pancreatic ductal adenocarcinoma (PDAC) (48). TGF-β1 activated cancer-associated fibroblasts to promote breast cancer invasion, metastasis, and epithelial-mesenchymal transition by autophagy (49). These studies showed that TGF-β1 can promote autophagy in the development of cancer. In our research, the autophagy level was determined by MDC staining and WB, which showed that the autophagy level of breast cancer cells was affected by TGF-β1 and was increased when TGF-β1 induced. We found that the autophagy levels of MDA-MB-231 and MCF-7 cells treated with TGF-β1 were improved, and there was a concentration-dependent relation between TGF-β1 and autophagy levels. Furthermore, WB results proved that the expression of TP63 was decreased with TGF-β1 induced. The above results proved that TGF-β1 can target TP63 to promote autophagy in breast cancer cells.

Autophagy and apoptosis are inseparable (50, 51). Therefore, TGF–β1 can also regulate tumor progression by affecting apoptosis. A study has suggested that TGF-β1 can influence cervical cancer cell proliferation and apoptosis and TGF-β is a potential target for cervical cancer therapeutics (52). TGF–β1 treatment protects tumor cells from various apoptotic stresses, including 5–fluorouracil, etoposide, and γ–irradiation in human colon cancer (53). TGF-β1 even plays an important role in the apoptosis of breast cancer (54). From the colony formation experiment, the number of cell clones in the experimental group treated with TGF-β1 was less than that in the control group. According to CCK-8 results, TGF-β1 had no effect on the proliferation ability of breast cancer cells until 48h. There was a time-dependent and concentration-dependent relation between TGF-β1 and the proliferation ability of breast cancer cells. In addition, we used flow cytometry to detect the apoptosis rates of MDA-MB-231 and MCF-7 cells after TGF-β1 treatment. The results of Annexin V-FITC/PI flow cytometric analysis showed that TGF-β1 inhibited the apoptosis level of MDA-MB-231 and MCF-7 cells. Similarly, TGF-β1 was determined to inhibit apoptosis of breast cancer cells by targeting TP63 from the WB results. In the future, we need to further explore about how autophagy and apoptosis regulating the tumor microenvironment *via* the TGF-β1/TP63 signaling pathway in breast cancer.

A large number of studies have reported that TP63 can be used as a prognostic factor for cancers such as salivary gland adenoid cystic carcinoma, anaplastic large cell lymphoma, and squamous cell carcinoma (55–58). The following analysis demonstrated that TP63 as an autophagy-related gene is a low-risk factor for the prognosis of breast cancer, that is, the lower the expression of TP63, the worse the prognosis of breast cancer. One point in our result is that TP63 was related to advanced Clinicopathological indicators from bioinformatics analysis. Possibly due to two different promoters of TP63 (P1 and P2), and two types of proteins are produced: TAp63 and ΔNp63. TP63 has two subtypes, but which one responsible for breast cancer is not specified. And also, breast cancer has many subtypes. In the bioinformatics analysis, it is not clearly that which subtype plays the important role in the database. In future studies, we will focus on this doubt. We explored that the prognostic value of TP63 in breast cancer by the Kaplan-Meier Plotter database. Therefore, TP63, as an important prognostic gene, may be expected to become a potential prognostic biomarker.

In summary, our study constructed a prognostic model related to autophagy in breast cancer, and TP63 was screened

out as a key factor in the prognostic model. TGF-β1 can promote autophagy and inhibit apoptosis on MDA-MB-231 and MCF-7 breast cancer cells by targeting TP63 to affect the occurrence and development of breast cancer. This may provide a new theoretical basis to the research on the mechanism of occurrence and development in breast cancer, as well as the value of prognostic prediction.

DATA AVAILABILITY STATEMENT

The original contributions presented in the study are included in the article/**Supplementary Material**. Further inquiries can be directed to the corresponding authors.

AUTHOR CONTRIBUTIONS

Data curation, YW. Formal analysis, YL. Funding acquisition, YW and XC. Investigation, ZW. Software, HL. Writing – review and editing, YW and XC. All authors contributed to the article and approved the submitted version.

FUNDING

This work was supported by the Natural Science Foundation of China (grant number 81902138), The Project of Public Welfare Technology Application of Zhejiang Province (grant number LGF22H200016) and the Hangzhou Medical and Health Science and Technology Project (grant no. B20220609).

SUPPLEMENTARY MATERIAL

The Supplementary Material for this article can be found online at: https://www.frontiersin.org/articles/10.3389/fonc.2022.865067/full#supplementary-material

Supplementary Figure S1 | The workflow for the construction of the prognostic risk model about autophagy-related genes in BC.

REFERENCES

1. DeSantis CE, Ma J, Gaudet MM, Newman LA, Miller KD, Goding Sauer A, et al. Breast Cancer Statistics, 2019. *CA Cancer J Clin* (2019) 69:438–51. doi: 10.3322/caac.21583
2. Siegel RL, Miller KD, Fuchs HE, Jemal A. Cancer Statistics, 2021. *CA Cancer J Clin* (2021) 71:7–33. doi: 10.3322/caac.21654
3. Fan L, Strasser-Weippl K, Li JJ, St Louis J, Finkelstein DM, Yu KD, et al. Breast Cancer in China. *Lancet Oncol* (2014) 15:e279–89. doi: 10.1016/S1470-2045(13)70567-9
4. Cheng Y, Li Z, Xie J, Wang P, Zhu J, Li Y, et al. MiRNA-224-5p Inhibits Autophagy in Breast Cancer Cells *via* Targeting Smad4. *Biochem Biophys Res Commun* (2018) 506:793–8. doi: 10.1016/j.bbrc.2018.10.150
5. Masso-Welch P, Girald Berlingeri S, King-Lyons ND, Mandell L, Hu J, Greene CJ, et al. LT-IIc, A Bacterial Type II Heat-Labile Enterotoxin, Induces Specific Lethality in Triple Negative Breast Cancer Cells by Modulation of Autophagy and Induction of Apoptosis and Necroptosis. *Int J Mol Sci* (2018) 20(1). doi: 10.3390/ijms20010085
6. Choi AM, Ryter SW, Levine B. Autophagy in Human Health and Disease. *N Engl J Med* (2013) 368:651–62. doi: 10.1056/NEJMra1205406
7. Glick D, Barth S, Macleod KF. Autophagy: Cellular and Molecular Mechanisms. *J Pathol* (2010) 221:3–12. doi: 10.1002/path.2697
8. Jiang Y, Woosley AN, Sivalingam N, Natarajan S, Howe PH. Cathepsin-B-Mediated Cleavage of Disabled-2 Regulates TGF-β-Induced Autophagy. *Nat Cell Biol* (2016) 18:851–63. doi: 10.1038/ncb3388
9. Cicchini M, Chakrabarti R, Kongara S, Price S, Nahar R, Lozy F, et al. Autophagy Regulator BECN1 Suppresses Mammary Tumorigenesis Driven by WNT1 Activation and Following Parity. *Autophagy* (2014) 10:2036–52. doi: 10.4161/auto.34398
10. Ren Y, Chen Y, Liang X, Lu Y, Pan W, Yang M. MiRNA-638 Promotes Autophagy and Malignant Phenotypes of Cancer Cells *via* Directly Suppressing DACT3. *Cancer Lett* (2017) 390:126–36. doi: 10.1016/j.canlet.2017.01.009
11. Vera-Ramirez L, Vodnala SK, Nini R, Hunter KW, Green JE. Autophagy Promotes the Survival of Dormant Breast Cancer Cells and Metastatic Tumour Recurrence. *Nat Commun* (2018) 9:1944. doi: 10.1038/s41467-018-04070-6
12. Fernández A, Ordóñez R, Reiter RJ, González-Gallego J, Mauriz JL. Melatonin and Endoplasmic Reticulum Stress: Relation to Autophagy and Apoptosis. *J Pineal Res* (2015) 59:292–307. doi: 10.1111/jpi.12264
13. Kaminskyy VO, Zhivotovsky B. Free Radicals in Cross Talk Between Autophagy and Apoptosis. *Antioxid Redox Signal* (2014) 21:86–102. doi: 10.1089/ars.2013.5746
14. Doherty J, Baehrecke EH. Life, Death and Autophagy. *Nat Cell Biol* (2018) 20:1110–7. doi: 10.1038/s41556-018-0201-5
15. Pistritto G, Trisciuoglio D, Ceci C, Garufi A, D'Orazi G. Apoptosis as Anticancer Mechanism: Function and Dysfunction of its Modulators and Targeted Therapeutic Strategies. *Aging (Albany NY)* (2016) 8:603–19. doi: 10.18632/aging.100934
16. Gordy C, He YW. The Crosstalk Between Autophagy and Apoptosis: Where Does This Lead? *Protein Cell* (2012) 3:17–27. doi: 10.1007/s13238-011-1127-x
17. Tang X, Shi L, Xie N, Liu Z, Qian M, Meng F, et al. SIRT7 Antagonizes TGF-β Signaling and Inhibits Breast Cancer Metastasis. *Nat Commun* (2017) 8:318. doi: 10.1038/s41467-017-00396-9
18. Tao MZ, Gao X, Zhou TJ, Guo QX, Zhang Q, Yang CW. Effects of TGF-β1 on the Proliferation and Apoptosis of Human Cervical Cancer Hela Cells *In Vitro*. *Cell Biochem Biophys* (2015) 73:737–41. doi: 10.1007/s12013-015-0673-x
19. Ghavami S, Cunnington RH, Gupta S, Yeganeh B, Filomeno KL, Freed DH, et al. Autophagy is a Regulator of TGF-β1-Induced Fibrogenesis in Primary Human Atrial Myofibroblasts. *Cell Death Dis* (2015) 6:e1696. doi: 10.1038/cddis.2015.36
20. Kiyono K, Suzuki HI, Matsuyama H, Morishita Y, Komuro A, Kano MR, et al. Autophagy is Activated by TGF-Beta and Potentiates TGF-Beta-Mediated Growth Inhibition in Human Hepatocellular Carcinoma Cells. *Cancer Res* (2009) 69:8844–52. doi: 10.1158/0008-5472.CAN-08-4401
21. He R, Wang M, Zhao C, Shen M, Yu Y, He L, et al. TFEB-Driven Autophagy Potentiates TGF-β Induced Migration in Pancreatic Cancer Cells. *J Exp Clin Cancer Res* (2019) 38:340. doi: 10.1186/s13046-019-1343-4
22. Zhang Y, Alexander PB, Wang XF. TGF-β Family Signaling in the Control of Cell Proliferation and Survival. *Cold Spring Harb Perspect Biol* (2017) 9(4). doi: 10.1101/cshperspect.a022145
23. Vasilaki E, Morikawa M, Koinuma D, Mizutani A, Hirano Y, Ehata S, et al. Ras and TGF-β Signaling Enhance Cancer Progression by Promoting the Δnp63 Transcriptional Program. *Sci Signal* (2016) 9:ra84. doi: 10.1126/scisignal.aag3232
24. Gatti V, Bongiorno-Borbone L, Fierro C, Annicchiarico-Petruzzelli M, Melino G, Peschiaroli A, et al. P63 at the Crossroads Between Stemness and Metastasis in Breast Cancer. *Int J Mol Sci* (2019) 20(11). doi: 10.3390/ijms20112683
25. Sundqvist A, Vasilaki E, Voytyuk O, Bai Y, Morikawa M, Moustakas A, et al. Tgfβ and EGF Signaling Orchestrates the AP-1- and P63 Transcriptional Regulation of Breast Cancer Invasiveness. *Oncogene* (2020) 39:4436–49. doi: 10.1038/s41388-020-1299-z
26. Anastasiadi Z, Lianos GD, Ignatiadou E, Harissis HV, Mitsis M. Breast Cancer in Young Women: An Overview. *Updates Surg* (2017) 69:313–7. doi: 10.1007/s13304-017-0424-1

27. DeSantis C, Ma J, Bryan L, Jemal A. Breast Cancer Statistics, 2013. *CA Cancer J Clin* (2014) 64:52–62. doi: 10.3322/caac.21203
28. Leignadier J, Dalenc F, Poirot M, Silvente-Poirot S. Improving the Efficacy of Hormone Therapy in Breast Cancer: The Role of Cholesterol Metabolism in SERM-Mediated Autophagy, Cell Differentiation and Death. *Biochem Pharmacol* (2017) 144:18–28. doi: 10.1016/j.bcp.2017.06.120
29. Liang Y, Zhang H, Song X, Yang Q. Metastatic Heterogeneity of Breast Cancer: Molecular Mechanism and Potential Therapeutic Targets. *Semin Cancer Biol* (2020) 60:14–27. doi: 10.1016/j.semcancer.2019.08.012
30. Ostendorf BN, Tavazoie SF. Autophagy Suppresses Breast Cancer Metastasis. *Dev Cell* (2020) 52:542–4. doi: 10.1016/j.devcel.2020.02.005
31. Li ZL, Zhang HL, Huang Y, Huang JH, Sun P, Zhou NN, et al. Autophagy Deficiency Promotes Triple-Negative Breast Cancer Resistance to T Cell-Mediated Cytotoxicity by Blocking Tenascin-C Degradation. *Nat Commun* (2020) 11:3806. doi: 10.1038/s41467-020-17395-y
32. El-Ashmawy NE, Al-Ashmawy GM, Amr EA, Khedr EG. Inhibition of Lovastatin- and Docosahexaenoic Acid-Initiated Autophagy in Triple Negative Breast Cancer Reverted Resistance and Enhanced Cytotoxicity. *Life Sci* (2020) 259:118212. doi: 10.1016/j.lfs.2020.118212
33. Sachs N, de Ligt J, Kopper O, Gogola E, Bounova G, Weeber F, et al. A Living Biobank of Breast Cancer Organoids Captures Disease Heterogeneity. *Cell* (2018) 172:373–86.e10. doi: 10.1016/j.cell.2017.11.010
34. Wang Z, Feng X, Molinolo AA, Martin D, Vitale-Cross L, Nohata N, et al. 4e-BP1 Is a Tumor Suppressor Protein Reactivated by mTOR Inhibition in Head and Neck Cancer. *Cancer Res* (2019) 79:1438–50. doi: 10.1158/0008-5472.CAN-18-1220
35. Rutkovsky AC, Yeh ES, Guest ST, Findlay VJ, Muise-Helmericks RC, Armeson K, et al. Eukaryotic Initiation Factor 4E-Binding Protein as an Oncogene in Breast Cancer. *BMC Cancer* (2019) 19:491. doi: 10.1186/s12885-019-5667-4
36. Ganapathi SK, Eggs AD, Hodgson SV, Kumar D. Expression and DNA Methylation of TNF, IFNG and FOXP3 in Colorectal Cancer and Their Prognostic Significance. *Br J Cancer* (2014) 111:1581–9. doi: 10.1038/bjc.2014.477
37. Bankhead A 3rd, McMaster T, Wang Y, Boonstra PS, Palmbos PL. TP63 Isoform Expression is Linked With Distinct Clinical Outcomes in Cancer. *EBioMedicine* (2020) 51:102561. doi: 10.1016/j.ebiom.2019.11.022
38. Smirnov A, Anemona L, Novelli F, Piro CM, Annicchiarico-Petruzzelli M, Melino G, et al. P63 Is a Promising Marker in the Diagnosis of Unusual Skin Cancer. *Int J Mol Sci* (2019) 20(22). doi: 10.3390/ijms20225781
39. Kumar S, Wilkes DW, Samuel N, Blanco MA, Nayak A, Alicea-Torres K, et al. ΔNp63-Driven Recruitment of Myeloid-Derived Suppressor Cells Promotes Metastasis in Triple-Negative Breast Cancer. *J Clin Invest* (2018) 128:5095–109. doi: 10.1172/JCI99673
40. Mendoza-Rodríguez MG, Ayala-Sumuano JT, García-Morales L, Zamudio-Meza H, Pérez-Yepez EA, Meza I. IL-1β Inflammatory Cytokine-Induced TP63 Isoform ΔNp63α Signaling Cascade Contributes to Cisplatin Resistance in Human Breast Cancer Cells. *Int J Mol Sci* (2019) 20. doi: 10.3390/ijms20020270
41. Ding L, Su Y, Fassl A, Hinohara K, Qiu X, Harper NW, et al. Perturbed Myoepithelial Cell Differentiation in BRCA Mutation Carriers and in Ductal Carcinoma in Situ. *Nat Commun* (2019) 10:4182. doi: 10.1158/1557-3125.ADVBC17-B62
42. Adorno M, Cordenonsi M, Montagner M, Dupont S, Wong C, Hann B, et al. A Mutant-P53/Smad Complex Opposes P63 to Empower TGFbeta-Induced Metastasis. *Cell* (2009) 137:87–98. doi: 10.1016/j.cell.2009.01.039
43. Klein K, Habiger C, Iftner T, Stubenrauch F. A TGF-β- and P63-Responsive Enhancer Regulates IFN-κ Expression in Human Keratinocytes. *J Immunol* (2020) 204:1825–35. doi: 10.4049/jimmunol.1901178
44. Bui NHB, Napoli M, Davis AJ, Abbas HA, Rajapakshe K, Coarfa C, et al. Spatiotemporal Regulation of Δnp63 by Tgfβ-Regulated miRNAs Is Essential for Cancer Metastasis. *Cancer Res* (2020) 80:2833–47. doi: 10.1158/0008-5472.CAN-19-2733
45. Zhao X, Su L, He X, Zhao B, Miao J. Long Noncoding RNA CA7-4 Promotes Autophagy and Apoptosis *via* Sponging MIR877-3P and MIR5680 in High Glucose-Induced Vascular Endothelial Cells. *Autophagy* (2020) 16:70–85. doi: 10.1080/15548627.2019.1598750
46. Chung Y, Lee J, Jung S, Lee Y, Cho JW, Oh YJ. Dysregulated Autophagy Contributes to Caspase-Dependent Neuronal Apoptosis. *Cell Death Dis* (2018) 9:1189. doi: 10.1038/s41419-018-1229-y
47. Wu J, Zhou Y, Yuan Z, Yi J, Chen J, Wang N, et al. Autophagy and Apoptosis Interact to Modulate T-2 Toxin-Induced Toxicity in Liver Cells. *Toxins (Basel)* (2019) 11(1). doi: 10.3390/toxins11010045
48. Liang C, Xu J, Meng Q, Zhang B, Liu J, Hua J, et al. TGFB1-Induced Autophagy Affects the Pattern of Pancreatic Cancer Progression in Distinct Ways Depending on SMAD4 Status. *Autophagy* (2020) 16:486–500. doi: 10.1080/15548627.2019.1628540
49. Huang M, Fu M, Wang J, Xia C, Zhang H, Xiong Y, et al. TGF-β1-Activated Cancer-Associated Fibroblasts Promote Breast Cancer Invasion, Metastasis and Epithelial-Mesenchymal Transition by Autophagy or Overexpression of FAP-α. *Biochem Pharmacol* (2021), 114527. doi: 10.1016/j.bcp.2021.114527
50. Su Z, Yang Z, Xu Y, Chen Y, Yu Q. Apoptosis, Autophagy, Necroptosis, and Cancer Metastasis. *Mol Cancer* (2015) 14:48. doi: 10.1186/s12943-015-0321-5
51. Yoshida GJ. Therapeutic Strategies of Drug Repositioning Targeting Autophagy to Induce Cancer Cell Death: From Pathophysiology to Treatment. *J Hematol Oncol* (2017) 10:67. doi: 10.1186/s13045-017-0436-9
52. Cao Z, Zhang G, Xie C, Zhou Y. MiR-34b Regulates Cervical Cancer Cell Proliferation and Apoptosis. *Artif Cells Nanomed Biotechnol* (2019) 47:2042–7. doi: 10.1080/21691401.2019.1614013
53. Moon JR, Oh SJ, Lee CK, Chi SG, Kim HJ. TGF-β1 Protects Colon Tumor Cells From Apoptosis Through XAF1 Suppression. *Int J Oncol* (2019) 54:2117–26. doi: 10.3892/ijo.2019.4776
54. Moses H, Barcellos-Hoff MH. TGF-Beta Biology in Mammary Development and Breast Cancer. *Cold Spring Harb Perspect Biol* (2011) 3:a003277. doi: 10.1101/cshperspect.a003277
55. Ferrarotto R, Mitani Y, McGrail DJ, Li K, Karpinets TV, Bell D, et al. Proteogenomic Analysis of Salivary Adenoid Cystic Carcinomas Defines Molecular Subtypes and Identifies Therapeutic Targets. *Clin Cancer Res* (2021) 27:852–64. doi: 10.1158/1078-0432.CCR-20-1192
56. Parrilla Castellar ER, Jaffe ES, Said JW, Swerdlow SH, Ketterling RP, Knudson RA, et al. ALK-Negative Anaplastic Large Cell Lymphoma is a Genetically Heterogeneous Disease With Widely Disparate Clinical Outcomes. *Blood* (2014) 124:1473–80. doi: 10.1182/blood-2014-04-571091
57. Yi M, Tan Y, Wang L, Cai J, Li X, Zeng Z, et al. TP63 Links Chromatin Remodeling and Enhancer Reprogramming to Epidermal Differentiation and Squamous Cell Carcinoma Development. *Cell Mol Life Sci* (2020) 77:4325–46. doi: 10.1007/s00018-020-03539-2
58. Li LY, Yang Q, Jiang YY, Yang W, Jiang Y, Li X, et al. Interplay and Cooperation Between SREBF1 and Master Transcription Factors Regulate Lipid Metabolism and Tumor-Promoting Pathways in Squamous Cancer. *Nat Commun* (2021) 12:4362. doi: 10.1038/s41467-021-24656-x

Conflict of Interest: The authors declare that the research was conducted in the absence of any commercial or financial relationships that could be construed as a potential conflict of interest.

Publisher's Note: All claims expressed in this article are solely those of the authors and do not necessarily represent those of their affiliated organizations, or those of the publisher, the editors and the reviewers. Any product that may be evaluated in this article, or claim that may be made by its manufacturer, is not guaranteed or endorsed by the publisher.

Copyright © 2022 Wang, Lu, Wang, Li and Chen. This is an open-access article distributed under the terms of the Creative Commons Attribution License (CC BY). The use, distribution or reproduction in other forums is permitted, provided the original author(s) and the copyright owner(s) are credited and that the original publication in this journal is cited, in accordance with accepted academic practice. No use, distribution or reproduction is permitted which does not comply with these terms.

frontiers | Frontiers in Oncology

ORIGINAL RESEARCH
published: 07 June 2022
doi: 10.3389/fonc.2022.885656

Targeting MDK Abrogates IFN-γ-Elicited Metastasis in Cancers of Various Origins

Luyu Zheng[1†], Qun Liu[2†], Ruijun Li[1], Shibin Chen[1], Jingyu Tan[1], Lina Li[1], Xichen Dong[1], Changzhi Huang[3], Tao Wen[1*] and Jian Liu[1,4*]*

[1] Medical Research Center, Beijing Chao-Yang Hospital, Capital Medical University, Beijing, China, [2] Department of Obstetrics and Gynaecology, Beijing Anzhen Hospital, Capital Medical University, Beijing, China, [3] State Key Laboratory of Molecular Oncology, Beijing Key Laboratory for Carcinogenesis and Cancer Prevention, Department of Etiology and Carcinogenesis, National Cancer Center/Cancer Hospital, Chinese Academy of Medical Sciences and Peking Union Medical College, Beijing, China, [4] Department of Oncology, Beijing Chao-Yang Hospital Capital Medical University, Beijing, China

IFN-γ is a pleiotropic cytokine with immunomodulatory and tumoricidal functions. It has been used as an anti-tumor agent in adjuvant therapies for various cancers. Paradoxically, recent advances have also demonstrated pro-tumorigenic effects of IFN-γ, especially in promoting cancer metastasis, with the mechanism remains unclear. This will undoubtedly hinder the application of IFN-γ in cancer treatment. Here, we verified that IFN-γ treatment led to activation of the epithelial-to-mesenchymal transition (EMT) programme and metastasis in cell lines of various cancers, including the kidney cancer cell line Caki-1, the lung cancer cell line A549, the cervical carcinoma cell line CaSki, the breast cancer cell line BT549 and the colon cancer cell line HCT116. We further disclosed that midkine (MDK), an emerging oncoprotein and EMT inducer, is a common responsive target of IFN-γ in these cell lines. Mechanistically, IFN-γ upregulated MDK *via* STAT1, a principle downstream effector in the IFN-γ signalling. MDK is elevated in the majority of cancer types in the TCGA database, and its overexpression drove EMT activation and cancer metastasis in all examined cell lines. Targeting MDK using a specific MDK inhibitor (iMDK) broadly reversed IFN-γ-activated EMT, and subsequently abrogated IFN-γ-triggered metastasis. Collectively, our data uncover a MDK-dependent EMT inducing mechanism underlying IFN-γ-driven metastasis across cancers which could be attenuated by pharmacological inhibition of MDK. Based on these findings, we propose that MDK may be used as a potential therapeutic target to eliminate IFN-γ-elicited pro-metastatic adverse effect, and that combined MDK utilization may expand the application of IFN-γ in cancer and improve the clinical benefits from IFN-γ-based therapies.

Keywords: cancer, IFN-γ, MDK, epithelial-to-mesenchymal transition, metastasis

OPEN ACCESS

Edited by:
Tao Sun,
Nankai University, China

Reviewed by:
Yi Zhang,
First Affiliated Hospital of Zhengzhou University, China
Junyan Tao,
University of Pittsburgh, United States
Ke Li,
Peking Union Medical College Graduate School, China

***Correspondence:**
Jian Liu
liujian2004811@126.com
Tao Wen
wentao5281@163.com
Changzhi Huang
huangcz@cicams.ac.cn

†These authors have contributed equally to this work

Specialty section:
This article was submitted to Pharmacology of Anti-Cancer Drugs, a section of the journal Frontiers in Oncology

Received: *28 February 2022*
Accepted: *18 May 2022*
Published: *07 June 2022*

Citation:
Zheng L, Liu Q, Li R, Chen S, Tan J, Li L, Dong X, Huang C, Wen T and Liu J (2022) Targeting MDK Abrogates IFN-γ-Elicited Metastasis in Cancers of Various Origins. Front. Oncol. 12:885656. doi: 10.3389/fonc.2022.885656

INTRODUCTION

Interferons (IFNs) constitute a family of cytokines that have antiviral, antiproliferative and immunomodulatory properties (1). There are three main classes of cytokines in the IFN family: IFN-I (IFN-α, β, ϵ, κ, and ω), IFN-II (IFN-γ), and IFN-III (IFN-λ1, λ2, λ3, and λ4) (2). These cytokines play pivotal roles in host defense against viral and bacterial infections, as well as immunosurveillance for malignant cells (3).

IFN-γ, encoded by the gene *IFNG*, is the only member of IFN-II. It is a pleiotropic cytokine with a long history of clinical trials in cancer treatment (4, 5). Since the first clinical trial conducted in 1985 (6), the therapeutic application of IFN-γ has been tested in a variety of malignancies, including melanoma, leukemia, ovarian cancer, renal cell carcinoma, hepatocellular carcinoma, lung cancer, breast cancer, bladder cancer and colorectal cancer (7). Clinical benefits derived from IFN-γ-based therapies have been reported in several cancers (8–10), highlighting the therapeutic value of IFN-γ in combating cancers.

IFN-γ exerts anti-tumor effects by boosting antitumor immunity and by direct effects on cancer cells (1, 11). IFN-γ enhances the activity of cytotoxic CD8 T cells, NK cells, Th1 cells, dendritic cells and macrophages; stimulates the expression of the major histocompatibility complex (MHC) class I and II molecules in tumor cells and APCs; promotes differentiation of macrophages towards a pro-inflammatory (M1-like) phenotype; and bridges the innate and adaptive immune responses (3, 12, 13). IFN-γ also exerts direct cytotoxic effects on neoplastic cells through anti-proliferative, anti-angiogenic and pro-apoptotic mechanisms (7, 14, 15).

Despite these anti-tumor activities, IFN-γ has been paradoxically reported to increase the risk of tumor metastasis (16–22). This pro-tumorigenic activity has been reported in colon adenocarcinoma (16), non-small cell lung cancer (20), prostate cancer (17), renal cancer (18), triple-negative breast cancer (21), and melanoma (19, 22) *via* multiple mechanisms. However, the mechanisms underlying IFN-γ-induced metastasis remain unclear, and whether there is a shared mechanism mediating IFN-γ-induced metastasis in cancers of different origins is still unknown.

Here, we reveal, for the first time, that the EMT inducer MDK, is a common responsive target of IFN-γ in all examined five cancer cell lines, and that MDK confers the pro-metastatic function of IFN-γ in these cell lines by activating the EMT programme; while pharmacologically targeting MDK using a specific inhibitor globally attenuated IFN-γ treatment-induced EMT and metastasis in all examined cancers. We thus propose that blocking the pro-tumorigenic activities of IFN-γ using MDK inhibitors may help to improve the clinical benefits from IFN-γ-based therapies.

MATERIALS AND METHODS

Cell Lines and Culture

The human renal cancer cell line Caki-1, human lung cancer cell line A549, human colorectal adenocarcinoma cell line HCT116, cervical cancer cell line CaSki, human breast cancer cell line BT549 and human embryonic kidney cell line HEK293T were acquired from National Collection of Authenticated Cell Cultures (Beijing, China). Caki-1, A549 and HCT116 cells were maintained in McCoy's 5A medium modified (KeyGEN BioTECH, Jiangsu, China). CaSki and BT549 cells were cultured in RPMI-1640 medium (SIGMA, Vienna, Austria). HEK293T were maintained in DMEM medium (Gibco, California, USA). All mediums contained 10% fetal bovine serum (FBS, Ausbian, Australia) and 1% penicillin–streptomycin mixture (Solarbio, Beijing, China). All cell lines were incubated at 37°C with 5% CO_2 in a humidified incubator.

Antibodies and Reagents

MDK antibody (1:1000 dilution, 11009-1-AP) was purchased from Proteintech Group Inc (Rosemont, IL, USA). E-cadherin antibody (1:1000 dilution, 3195T), ZO1 antibody (1:1000 dilution, 8193T), Vimentin antibody (1:1500 dilution, 5741T) and Snail antibody (1:500 dilution, 3879T) were from Cell Signaling Technology (Danvers, Massachusetts, USA). STAT1 antibody (1:5000 dilution, ab109320) and phospho-STAT1 (phosphor Y701) antibody (1:1000 dilution, ab109457) were purchased from Abcam (Cambridge, UK). β-actin antibody (1:1000 dilution, AF5001) was from Beyotime Biotechnology (Shanghai, China). Recombinant human IFN-γ was acquired from PeproTech (Rocky Hill, NJ, USA) and used at a concentration of 50 ng/ml for 48h. The MDK inhibitor iMDK was bought from Merck Millipore (Darmstadt, Germany) and diluted to a final concentration of 100nM in growth mediums. The STAT1 inhibitor Fludarabine was purchased from Med Chem Express (New Jersey, USA) and used at a concentration of 5 μM for 48h.

RNA Isolation and Quantitative Real-Time PCR (qRT-PCR)

Total RNA was extracted using TRIeasy reagent (Yeasen Biotechnology, Shanghai, China) according to the manufacturer's instruction. The concentration and purity of RNA were determined by Nanodrop 1000. The ratio of OD 260/OD 280 falling between 1.8 and 2.0 indicates acceptable values. Reverse transcription was achieved with a total of 1 μg RNA using the cDNA Synthesis SuperMix (Yeasen Biotechnology, Shanghai, China). The primers (5′-3′) synthesized by Rui Biotech (Beijing, China) were listed in **Table S1**. QRT-PCR was performed using qPCR SYBR Green Master Mix (Yeasen Biotechnology, Shanghai, China). Each sample was run in 3 duplicate wells, and the relative RNA expression levels between different samples were analyzed by $2^{-\Delta\Delta Ct}$ method, with β-actin as an internal control.

Lentivirus Production and MDK Overexpression

The human MDK overexpression lentiviral vector (YOE-LV004-hMDK) with neomycin resistance and the corresponding control vector (YOE-LV004-Ctrl) were purchased form UBIGENE (Guangzhou, China). Lentivirus was produced in HEK293T cells by co-transfecting the lentiviral vector with the psPAX2 and pMD2G packaging vectors using Lipofectamine 3000

(Invitrogen, Carlsbad, CA, USA). Caki-1, A549, HCT116, CaSki and BT549 cells were infected with the packaged lentiviruses with polybrene, and then selected with G418 (Solarbio, Beijing, China) at a concentration of 400 μg/ml. The empty plasmid (YOE-LV004-Ctrl) was used as a control.

Transwell Assay

Transwell assays were used to assess the invasion and migration abilities of cancer cells. Briefly, 1×10^5 cells in serum-free medium were seeded into the upper chamber of transwell plates (Corning, NY, USA), while the lower chamber was added with 10% FBS medium. For invasion assay, the transwell chambers were pre-coated with Matrigel (BD Biosciences, Palo Alto, CA). Approximately 16-24 h after seeding, the cells remaining on the upper chamber were carefully wiped off with cotton swabs, while the migrated cells were fixed in 4% paraformaldehyde for 20 minutes and then stained in 0.2% crystal violet solution for 20-25 minutes. After cleaning the chamber with wash buffer for three times, the migrated cells were counted under an inverted bright-field microscope.

Western Blotting Assay

Cell lysates were prepared in RIPA lysis buffer (Beyotime Biotechnology, Shanghai, China) supplemented with 1x protease inhibitor cocktail (Beyotime Biotechnology) and 1x phenylmethylsulfonyl fluoride (PMSF, APPLYGEN, Beijing, China). Protein concentrations were measured with a BCA assay kit (KeyGEN BioTECH, Jiangsu, China). The protein samples (50 μg) were boiled at 100°C for 10 minutes, separated by 10-12% SDS-PAGE, and then transferred onto PVDF membranes (Merck Millipore, MA, USA) *via* semi-dry transfer unit. After blocked in 5% skim milk at room temperature for 1h, the membranes were incubated overnight at 4°C with primary antibodies, and then incubated with anti-rabbit or mouse IgG-HRP secondary antibody for 2h at room temperature. Membranes were visualized using Baygene Chemilmaging system (Baygene Biotech, Beijing, China) with Super ECL Detection Reagent (Yeasen Biotechnology, Shanghai, China).

Statistical Analysis

All statistical analysis was performed in GraphPad Prism 8.0 (GraphPad Software, La Jolla, CA, USA). Unpaired and multiple T-test were used to assess the differences between control and experimental groups. P value < 0.05 was considered statistically significant. The results were presented as mean ± standard deviation (SD). *P<0.05, **P<0.01, ***P<0.001, ****P<0.0001.

RESULTS

IFN-γ Treatment Enhances EMT and Metastasis in Various Tumors

Interferon-gamma (IFN-γ) is a pleiotropic cytokine with antiproliferative, pro-apoptotic and immunomodulatory functions. IFN-γ has been used to treat a variety of malignancies in pre-clinical and clinical trials; however, limited benefits have been achieved, presumably due to its pro-tumor adverse effects, including eliciting metastasis (23). Prior to deciphering the mechanism underlying IFN-γ-induced cancer metastasis, we first verified the pro-metastatic effect of IFN-γ in five cell lines of different human cancers (**Figure 1A**): the kidney cancer cell line Caki-1, the lung cancer cell line A549, the cervical carcinoma cell line CaSki, the breast cancer cell line BT549, and the colon cancer cell line HCT116. Transwell assays demonstrated that IFN-γ exposure obviously increased the migration and invasion abilities of all the five cancer cell lines (**Figure 1A**). This is in line with the previous findings in colon cancer (16), prostate cancer (17), non-small cell lung cancer (20), and melanoma (19), suggesting that IFN-γ treatment could globally enhance metastasis of cancers.

EMT is a common mechanism driving metastasis of cancers (24). We then examined the role of IFN-γ in the EMT programme. Western blotting results showed that IFN-γ treatment led to decreased expression of epithelial markers, including ZO-1 and E-cadherin, and concomitant upregulation of mesenchymal markers, such as Vimentin, Snail and Slug in the above cell lines at the protein level (**Figure 1B**). The alterations in expression of EMT markers were further verified at the mRNA level (**Figure 1C**). These data indicate that IFN-γ may promote metastasis by activating the EMT programme in cancers.

IFN-γ Exposure Promotes MDK Expression in Cancers

MDK is a heparin-binding growth factor well-documented to promote EMT and cancer metastasis (25). Though there is no evidence suggesting the regulatory relationship between IFN-γ and MDK in the cancerous context, we found a previous report indicating that the MDK expression in lymphocytes is upregulated in response to IFN-γ treatment (26). This gave rise to the speculation that whether IFN-γ treatment in cancers would result in MDK activation, thereby triggering EMT and metastasis. To verify this hypothesis, we treated different cancer cell lines with IFN-γ (50 ng/ml) and then examined the alterations of MDK expression in the mRNA and protein levels. Real-time qPCR assays demonstrated a dramatic upregulation of MDK mRNA by IFN-γ in all examined cancer cell lines (**Figure 2A**), including the kidney cancer Caki-1, the lung cancer A549, the cervical carcinoma CaSki, the breast cancer BT549, and the colon cancer HCT116, which was further validated by Western blotting at the protein level (**Figure 2B**), suggesting that this is a shared regulation across different types of cancers.

To further validate the IFN-γ-MDK regulatory axis, we treated the HCT116 cancer cell line with different concentrations of IFN-γ and verified that activation of MDK by IFN-γ was dose-dependent at both the mRNA (**Figure 3A**) and protein (**Figure 3B**) levels. Furthermore, IFN-γ treatment also caused an obviously time-dependent upregulation of MDK at both the mRNA (**Figure 3C**) and protein (**Figure 3D**) levels, as well as time-dependent activation of EMT evidenced by time-dependent downregulation of E-cad and ZO-1 but upregulation of Slug and Snail (**Figures 3D, E**).

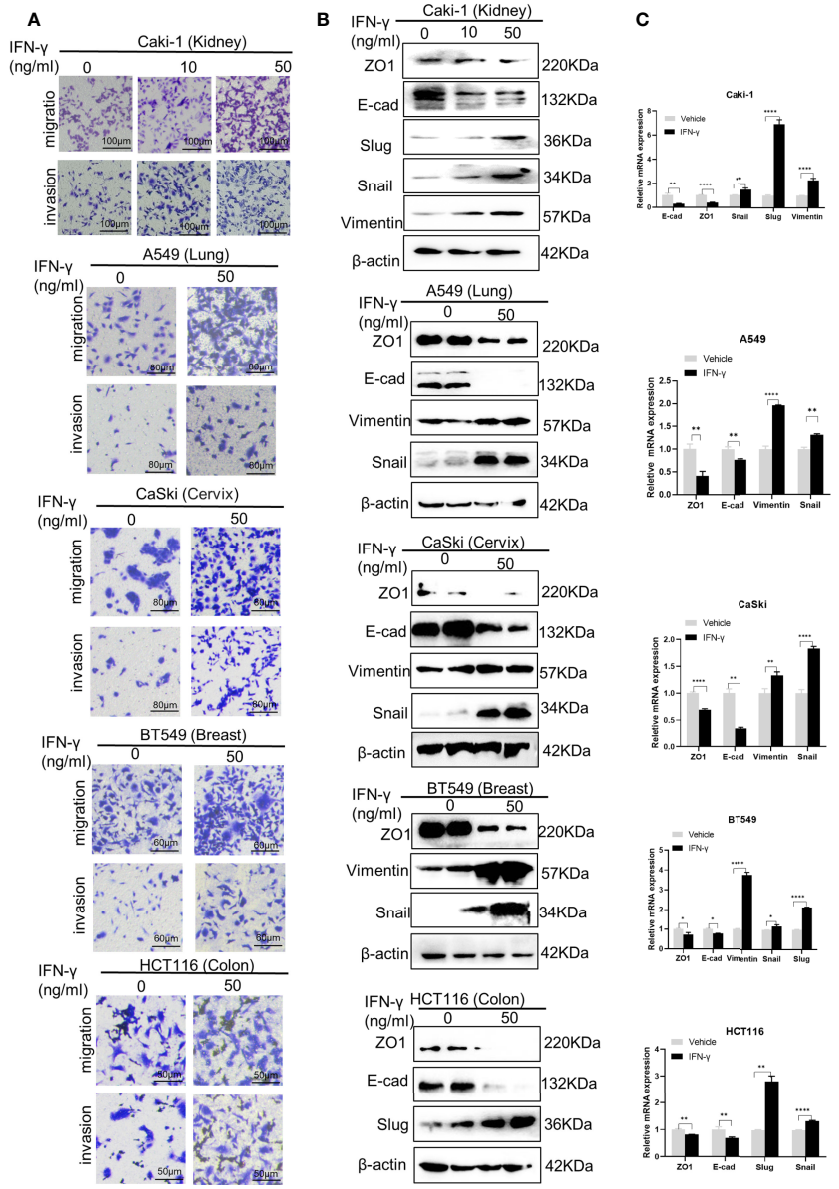

FIGURE 1 | IFN-γ treatment enhances epithelial-mesenchymal transition (EMT) and metastasis in various tumors. **(A)** Transwell assays to detect the migration and invasion abilities of different cancer cell lines without and with IFN-γ treatment (50 ng/ml, 48 h). **(B)** Western blotting assays to examine the effect of IFN-γ treatment (50 ng/ml, 48 h) on expression of EMT markers at the protein level. **(C)** RT-qPCR assays to detect the changes in expression of EMT markers at the mRNA level after IFN-γ treatment (50 ng/ml, 48 h). Data are shown as the mean ± standard deviation (SD). *P < 0.05, **P < 0.01, ****P < 0.0001.

IFN-γ Activates MDK in a STAT1-Dependent Manner

STAT1 is a key downstream effector in the IFN-γ signalling (2), which leads us to speculate that the IFN-γ-MDK regulation may rely on IFN-γ-induced STAT1 activation. This speculation was preliminarily supported by the significant correlations between STAT1 and MDK in various cancers in the TCGA database (**Figure 4A**). Moreover, as reported, real-time qPCR and Western blotting assays showed that IFN-γ exposure caused a significant upregulation in levels of STAT1 abundance and phosphorylation (**Figure 4B**). Then we blocked STAT1 activation using a specific STAT1 inhibitor Fludarabine and assessed its influence on IFN-γ activation of MDK. Notably, STAT1 inhibitor remarkably diminished IFN-γ-induced STAT1 activation, and substantially abrogated IFN-γ-induced MDK activation at the mRNA level in all examined cell lines (**Figure 4C**), which was further validated at the protein level by Western blotting analyses (**Figure 4D**). All these demonstrate that IFN-γ activates MDK *via* STAT1 in cancer cells.

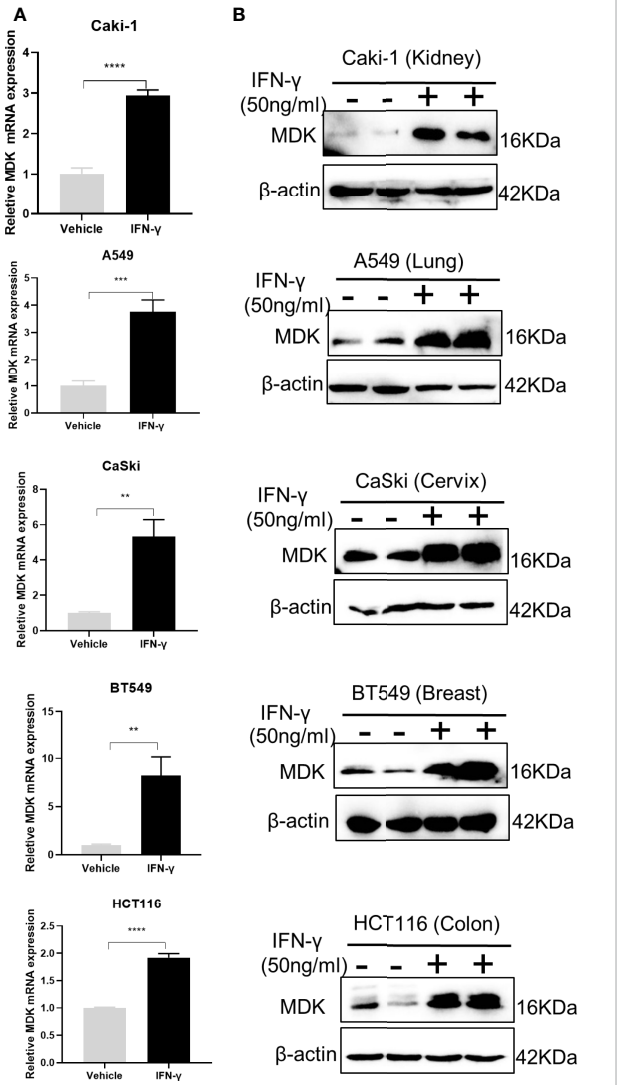

FIGURE 2 | IFN-γ treatment promotes MDK expression in different cancers. **(A)** RT-qPCR assays to detect the expression of MDK in five cancer cell lines without and with IFN-γ treatment (50 ng/ml, 48 h). **(B)** Western blotting assay to determine the influence of IFN-γ treatment (50 ng/ml, 48 h) on MDK protein levels in five cancer cell lines. Data are shown as the mean ± standard deviation (SD). **P < 0.01, ***P < 0.001, ****P < 0.0001.

MDK Promotes Cancer Metastasis by Activating the EMT Programme

To further explore the possibility that MDK is a shared mechanism underlying IFN-γ-triggered metastasis in various cancers, we first examined the effect of MDK on cancer metastasis in the above cancer cell lines. Transwell assays clearly showed that MDK overexpression (**Figure 5A**) enhanced the migration and invasion capacities of all five cancer cell lines (**Figure 5B**). In accordance, MDK overexpression resulted in activation of the EMT programme, as evidenced by loss of epithelial markers, and concomitant gain of mesenchymal markers at the both protein (**Figure 5C**) and mRNA (**Figure 5D**) levels. To further validate that MDK is necessary for cancer metastasis, we silenced MDK expression using a specific MDK inhibitor iMDK, which demonstrated high efficiency in decreasing endogenous MDK expression (**Figure 5E**) and subsequent EMT activation in all five cell lines (**Figure 5F**). In accordance, iMDK suppressed the migration and invasion in all five cell lines in transwell assays (**Figure 5G**). In line with its oncogenic role, MDK is elevated in the majority of cancer types in the TCGA dataset (**Figure S1**).

Pharmacologically Targeting MDK Abrogates IFN-γ-Induced Metastasis

To test whether MDK inhibition would attenuate IFN-γ-induced metastasis, we added iMDK (100 nM) to the IFN-γ-treated cancer cells, which resulted in no conspicuous cell death under microscope. As expected, iMDK efficiently eliminated IFN-γ-induced MDK expression at both the mRNA and protein levels (**Figures 6A, B**), reversed IFN-γ-driven EMT activation determined by Western blotting and RT-qPCR (**Figure 6B**), and subsequently abrogated IFN-γ-triggered migration and invasion as shown in transwell assays (**Figure 6C**) in all examined cancer cell lines. These data suggest that MDK confers the IFN-γ-elicited metastasis in various cancers, and that pharmacologically inhibiting MDK can broadly and efficiently abrogate IFN-γ treatment-induced cancer metastasis.

DISCUSSION

Accumulative evidence suggests that IFN-γ functions as a "two-edged sword" in cancer treatment (15, 23). IFN-γ is conventionally considered a promising cancer therapeutic agents for its potent tumoricidal and immunoregulatory activities, and certain positive responses have been reported in multiple pre-clinical and clinical trials (7). Tamura et al. reported that intralesional injection of IFN-γ could induce lasting remissions of T cell leukemia (8). Giannopoulos et al. demanstrated that intravesicle instillation of IFN-γ was effective in preventing bladder cancer recurrence (9). A randomized phase III trial showed that inclusion of IFN-γ in the first-line chemotherapy could prolong the progression-free survival of ovarian cancer patients (10).

Despite these encouraging results, a lack of beneficial effect has been observed in small-cell lung cancer, advanced colon cancer, metastatic renal cell carcinoma, and breast cancer (12, 15, 23). On the contrary, the pro-metastatic adverse effect of IFN-γ mediated by multiple mechanisms have been reported. Preincubation of murine colon adenocarcinoma cells with IFN-γ produced a significant increase in pulmonary metastases in mice (16). IFN-γ induced cancer invasiveness in prostate cancer *via* transcription of IFN-induced tetratricopeptide repeat 5 (IFIT5) (17). Low-dose IFN-γ enhanced the stemness and metastasis of non–small cell lung cancer *via* the intercellular adhesion molecule-1 (ICAM1)-PI3K-Akt-Notch1 axis (20). IFN-γ withdrawal after immunotherapy potentiates B16 melanoma invasion and metastasis by intensifying tumor integrin αvβ3

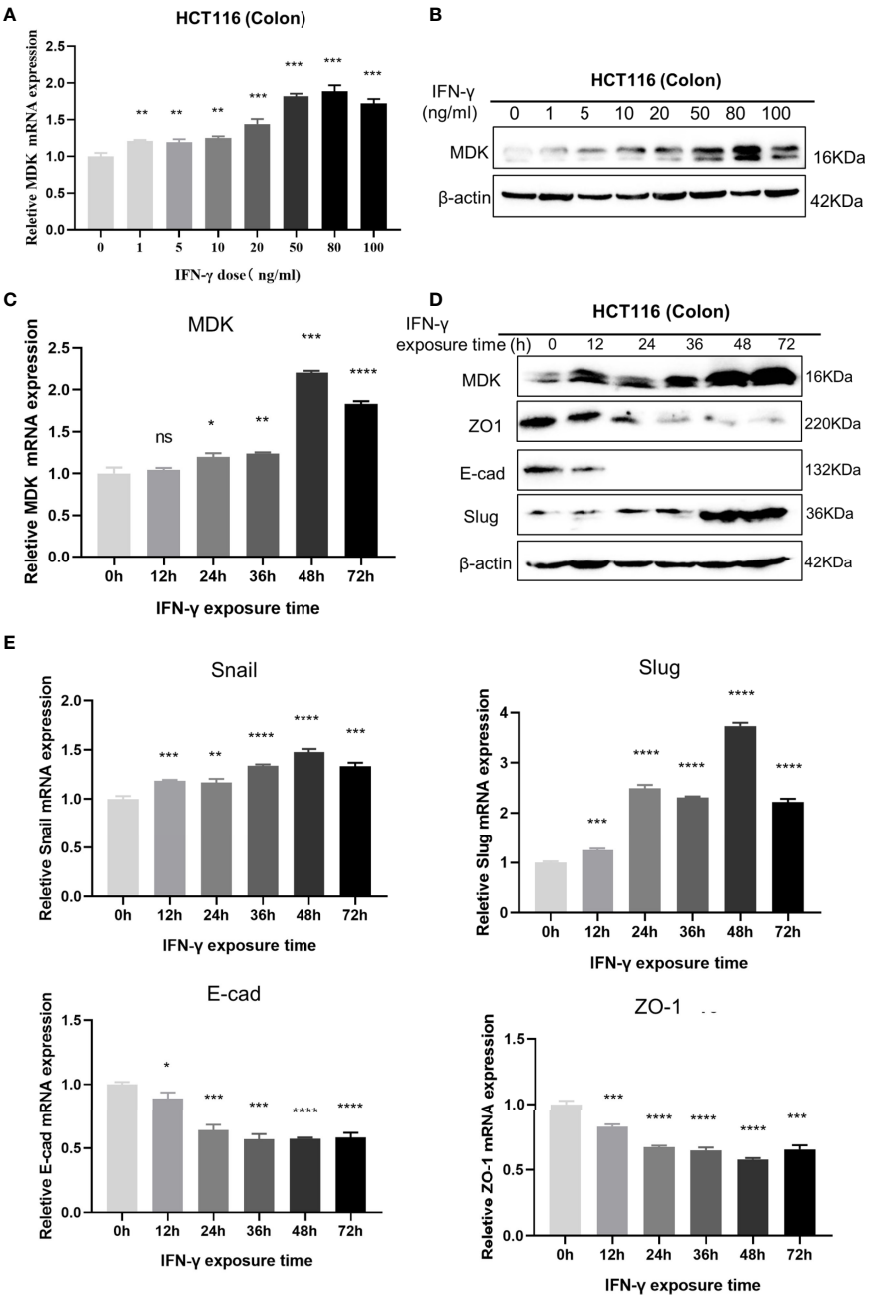

FIGURE 3 | Dose- and time-dependent effects of IFN-γ on MDK induction. **(A)** RT-qPCR assays to examine the effect of IFN-γ concentration on MDK induction in the HCT116 cell line. **(B)** Western blotting assays to examine the effect of IFN-γ concentration on MDK induction in the HCT116 cell line. **(C)** RT-qPCR assays to examine the effect of IFN-γ treatment time on MDK induction in the HCT116 cell line. **(D)** Western blotting assays to examine the effect of IFN-γ treatment time on MDK induction and EMT activation in the HCT116 cell line. **(E)** RT-qPCR assays showing the effect of IFN-γ treatment time on EMT markers in the HCT116 cell line. *P < 0.05, **P < 0.01, ***P < 0.001, ****P < 0.0001. ns, not significant.

signaling (19). More recently, Singh et al. reported that loss of the tumor suppressive transcription factor Elf5 in triple-negative breast cancer mediated IFN-γ signalling-promoted tumor progression and metastasis (21).

Though the IFN-γ-mediated metastasis has been indicated in a variety of cancers, no shared mechanism has been revealed. Here, we verified that IFN-γ exerted its pro-metastatic effect *via* a common EMT activating mechanism in all examined cancer cell lines, including the kidney cancer Caki-1, the lung cancer A549, the cervical carcinoma CaSki, the breast cancer BT549, and the colon cancer HCT116. The EMT programme is a developmental program broadly promoting metastasis of various cancers.

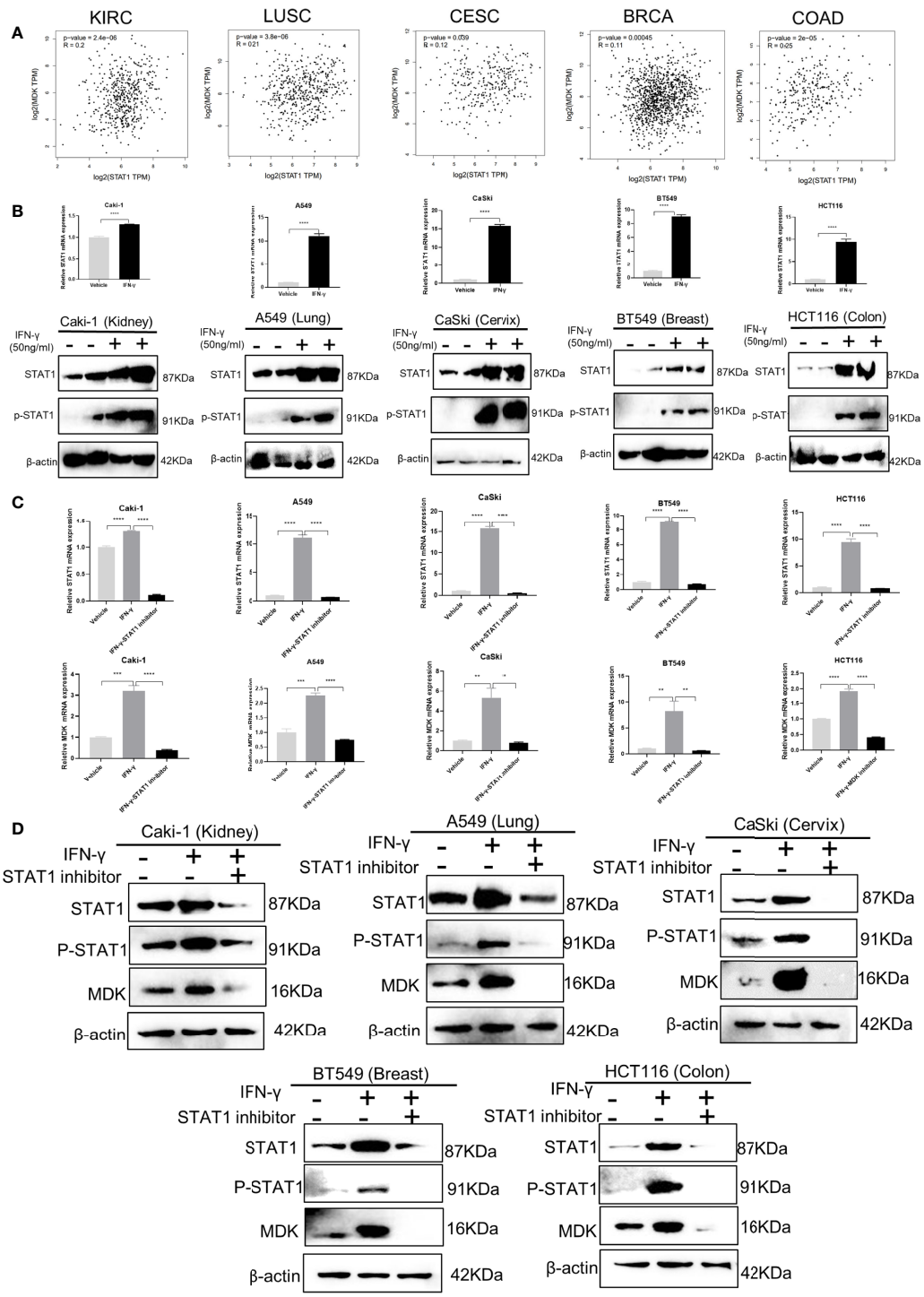

FIGURE 4 | IFN-γ activates MDK *via* STAT1. **(A)** Correlation analyses using the GEPIA 2 online tool (http://gepia2.cancer-pku.cn/#correlation) to shown the correlation relationship between STAT1 and MDK using the RNA-seq data of different cancers from the Cancer Genome Atlas (TCGA) database. KIRC, kidney renal clear cell carcinoma; LUSC, Lung squamous cell carcinoma; CESC, Cervical squamous cell carcinoma and endocervical adenocarcinoma; BRCA, breast invasive carcinoma; COAD, colorectal adenocarcinoma. **(B)** RT-qPCR and Western blotting assays to detect the effect of IFN-γ treatment (50 ng/ml, 48h) on levels of STAT1 and phosphorylated STAT1 (p-STAT1) in five cancer cell lines. **(C)** RT-qPCR assays to the effect of STAT1 inhibitor on mRNA levels of STAT1 and MDK in five cancer cell lines. **(D)** Western blotting assays to examine the effect of STAT1 inhibitor on protein levels of STAT1, p-STAT1 and MDK in five cancer cell lines. Data are shown as the mean ± standard deviation (SD). **P < 0.01, ***P < 0.001, ****P < 0.0001.

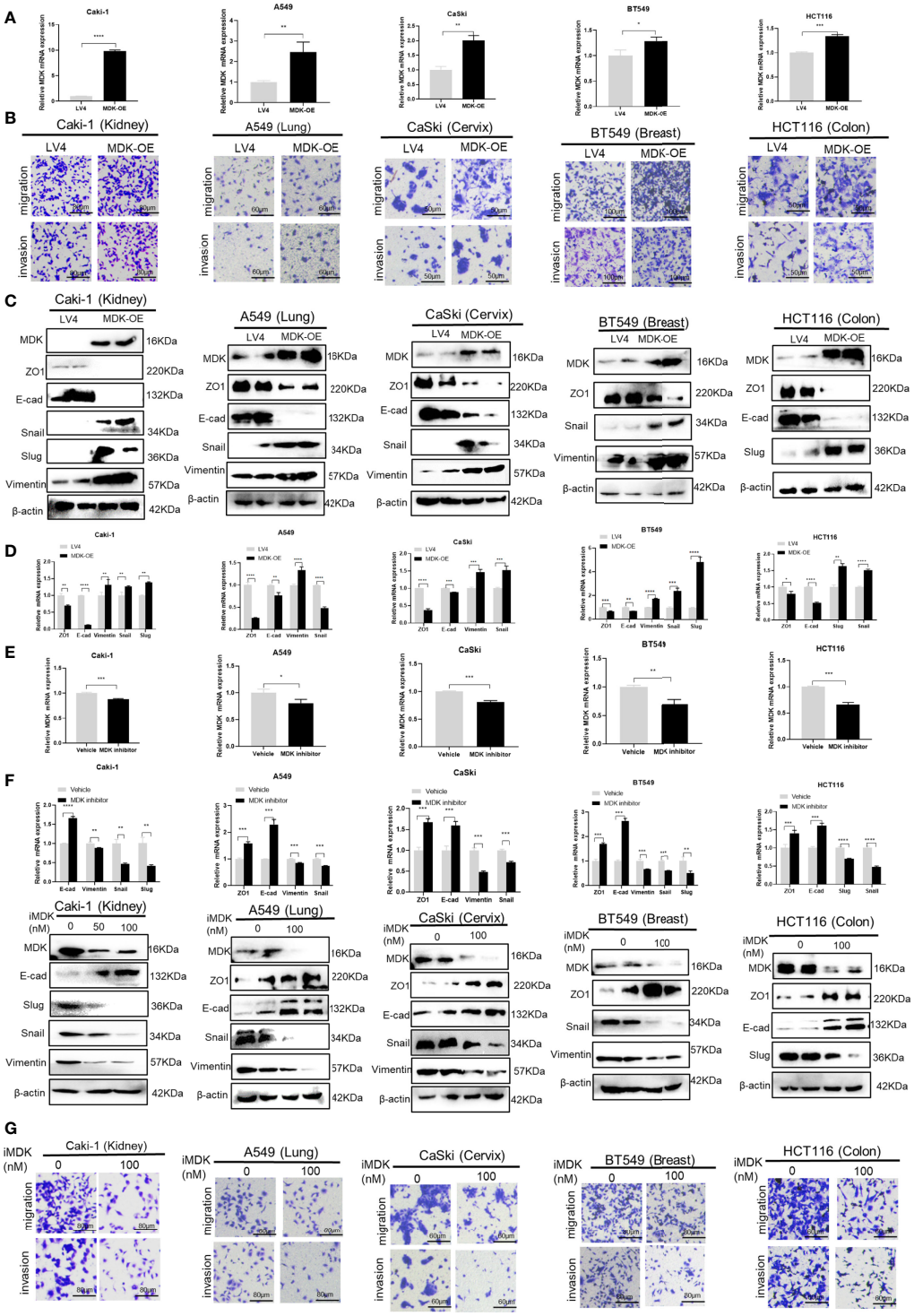

FIGURE 5 | MDK promotes cancer metastasis by activating the EMT programme. **(A)** RT-qPCR validation of MDK overexpression in five cancer cell lines. **(B)** Transwell assays to assess the alteration of cell invasion and migration abilities by MDK overexpression in five cancer cell lines. **(C)** Western blotting assays to assess the effect of MDK overexpression on expression of EMT markers. **(D)** RT-qPCR assays to assess the effect of MDK overexpression on expression of EMT markers. **(E)** RT-qPCR validation of MDK inhibition by iMDK (100nM, 48h). **(F)** RT-qPCR and Western blotting assays to assess the effect of iMDK on EMT in five cancer cell lines. **(G)** Transwell assays to assess the effect of iMDK on cell invasion and migration in five cancer cell lines. Data are shown as the mean ± standard deviation (SD). *P < 0.05, **P < 0.01, ***P < 0.001, ****P < 0.0001.

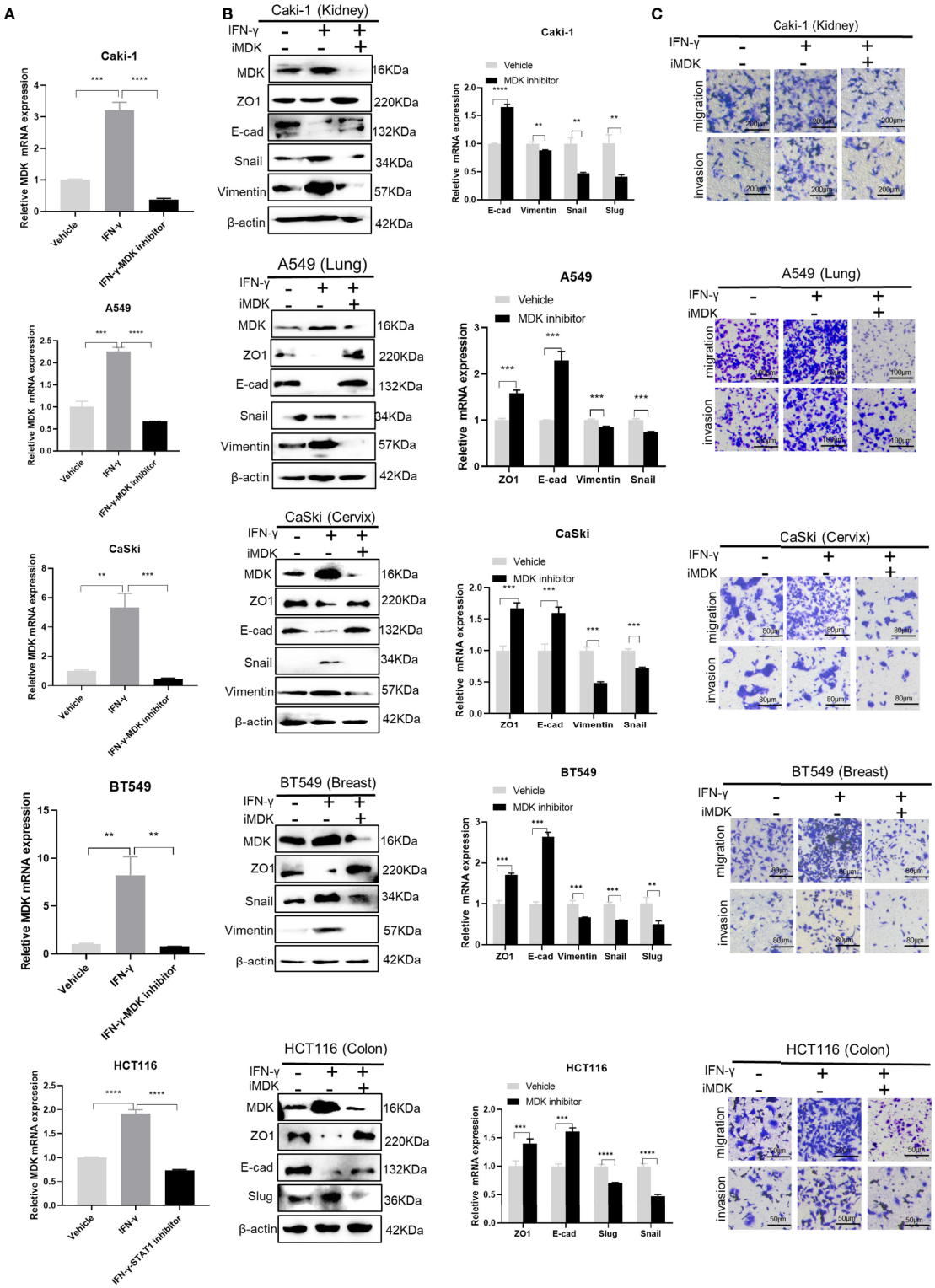

FIGURE 6 | Targeting MDK abrogates IFN-γ-induced tumor metastasis. **(A)** RT-qPCR validation of MDK suppression by MDK inhibitor in IFN-γ-treated cancer cells. **(B)** Western blotting and RT-qPCR assays to assess the effect of iMDK on IFN-γ-activated EMT in five cancer cell lines. **(C)** Transwell assays to examine the effect of iMDK on IFN-γ-driven cell invasion and migration. Data are shown as the mean ± standard deviation (SD). **P < 0.01, ***P < 0.001, ****P < 0.0001.

Activation of EMT enables cancer cells to lose their epithelial property but acquire a mesenchymal, migratory phenotype through downregulating epithelial markers including ZO-1 and E-cadherin and upregulating mesenchymal markers such as N-cadherin and Vimentin (24). In consistence with our finding, IFN-γ activation of EMT has also been reported in prostate cancer (17), suggesting that EMT activation is a common mechanism underlying IFN-γ-driven metastasis in different cancers.

To further deep into the mechanism mediating IFN-γ-triggered EMT activation, we focused on MDK, which is a heparin-binding growth factor and an emerging oncoprotein well implicated in induction of EMT and cancer metastasis (25). Indeed, we validated that MDK overexpression led to EMT and metastasis in all five cancer cell lines. MDK has been reported to promote cancer EMT *via* TGF-β, WNT and Notch 2 signalings (25). Additionally, MDK has also been implicated in promoting cancer proliferation (27), angiogenesis (28), stemness (29), drug resistance (30), immunosuppression (31), and resistance to immune checkpoint blockade (31), closely correlated with advanced cancer progression and poor survival (27, 32, 33).

Our data demonstrated that IFN-γ exposure resulted in a dramatic upregulation of MDK in all examined five cancer cell lines, suggesting this is a universal regulatory mechanism across cancers. To our knowledge, this is the first report demonstrating the common IFN-γ-MDK transduction cascade in the cancerous context. However, MDK was also previously reported to be elevated in peripheral blood lymphocytes in response to IFN-γ treatment when investigating its anti-HIV function (26), suggesting that this regulation may also exist in non-cancerous cells.

MDK is upregulated in the majority of cancers (at least 20 different cancer types), such as breast, lung, ovary, prostate, colon, gastric and pancreatic cancers, whereas its expression is generally low or undetectable in normal adult tissues (25, 34). However, the regulatory mechanism mediating MDK elevation is still largely obscure. There is evidence indicating that MDK is induced by hypoxia in a HIF-1α dependent manner (35). Here, we further indicate that MDK is also an IFN-γ inducible protein, which provides more insights into the MDK regulatory network in cancer.

STAT1 is the major IFN-γ-activated transcription factor responsible for the downstream signaling triggered by IFN-γ (2). The binding of IFN-γ to IFNGR1 triggers the formation of the IFNGR complex consisting of two IFNGR1 and two IFNGR2 subunits. This complex induces JAK1 and JAK2 phosphorylation, and further recruits and phosphorylates two STAT1 molecules. Phosphorylated STAT1 homodimerizes and translocates to the nucleus to initiate transcription of IFN-γ induced genes (3, 13). Our data demonstrated that STAT1 inhibition efficiently abrogated IFN-γ-induced MDK activation in all examined cancer cell lines, suggesting that the IFN-γ-MDK transduction is dependent on STAT1 in cancer.

To validate the role of MDK in mediating IFN-γ-activated EMT and metastasis, we pharmacologically silenced MDK expression using a specific inhibitor iMDK. The inhibitor iMDK is a small low molecular weight compound, demonstrating high efficiency and specificity in suppressing MDK expression in cancer cells (36, 37). iMDK decreased cell viability of the MDK-positive cancer cells in a dose-dependent manner, but less affected the MDK-negative cancer and non-transformed cells (36). The inhibitory effect of iMDK on cancer malignant behaviors has been validated in oral squamous cell carcinoma (37), non-small cell lung cancer (36, 38), and prostate cancer (39). Importantly, systemic administration of iMDK in mouse didn't cause obvious systemic toxicity (36), highlighting a high safety for potential clinical use. Our data indicated that iMDK application could globally eliminate IFN-γ-induced MDK, reverse IFN-γ-induced EMT activation, and ultimately abrogate IFN-γ-triggered cancer migration and invasion in all examined cancer cell lines.

Collectively, our data identify a novel IFN-γ-STAT1-MDK signalling axis (**Figure 7**), which confers the pro-metastatic adverse effect of IFN-γ in immunotherapy, whereas targeting

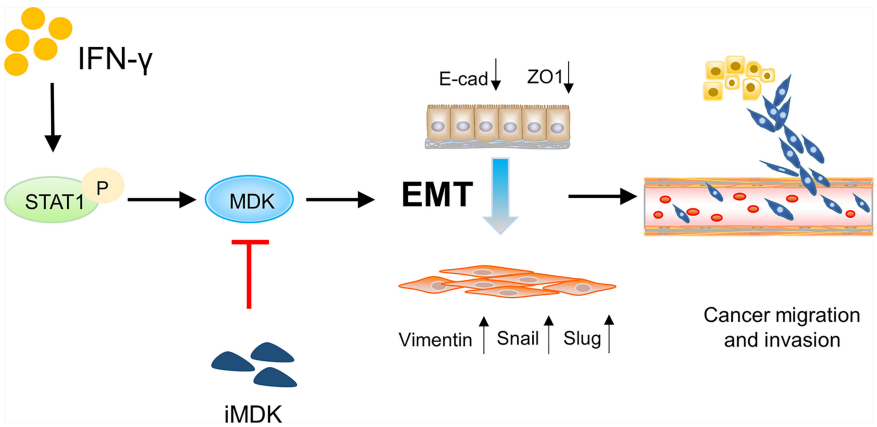

FIGURE 7 | Schematic diagram showing the IFN-γ-STAT1-MDK signalling axis in driving cancer metastasis. The IFN-γ-STAT1-MDK signalling axis promotes cancer metastasis by activating EMT, whereas MDK inhibition by iMDK can abrogate IFN-γ-induced EMT and tumor metastasis.

MDK may efficiently abrogate IFN-γ-elicited cancer metastasis. Attenuation of the pro-metastatic activity of IFN-γ may help to augment its anti-tumor effects during cancer treatment, thus our data propose a combined use of MDK inhibitors in IFN-γ-based cancer therapies.

DATA AVAILABILITY STATEMENT

The original contributions presented in the study are included in the article/**Supplementary Material**. Further inquiries can be directed to the corresponding authors.

AUTHOR CONTRIBUTIONS

JL, TW, and CH designed and conceived the study. LZ, QL, RL, SC, JT, LL, and XD performed the experiments. LZ and QL analyzed the data. LZ and QL wrote the manuscript. JL and TW revised the manuscript. All authors contributed to the article and approved the submitted version.

FUNDING

This work was financially supported by grants from the National Natural Science Foundation of China (No. 82172913, 82173234 and 82002754), and Open Funding of the State Key Laboratory of Molecular Oncology (SKLMO-KF2021-19).

SUPPLEMENTARY MATERIAL

The Supplementary Material for this article can be found online at: https://www.frontiersin.org/articles/10.3389/fonc.2022.885656/full#supplementary-material

Supplementary Figure 1 | MDK is elevated in the majority of cancer types in the TCGA database. Red, cancer; blue, adjacent normal.

REFERENCES

1. Parker BS, Rautela J, Hertzog PJ. Antitumour Actions of Interferons: Implications for Cancer Therapy. *Nat Rev Cancer* (2016) 16(3):131–44. doi: 10.1038/nrc.2016.14
2. Chow KT, Gale MJr. SnapShot: Interferon Signaling. *Cell* (2015) 163(7):1808–1808.e1. doi: 10.1016/j.cell.2015.12.008
3. Platanias LC. Mechanisms of Type-I- and Type-II-Interferon-Mediated Signalling. *Nat Rev Immunol* (2005) 5(5):375–86. doi: 10.1038/nri1604
4. Dighe AS, Richards E, Old LJ, Schreiber RD. Enhanced *In Vivo* Growth and Resistance to Rejection of Tumor Cells Expressing Dominant Negative IFN Gamma Receptors. *Immunity* (1994) 1(6):447–56. doi: 10.1016/1074-7613(94)90087-6
5. Miller CH, Maher SG, Young HA. Clinical Use of Interferon-Gamma. *Ann N Y Acad Sci* (2009) 1182:69–79. doi: 10.1111/j.1749-6632.2009.05069.x
6. Foon KA, Sherwin SA, Abrams PG, Stevenson HC, Holmes P, Maluish AE, et al. A Phase I Trial of Recombinant Gamma Interferon in Patients With Cancer. *Cancer Immunol Immunother* (1985) 20(3):193–7. doi: 10.1007/BF00205575
7. Shen J, Xiao Z, Zhao Q, Li M, Wu X, Zhang L, et al. Anti-Cancer Therapy With Tnfα and Ifnγ: A Comprehensive Review. *Cell Prolif* (2018) 51(4):e12441. doi: 10.1111/cpr.12441
8. Tamura K, Makino S, Araki Y, Imamura T, Seita M. Recombinant Interferon Beta and Gamma in the Treatment of Adult T-Cell Leukemia. *Cancer* (1987) 59(6):1059–62. doi: 10.1002/1097-0142(19870315)59:6<1059::AID-CNCR2820590602>3.0.CO;2-M
9. Giannopoulos A, Constantinides C, Fokaeas E, Stravodimos C, Giannopoulou M, Kyroudi A, et al. The Immunomodulating Effect of Interferon-Gamma Intravesical Instillations in Preventing Bladder Cancer Recurrence. *Clin Cancer Res* (2003) 9(15):5550–8.
10. Windbichler GH, Hausmaninger H, Stummvoll W, Graf AH, Kainz C, Lahodny J, et al. Interferon-Gamma in the First-Line Therapy of Ovarian Cancer: A Randomized Phase III Trial. *Br J Cancer* (2000) 82(6):1138–44. doi: 10.1054/bjoc.1999.1053
11. Du W, Frankel TL, Green M, Zou W. Ifnγ Signaling Integrity in Colorectal Cancer Immunity and Immunotherapy. *Cell Mol Immunol* (2022) 19(1):23–32. doi: 10.1038/s41423-021-00735-3
12. Castro F, Cardoso AP, Gonçalves RM, Serre K, Oliveira MJ. Interferon-Gamma at the Crossroads of Tumor Immune Surveillance or Evasion. *Front Immunol* (2018) 9:847. doi: 10.3389/fimmu.2018.00847
13. Martínez-Sabadell A, Arenas EJ, Arribas J. Ifnγ Signaling in Natural and Therapy-Induced Antitumor Responses. *Clin Cancer Res* (2022) 28(7):1243–9. doi: 10.1158/1078-0432.CCR-21-3226
14. Ealick SE, Cook WJ, Vijay-Kumar S, Carson M, Nagabhushan TL, Trotta PP, et al. Three-Dimensional Structure of Recombinant Human Interferon-Gamma. *Science* (1991) 252(5006):698–702. doi: 10.1126/science.1902591
15. Jorgovanovic D, Song M, Wang L, Zhang Y. Roles of IFN-γ in Tumor Progression and Regression: A Review. *biomark Res* (2020) 8:49. doi: 10.1186/s40364-020-00228-x
16. Kelly SA, Gschmeissner S, East N, Balkwill FR. Enhancement of Metastatic Potential by Gamma-Interferon. *Cancer Res* (1991) 51(15):4020–7.
17. Lo UG, Pong RC, Yang D, Gandee L, Hernandez E, Dang A, et al. Ifnγ-Induced IFIT5 Promotes Epithelial-To-Mesenchymal Transition in Prostate Cancer *via* miRNA Processing. *Cancer Res* (2019) 79(6):1098–112. doi: 10.1158/0008-5472.CAN-18-2207
18. Lo UG, Bao J, Cen J, Yeh HC, Luo J, Tan W, et al. Interferon-Induced IFIT5 Promotes Epithelial-to-Mesenchymal Transition Leading to Renal Cancer Invasion. *Am J Clin Exp Urol* (2019) 7(1):31–45.
19. Gong W, Zhang GM, Liu Y, Lei Z, Li D, Yuan Y, et al. IFN-Gamma Withdrawal After Immunotherapy Potentiates B16 Melanoma Invasion and Metastasis by Intensifying Tumor Integrin Alphavbeta3 Signaling. *Int J Cancer* (2008) 123(3):702–8. doi: 10.1002/ijc.23553
20. Song M, Ping Y, Zhang K, Yang L, Li F, Zhang C, et al. Low-Dose Ifnγ Induces Tumor Cell Stemness in Tumor Microenvironment of Non-Small Cell Lung Cancer. *Cancer Res* (2019) 79(14):3737–48. doi: 10.1158/0008-5472.CAN-19-0596
21. Singh S, Kumar S, Srivastava RK, Nandi A, Thacker G, Murali H, et al. Loss of ELF5-FBXW7 Stabilizes IFNGR1 to Promote the Growth and Metastasis of Triple-Negative Breast Cancer Through Interferon-γ Signalling. *Nat Cell Biol* (2020) 22(5):591–602. doi: 10.1038/s41556-020-0495-y
22. Zaidi MR, Davis S, Noonan FP, Graff-Cherry C, Hawley TS, Walker RL, et al. Interferon-γ Links Ultraviolet Radiation to Melanomagenesis in Mice. *Nature* (2011) 469(7331):548–53. doi: 10.1038/nature09666
23. Zaidi MR, Merlino G. The Two Faces of Interferon-γ in Cancer. *Clin Cancer Res* (2011) 17(19):6118–24. doi: 10.1158/1078-0432.CCR-11-0482
24. Li L, Liu J, Xue H, Li C, Liu Q, Zhou Y, et al. A TGF-β-MTA1-SOX4-EZH2 Signaling Axis Drives Epithelial-Mesenchymal Transition in Tumor Metastasis. *Oncogene* (2020) 39(10):2125–39. doi: 10.1038/s41388-019-1132-8
25. Filippou PS, Karagiannis GS, Constantinidou A. Midkine (MDK) Growth Factor: A Key Player in Cancer Progression and a Promising Therapeutic Target. *Oncogene* (2020) 39(10):2040–54. doi: 10.1038/s41388-019-1124-8
26. Callebaut C, Nisole S, Briand JP, Krust B, Hovanessian AG. Inhibition of HIV Infection by the Cytokine Midkine. *Virology* (2001) 281(2):248–64. doi: 10.1006/viro.2000.0767
27. Cubillos-Zapata C, Martínez-García MÁ, Díaz-García E, Toledano V, Campos-Rodríguez F, Sánchez-de-la-Torre M, et al. Proangiogenic Factor

Midkine is Increased in Melanoma Patients With Sleep Apnea and Induces Tumor Cell Proliferation. *FASEB J* (2020) 34(12):16179–90. doi: 10.1096/fj.202001247RR
28. Sheng B, Wei Z, Wu X, Li Y, Liu Z. USP12 Promotes Breast Cancer Angiogenesis by Maintaining Midkine Stability. *Cell Death Dis* (2021) 12 (11):1074. doi: 10.1038/s41419-021-04102-y
29. López-Valero I, Dávila D, González-Martínez J, Salvador-Tormo N, Lorente M, Saiz-Ladera C, et al. Midkine Signaling Maintains the Self-Renewal and Tumorigenic Capacity of Glioma Initiating Cells. *Theranostics* (2020) 10 (11):5120–36. doi: 10.7150/thno.41450
30. Lu Y, Yan B, Guo H, Qiu L, Sun X, Wang X, et al. Effect of Midkine on Gemcitabine Resistance in Biliary Tract Cancer. *Int J Mol Med* (2018) 41 (4):2003–11. doi: 10.3892/ijmm.2018.3399
31. Cerezo-Wallis D, Contreras-Alcalde M, Troulé K, Catena X, Mucientes C, Calvo TG, et al. Midkine Rewires the Melanoma Microenvironment Toward a Tolerogenic and Immune-Resistant State. *Nat Med* (2020) 26(12):1865–77. doi: 10.1038/s41591-020-1073-3
32. Kemper M, Hentschel W, Graß JK, Stüben BO, Konczalla L, Rawnaq T, et al. Serum Midkine is a Clinical Significant Biomarker for Colorectal Cancer and Associated With Poor Survival. *Cancer Med* (2020) 9(6):2010–8. doi: 10.1002/cam4.2884
33. Ma MC, Chen YJ, Chiu TJ, Lan J, Liu CT, Chen YC, et al. Positive Expression of Midkine Predicts Early Recurrence and Poor Prognosis of Initially Resectable Combined Hepatocellular Cholangiocarcinoma. *BMC Cancer* (2018) 18(1):227. doi: 10.1186/s12885-018-4146-7
34. Jones DR. Measuring Midkine: The Utility of Midkine as a Biomarker in Cancer and Other Diseases. *Br J Pharmacol* (2014) 171(12):2925–39. doi: 10.1111/bph.12601
35. Shin DH, Jo JY, Kim SH, Choi M, Han C, Choi BK, et al. Midkine Is a Potential Therapeutic Target of Tumorigenesis, Angiogenesis, and Metastasis in Non-Small Cell Lung Cancer. *Cancers (Basel)* (2020) 12(9):2402. doi: 10.3390/cancers12092402
36. Hao H, Maeda Y, Fukazawa T, Yamatsuji T, Takaoka M, Bao XH, et al. Inhibition of the Growth Factor MDK/midkine by a Novel Small Molecule Compound to Treat non-Small Cell Lung Cancer. *PloS One* (2013) 8(8): e71093. doi: 10.1371/journal.pone.0071093
37. Masui M, Okui T, Shimo T, Takabatake K, Fukazawa T, Matsumoto K, et al. Novel Midkine Inhibitor iMDK Inhibits Tumor Growth and Angiogenesis in Oral Squamous Cell Carcinoma. *Anticancer Res* (2016) 36(6):2775–81.
38. Ishida N, Fukazawa T, Maeda Y, Yamatsuji T, Kato K, Matsumoto K, et al. A Novel PI3K Inhibitor iMDK Suppresses non-Small Cell Lung Cancer Cooperatively With A MEK Inhibitor. *Exp Cell Res* (2015) 335(2):197–206. doi: 10.1016/j.yexcr.2015.03.019
39. Erdogan S, Doganlar ZB, Doganlar O, Turkekul K, Serttas R. Inhibition of Midkine Suppresses Prostate Cancer CD133+ Stem Cell Growth and Migration. *Am J Med Sci* (2017) 354(3):299–309. doi: 10.1016/j.amjms.2017.04.019

Conflict of Interest: The authors declare that the research was conducted in the absence of any commercial or financial relationships that could be construed as a potential conflict of interest.

Publisher's Note: All claims expressed in this article are solely those of the authors and do not necessarily represent those of their affiliated organizations, or those of the publisher, the editors and the reviewers. Any product that may be evaluated in this article, or claim that may be made by its manufacturer, is not guaranteed or endorsed by the publisher.

Copyright © 2022 Zheng, Liu, Li, Chen, Tan, Li, Dong, Huang, Wen and Liu. This is an open-access article distributed under the terms of the Creative Commons Attribution License (CC BY). The use, distribution or reproduction in other forums is permitted, provided the original author(s) and the copyright owner(s) are credited and that the original publication in this journal is cited, in accordance with accepted academic practice. No use, distribution or reproduction is permitted which does not comply with these terms.

frontiers | Frontiers in Oncology

TYPE Original Research
PUBLISHED 17 August 2022
DOI 10.3389/fonc.2022.942020

Check for updates

OPEN ACCESS

EDITED BY
Weilong Zhong,
Tianjin Medical University General Hospital, China

REVIEWED BY
Gisela D'Angelo,
UMR 144 CNRS institut Curie, France
Hiu Yee Kwan,
Hong Kong Baptist University, SAR China

*CORRESPONDENCE
Li-wei Sun
sunnylilwei@163.com
Da-qing Zhao
zhaodaqing1963@163.com

SPECIALTY SECTION
This article was submitted to Pharmacology of Anti-Cancer Drugs, a section of the journal Frontiers in Oncology

RECEIVED 12 May 2022
ACCEPTED 13 July 2022
PUBLISHED 17 August 2022

CITATION
Yang L, Jin W-q, Tang X-l, Zhang S, Ma R, Zhao D-q and Sun L-w (2022) Ginseng-derived nanoparticles inhibit lung cancer cell epithelial mesenchymal transition by repressing pentose phosphate pathway activity. *Front. Oncol.* 12:942020. doi: 10.3389/fonc.2022.942020

COPYRIGHT
© 2022 Yang, Jin, Tang, Zhang, Ma, Zhao and Sun. This is an open-access article distributed under the terms of the Creative Commons Attribution License (CC BY). The use, distribution or reproduction in other forums is permitted, provided the original author (s) and the copyright owner(s) are credited and that the original publication in this journal is cited, in accordance with accepted academic practice. No use, distribution or reproduction is permitted which does not comply with these terms.

Ginseng-derived nanoparticles inhibit lung cancer cell epithelial mesenchymal transition by repressing pentose phosphate pathway activity

Lan Yang[1], Wen-qi Jin[1], Xiao-lei Tang[1], Shuai Zhang[2], Rui Ma[1], Da-qing Zhao[2,3]* and Li-wei Sun[1,3]*

[1]Research Center of Traditional Chinese Medicine, The Affiliated Hospital to Changchun University of Chinese Medicine, Changchun, China, [2]Jilin Ginseng Academy, Changchun University of Chinese Medicine, Changchun, China, [3]Key Laboratory of Active Substances and Biological Mechanisms of Ginseng Efficacy, Ministry of Education, Changchun, China

It is unclear whether ginseng-derived nanoparticles (GDNPs) can prevent tumor cell epithelial-mesenchymal transition (EMT). Here, we describe typical characteristics of GDNPs and possible underlying mechanisms for GDNP antitumor activities. First, GDNPs particle sizes and morphology were determined using nanoparticle tracking analysis (NTA) and transmission electron microscopy (TEM), respectively, while cellular uptake of PKH67-labeled GDNPs was also assessed. Next, we evaluated GDNPs antitumor effects by determining whether GDNPs inhibited proliferation and migration of five tumor cell lines derived from different cell types. The results indicated that GDNPs most significantly inhibited proliferation and migration of lung cancer-derived tumor cells (A549, NCI-H1299). Moreover, GDNPs treatment also inhibited cell migration, invasion, clonal formation, and adhesion tube formation ability and reduced expression of EMT-related markers in A549 and NCI-H1299 cells in a dose-dependent manner. Meanwhile, Kaplan-Meier analysis of microarray data revealed that high-level thymidine phosphorylase (TP) production, which is associated with poor lung cancer prognosis, was inhibited by GDNPs treatment, as reflected by decreased secretion of overexpressed TP and downregulation of TP mRNA-level expression. In addition, proteomic analysis results indicated that GDNPs affected pentose phosphate pathway (PPP) activity, with ELISA results confirming that GDNPs significantly reduced levels of PPP metabolic intermediates. Results of this study also demonstrated that GDNPs-induced downregulation of TP expression led to PPP pathway inhibition and repression of lung cancer cell metastasis, warranting further studies of nano-drugs as a new and promising class of anti-cancer drugs.

KEYWORDS

ginseng-derived nanoparticles, EMT, lung cancer, pentose phosphate pathway, migration

Introduction

Lung cancer, a major threat to human health and survival, accounts for the highest cancer incidence and mortality rates worldwide (1). In fact, nearly 80% of lung cancer patients are diagnosed during advanced stages of the disease, with very poor prognosis for most patients resulting from disease recurrence and distant metastasis. Non-small cell lung cancer (NSCLC) accounts for approximately 85% of all lung cancer cases (2, 3). During NSCLC disease progression a critical process occurs, epithelial mesenchymal transition (EMT), that endows the cells with enhanced migratory ability, invasiveness, and metastatic capability, thereby increasing cancer cell survival rates (4).

The root of *Panax ginseng* C.A. Meyer (Araliaceae) is famous for its many pharmacological properties that stem from regulatory activities of its constituent components of signal pathways related to inflammation, oxidative stress, angiogenesis, and cancer metastasis (5, 6). In recent years, it has been reported that ginseng extract has good efficacy as a cancer treatment, due to antitumor activities of components that include Rh2, Rg3, and Rg5 saponins. However, mechanisms underlying ginseng antitumor effects are still only partially understood (7–9).

Physiological cell-to-cell communication is essential for maintaining tissue homeostasis and biological integrity, with most cell-to-cell communication coordinated through multiple informational exchange mechanisms (10, 11). In recent years, nanovesicle-mediated cell communication has become a research hotspot, since nanovesicles can transfer diverse types of molecules from producing cells to target cells through extracellular transport as special extracellular vesicles (EVs) called exosomes (12). Plant exosome-like nanovesicles, nano-sized particles, are known to play a role in cell communication by transporting mRNA, miRNA, bioactive lipids, and multiple proteins between cells that allow different cells to work together as a functional unit. Importantly, nanovesicles can freely enter target cells and thus are viewed as a potentially useful vehicle for drug delivery (13–15). Recent studies have indicated that exosome-like nanoparticles released from edible plants (grapes, grapefruit, ginger, and carrots) have anti-inflammatory properties that appear to alleviate inflammatory bowel diseases (16–20), while ginseng-derived nanoparticles have been shown to exert an immunomodulatory effect on murine macrophages to inhibit tumor growth (21). Notably, lemon-derived nanovesicles have been shown to trigger TRAIL-mediated apoptosis that can effectively kill tumor cells (11).

Tumor cells can grow rapidly in an uncontrolled manner that is related to reprogramming of tumor cell metabolism. Unlike normal cells, which obtain energy from glycolysis and aerobic respiration, most tumor cells can also obtain energy through the pentose phosphate pathway (PPP), due to a phenomenon known as the Warburg effect. In fact, cancer cells are known to rely significantly on the PPP pathway to obtain energy and reducing equivalents needed for cell proliferation, invasiveness, drug resistance, and metastasis that enhance cell survival (22). Therefore, inhibition of the PPP pathway may significantly prevent tumor cell proliferation and metastasis (23). At the same time, cancer cells can also avoid metabolic regulatory roadblocks by deleting or acquiring key tumor suppressor genes and oncogenes, respectively (24, 25). For example, Twist1, a key transcription factor associated with tumor cell-associated EMT, promotes increased expression of thymidine phosphorylase (TP), a rate-limiting PPP enzyme belonging to the thymidine catabolic pathway. Importantly, studies have demonstrated that TP is overexpressed in human tumors, including those associated with non-small cell lung cancer (NSCLC), with TP expression level shown to be positively correlated with advanced-stage tumor metastasis and poor prognosis (26, 27).

In this study, antitumor effects of GDNPs on five different cancer cell lines were evaluated. The results demonstrated that GDNPs exhibited excellent antitumor effects against lung cancer-derived A549 and NCI-H1299 cells, warranting further development of nano-drugs for use as anti-cancer therapies.

Materials and methods

Cell culture

Cell lines used in this study, which included lines derived from hepatocellular carcinoma cells (HpG2), lung cancer cells (NCI-A549, hereafter referred to as A549 cells; NCI-H1299, hereafter referred to as H1299 cells), breast cancer cells (MCF-7), colorectal cancer cells (HCT-8), and pancreatic cancer cells (PANC-1), were obtained from KeyGen Biotech (Nanjing, China). All cells were cultured in RPMI 1640 or DMEM media supplemented with 10% fetal bovine serum under conditions of 37°C, 95% humidity, and 5% CO_2 (hereafter referred to as standard cell culture conditions). No primary human tumor specimens were used in this study.

Plasmid construction and cell transfection

The pcDNA3.1-TP plasmids were purchased from GeneCopoeia (Guangzhou, China). TP enzyme inhibitor (TPI) tipiracil (10μM, Meilunbio, China) was added to the medium for

enzyme inhibition experiments. Plasmid vectors were transfected into cells using Lipofectamine 2000 (Invitrogen, Shanghai, China).

Isolation of GDNPs

For isolation of GDNPs, fresh ginseng roots were purchased from Panax Ginseng Base Co. (Songyuan, Jilin, China). After roots were washed three times with deionized water at room temperature (RT), roots were pulverized using a juicer to yield juice. The resulting juice was centrifuged 300 × g for 30 min then was filtered through a 0.45-μm membrane and the supernatant was retained. Next, the supernatant was centrifuged at 2000 × *g* for 20 min and the resulting supernatant was retained and centrifuged at 10000 × *g* for 40 min through a 0.45-μm membrane to remove large particles and fibers. Thereafter, the supernatant was filtered through a 0.22-μm membrane then the resulting pellet that contained GDNPs was resuspended. The suspension was then concentrated by ultracentrifugation at 100000 × *g* for 60 min (Beckman at Optima XE-100, Beckman, USA). Next, the pellet was resuspended in 100 μL of pre-cooled vesicle isolation buffer (VIB, 20 mm MES, 2 mM $CaCl_2$, 0.1 M NaCl, pH 6), then the protein concentration of the GDNPs preparation was determined using a BCA protein assay kit (12, 28).

GDNPs characterization and nanoparticle tracking analysis

GDNPs size distribution and concentration were determined *via* nanoparticle tracking analysis (NTA), a method based on light scattering properties of particles. NTA was conducted using a Zetasizer Nano ZS90 system (Malvern Instruments, England) equipped with a blue laser (405 nm) according to the manufacturer's instructions provided with the system.

Transmission electron microscope analysis of GDNPs

For TEM, 10 μL of sample solution was loaded onto copper mesh-coated carbon film then the sample was allowed to adsorb to the film for 1 min at room temperature. After removal of the remaining solution by dabbing the film with filter paper, the adsorbed sample was negatively stained with 10 μL uranyl acetate for 1 min. Thereafter, the excess staining solution was gently removed by dabbing the edge of the copper mesh with filter paper then the mesh was allowed to air-dry. Imaging was performed using a TEM system (HT-7700, Hitachi, Japan) operated at 100 kV.

PKH67 labeling of GDNPs

Isolated GDNPs were labeled with the green fluorescent, lipophilic dye PKH67 (Umibio, UR52303) according to the manufacturer's protocol. Briefly, to prepare the fluorescent dye, 1 μL PKH67 and 9 μL Diluent C were mixed and added to GDNPs then the mixture was incubated in the dark at RT for 10 min. Next, 1 mL of PBS was added then the mixture was ultracentrifuged at 100000 × *g* for 17 min and the supernatant was discarded. The pellet containing fluorescently labeled GDNPs was washed three times with phosphate-buffered saline (PBS) and 10 μL was removed and analyzed for protein content using a BCA protein assay kit. Next, PKH67-labeled GDNPs were added to A549 cells (5×10^5/well) grown to 70% confluence in wells of in 24-well sterile were incubated for 0 h, 6 h, or 12 h. After incubation, the co-cultured cells and GDNPs in wells of plates were washed three times with PBS, fixed in 4% paraformaldehyde (PFA) at RT for 30 min, washed three times with PBS, then were stained with DAPI for 5 min. Images were taken of cells viewed under a Nikon confocal microscope.

Flow cytometry

An A549 cell suspension (2×10^6 cells/well) was inoculated into 6-well plates followed by incubation of plates under normal culture conditions for 24 h. After incubation, PKH67-labeled GDNPs were added to cells followed by incubation as mentioned above for 6 or 12 h. Cells were collected then washed twice with PBS after centrifugation at 1000 rpm for 5 min. Cell samples were prepared and analyzed using a FACSAria™ II system (BD Biosciences, USA).

Cell viability assay

After A549 and H1299 cells (4-6 × 10^3/well) were cultured overnight in 96-well plates, various concentrations of GNDPs were added to wells then the plates were incubated for 48 h under normal cell culture conditions. Next, cytotoxicity was determined *via* MTT assay whereby 10 μL of MTT solution (5 mg/mL) was added to each well then plates were incubated for 4 h. Next, 100 μL DMSO solution was added per well then absorbance values of wells were measured at 490 nm using a spectrophotometer, with untreated cells serving as the negative control.

Wound healing assay

Cells were seeded into wells of 24-well plates (5×10^5 cells/well). to create a confluent monolayer. Next, a scratch wound

was made in the monolayer in a straight line using a 200-μL pipette tip. The cells adhering to plates were removed and incubated with serum-free medium containing GDNPs (40 or 80 μg/mL). Images of wounds were captured under a microscope at 0 h and 48 h.

Cell invasion assay

Cell invasion capacity was assessed using transwell plates containing membrane inserts with 0.8-μm pores (Corning, USA). Membrane inserts were coated with Matrigel (BD Biosciences) then complete culture medium (600 μL) was added to the lower chamber followed by insertion of membrane inserts into transwell plates. Next, 200 μL of cell suspension in serum-free medium (1×10^5 cells/mL) with or without GDNPs was added to the upper chamber. After 24 h of incubation under standard cell culture conditions, non-invasive cells were removed from the upper chamber with a cotton swab then remaining cells on membrane inserts were fixed in 4% PFA for 15 min at RT. Next, cells were stained with 0.1% crystal violet solution for 20 min. Cell invasion was visually assessed microscopically based on counting of cells in five random fields per well.

Cell adhesion assay

Cells adhesion was assessed using 96-well plates coated with Matrigel (30 μL/well). GDNPs-treated cell suspensions (5×10^4) were added to wells then plates were incubated for 2 h. After non-adherent cells were removed by washing with PBS, remaining adherent cells were fixed in 4% PFA for 10 min then were stained with 0.1% crystal violet solution for 10 min then cell adhesion was observed under a microscope for five randomly selected fields per well.

Colony formation assay

A549 and H1299 cell suspensions were seeded at 400 cells/well in 6-well plates then medium containing GDNPs was added to wells and replaced every 3 days. After 12 days of incubation, cell colonies that had formed were fixed in 4% PFA and stained with 0.1% crystal violet solution as described above. A digital camera was used to record images of stained cells.

Tube formation assay

Wells of 96-well plates were coated with Matrigel (40 μL/well, 0.3 mg/ml, BD, USA) then plates were incubated under standard cell culture conditions for 2 h. Next, A549 and H1299 cell suspensions pretreated with GDNPs were added into Matrigel-coated plate wells then plates were incubated for 8 h under standard cell culture conditions. After incubation, tube formation ability of cells was evaluated based on images of cells obtained under a microscope.

Immunofluorescent staining

Cells were seeded into wells of 24-well plates at an appropriate concentration and incubated at 37°C overnight. After treatment of cells with various concentrations of GDNPs for 24 h, cells were fixed in 4% PFA for 10 min, permeabilized in 0.1% Triton X-100 for 20 min, and washed three times with PBS-T (3 min/wash). Next, cells were blocked in 3% BSA for 1 h then were incubated overnight with primary antibody (anti-E-cadherin or anti-vimentin antibody) diluted 1:200 (Affinity) at 4°C. After three PBS washes, cells were incubated with Alexa Fluor 546-conjugated secondary antibody at RT for 2 h in the dark. Finally, nuclear staining was performed by incubation of cells with DAPI for 5 min. Images of labeled/stained cells were obtained using a laser scanning confocal microscope.

Western blot analysis

Cells were lysed in radioimmunoprecipitation buffer (RIPA) containing halt protease and phosphatase inhibitor cocktail for 10 min on ice then were centrifuged at 12000 rpm for 15 min. Next, equal amounts of protein were separated by SDS-PAGE and transferred to PVDF membranes. Thereafter, membranes were blocked with 5% milk solution for 1 h then were incubated with primary antibodies specific for Twist1, E-cadherin, vimentin, or GAPDH (diluted 1:1000) at 4°C overnight. Next, membranes were washed then incubated with appropriate HRP-conjugated secondary antibodies at RT for 2 h. Finally, antibody-bound proteins were visualized on membranes using an enhanced chemiluminescent (ECL) kit.

Quantitative real-time PCR

Total RNA isolation from A549 cells was performed using TRIzol Reagent (Invitrogen, USA) then cDNA synthesis was performed using a cDNA reverse transcription kit (TIANGEN, China). Next, quantitative real-time PCR (qRT-PCR) was performed using a 2× Taq Plus PCR MasterMix kit (TIANGEN, China) and PCR primers with sequences as listed in Table 1.

TABLE 1 PCR primer sequences.

Gene	Forward primer ((5′- to 3′))	Reverse primer (5′- to 3′)
E-Cadherin	CGAGAGCTACACGTTCACGG	GGGTGTCGAGGGAAAAATAGG
Vimentin	GACGCCATCAACACCGAGTT	CTTTGTCGTTGGTTAGCTGGT
Twist1	GTCCGCAGTCTTACGAGGAG	GCTTGAGGGTCTGAATCTTGCT
snail	TCGGAAGCCTAACTACAGCGA	AGATGAGCATTGGCAGCGAG
Slug	TGGTCAAGAAACATTTCAACG	GGTGAGGATCTCTGGTTTT GG
TP	CACATGCAGCAACCAGTCCA	GGGAGAAGCCTTGGTAGGGT
GAPDH	GGAGCGAGATCCCTCCAAAAT	GGCTGTTGTCATACTTCTCATGG

Mass spectrometric analysis and bioinformatics analysis

Mass spectrometric assays were performed as previously reported with modifications (29). First, GDNPs frozen in liquid nitrogen were ground into powder then the powder was transferred to a centrifuge tube. Subsequently, a volume of lysate buffer equivalent to 4-times the powder volume was added to the powder then the mixture was sonicated three times on ice followed by centrifugation 2000 × *g* for 10 min to remove debris. Next, precooled (-20°C) 20% TCA was added to the supernatant followed by gentle mixing and incubation at -20°C for 2 h to allow precipitation to occur. Finally, the mixture was centrifuged at 12000 × *g* for 10 min then the supernatant was removed and the precipitate was washed three times with pre-cooled acetone (-20°C). The remaining protein-containing solid was dissolved in 8 M urea and the protein concentration was determined using a BCA kit according to the manufacturer's instructions. Next, the Gene Ontology (GO)-annotated proteome was obtained using the UniProt-GOA database (https://www.ebi.ac.uk/GOA/). First, the identified protein ID was converted to a UniProt ID, then each protein was mapped to a GO ID based on its UniProt ID. Subsequently, each protein was assigned a Gene Ontology functional classification based on three categories: biological process (BP), cellular component (CC), or molecular function (MF). Kyoto Encyclopedia of Genes and Genomes (KEGG) biological pathway analysis (https://www.genome.jp/kegg/pathway.html).

Enzyme-linked immunosorbent assay

Cell culture supernatants collected from A549 and H1299 cell cultures were analyzed for human thymidine phosphorylase (TP) and ribulose-5-phosphate (Ru5P) contents using ELISA kits (J&l Biological, China) in accordance with the manufacturer's instructions.

G6PD activity assay and $NADP^+$/NADPH assay

A549 cells were seeded into wells containing culture medium and cultured for 24 h. Next, cells were lysed, cell lysates were centrifuged, then supernatants were collected. G6PD activity of supernatants was determined using a kit (Beyotime, China) according to the manufacturer's instructions based on absorbance values measured at 450 nm. G6PD activity was proportional to NADPH concentration, as determined using a $NADP^+$/NADPH Assay Kit (Beyotime, China) according to the manufacturer's instructions.

Cancer genome atlas -based data analysis

Representative immunohistochemical assay images were downloaded from the Human Protein Atlas (https://www.proteinatlas.org) image archive. Lung cancer patient data were downloaded from The Cancer Genome Atlas Lung Adenocarcinoma (TCGA-LUAD) database (https://portal.gdc.cancer.gov/projects/TCGA-LUAD) and additional data were obtained from The Tumor Immune Estimation Resource 2.0 (TIMER2.0) database, a publicly available repository of data related to tumor immunity and tumor gene expression (http://timer.cistrome.org/). For data analysis, first the Gene DE module was used to study differential expression of TP among various types of tumors then the Gene Corr module was used to verify correlations between TP and Twist1 expression based on Spearman analysis of LUAD data. Kaplan-Meier Plotter (https://kmplot.com/analysis/) was used for prognostic analysis. Based on the median TP expression level, patient samples were divided into two groups then the two groups were compared with respect to overall survival (OS), first-progression (FP) survival, and post-progression survival (PPS).

Statistical analysis

For each study involving A549 and H1299 cells, three independent experiments were performed and statistical analysis of results was conducted using GraphPad Prism. All data in the study were evaluated using SPSS 24.0 statistical software. For each group were analyzed by one-way analysis. Measurement data were expressed as means ± SD (X ± SD). A difference of $P< 0.05$ was considered statistically significant.

Results

Isolation and characterization of ginseng-derived nanoparticles

First, we prepared plant-derived GDNPs by extracting juice from ginseng roots followed by processing of juice *via* centrifugation and filtration to isolate GDNPs. The result showed that GDNPs have an intact membrane and clearly visible the vesicle-like structure, and was generally spherical by Transmission electron microscopy (TEM) (Figure 1A). Meanwhile, Nanoparticle Tracking Analysis (NTA) revealed that the average diameter of GDNPs was about 119.7 nm, accounting for more than 93.5% of the total particle size, and also revealing a total particle concentration of 7.7E+6 particles/mL (Supplementary Table 1, Figures 1B, C). After GDNPs protein concentration was quantified using a BCA protein assay kit, GDNPS at various concentrations were evaluated for anticancer effects against five types of cancer cells (HepG2, HCT-116, A549, PANC-1, and MCF-7). Notably, results of MTT assays revealed that the GDNPs IC_{50} for A549 cells was approximately 80 μg/mL, a lower value than values obtained for the other cell lines (Figure 1D). To confirm this GDNPs effect on A549 cells, we also evaluated A549 cell uptake of PKH-67-labeled GDNPs by incubating A549 cells with 10 μg of PKH-67-labeled GDNPs for 0 h, 6 h, or 12 h. Immunofluorescence staining results demonstrated increased uptake with longer incubation times (Figure 1E, Supplementary Figure 1A). The results of flow cytometric analysis showed an increase in percentage of GDNPs-containing cells over time, as reflected by increasing absorption efficiency with time (Supplementary Figures 1B, C).

GDNPs treatment inhibited cancer cell migration and proliferation activities

Next, we studied GDNPs effects on cell migration using a wound-healing assay. Results of wound-healing assays indicated that GDNPs most significantly inhibited migration of A549 cells as compared to effects on migration of other cancer cell types (Figures 2A–F).

GDNPs treatment inhibited migration, invasion, clonal formation, and adhesion of human NSCLC cells

Based on findings of this study showing that GDNPs exerted excellent antitumor effects on A549 lung cancer cells, we next investigated whether GDNPs could exert additional antitumor effects on NSCLC cell-derived cells (A549 and H1299) in order to better understand mechanisms underlying GDNPs antitumor effects. First, GDNPs were assessed for their ability to inhibit migration and invasion activities of A549 and H1299 cells. Based on wound-healing assay results, GDNPs treatment resulted in significantly greater inhibition of migration of both cell types at 48 h as compared with results obtained for the untreated control group (Figure 3A). We next determined whether GDNPs could inhibit lung cancer cell invasion and adhesion activities. The results revealed that GDNPs were able to inhibit cell invasion and cell adherence (as based on cell numbers obtained in each assay) in a dose-dependent manner as compared to corresponding results obtained for the untreated group (Figures 3B, C). In addition, a cloning formation assay was performed that revealed that GDNPs inhibited cell clone formation ability in a dose-dependent manner (Figure 3D).

GDNPs treatment of human NSCLC cells inhibited adhesion tube formation and reduced levels of EMT-related markers

Emerging evidence has confirmed that EMT is associated with increases in migration, invasion, and unique vasculogenic mimicry (VM) abilities associated with aggressive cancer cells such as NSCLC cells. To elucidate the mechanism associated with GDNPs-mediated inhibition of metastatic activities of A549 and H1299 cells, effects of GDNPs treatment on EMT were evaluated. First, A549 and H1299 cells were treated with various doses of exosomes for 24 h. Next, the GDNPs effect on cell VM formation was investigated using tube formation assay, with results revealing that GDNPs treatment significantly reduced the number of tube-like structures as compared to numbers in the untreated control group (Figures 4A, B). Additionally, immunofluorescence assay results showed that GDNPs treatment led to significantly increased expression of epithelial cell marker E-cadherin and decreased expression of mesenchymal cell marker vimentin in a dose-dependent manner (Figures 4C, D). Moreover, qRT-PCR results revealed GDNPs treatment-induced decreases in levels of transcription

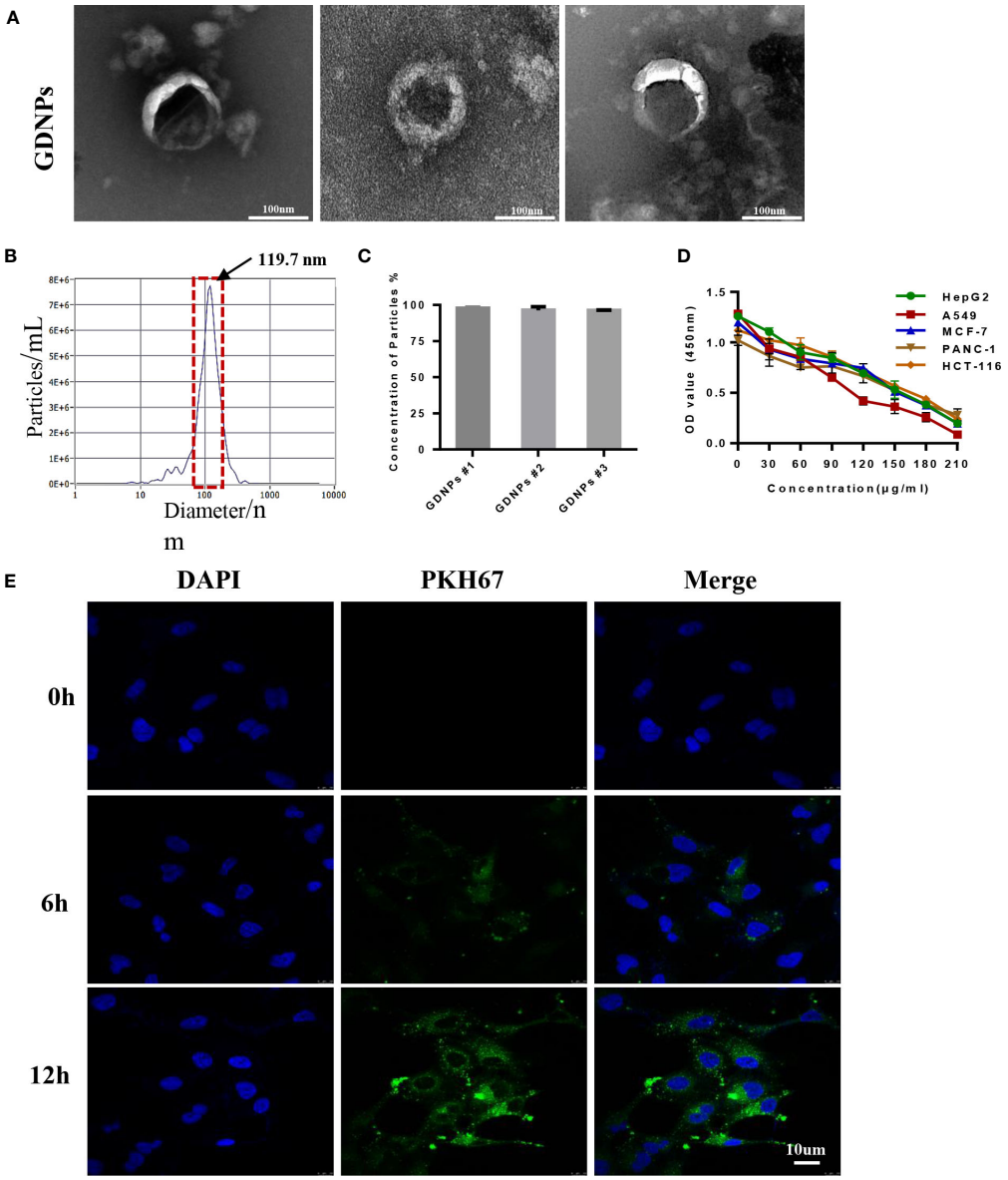

FIGURE 1
Characterization of nanoparticles derived from ginseng root. **(A)** The morphology of GDNPs was observed by TEM, scale bar = 100 nm (n = 3). **(B)** Nanoparticle tracking analysis (NTA)-based determination of GDNPs number and size distribution (n = 3). **(C)** GDNPs concentration expressed as percentage per batch (n = 3). **(D)** GDNPs effects on cell viability of HepG2, HCT-116, A549, PANC-1, and MCF-7 cells as analyzed *via* MTT assay. **(E)** Confocal microscopic image showing internalization of PKH-67-labeled GDPNs by A549 cells at indicated timepoints. Data are presented as the mean ± SD of three experiments.

factor proteins Twist1, Snail, and Slug (Figures 5A, B), while Western blot results revealed that E-cadherin and vimentin protein expression levels were consistent with immunofluorescence assay results showing GDNPs inhibition of Twist1 expression (Figures 5C, D). Therefore, these results collectively suggest that GDNPs inhibited both EMT occurrence and VM channel formation in lung cancer cells.

TP mRNA and protein levels were reduced after GDPNs treatment of A549 and H1299 cells

Previous studies had confirmed that main metabolic pathways associated with TP expression included the PPP and glycolysis, whereby TP expression was positively

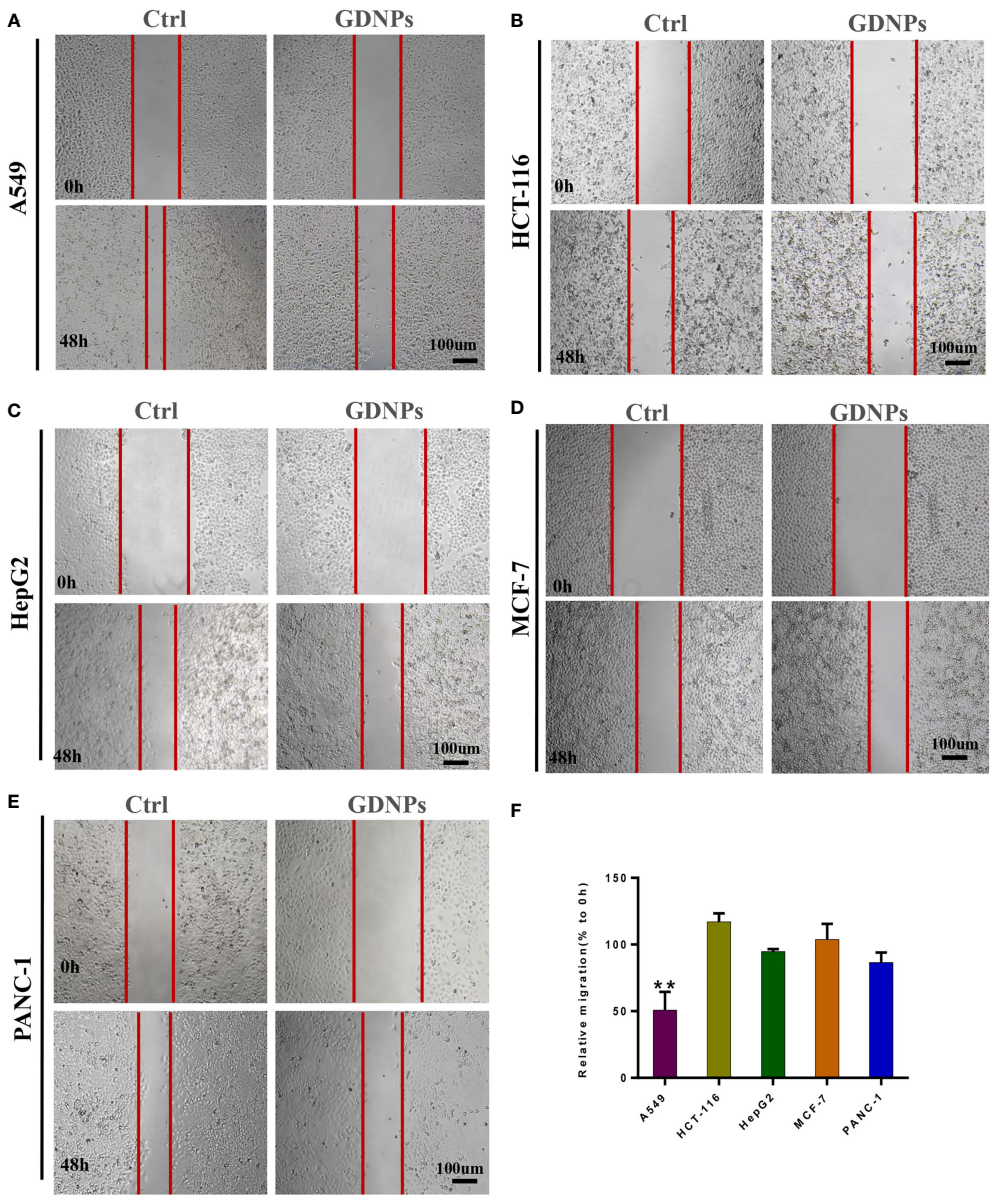

FIGURE 2
Effect of GDNPs on cancer cell migratory ability. **(A)** Analysis of A549 cells *via* wound-healing assay. **(B)** Analysis of HCT-116 cells *via* wound-healing assay. **(C)** Analysis of HepG2 cells *via* wound-healing assay. **(D)** Analysis of PANC-1 cells *via* wound-healing assay. **(E)** Analysis of MCF-7 cells *via* wound-healing assay. Images were acquired at 0 and 48 h. **(F)** Quantitative analysis of wound-healing assay data. Images were captured at 0 h and 48 h after wound formation, then the mean (%) change in width of the wound during healing was calculated by comparing wound width after 48-h healing (closure) to wound width at 0 h. Data are presented as the mean ± SD of three experiments (*P < 0.05).

correlated with tumor stage, metastasis, and poor prognosis (30, 31). Due to the fact that TP enzymatic activity is required for angiogenesis, tumor growth and metastasis, we verified effects of GDNPs treatment on TP expression by measuring cell contents of TP protein and TP-encoding mRNA. ELISA results showed that GDNPs treatment of A549 and H1299 cells significantly inhibited cellular secretion of overexpressed TP protein, as did treatment of cells with TPI (Figure 5E); similar results were obtained for TP mRNA levels (Figure 5F). Therefore, we hypothesized that GDNPs inhibited lung cancer metastasis by downregulating TP as a potential anticancer strategy.

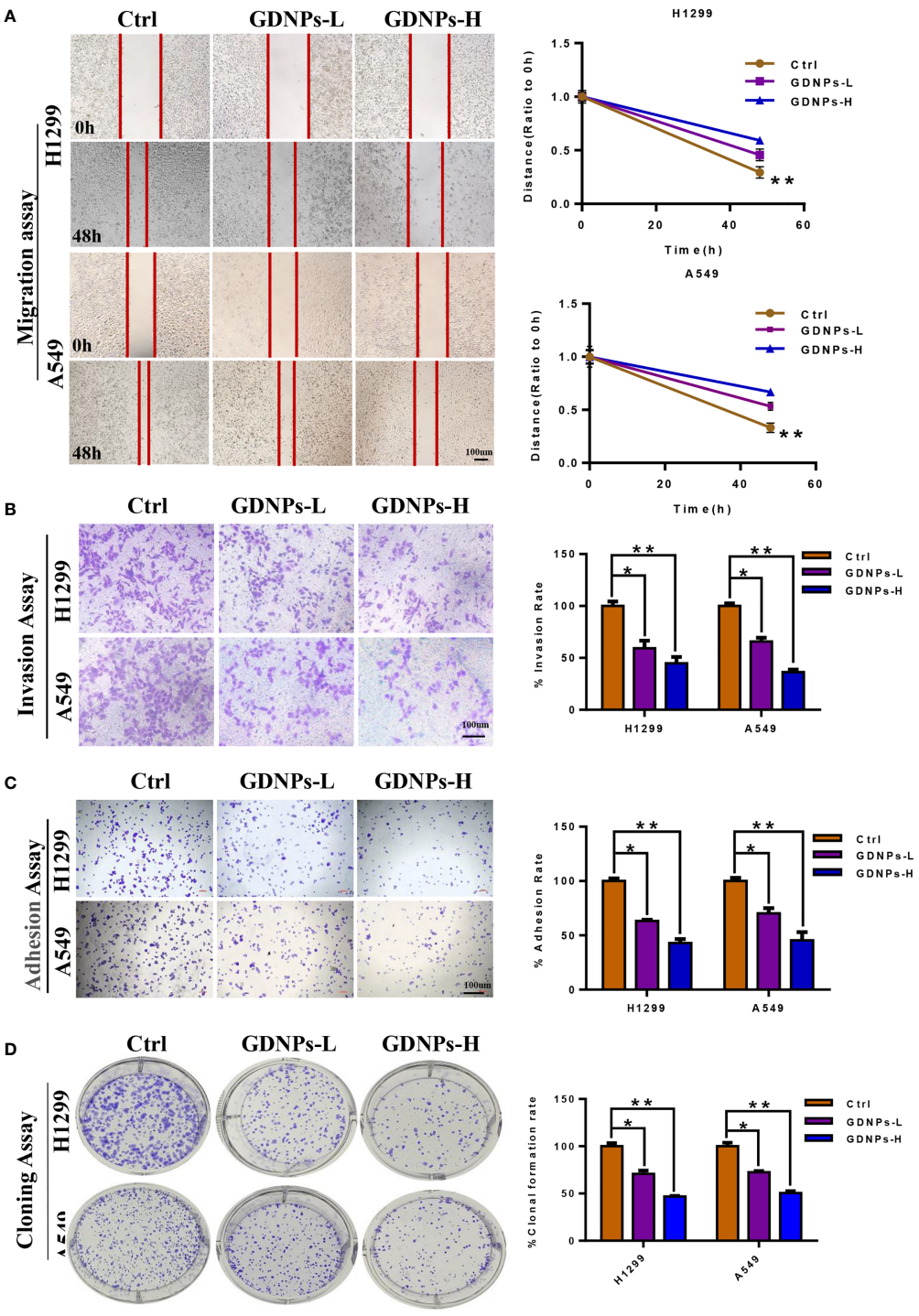

FIGURE 3
GDNPs inhibited human NSCLC cell migration, invasion, and colony formation. **(A)** GDNPs significantly inhibited migratory abilities of A549 and H1299 cells as compared with the untreated group cells as measured *via* the wound healing assay. **(B)** GDNPs significantly inhibited invasion abilities of two lung cancer cell lines as compared with the untreated group cells as measured vis the transwell assay. **(C)** GDNPs inhibited the adhesion of A549 and H1299 cells. **(D)** GDNPs inhibited colony formation by A549 and H1299 cells. GDNPs-H designates GDNPs at high concentration (60 μg/mL) and GDNPs-L designates GDNPs at low concentration (30 μg/mL). Statistical results are summarized in the right panel. Data are presented as the mean ± SD of three experiments (*P < 0.05 and **P < 0.01).

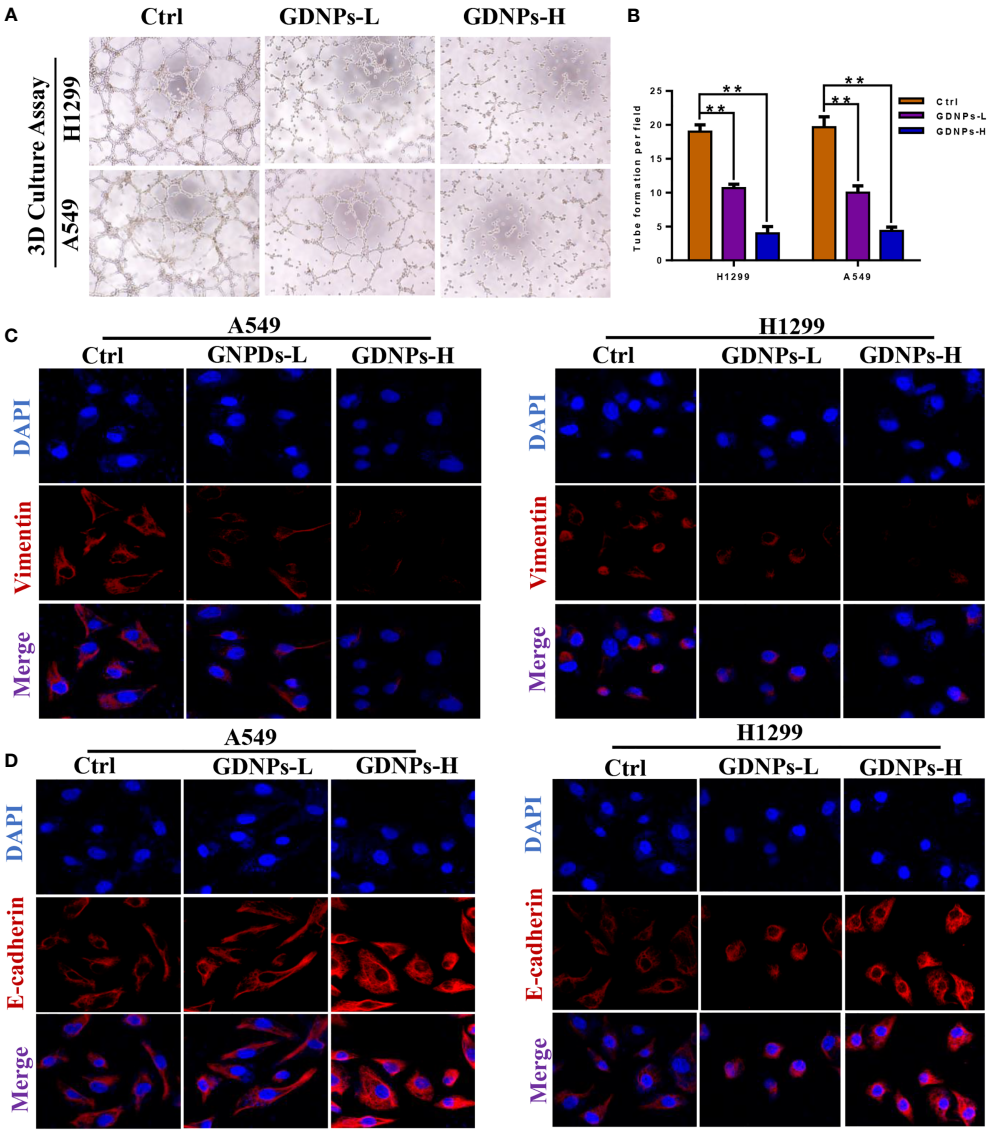

FIGURE 4
GDNPs treatment inhibited VM formation and reversed EMT biomarker changes. **(A, B)** Tube formation revealing decreased VM formation following GDNPs treatment, with statistical results summarized in panels to the right **(C, D)** Immunofluorescence assays revealed increased E-cadherin expression and decreased vimentin expression as compared with untreated group cells. Data are presented as the mean ± SD of three experiments (*P < 0.05).

Association of TP with clinical characteristics of lung cancer patients

To further elucidate the role of TP in lung cancer patient survival, we compared TP expression levels of different tumor types to TP expression in normal tissues based on data obtained from the TIMER2.0 database. Results of this analysis demonstrated higher TP expression levels in lung cancer cells versus normal lung cells (Figure 6A). In addition, we also obtained data from the Human Protein Atlas database to compare TP expression levels, as determined using immunohistochemical analysis, between lung cancer tissues and adjacent normal tissues. The results revealed that TP was expressed at higher levels in tumor tissues than in adjacent normal (non-tumor) tissues (Figure 6B). Concurrently, analysis of TCGA results (Normal n = 59, Tumor n = 53) showed that TP mRNA-level expression was higher in tumor tissues than in normal tissues (Figure 6C). Next, we analyzed the relationship

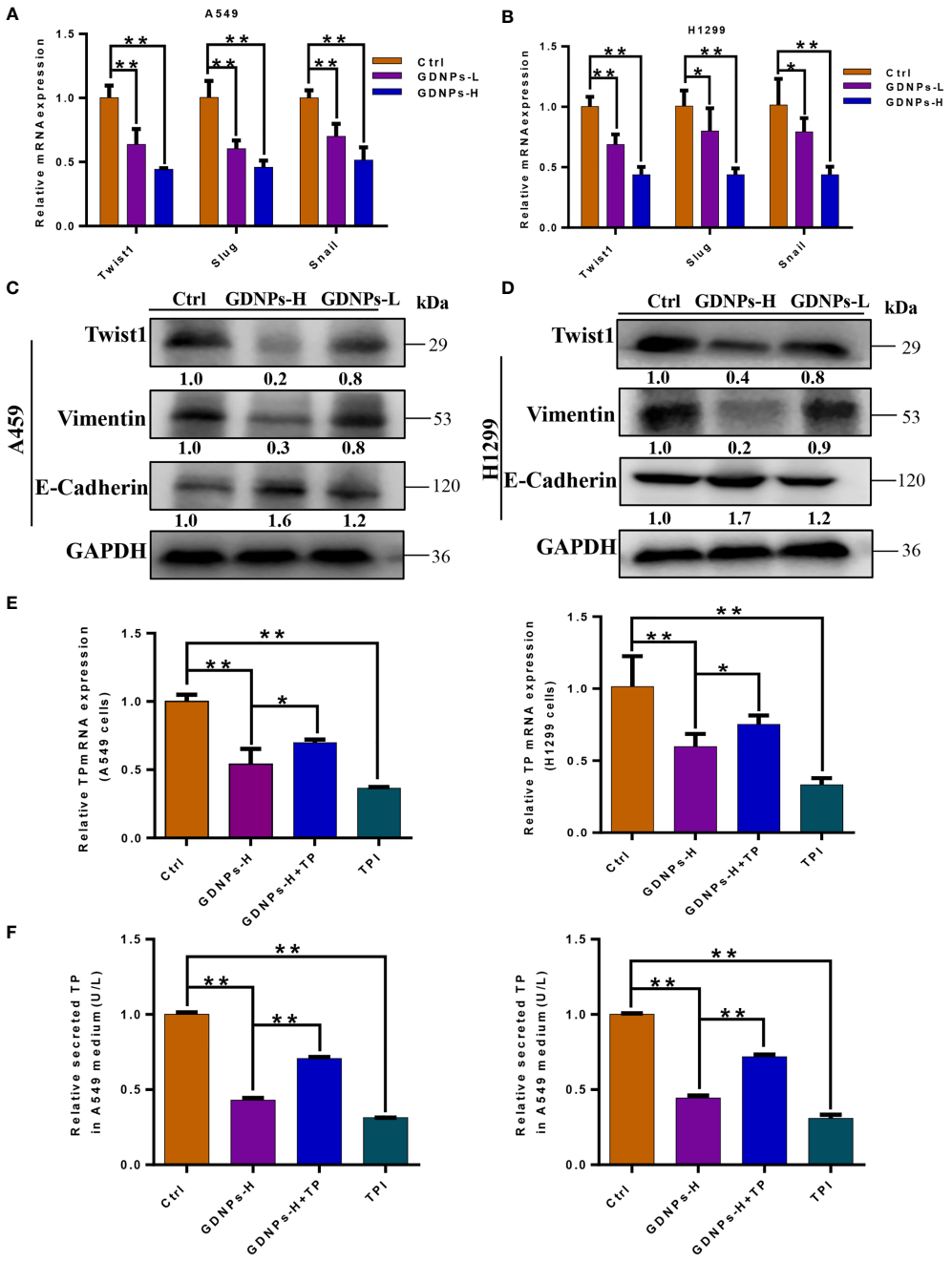

FIGURE 5
GDNPs treatment reduced levels of EMT-related makers and TP expression. **(A, B)** Expression of genes encoding epithelial and mesenchymal marker proteins in A549 and H1299 cells as measured *via* qRT-PCR after treatment of cells with GDNPs for 24 h. **(C, D)** Western blot results showing A549 and H1299 cells treated with GDNPs exhibited relatively decreased levels of vimentin and Twist1 and increased E-cadherin level as compared to untreated cells. **(E)** Results of qRT-PCR analysis showing expression levels of TP mRNA in A549 and H1299 cells. **(F)** Enzyme-linked immunosorbent assay results showing TP levels in medium of cultured cells. Data are presented as the mean ± SD of three experiments (*P < 0.05 and **P < 0.01).

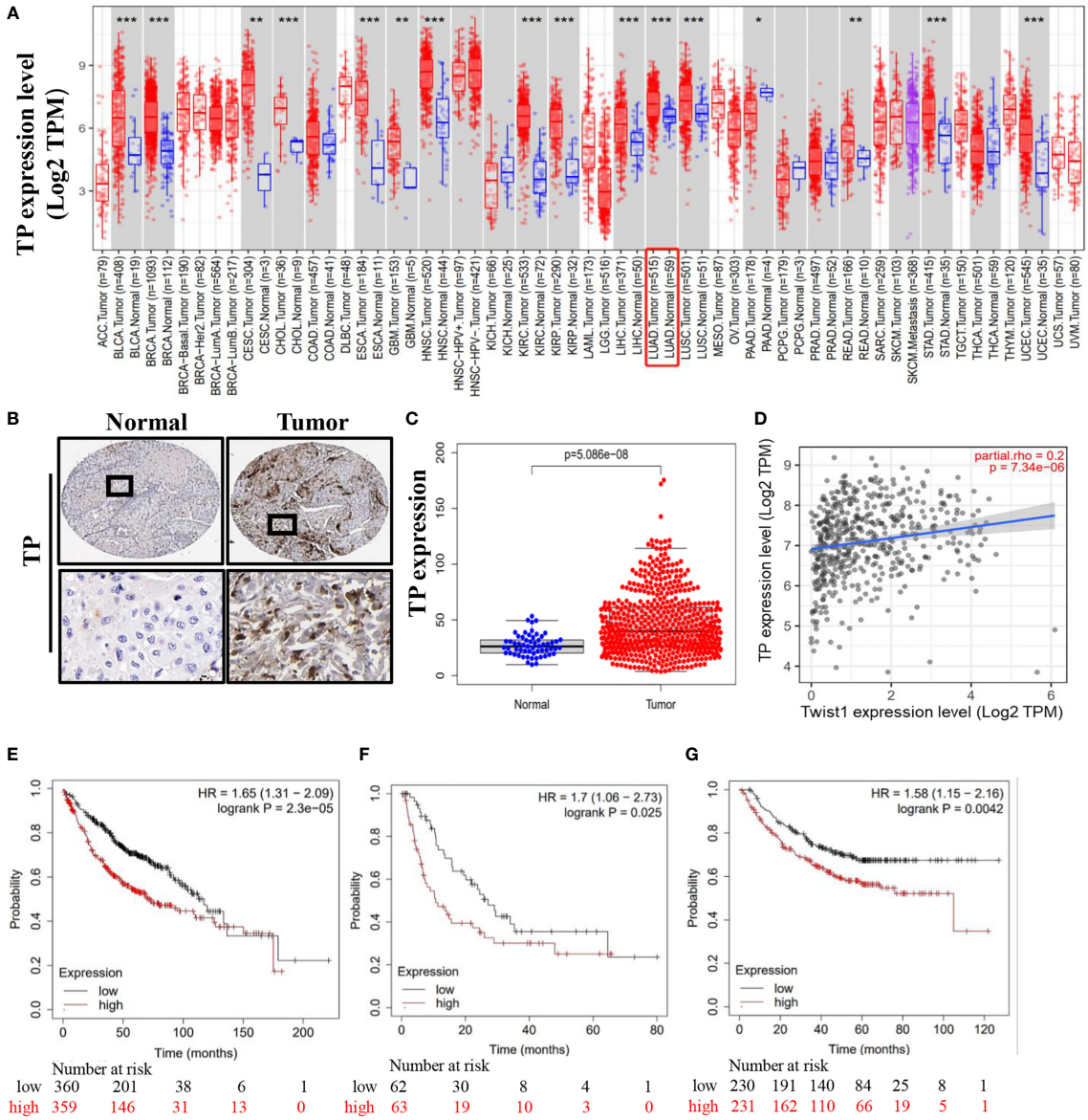

FIGURE 6
Lung cancer patient tissue TP levels as an indicator of poor prognosis. **(A)** High-level TP expression in lung cancer tissues. **(B, C)** Representative images derived from immunohistochemical staining of normal and lung cancer tumor tissues showing high tumor cell TP levels. **(D)** Correlation between TP and Twist1 expression levels. **(E)** Overall survival (OS). **(F)** First-progression survival (FP). **(G)** Post-progression survival (PPS). Data were obtained from the Human Protein Atlas and the TIMER2.0 database. (*P < 0.05 and **P < 0.01 and *** P < 0.001).

between TP expression and lung cancer patient prognosis. The results revealed that TP expression level was significantly and positively correlated with Twist1 expression in lung cancer cells (Figure 6D). Moreover, results of Kaplan–Meier analysis of microarray data showed that high TP expression was associated with poor prognosis, as reflected by low OS, PPS, and FP values associated with lung cancer patients (Figures 6E-G).

Proteomic analysis of GDNPs

Analysis of GDNPs proteins led to identification of proteins belonging to all three GO categories of Biological Process (BP), Cellular Component (CC), and Molecular Function (MF). GO analysis results revealed that: BP protein functional terms were mainly associated positive regulation of catabolism, small molecule metabolism process, intracellular protein transport, ribose

phosphate metabolic process, and small molecule biosynthesis process functions (Figure 7A); CC terms were mainly associated with cell-cell junction and endomembrane system functions (Figure 7B); and MF terms were mainly associated with small molecule binding, drug binding, coenzyme binding, and transferase activity functions (Figure 7C). We then investigated possible biological roles of exosome proteins based on KEGG pathway analysis. The results of KEGG analysis revealed that exosome proteins were mainly involved in several metabolic pathways, including the TCA cycle, PPP, pyruvate metabolism, and several other pathways (Figure 7D).

GDNPs reduced PPP activity by blocking the warburg effect in NSCLC cells

G6PD is the rate-limiting enzyme within the PPP, a pathway that serves as the main source of reducing equivalents (NADPH) and pentose phosphate needed for tumor cell activities. To investigate effects of GDNPs on PPP metabolism in NSCLC cells, we added the effective antimetabolic drug aminonicotinamide (6-AN, G6PD inhibitor) and TP expression to investigate GDNP effects on cellular levels of NADPH and PPP rate-limiting enzyme G6PD and production of PPP intermediate metabolite R-5-P. The results showed that, as compared with the control, treatment of cells with GDNPs significantly inhibited G6PD expression and reduced cellular NADPH levels (as reflected by a decrease in the NADP +/NADPH ratio). Meanwhile, compared with the GDNPs treatment group, with more pronounced inhibition observed when cells were treated with both GDNPs and 6-AN than when either treatment alone, but TP expression group attenuated the inhibitory effect of GDNPs. In addition, we measured levels of the PPP intermediate metabolite R-5-P. The results showed that GDNPs could effectively inhibit production of R-5-P, with the combination of GDNPS and 6-AN also significantly reducing production of intermediate metabolites (Figure 8A). Furthermore, results showing the effect of PPP activity on

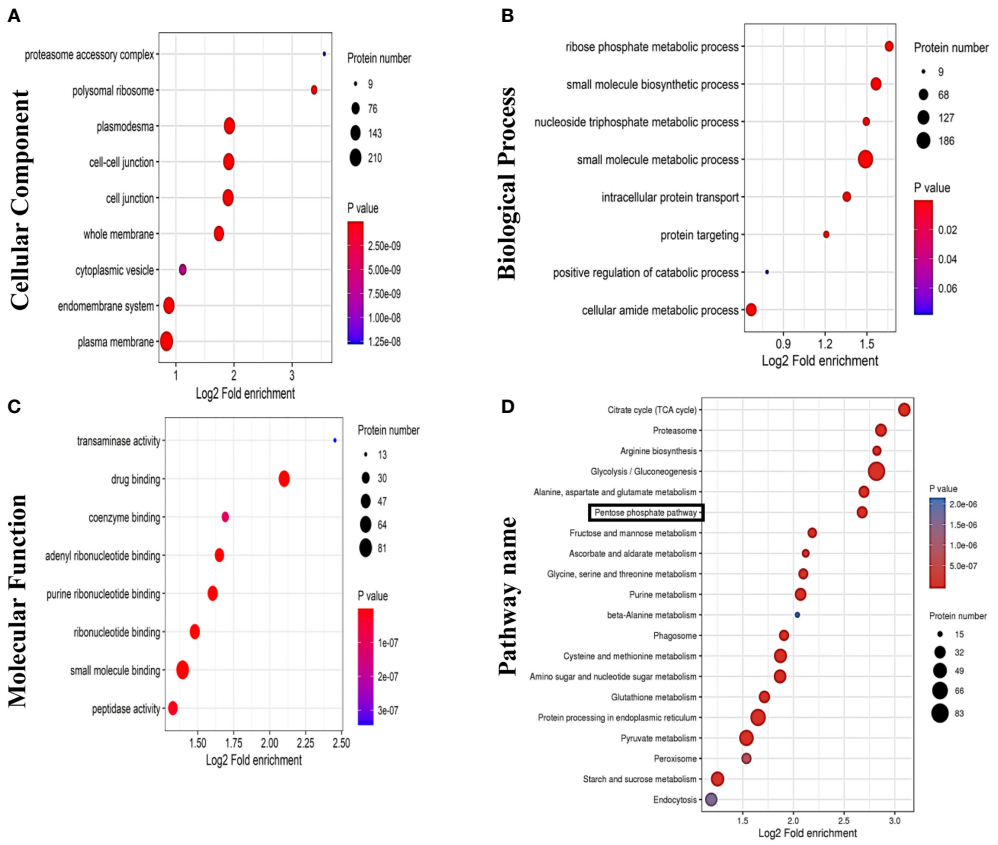

FIGURE 7
Results of proteomics analyses showing GDNPs effects on pentose phosphate pathway (PPP) activity. GO annotation results are listed under three main categories: **(A)** Biological Process. **(B)** Molecular Function. **(C)** Cellular Component. **(D)** KEGG pathway annotation analysis.

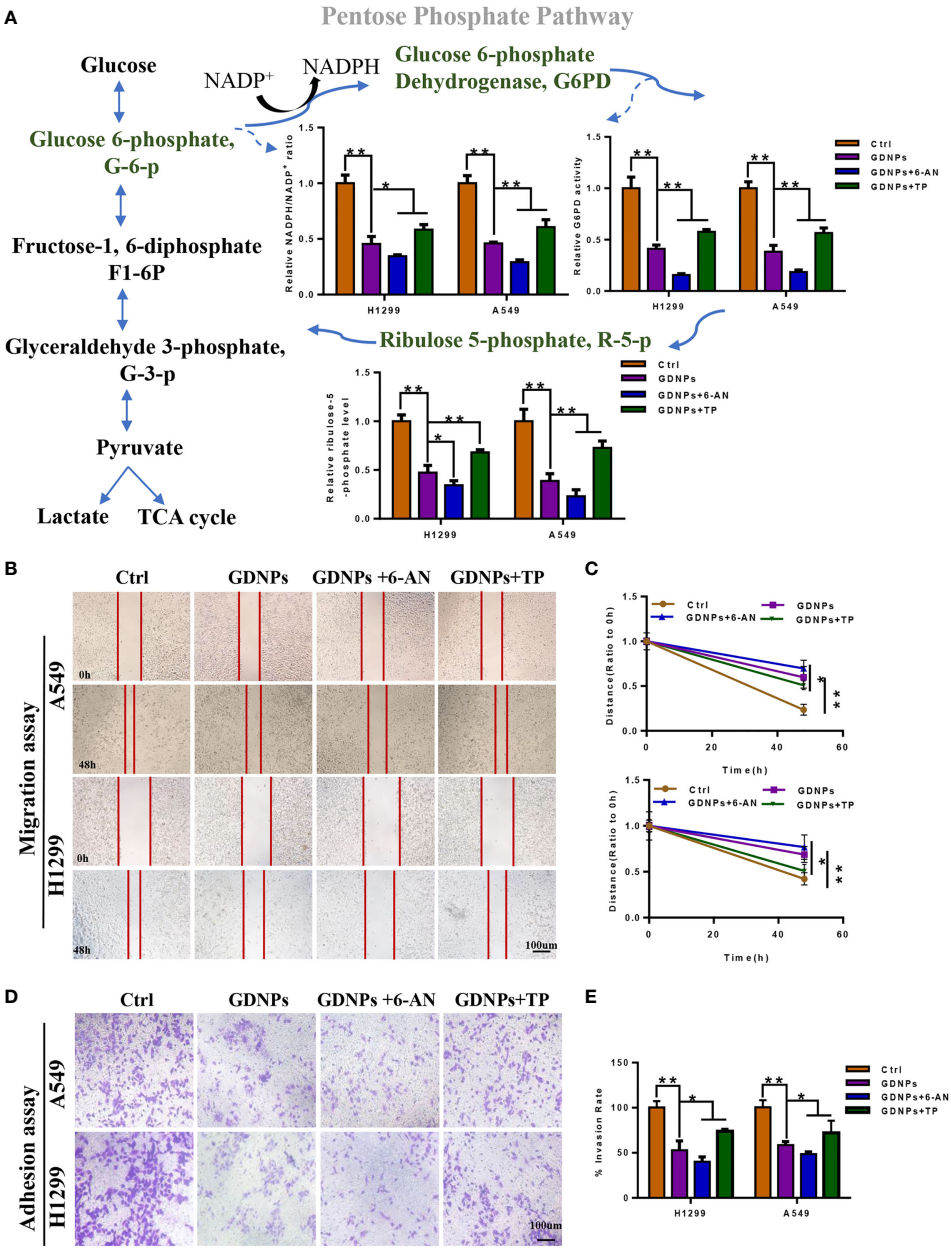

FIGURE 8
GDNPs and 6-AN can synergistically inhibit pentose phosphate pathway activities. **(A)** Contents of $NADP^+$/NADPH and relative G6PD activities in A549 and H1299 cells of control and treated groups. Detection of contents of intermediate pentose phosphate pathway metabolites in A549 and H1299 cells treated with GDNPs and 6-AN. **(B-E)** Effect of GDNPs and 6-AN on migration and invasion of A549 and H1299 cells. Images were obtained at 200× magnification. Cells were then treated with 6-AN (50 μM). Data are presented as the mean ± SD of three experiments (*P < 0.05 and **P < 0.01).

migration of lung cancer cells revealed that treatment of A549 and H1299 cells with GDNPs in combination with 6-AN significantly inhibited cell migration and TP expression group attenuated the inhibitory effect of GDNPs (relative to results obtained for the GDNPs group) (Figures 8B-E). Taken together, these results suggest that PPP is one of the key metabolic pathways affected by GDNPs -induced downregulation of TP expression.

Discussion

Lung cancer, a life-threatening oncological disease, is the leading cause of cancer-related deaths worldwide. It is well known that the majority of oncologic-related deaths are not caused by primary tumors but are instead caused by metastatic tumors (32, 33). The core process that is generally thought to drive tumor metastasis is the epithelial-mesenchymal transition (EMT), a process by which cells lose epithelial characteristics associated with low metastatic potential and gain mesenchymal cell characteristics associated with high metastatic potential (34). Main EMT hallmarks include loss of functional E-cadherin and overexpression of vimentin (35).

Extracellular vesicles (EVs) of mammalian cells, which can be internalized *via* endocytosis or phagocytosis, fuse with the target cell membrane then deliver their contents into the cytosol to influence cellular physiological and pathological processes (e.g., cancer, inflammatory bowel disease, and degenerative diseases) (36, 37). However, before EVs can be used to treat human diseases, challenges remain despite recent progress made in understanding EVs formation and secretion processes (38). Nevertheless, as compared to animal EVs, nanoparticles derived from edible plants are nontoxic, have low immunogenicity, can cross the blood-brain barrier, have target tissue specificity, can be internalized at high levels, and can be produced in large quantities (39, 40). To our knowledge, to date no applications of plant-derived nanoparticles for use in blocking cancer development have ever been described. This is surprising, due to the fact that from medicinal and functional perspectives, herbal nanoparticles appear to be easily internalized by mammalian cells and thus are amenable to experimental study for determining whether they can mediate cross-species communication (41).

In this study, we evaluated the integrity and size of GDNPs by TEM and NTA analysis. The results showed that GDNPs were in nanometer scale and have intact membranes with an average diameter of GDNPs was about 119.7 nm. Furthermore, our results revealed that GDNPs are stable and capable of functionally engaging in cross-species communication. In particular, here we demonstrated for the first time that GDNPs could be used to selectively inhibit growth of various types of cancer cells, while also significantly reducing migratory, infiltration, and clone formation abilities of A549 and H1299 lung cancer-derived cells. Moreover, GDNPs treatment also inhibited EMT and VM processes, upregulated E-cadherin expression, and decreased expression levels of vimentin and Twist1 to achieve an overall excellent antitumor effect.

Previous results reported by researchers associate with this study found that Twist1 production depends on TP-induced reprogramming of tumor metabolism to promote HCC cell VM formation and metastasis by invoking the pentose Warburg effect, thereby promoting tumor development (30). In this study, analysis of clinical data also revealed that high-level TP expression was positively correlated with low NSCLC patient prognostic indicator values for OS, PPS, and FP. The PPP, a major glucose metabolic pathway that is upregulated in cancer cells, depends on TP activity to convert pentose into glycerol-3-phosphate (G-3-P), a glycolytic pathway intermediate that links pentose metabolism with the glycolytic pathway. The results confirmed that GDNPs can inhibit PPP activity of lung cancer cells to reduce PPP-associated energy generation and PPP metabolic intermediates to ultimately inhibit tumor cell proliferation and other tumor-associated physiological processes. However, it remains to be determined whether ginseng-derived nanoparticles (GDNPs) inhibit lung cancer cell metastasis by downregulating TP expression through mechanisms involving miRNA- or protein-based PPP inhibition, warranting further study.

In summary, here we demonstrated for the first time that GDNPs could exert antitumor effects that effectively inhibited tumor cell proliferation, migration, invasion, and EMT occurrence. Mechanistically, antitumor GDNPs effects may be associated with downregulated TP expression resulting from PPP inhibition. These findings provide insights to guide future research on mechanisms underlying NSCLC progression and describe a new class of nano-drugs with potential activities for inhibiting cancer metastasis.

Data availability statement

The original contributions presented in the study are included in the article/Supplementary materials. Further inquiries can be directed to the corresponding authors.

Author contributions

LY, L-WS, and D-QZ conceived and designed the study. LY conducted the experiments and prepared the figures and tables. LY provided data analysis and wrote the original draft. W-QJ, X-LT, SZ, and RM supervised the research. All authors contributed to the article and approved the submitted version.

Funding

This work was supported by the National Natural Science Foundation of China (Grant No. U20A20402, 82104428). The Science and Technology Development of Jilin Province (No. 20210304002YY).

Conflict of interest

The authors declare that the research was conducted in the absence of any commercial or financial relationships that could be construed as a potential conflict of interest.

Publisher's note

All claims expressed in this article are solely those of the authors and do not necessarily represent those of their affiliated organizations, or those of the publisher, the editors and the reviewers. Any product that may be evaluated in this article, or claim that may be made by its manufacturer, is not guaranteed or endorsed by the publisher.

Supplementary material

The Supplementary Material for this article can be found online at: https://www.frontiersin.org/articles/10.3389/fonc.2022.942020/full#supplementary-material

References

1. Bonanno L, Pavan A, Ferro A, Calvetti L, Frega S, Pasello G, et al. Clinical impact of plasma and tissue next-generation sequencing in advanced non-small cell lung cancer: A real-world experience. *Oncologist* (2020) 25(12):e1996–2005. doi: 10.1634/theoncologist.2020-0148

2. Coudray N, Ocampo PS, Sakellaropoulos T, Narula N, Snuderl M, Fenyo D, et al. Classification and mutation prediction from non-small cell lung cancer histopathology images using deep learning. *Nat Med* (2018) 24(10):1559–67. doi: 10.1038/s41591-018-0177-5

3. Zhang P, Li Z, Yang G. Silencing of ISLR inhibits tumour progression and glycolysis by inactivating the IL6/JAK/STAT3 pathway in nonsmall cell lung cancer. *Int J Mol Med* (2021) 48(6):222. doi: 10.3892/ijmm.2021.5055

4. Giannos P, Kechagias KS, Gal A. Identification of prognostic gene biomarkers in non-small cell lung cancer progression by integrated bioinformatics analysis. *Biol (Basel)* (2021) 10(11):1200. doi: 10.3390/biology10111200

5. Jimenez Perez ZE, Mathiyalagan R, Markus J, Kim YJ, Kang HM, Abbai R, et al. Ginseng-berry-mediated gold and silver nanoparticle synthesis and evaluation of their *in vitro* antioxidant, antimicrobial, and cytotoxicity effects on human dermal fibroblast and murine melanoma skin cell lines. *Int J Nanomed* (2017) 12:709–23. doi: 10.2147/IJN.S118373

6. Kim JH, Kim M, Yun SM, Lee S, No JH, Suh DH, et al. Ginsenoside Rh2 induces apoptosis and inhibits epithelial-mesenchymal transition in HEC1A and ishikawa endometrial cancer cells. *Biomed Pharmacother Biomed Pharmacother* (2017) 96:871–6. doi: 10.1016/j.biopha.2017.09.033

7. Lee H, Lee S, Jeong D, Kim SJ. Ginsenoside Rh2 epigenetically regulates cell-mediated immune pathway to inhibit proliferation of MCF-7 breast cancer cells. *J Ginseng Res* (2018) 42(4):455–62. doi: 10.1016/j.jgr.2017.05.003

8. Liu Y, Fan D. Ginsenoside Rg5 induces apoptosis and autophagy *via* the inhibition of the PI3K/Akt pathway against breast cancer in a mouse model. *Food Funct* (2018) 9(11):5513–27. doi: 10.1039/C8FO01122B

9. Tian L, Shen D, Li X, Shan X, Wang X, Yan Q, et al. Ginsenoside Rg3 inhibits epithelial-mesenchymal transition (EMT) and invasion of lung cancer by down-regulating FUT4. *Oncotarget* (2016) 7(2):1619–32. doi: 10.18632/oncotarget.6451

10. Corrado C, Raimondo S, Chiesi A, Ciccia F, De Leo G, Alessandro R. Exosomes as intercellular signaling organelles involved in health and disease: basic science and clinical applications. *Int J Mol Sci* (2013) 14(3):5338–66. doi: 10.3390/ijms14035338

11. Raimondo S, Naselli F, Fontana S, Monteleone F, Lo Dico A, Saieva L, et al. Citrus limon-derived nanovesicles inhibit cancer cell proliferation and suppress CML xenograft growth by inducing TRAIL-mediated cell death. *Oncotarget* (2015) 6(23):19514–27. doi: 10.18632/oncotarget.4004

12. Sahin F, Kocak P, Gunes MY, Ozkan I, Yildirim E, Kala EY. *In vitro* wound healing activity of wheat-derived nanovesicles. *Appl Biochem Biotechnol* (2019) 188 (2):381–94. doi: 10.1007/s12010-018-2913-1

13. Mu J, Zhuang X, Wang Q, Jiang H, Deng ZB, Wang B, et al. Interspecies communication between plant and mouse gut host cells through edible plant derived exosome-like nanoparticles. *Mol Nutr Food Res* (2014) 58(7):1561–73. doi: 10.1002/mnfr.201300729

14. Dad HA, Gu TW, Zhu AQ, Huang LQ, Peng LH. Plant exosome-like nanovesicles: Emerging therapeutics and drug delivery nanoplatforms. *Mol Ther* (2021) 29(1):13–31. doi: 10.1016/j.ymthe.2020.11.030

15. Vashisht M, Rani P, Onteru SK, Singh D. Curcumin encapsulated in milk exosomes resists human digestion and possesses enhanced intestinal permeability in vitro. *Appl Biochem Biotechnol* (2017) 183(3):993–1007. doi: 10.1007/s12010-017-2478-4

16. Ju S, Mu J, Dokland T, Zhuang X, Wang Q, Jiang H, et al. Grape exosome-like nanoparticles induce intestinal stem cells and protect mice from DSS-induced colitis. *Mol Ther* (2013) 21(7):1345–57. doi: 10.1038/mt.2013.64

17. Wang B, Zhuang X, Deng ZB, Jiang H, Mu J, Wang Q, et al. Targeted drug delivery to intestinal macrophages by bioactive nanovesicles released from grapefruit. *Mol Ther* (2014) 22(3):522–34. doi: 10.1038/mt.2013.190

18. Zhang M, Viennois E, Prasad M, Zhang Y, Wang L, Zhang Z, et al. Edible ginger-derived nanoparticles: A novel therapeutic approach for the prevention and treatment of inflammatory bowel disease and colitis-associated cancer. *Biomaterials* (2016) 101:321–40. doi: 10.1016/j.biomaterials.2016.06.018

19. Teng Y, Ren Y, Sayed M, Hu X, Lei C, Kumar A, et al. Plant-derived exosomal MicroRNAs shape the gut microbiota. *Cell Host Microbe* (2018) 24 (5):637–52.e638. doi: 10.1016/j.chom.2018.10.001

20. Zhang M, Xiao B, Wang H, Han MK, Zhang Z, Viennois E, et al. Edible ginger-derived nano-lipids loaded with doxorubicin as a novel drug-delivery approach for colon cancer therapy. *Mol Ther* (2016) 24(10):1783–96. doi: 10.1038/mt.2016.159

21. Cao M, Yan H, Han X, Weng L, Wei Q, Sun X, et al. Ginseng-derived nanoparticles alter macrophage polarization to inhibit melanoma growth. *J Immunother Cancer* (2019) 7(1):326. doi: 10.1186/s40425-019-0817-4

22. Polat IH, Tarrado-Castellarnau M, Benito A, Hernandez-Carro C, Centelles J, Marin S, et al. Glutamine modulates expression and function of glucose 6-phosphate dehydrogenase *via* NRF2 in colon cancer cells. *Antioxid (Basel)* (2021) 10(9):1349. doi: 10.3390/antiox10091349

23. Ghanem N, El-Baba C, Araji K, El-Khoury R, Usta J, Darwiche N. The pentose phosphate pathway in cancer: Regulation and therapeutic opportunities. *Chemotherapy* (2021) 66(5-6):179–91. doi: 10.1159/000519784

24. Vander Heiden MG, Cantley LC, Thompson CB. Understanding the warburg effect: the metabolic requirements of cell proliferation. *Science* (2009) 324(5930):1029–33. doi: 10.1126/science.1160809

25. Cho ES, Cha YH, Kim HS, Kim NH, Yook JI. The pentose phosphate pathway as a potential target for cancer therapy. *Biomol Ther (Seoul)* (2018) 26 (1):29–38. doi: 10.4062/biomolther.2017.179

26. Tabata S, Yamamoto M, Goto H, Hirayama A, Ohishi M, Kuramoto T, et al. Thymidine catabolism promotes NADPH oxidase-derived reactive oxygen species (ROS) signalling in KB and yumoto cells. *Sci Rep* (2018) 8(1):6760. doi: 10.1038/s41598-018-25189-y

27. Ko JC, Chen JC, Chen TY, Yen TC, Ma PF, Lin YC, et al. Inhibition of thymidine phosphorylase expression by Hsp90 inhibitor potentiates the cytotoxic effect of salinomycin in human non-small-cell lung cancer cells. *Toxicology* (2019) 417:54–63. doi: 10.1016/j.tox.2019.02.009

28. Lee R, Ko HJ, Kim K, Sohn Y, Min SY, Kim JA, et al. Anti-melanogenic effects of extracellular vesicles derived from plant leaves and stems in mouse melanoma cells and human healthy skin. *J Extracell Vesicles* (2020) 9(1):1703480. doi: 10.1080/20013078.2019.1703480

29. Gao Z, Han X, Zhu Y, Zhang H, Tian R, Wang Z, et al. Drug-resistant cancer cell-derived exosomal EphA2 promotes breast cancer metastasis *via* the EphA2-

ephrin A1 reverse signaling. *Cell Death Dis* (2021) 12(5):414. doi: 10.1038/s41419-021-03692-x

30. Zhang Q, Qin Y, Zhao J, Tang Y, Hu X, Zhong W, et al. Thymidine phosphorylase promotes malignant progression in hepatocellular carcinoma through pentose warburg effect. *Cell Death Dis* (2019) 10(2):43. doi: 10.1038/s41419-018-1282-6

31. Bijnsdorp IV, Azijli K, Jansen EE, Wamelink MM, Jakobs C, Struys EA, et al. Accumulation of thymidine-derived sugars in thymidine phosphorylase overexpressing cells. *Biochem Pharmacol* (2010) 80(6):786–92. doi: 10.1016/j.bcp.2010.05.009

32. Kejik Z, Kaplanek R, Dytrych P, Masarik M, Vesela K, Abramenko N, et al. Circulating tumour cells (CTCs) in NSCLC: From prognosis to therapy design. *Pharmaceutics* (2021) 13(11):1879. doi: 10.3390/pharmaceutics13111879

33. Šutić M, Vukić A, Baranašić J, Försti A, Džubur F, Samaržija M, et al. Diagnostic, predictive, and prognostic biomarkers in non-small cell lung cancer (NSCLC) management. *J Personalized Med* (2021) 11(11):1102. doi: 10.3390/jpm11111102

34. Chaw SY, Abdul Majeed A, Dalley AJ, Chan A, Stein S, Farah CS. Epithelial to mesenchymal transition (EMT) biomarkers–e-cadherin, beta-catenin, APC and vimentin–in oral squamous cell carcinogenesis and transformation. *Oral Oncol* (2012) 48(10):997–1006. doi: 10.1016/j.oraloncology.2012.05.011

35. Li S, Zhang HY, Du ZX, Li C, An MX, Zong ZH, et al Induction of epithelial–mesenchymal transition (EMT). by *Beclin 1 knockdown via posttranscriptional upregulation of ZEB1 in thyroid cancer cells. Oncotarget.* (2016) 7(43):70364–70377. doi: 10.18632/oncotarget.12217

36. Saman S, Kim W, Raya M, Visnick Y, Miro S, Saman S, et al. Exosome-associated tau is secreted in tauopathy models and is selectively phosphorylated in cerebrospinal fluid in early Alzheimer disease. *J Biol Chem* (2012) 287(6):3842–9. doi: 10.1074/jbc.M111.277061

37. Guo S, Chen J, Chen F, Zeng Q, Liu WL, Zhang G. Exosomes derived from fusobacterium nucleatum-infected colorectal cancer cells facilitate tumour metastasis by selectively carrying miR-1246/92b-3p/27a-3p and CXCL16. *Gut* (2020) 71(2):e1–e3. doi: 10.1136/gutjnl-2020-321187

38. Colombo M, Raposo G, Théry C. Biogenesis, secretion, and intercellular interactions of exosomes and other extracellular vesicles. *Annu Rev Cell Dev Biol* (2014) 30(1):255–89. doi: 10.1146/annurev-cellbio-101512-122326

39. Sarvarian P, Samadi P, Gholipour E, Shams Asenjan K, Hojjat-Farsangi M, Motavalli R, et al. Application of emerging plant-derived nanoparticles as a novel approach for nano-drug delivery systems. *Immunol Invest* (2021), 51(4):1–21. doi: 10.1080/08820139.2021.1891094

40. Wong AS, Che CM, Leung KW. Recent advances in ginseng as cancer therapeutics: a functional and mechanistic overview. *Nat Prod Rep* (2015) 32 (2):256–72. doi: 10.1039/C4NP00080C

41. Mathiyalagan R, Yang DC. Ginseng nanoparticles: a budding tool for cancer treatment. *Nanomed (Lond)* (2017) 12(10):1091–4. doi: 10.2217/nnm-2017-0070

frontiers | Frontiers in Oncology

TYPE Review
PUBLISHED 24 August 2022
DOI 10.3389/fonc.2022.968591

Check for updates

OPEN ACCESS

EDITED BY
Tao Sun,
Nankai University, China

REVIEWED BY
Evin Iscan,
Dokuz Eylül University, Turkey
Jiang Chen,
Zhejiang University, China
P. Lin,
Cytelligen, United States

*CORRESPONDENCE
Zhiming Li
lzmleo@xmu.edu.cn
Yong Yan
2246827070@qq.com

SPECIALTY SECTION
This article was submitted to Pharmacology of Anti-Cancer Drugs, a section of the journal Frontiers in Oncology

RECEIVED 14 June 2022
ACCEPTED 01 August 2022
PUBLISHED 24 August 2022

CITATION
Hua Y, Dong J, Hong J, Wang B, Yan Y and Li Z (2022) Clinical applications of circulating tumor cells in hepatocellular carcinoma. *Front. Oncol.* 12:968591. doi: 10.3389/fonc.2022.968591

COPYRIGHT
© 2022 Hua, Dong, Hong, Wang, Yan and Li. This is an open-access article distributed under the terms of the Creative Commons Attribution License (CC BY). The use, distribution or reproduction in other forums is permitted, provided the original author(s) and the copyright owner(s) are credited and that the original publication in this journal is cited, in accordance with accepted academic practice. No use, distribution or reproduction is permitted which does not comply with these terms.

Clinical applications of circulating tumor cells in hepatocellular carcinoma

Yinggang Hua[1], Jingqing Dong[1], Jinsong Hong[1], Bailin Wang[1], Yong Yan[1*] and Zhiming Li[2*]

[1]Department of General Surgery, Guangzhou Red Cross Hospital, Jinan University, Guangzhou, China, [2]Institute of Reproductive Health, Tongji Medical College, Huazhong University of Science and Technology, Wuhan, China

Hepatocellular carcinoma (HCC) is a highly malignant tumor and ranked as the fourth cause of cancer-related mortality. The poor clinical prognosis is due to an advanced stage and resistance to systemic treatment. There are no obvious clinical symptoms in the early stage and the early diagnosis rate remains low. Novel effective biomarkers are important for early diagnosis and tumor surveillance to improve the survival of HCC patients. Circulating tumor cells (CTCs) are cancer cells shed from primary or metastatic tumor and extravasate into the blood system. The number of CTCs is closely related to the metastasis of various solid tumors. CTCs escape from blood vessels and settle in target organs, then form micro-metastasis. Epithelial-mesenchymal transformation (EMT) plays a crucial role in distant metastasis, which confers strong invasiveness to CTCs. The fact that CTCs can provide complete cellular biological information, which allows CTCs to be one of the most promising liquid biopsy targets. Recent studies have shown that CTCs are good candidates for early diagnosis, prognosis evaluation of metastasis or recurrence, and even a potential therapeutic target in patients with HCC. It is a new indicator for clinical application in the future. In this review, we introduce the enrichment methods and mechanisms of CTCs, and focus on clinical application in patients with HCC.

KEYWORDS

circulating tumor cells, hepatocellular carcinoma, epithelial-mesenchymal transformation, clinical application, detection methods

Abbreviations: AFP, alpha-fetoprotein; ASGPR, sialoglycoprotein receptor; BCLC, Barcelona clinic liver cancer; CD44, cluster of differentiation 44; CD45, cluster of differentiation 45; CD90, cluster of differentiation 90; CD133, cluster of differentiation 133; CPS1, carbamoyl phosphate synthetase 1; CSCs, circulating cancer stem cells; CTCs, Circulating tumor cells; EMT, Epithelial-mesenchymal transformation; EpCAM, epithelial Cell adhesion molecule; GPC3, glypican-3; HCC, Hepatocellular carcinoma; Hep Par 1, hepatocyte paraffin 1; IF, immunofluorescence; iFISH, immunofluorescence *in situ* hybridization; MET, mesenchymal-epithelial transition; MMP, matrix metalloproteinase; pAkt, phosphorylated protein kinase B; PD-L1, programmed cell death ligand 1; pERK, phosphorylated extracellular signal-regulated kinase; qRT-PCR, quantitative real-time PCR; TNM, tumor-node-metastasis; AUC, area under the curve; BLD, benign liver disease; CTCs, circulating tumor cells; DFS, disease-free survival; EMT, epithelial to mesenchymal transition; HCC, hepatocellular carcinoma; HV, healthy volunteers; IF, immunofluorescence; LTx, liver transplantation; OS, overall survival; PFS, progression-free survival; RFS, recurrence-free survival; TACE, transcatheter arterial chemoembolization; TNM, tumor-node-metastasis

Introduction

Hepatocellular carcinoma (HCC) accounts for about 90% of all primary hepatic malignancies and is one of the most common malignancies. HCC ranks as the sixth most common tumor and its mortality ranks fourth in cancer-related death worldwide, with a high incidence in Asia and Africa (1). Patients with early-stage HCC may undergo curative therapies such as surgical liver resection (LR), liver transplantation (LT) and local ablation. On the other hand, patients with advanced-stage HCC usually accept non-curative therapies such as transcatheter arterial chemoembolization, radiotherapy and systemic therapies (2). Due to the absence of obvious clinical symptoms in the early stage of HCC, most patients are diagnosed with advanced HCC for the first time. The existing methods are difficult to effectively prolong the survival of patients, with a 5-year survival rate of less than 20%. Therefore, the key to improving the prognosis of HCC patients are to find effective means for early diagnosis, surveillance response of treatment, and early intervention (3).

Currently, the diagnosis of HCC mainly depends on serum markers, imaging examination and liver biopsy. Serum alpha-fetoprotein (AFP) is the most widely used tumor marker for early screening and surveillance progression of HCC, nevertheless, it has unsatisfactory performance with a sensitivity of only 60% and specificity of only 80% (4, 5). The updated American Association for the Study of Liver Disease (AASLD) guidelines no longer recommended AFP testing as part of HCC diagnostic criteria (6). Other serum markers, such as osteopontin, Golgi protein-73 or glypican-3 may offer information about the biological aggressiveness of HCC, but they are not erratic and accurate enough to form part of a screening strategy (7–9). Medical imaging methods including B-ultrasound, computed tomography (CT), and magnetic resonance imaging (MR) are recommended for the diagnosis of HCC, however, those methods are difficult to detect early-stage liver cancer with a diameter of less than 1 cm. Although liver biopsy can provide definitely a pathological diagnosis, there is a debate on the widespread use of liver biopsy due to the risks of bleeding and tumor seeding (10). Therefore, we need to find effective markers for early diagnosis and monitoring of recurrence and metastasis in patients with HCC.

In recent years, liquid biopsy technology has gradually emerged and has become one of the most promising methods for early diagnosis and real-time progress assessment of tumors with the advantages of non-invasive and repeated sampling. CTCs, which are the most concerned tumor detection method in liquid biopsy, is obtained from the peripheral blood of patients and carry much comprehensive tumor information for early diagnosis and monitoring of tumors. CTCs were originally discovered in the blood of breast cancer patients by Australian physicians Thomas Ashworth (11). CTCs are a very scarce sub-population of cancer cells released from primary solid tumors or metastatic sites into the peripheral circulation and eventually form metastatic lesions in other target organs (12). The number of CTCs in the circulating system is extremely rare (only a few CTCs in billions of blood cells), a range of 0 – 86 CTCs were detected in 5 mL of blood in HCC patients (13).

In the early stages, little is known about the characteristics and phenotypes of CTCs, and the limitation of enrichment technique leads to a big challenge for the detection of CTCs. With the emergence of new technologies, the improvement of existing technologies and the deepening of understanding of oncology, the detection rate of CTCs has been greatly improved. Currently, CTCs detection has been applied in clinical trials on a small scale. The CellSearch system for CTCs detection, the only approved technology by the US Food and Drug Administration, has been used for breast, lung, prostate and colon cancer (14–16). In recent years, CTCs detection plays an increasingly important role in HCC clinical management.

CTCs can not only provide information about abnormal protein expression, genomic mutation and mRNA variation of solid tumors, but also help people understand the mechanism of tumorigenesis, metastasis and drug resistance from aspects of cell morphology, migration ability and drug response (17–19). Correspondingly, CTCs detection can be used for early diagnosis, individualized treatment, and monitoring of prognosis and recurrence (20). In HCC, rich blood is present around the immediate vicinity of the tumor, allowing thousands of CTCs to be released into the blood circulation daily. CTCs carry a large amount of tumor information and are used as a clinical biomarker for HCC. In the present review, we introduce the enrichment methods and different phenotypes of CTCs and focus on clinical application in patients with HCC.

Enrichment and identification of CTCs

About 10^6 CTCs fall off into the peripheral blood circulation per gram of tumor primary or metastatic tissue daily, but more than 99.99% of CTCs lose their activity under the attack of the human immune defense system, and only <0.01% of CTCs can survive (21). Every milliliter of blood contains only a few of CTCs, while there are billions of normal blood cells, various proteins, nucleic acids, carbohydrates and other substances. The sensitivity of the enrichment effect is greatly affected by the background interference. Most of the CTCs travel as individual cell, but some as clusters, also known as micro-emboli. Micro-emboli are more easily infiltrate distant tissues and form metastases than individual cell in cancers (22–24). In addition,

some CTCs can interact with platelets in the blood and accomplish the phenotypic transformation of tumor cells, resulting in poor prognosis (25, 26). A series of techniques recently have been developed to separate and enrich CTCs from complex background. The capture methods can be divided into the physical techniques and biological techniques according to the properties of CTCs.

Physical methods capture CTCs from erythrocytes and leukocytes through the physical properties of CTCs, including size, density, deformability, and electrical charge. Density gradient centrifugation is based on the difference in density and sedimentation rate between CTCs and blood cells. CTCs and blood components are distributed to specific positions under a certain centrifugal force (27). This method is simple to operate, but is not widely used due to its low sensitivity, specificity and time-consuming. Microfiltration is a physical method based on the assumption that the diameter of tumor cells is too larger than erythrocytes and leukocytes to pass through a filter with lots of small pores (28, 29). However, some studies showed the cell-size based microfiltration loss amount of small size CTCs, resulting in false negative results (30–32). The CTCs ≤ 5μm are particularly observed in a majority of HCC CTCs, which is lost during microfiltration (30). Dielectrophoresis is a method to separate CTCs from blood according to the difference of charge between CTCs and other blood cells (33). Other physical separation and enrichment techniques include microfluidic, acoustophoresis, et al. (34, 35). CTCs enrichment based on physical properties enables high-throughput, but these methods possess a low specificity and a higher false-positive rate due to some blood cells may exhibit similar physical properties to CTCs.

Biological methods capture CTCs based on cellular immune characteristics that specific antibodies or ligands target to the antigens presented on the cell membrane of CTCs. The affinity ligands or antibodies are immobilized on microdevices or magnetic beads to bind with antigens on the cell membrane of CTCs, which achieve efficient and high-purity enrichment (36). Biological methods can be divided into two subcategories: positive techniques and negative techniques. Cellsearch system is the most representative of positive enrichment methods, which is only approved by the US Food and Drug Administration for the detection of CTCs (16). This system employs immunomagnetic beads coated with an antibody specifically against the epithelial Cell adhesion molecule (EpCAM) antigens on CTCs cell surface, and has already been applied in HCC (37–44). However, several types of tumor cells express low level of EpCAM, and some CTCs may lose the expression of EpCAM during the process of EMT (Figure 1). This largely limits the sensitivity of Cellsearch system for EpCAM negative tumor cells (45, 46). The negative enrichment method employs immunomagnetic beads coated with CD45 antibodies to bind the antigens on the surface of leukocytes, and then the binding leukocytes are removed with the beads (47, 48). This indirectly enriching CTCs method makes up for the limitation that the Cellsearch system is highly dependent on EpCAM. Additionally, many research studies show that CTCs detection with a single marker is inefficient. The combination of multiple markers and a physical enrichment method could increase the sensitivity and specificity of CTCs detection.

The most common method to identify CTCs are through immunofluorescence (IF), which provides the size and morphology of CTCs (49). Other identification methods includes flow cytometry (50), quantitative real-time PCR (qRT-PCR) (51) and immunofluorescence *in situ* hybridization (iFISH) (52). Now multiple detection methods have been used together to improve enrichment efficiency. Microfluidic chips achieve a high sensitivity and specificity in the separation of CTCs by the combination of cell size and immunoaffinity (53, 54). The CanPatrol system combines microfiltration and RNA *in situ* hybridization, which can simultaneously identify CTCs with EMT phenotype and has been widely used in various tumors including HCC (13, 22, 52, 55–61). A novel integrated strategy, subtraction enrichment (SE)-iFISH, improved the detection of HCC CTCs (30). $EpCAM^+$ CTCs and $EpCAM^-$ CTCs, each with different ploidy of chromosome 8, were effectively detected in patients with hepatobiliary malignances.

EMT and CTCs

Many evidence shows a strong relationship between EMT and CTC. EMT is a dynamic process in which the epithelial phenotype cells transition into mesenchymal phenotype cells with the downregulation of epithelial markers (E-cadherin, EpCAM) and upregulation of mesenchymal markers (N-cadherin, vimentin) (62, 63). EMT is critical for embryonic development and tissue repair under physiological conditions, however, it is also thought to play a crucial role in tumor progression by promoting tissue infiltration and metastases (64, 65). EMT is a complex process involving multiple signaling pathways and transcription factor regulation, the up-regulation of mesenchymal genes and suppression of epithelial genes lead to the transformation of cell morphology and acquisition of stronger invasive migration capability (66). Many changes in cellular shape and vitality, such as loss of cellular polarity, the disappearance of intercellular adhesion, and the acquisition of enhanced motility, which promote cells to fall off from tumor tissues and invade into blood vessels (64, 67, 68). EMT process facilitates the secretion of matrix metalloproteinase (MMP), which degrades the extracellular matrix to cause cell migration, tissue invasion and blood vessel infiltration (69). EMT is believed to play an important role in tumor

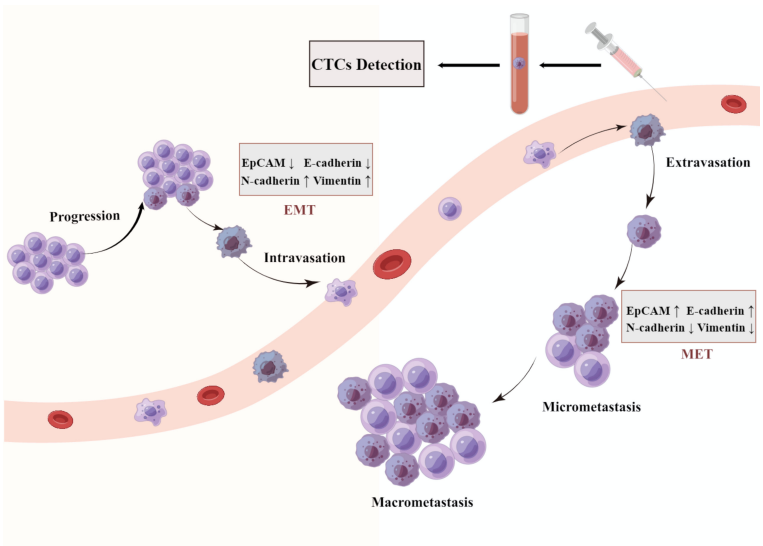

FIGURE 1
A schematic representation of epithelial mesenchymal transition (EMT). Cancer cells detach from the basement membrane and intravasate to the nearby blood vessels as CTC and travel through blood vessels to a secondary site in a process described as metastasis. They get lodged in different organs by a process termed as mesenchymal epithelial transition (MET).

occurrence and progression. The studies have demonstrated that the expression of EMT markers is associated with an aggressive malignant phenotype and with poor prognosis in cancer patients (65, 67, 70).

Recent studies found that tumor cells undergoing EMT are associated with the acquisition of stem cell characteristics (71), immunosuppression (72), resistance to radiotherapy (73) and chemotherapy (74, 75). A recent study in patients with HCC reported that the presence of mesenchymal phenotype CTCs was significantly correlated with high AFP levels, multiple tumors, advanced TNM stages, presence of embolus or micro-embolus, and earlier recurrence (57). Another study showed that mesenchymal phenotype CTCs were an independent risk factor for early recurrence, indicating a shorter postoperative disease-free survival in patients with HCC (60).

EMT promotes the spread of cancer cells from the primary tumor into the blood. Upon arrival at a suitable secondary location, CTCs undergo the MET transformation from the non-proliferative or low-proliferative migratory phenotype to a proliferative type, resulting in distant metastasis (64, 67, 76). To form micro-metastases or develop into metastatic cancers, CTCs are considered to have a corresponding colonization ability in the blood circulation (77, 78). The hypothesis proposes that there may be a reversible switch between epithelial-mesenchymal transition (EMT) and mesenchymal-epithelial transition (MET) (79, 80). Contrary to the physiological process of EMT, mesenchymal phenotype cells transform into epithelial phenotype cells by recovery of intercellular adhesion and reduced mobility during MET, providing the ability of distant colonization and establishment of metastases.

Biomarkers of CTCs in HCC

The biomarkers only expressed on the surface of liver tumor cells and rarely or not expressed in blood cells, which are used for CTCs detection in HCC patients. The biomarkers include epithelial markers, EMT-related markers, hepatocytes and HCC specific markers, and cancer stem-cell markers, as shown in Table 1.

Epithelial markers

EpCAM is one of the most commonly used epithelial markers on the cell membrane, and is widely used for isolating CTCs from peripheral blood. $EpCAM^+$ CTCs enriched by CellSearch system were detected in a cohort of 29 patients, including 20 in the HCC group and 9 in the control group (39). A total of 7/20 (35%) HCC patients had more than two CTCs per 7.5 mL in peripheral blood. Although no patients with non-malignant liver diseases were detected with CTCs, the presence of CTCs was associated with AFP level and vascular invasion. Sequence analysis of CTCs DNA showed that low frequency variants exist in $EpCAM^+$ CTCs. Another study consists of 197 HCC patients who underwent curative surgical resection and show that $EpCAM^+$ CTCs counts (≥3) were associated with

TABLE 1 Summary of clinical application of CTCs in HCC.

CTC Marker	Method	Specimen	Main finding
Epithelial Marker			
EpCAM	CellSearch system	59 HCC; 19 BLD	CTCs were detected in 18/59 HCC patients and 1/19 in control patients. Patients with the presence of CTCs had shorter OS. Schulze et al., 2013 (38)
EpCAM	Negative enrichment+ qRT-PCR	122 HCC; 120 BLD	Preoperative CTC levels showed prognostic significance in HCC patients with surgical treatment. Combined with the AFP level, the AUC was 0.857 with a sensitivity of 73.0% and specificity of 93.4%. Guo et al., 2014 (51)
EpCAM	Magnetic separation + IF	42 HCC; 10 BLD; 10 HV	Shedding of tumor cells during TACE did not affect the time to progression of HCC patients. Fang et al., 2014 (81)
EpCAM	CellSearch system	20 HCC; 9 BLD	CTCs were detected in 7 of 20 HCC and 0 of 9 BLD. The presence of CTCs was associated with AFP levels and vascular invasion. Kelley et al., 2015 (39)
EpCAM	CellSearch system	57 HCC	HCC patients with CTCs before the operation had a higher risk of recurrence and shorter RFS. Felden et al., 2017 (40)
EpCAM	CellSearch system	139 HCC	The increased postoperative CTC counts were significantly associated with the macroscopic tumor thrombus status, shorter DFS and OS. Yu et al., 2018 (41)
EpCAM	CellSearch system	309 HCC	Preoperative CTC counts were correlated with microvascular invasion, and patients with positive CTC should have enough surgical margins to protect against early recurrence. Zhou et al., 2020 (42)
EpCAM	CellSearch system	344 HCC	CTC-positive patients treated with adjuvant TACE had lower early recurrence, longer OS and time to recurrence. Wang et al., 2020 (43)
EpCAM	CellSearch system	197 HCC	The postoperative CTC counts ≥3 were associated with postoperative extrahepatic metastases and shorter median overall survival. Sun et al., 2020 (44)
EMT related Marker			
Twist, Vimentin, ZEB1, ZEB2, Snail, Slug, ASGPRs, E-cadherin	Magnetic separation + IF	60 HCC	CTCs were detected in 46/60 HCC patients. Co-expression of Twist and vimentin in CTCs was closely correlated with portal vein tumor thrombus, TNM classification and tumor size. Li et al., 2013 (82)
EpCAM, Vimentin, CK8/18/19	CanPatrol system	40 HCC; 124 other cancers; 27 HV	CTCs were detected in 107/164 different cancer patients. The presence of mesenchymal CTCs tended to occur in patients with metastatic stages in different types of cancers. Wu et al., 2015 (22)
EpCAM, Vimentin, CK8/18/19, Twist	CanPatrol system	33 HCC; 10 HV	Epithelial-mesenchymal-mixed CTCs play an important role in EMT transition in HCC, mixed CTCs might be a vital factor for intrahepatic metastasis, and mesenchymal CTCs had the potential to be a predictor of extrahepatic metastasis. Liu et al., 2016 (56)
EpCAM, Vimentin, CK8/18/19, Twist, E-cadherin, AKT2, Snail,	CanPatrol system	195 HCC	CTCs were present in 95% of HCC patients. Mesenchymal and hybrid CTCs were correlated with ages, BCLC stages, metastasis, AFP levels and recurrence. Chen et al., 2017 (13)
EpCAM, Vimentin, CK8/18/19, Twist	CanPatrol system	165 HCC	CTCs were present in 70.9% of HCC patients. The presence of mesenchymal CTCs was significantly correlated with high AFP levels, multiple tumors, advanced TNM and BCLC stage, presence of embolus or micro-embolus, and earlier recurrence. Ou et al., 2018 (57)
EpCAM, CK8/18/19	CanPatrol sytem	80 HCC; 10 HV	Twist+ CTCs were detected in 54/80 HCC patients. The ratios of Twist+ CTCs were correlated with advanced stage, rate of metastasis, recurrence and mortality. the prognostic evaluation of Twist+ CTCs was better CTCs alone. Yin et al., 2018 (58)
EpCAM, Vimentin, E-cadherin, Twist, CK8/18/19, BCAT1	CanPatrol system	112 HCC; 12 HBV; 20 HV	CTCs were present in 90.18% of HCC patients. Preoperative mesenchymal-CTC percentage ≥2% was closely correlated with early recurrence, lung metastasis and multi-intrahepatic recurrence. Qi et al., 2018 (59)
EpCAM, Vimentin, E-cadherin, CK	CellSearch system and qRT-PCR	73 HCC	CTCs and circulating tumor micro-emboli burden in hepatic veins and peripheral circulation predicted postoperative lung metastasis and intrahepatic recurrence, respectively. Sun et al., 2018 (83)
EpCAM, Vimentin, CK8/18/19, Twist	CanPatrol system	62 HCC	Mesenchymal CTCs and portal vein tumor thrombus were independent risk factors for early recurrence. Patients with positive mesenchymal CTCs had significantly shorter postoperative disease-free survival. Wang et al., 2018 (60)
EpCAM, Vimentin, CK8/18/19, Twist	CanPatrol system	113 HCC; 57 BLD	All types of CTCs in patients with HCC were significantly more numerous than in BLD group patients. The use of total CTCs was more effective than AFP for the diagnosis of HCC, the combination of total CTCs and AFP could promote diagnostic sensitivity. Cheng et al., 2019 (61)
CK, CD45	Tapered slit platform+ IF	105 HCC; 132 BLD	The changes in CTCs count before and after surgery was defined as ΔCTC, and the increased ΔCTC was significantly associated with recurrence. Ha et al., 2019 (84)
Vimentin, Twist	CanPatrol system	261 HCC	The combination of PA-TACE and hepatic resection showed improved RFS and OS than hepatic resection alone for mCTC-positive patients. Zhang et al., 2021 (52)

(Continued)

TABLE 1 Continued

CTC Marker	Method	Specimen	Main finding
CK, CD45	MCA system + IF	31 HCC; 14 BLD; 7 HV	The ratio of positive CTCs in HCC was higher than that in BLD. The enumeration of CTCs was associated with tumor stage and the presence of CTCs (≥10) tended to significantly reduce the cumulative survival. Takahashi et al., 2021 (85)
EpCAM, CK19, p-CK	ChimeraX®-i120 platform	193 HCC	Postoperative CTC count ≥1 was correlated with tumor recurrence after LTx, and postoperative serial CTC detection could be applied in surveillance for recurrence. Wang et al., 2021 (49)
Liver and HCC specific markers			
ASGPR, Hep Par 1	Magnetic separation + IF	85 HCC; 37 BLD; 20 HV; 14 other cancers	CTCs were present in 69/85 HCC patients, and no CTCs were detected in healthy, BLD or other cancer groups. The detection rate and enumeration of positive CTCs were significantly associated with tumor size, portal vein tumor thrombus and TNM stage. Xu et al., 2011 (86)
ASGPR, CPS1, P-CK	Magnetic separation + IF	27 HCC	CTCs were identified in 89% of HCC patients by this method, and no CTCs were found in the other test subjects. Li et al., 2014 (87)
ASGPR, CPS1	negative enrichment + IF	32 HCC; 40 BLD; 20 HV; 17 other cancers	CTCs with positive ASGPR and CPS1 were detected in 91% of HCC patients, and no CTCs were found in healthy volunteers, BLD group and other cancer patients. Liu et al., 2015 (47)
CK, EpCAM, AFP, GPC3, DNA-PK	imaging flow cytometry method	69 HCC; 31 controls	CTCs were detected in 45/69 HCC patients and 0/31 controls, the enumeration of positive CTCs was correlated with tumor size, portal vein thrombosis and shorter median survival. Ogle et al., 2016 (88)
TP53	CanPatrol system	42 HCC	The postoperative CTC counts (> 2) and changes in CTC counts between preoperation and postoperation could be independent prognostic indicators for PRS in patients with HCC. Ye et al., 2018 (89)
ASGPR, GPC3	magnetically assisted surface-enhanced Raman scattering	8 HCC; 5 HV; 5 other cancers	The platform with dual labeling of ASGPR and GPC3 had an effective ability in detecting HCC CTCs with a small number of peripheral blood samples in clinical diagnosis. Pang et al., 2018 (90)
GPC3	immunomagnetic positive enrichment +flow cytometry	85 HCC	The preoperative GPC3-positive CTCs were a risk factor for microscopic portal vein invasion and poor prognosis. Hamaoka et al., 2019 (50)
EpCAM, ASGPR	Microfluidic Synergetic-Chip	45 HCC	The platform with dual labeling of EpCAM and ASGPR had an effective ability in detecting HCC CTCs. CTCs were identified in 100% of HCC patients. Total CTCs and non-epithelial CTCs were associated with advanced stage and malignant progression. Zhu et al., 2020 (53)
Stem-cell markers			
CD90(+), CD44(+)	Multicolor flow cytometry	82 HCC	Circulating CSCs > 0.01% was correlated with intrahepatic recurrence and extrahepatic recurrence, also associated with lower RFS and OS. Fan et al., 2011 (91)
EpCAM, CD133, ABCG2	CellSearch system	123 HCC	CSC biomarkers CD133 and ABCG2 were displayed in EpCAM positive CTCs. Sun et al., 2013 (92)
GPC3, CS, CD44, Hep Par-1	The Labyrinth Chip +IF	42 HCC	CTCs were detected in 88.1% of HCC patients and CTCs with the expression of CD44 were observed in 71.4% of HCC patients. CTCs with GPC3, CS and HepPar-1 markers had a cancer stemness phenotype. Wan et al., 2019 (93)
Drug therapy monitoring			
pERK, pAkt	negative enrichment + IF	109 HCC	HCC patients with $pERK^+/pAkt^-$ CTCs were most sensitive to sorafenib. The proportion of $pERK^+/pAkt^-$ CTCs was significantly correlated with shorter PFS, and could be an independent predictive factor in HCC patients treated with sorafenib. Li et al., 2016 (48)
CK, PD-L1	NanoVelcro Chip	87 HCC; 7 BLD; 8 HV	PD-L1+ CTCs were identified in 8.2% of early-stage patients, 54.5% of locally advanced and 93.8% of metastatic patients. HCC patients with PD-L1+ CTCs had favorable treatment responses when receiving anti-PD-1 therapy. Winograd et al., 2020 (94)

postoperative extrahepatic metastases and shorter median overall survival. The HCC patients with high number of CTCs need more careful surveillance in early interventions (44). EpCAM-based enrichment methods are not able to be used in the enrichment of CTCs which express low level of EpCAM (95) or lose expression of EpCAM during the process of EMT (96, 97).

EMT-related markers

According to the expression patterns during EMT process, biomarkers are largely categorized into epithelial markers and mesenchymal markers. Epithelial markers contain E-cadherin, EpCAM and CK8/18/19. Mesenchymal markers include N-cadherin, vimentin and some transcription factors such as

ZEB1, ZEB2, twist, slug and Snail1 (98). Based on microfiltration enrichment and RNA *in situ* hybridization, the CanPatrol system captures CTCs and classifies them into epithelial phenotype, mesenchymal phenotype and mixed phenotype (52). A retrospective cohort study consists of 165 HCC patients who underwent curative surgical resection, and show that more than two preoperative CTCs were present in 117/165 (70.9%) of HCC patients and the elevated CTC counts were correlated with poor clinicopathological features (57). The presence of preoperative mesenchymal CTCs was significantly correlated with multiple tumors, high AFP levels, presence of embolus or micro-embolus, advanced TNM and BCLC stage, and earlier recurrence. Another recent study consists of 112 HCC patients who underwent surgical resection, 12 HBV patients and 20 healthy volunteers (59). A total of 101/112 (90.18%) HCC patients and 2/12 (16.67%) HBV patients were detected with CTCs. Two of HBV patients who were isolated CTCs and then were detected with small HCC within five months, nevertheless, none of the healthy volunteers were isolated CTCs. Preoperatively total CTCs or mesenchymal CTCs were closely correlated with early recurrence, lung metastasis and multi-intrahepatic recurrence. Mesenchymal positive CTCs are a high risk of early recurrence. The combination of epithelial and mesenchymal markers increases the sensitivity and specificity of CTCs detection. CTCs expressing EMT-related markers are significantly correlated with clinicopathological features, which allows adequate stratification for HCC patients' management.

Hepatocytes and HCC specific markers

Serum AFP is a predictor of prognostic evaluation because the high level of AFP is closely associated with HCC recurrence and metastasis (2, 99). AFP is common biomarker for HCC screening, however, in early HCC the detection rate of AFP is only 25-65% (100). There is an urgent need of HCC specific biomarkers in early detection. A number of hepatocytes and HCC specific markers, including sialoglycoprotein receptor (ASGPR), hepatocyte paraffin 1 (Hep Par 1), and glypican-3 (GPC3), show a diagnostic and prognostic value (47, 50, 53, 86–88, 90).

A study consist of 85 HCC patients, 37 patients with benign liver diseases, 14 patients with other cancers, and 20 healthy volunteers (86). The immunomagnetic enrichment of $ASGPR^+$ CTCs and subsequent identification by immunofluorescence staining with Hep Par 1 antibody were illustrated to be an effective strategy to identify CTCs from peripheral blood of HCC patients. ASGPR is a protein expressed in the outer membrane of hepatocytes and HCC cells. Hep Par 1 is a protein expressed on the mitochondrial membrane of hepatocytes. By this method, CTCs were present in 69/85 (81%) HCC patients, and no CTCs were detected in benign liver diseases, healthy volunteers, or other cancer groups. The counts of CTCs were significantly associated with tumor size, portal vein tumor thrombus and TNM stage. Another study consists of 32 HCC patients, 40 patients with benign liver diseases, 20 healthy volunteers and 20 healthy volunteers (47). The negative enrichment method with CD45 antibodies to remove leukocytes and subsequent identification using a combination of ASGPR and CPS1 antibodies were conducted to identify CTCs from peripheral blood of HCC patients. By this strategy, CTCs with positive ASGPR and CPS1 were detected in 29/32 (91%) of HCC patients, nevertheless, no CTCs were found in healthy volunteers, benign liver diseases and other cancer groups. Recently, Zhu and his colleagues designed and developed a microfluidic Synergetic-Chip, which combined physical size separation and immunological recognition (53). EpCAM and ASGPR antibodies were respectively coated in two parallel channels to capture CTCs, subsequently, enriched CTCs were identified by immunofluorescence staining. By this method, EpCAM or ASGPR positive CTCs were identified in 45/45 (100%) of HCC patients, and the sensitivity and specificity achieve 97.8% and 100%. The specific markers combined with EpCAM were also used and proved to be efficient in CTCs detection (53, 101).

Cancer stem-cell markers

Cancer stem cells (CSCs) are a specific sub-population of cancer cells in tumor tissue, which play an important role in the occurrence and metastasis of carcinoma. The origin of cancer stem cells remains controversial. One of the possible origins is the transformation through mutation and de-differentiation (102). These phenotypic changes are primarily the result of fundamental changes in gene expression concomitant with a diminished transcription of the relevant liver-specific genes, and can be interpreted as a 'de-differentiation' of hepatocytes. During the de-differentiation process, the overexpression of oncogenes and inactivation of tumor suppressor genes lead to uncontrolled excessive proliferation of cells and expression of stem cell markers (103). Currently, it is difficult to distinguish CTCs and CSCs due to the lack of a suitable markers. HCC cells and liver cancer stem cells are also derived from the de-differentiation of mature hepatocytes (103–105). Liver cancer stem cells are a unique subset of hepatocellular carcinoma cells with stem cell features and contribute to the disease recurrence, drug resistance and death (98).

Circulating CSCs are a few subpopulations of CTCs, which exhibit unlimited self-renewal and proliferation potential. They are associate with increased aggressiveness and poor prognosis (106). Some CTCs of peripheral blood of HCC patients

expressed stem cell markers such as CD44, CD90, and CD133 (91–93). $CD133^+$ $CD44^+$ CSCs had been proved to be associated with elevated serum AFP, serum transaminases and poorer prognosis in HCC patients (107). Based on the detection of $CD90^+$ $CD44^+$ CSCs by multicolor flow cytometry, the number of preoperative CSCs in patients with recurrence were higher compared with the patients without recurrence (91). Patients with $CD90^+$ $CD44^+$ CSCs had lower RFS and OS. Thus, preoperative CSCs can be used to predict post-hepatectomy recurrence of HCC. $EpCAM1^+$ CTCs of peripheral blood of HCC patients showed high tumorigenic capacity and low apoptotic tendency and expressed CSCs markers $CD133^+$ and $ABCG2^+$ (92). Through physical enrichment by Labyrinth chip and immunofluorescence staining using GPC3, CD44, and HepPar-1 antibodies, CTCs were detected in 37/42 (88.1%) of HCC patients, and $CD44^+$ CTCs were identified in 30/42 (71.4%) of HCC patients (93). The detection rate of $CD44^+$ CTCs was significantly higher in patients with advanced stages than those with early stages.

Clinical application of CTCs in HCC

CTCs may transfer through hematogenous metastasis in the early stage, so some HCC patients have distant metastasis before receiving treatment, which leads to a great challenge for HCC management. Therefore, early diagnosis of HCC is the key to receiving the effective treatment. Accumulated evidence indicates that CTCs detection is of great significance for early diagnosis HCC. Related detection markers, methods and clinical application of CTCs are shown in Figure 2.

Diagnosis and tumor staging

Many evidence indicates that CTCs detection with EMT-related markers are useful for early diagnosis and staging. $EpCAM^+$ CTCs were detected in 18/59 (30.5%) HCC patients and 1/19 (5.3%) individuals in the control group. The CTCs detection rates of patients with different BCLC stages were significant differences: stages A 1/9 (11.1%), B 6/31 (19.3%) and C 11/19 (57.9%) (38). CTCs were detected in 101/112 (90.12%) of HCC patients, even at an early stage (59). Patients with late BCLC stage had a higher mesenchymal phenotype CTCs counts than those in early stage. Mesenchymal phenotype CTCs counts (≥1) could be used to distinguish BCLC stage in HCC patients (61). The combination of total CTCs and AFP improve the sensitivity and specificity of 61.95% and 89.47%, respectively. $Twist^+$ $vimentin^+$ CTCs were detected in 33/46 (69.6%) of HCC patients. The CTCs detection rates were closely associated with tumor size, portal vein tumor thrombus, and TNM classification (82). CTCs were detected in 185/195 (95%) of HCC patients. The counts, mesenchymal and mixed phenotype of CTCs were correlated with the clinicopathologic features, such as ages, BCLC stages and AFP levels (13, 22, 52, 57, 58, 61).

HCC specific markers are efficient to detect CTCs clinically. CTCs were identified in 24/27 (89%) HCC patients by specific markers ASGPR, CPS1 and P-CK, and no CTCs were detected in other test subjects (87). $ASGPR^+CPS1^+$ CTCs were detected in 29/32 (91%) of HCC patients, and no CTCs were found in healthy volunteers, benign liver diseases and other cancers groups (47). $ASGPR^+$ $EpCAM^+$ CTCs were detected in 45/45 (100%) of HCC patients (53). Some study showed that CTCs counts through HCC specific markers or combination with

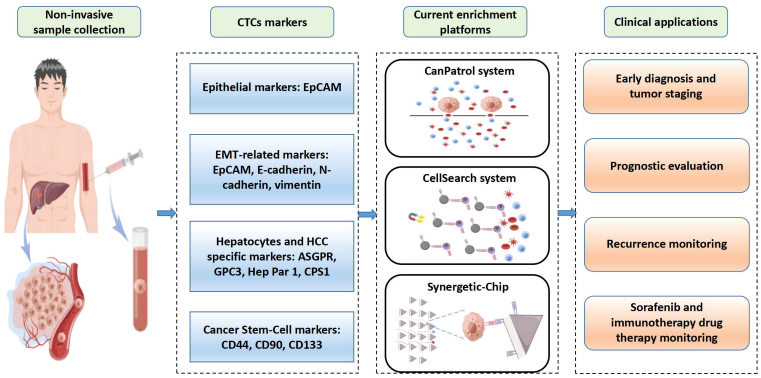

FIGURE 2
Overview of clinical applications of circulating tumor cells (CTCs) in hepatocellular carcinoma (HCC). CTCs are obtained from patients' blood samples in a non-invasive way. HCC CTCs are primarily isolated based on their unique biological markers. CellSearch is the only FDA-approved system for CTCs detection used clinically. CanPatol and CTC-chip are other CTCs detection systems. CTCs represent an independent factor for early diagnosis and tumor staging, prognostic evaluation, recurrence monitoring, and drug therapy monitoring.

other markers were correlated with tumor size, differentiation status, portal vein tumor thrombus and TNM stage (50, 53, 86, 88).

Prognostic evaluation and recurrence monitoring

The prognosis of HCC is closely related to the clinical stage. The common clinical prognostic models of HCC include the BCLC staging system and TNM staging system. BCLC staging system is based on tumor burden, liver function and physical status. The parameters of tumor burden are composed of the number and diameter of tumor, portal vein invasion and extrahepatic spread (108). TNM staging is evaluated by the number and diameter of tumors, vascular invasion, adjacent organs invasion, regional lymph nodes metastases and distant metastases (109, 110). Studies have shown that the counts of CTCs are associated with the parameters of BCLC staging and TNM staging in HCC patients (13, 52, 53, 59). Analysis of the CTCs by RNA *in situ* hybridization (RNA-ISH) revealed that positive rate of CTCs was 83.6% (46/55) and 96.5% (55/57) in patients with BCLC stage 0–A and stage B–C tumors (59). A meta-analysis study of twenty-three published studies showed that CTC positivity were also significantly associated with TNM Stage (RR 1.30, 95% CI: [1.02-1.65]; p=0.03), tumor size (RR 1.36, 95% CI: [1.09-1.69]; p=0.006), vascular invasion (RR 1.99, 95% CI: [1.43-2.77]; p<0.0001), portal vein tumor thrombus (RR 1.73, 95% CI: [1.42-2.11]; p=0.0001), serum AFP level (RR 2.05, 95% CI: [1.18-3.54]; p=0.01), suggesting a strong prognostic value of CTC in HCC (111).

The counts of CTCs make a difference in peripheral blood of HCC patients before and after treatment. Thus, CTCs detection is used to monitor the response of therapy and help clinicians to adjust their treatment plans. Recent study reported the relationship between ΔCTC and recurrence of HCC after hepatectomy. ΔCTC is defined as the changes of CTCs counts after surgery. The positive ΔCTC was correlated with higher recurrence and lower survival in HCC patients after surgical liver resection (84). HCC patients with postoperative $EpCAM^+$ CTCs counts < 2 had significantly longer disease-free survival and overall survival than the patients with CTCs counts ≥2, suggesting increased postoperative $EpCAM^+$ CTCs counts were related to a poor clinical outcome after surgical liver resection (41). Some studies provided evidence that mesenchymal phenotype CTCs could predict early recurrence, metastasis, shorter disease-free survival and overall survival (13, 52, 56, 57, 59, 82, 83). EMT-related phenotype CTCs play an important role in predicting metastasis and recurrence. A study reported that $Twist^+$ CTCs were associated with higher metastasis, recurrence and mortality rate (58). Another study found that mesenchymal phenotype CTCs were independent risk factors for early recurrence. HCC patients with postoperative mesenchymal phenotype CTCs counts ≥1 had a shorter disease-free survival after surgery (60). The preoperative $GPC3^+$CTCs were significantly correlated with the clinical outcome of HCC patients. $GPC3^+$ CTCs counts >5 were an independent risk factor for microscopic portal vein invasion. HCC patients with $GPC3^+$ CTCs counts >5 had lower disease-free survival and overall survival after hepatectomy (50). The preoperative $CD90^+$ $CD44^+$ CSCs were proved to be associated with intrahepatic and extrahepatic recurrence of patients after surgical resection. HCC patients with CSCs > 0.01% (the optimal cut-off point for gating percentages of circulating CSCs by calculating the AUROC) had lower disease-free survival and overall survival (91). HCC patients with $PD\text{-}L1^+$ CTCs had shorter overall survival than those patients without $PD\text{-}L1^+$ CTCs (94).

Drug therapy monitoring

Drug resistance is also an important factor affecting clinical prognosis. The acquired drug resistance of HCC cells leads to poor effects of systemic therapy (112). Sorafenib is a small molecule multi-kinase inhibitor with multiple antitumor effects and is the first-line targeted drug for the treatment of HCC in the advanced stage (113). Numerous studies have shown that the inactivation of Ras/Raf/ERK pathway and the activation of PI3K/Akt/mTOR pathway plays a crucial role in sorafenib resistance (114–117). CTCs are released from tumor tissue to the bloodstream and carry drug resistance information of the primary tumor or metastases, therefore pERK/pAkt phenotype of CTCs can be used to monitor the therapeutic effect and drug resistance of sorafenib (48). A study reported the association between $pERK^+$ $pAkt^-$ CTCs and the sensibility of sorafenib in HCC patients (48). During sorafenib treatment, the CTC counts showed a marked decrease in patients with $pERK^+$ $pAkt^-$ CTCs. HCC patients with $pERK^+$ $pAkt^-$ CTCs were sensitive to sorafenib-targeted therapy, whereas patients with other phenotype CTCs showed resistance to sorafenib therapy. So, they suggested the percentage of $pERK^+$ $pAkt^-$ CTCs could serve as an independent predictive factor for HCC patients treated with sorafenib.

The programmed cell death protein 1 (PD-1) and its ligand (PD-L1) axes is an inhibitory immune checkpoint that is involved in suppressing antitumor immunity. The overexpression of PD-L1 of tumor cells binding to PD-1 on the surface of T cells can induce T-cell anergy or apoptosis, which enables evasion of immune-mediated tumor surveillance (112). Inhibitors targeting PD-1 or PD-L1 can restrain this pathway and restore antitumor immunity (118). The advanced melanoma patients with $PD\text{-}L1^+$ CTCs showed a good response to PD-1 inhibitor immunotherapy, whereas those patients with the $PD\text{-}L1^-$ CTCs exhibited drug resistance (119). $PD\text{-}L1^+$ CTCs which were predominantly found in advanced-stage patients could accurately discriminate early-

stage from advanced-stage HCC patients (94). Subsequently, they followed up 10 HCC patients who received immunotherapy (PD-1 blockade), and found that 5 patients with PD-L1$^+$ CTCs had a good response to immunotherapy, and only 1 of 5 non-responders had PD-L1$^+$ CTCs. CTCs with specific phenotypes have the potentials to predict drug resistance to targeted therapy and immunotherapy, which provide clinical application in guiding individualized medicine.

Conclusions

The detection of CTCs is of great value in the early diagnosis and tumor staging, evaluation of recurrence and prognosis, and even prediction of drug resistance of targeted therapy and immunotherapy in patients with HCC. However, CTCs detection is not widely used in the clinical application of HCC due to several limitations, such as lack of standardized technical procedures, limitations of detection efficiency, extremely rare of CTCs in blood, and absence of external validation in many clinical studies. If technological advances could overcome the shortcomings of CTCs detection in the future, CTCs detection will be a breakthrough in HCC clinical management, especially in early diagnosis offering an opportunity for curative surgery before metastasis. EMT plays an important role in various pathophysiological processes of CTCs, such as tumor cells shedding and migrating, vascular invasion and distant implantation. More mechanisms of EMT in CTCs should be investigated, which is expected to provide new insight into HCC clinical management.

Author contributions

YY, JD, JH, and BW reviewed the literature. YH and YY drafted the manuscript and designed the figures. YY and ZL revised the manuscript. All authors read and approved the manuscript.

Funding

This work was supported by Guangdong Basic and Applied Basic Research Foundation (2021A1515011261).

Conflict of interest

The authors declare that the research was conducted in the absence of any commercial or financial relationships that could be construed as a potential conflict of interest.

Publisher's note

All claims expressed in this article are solely those of the authors and do not necessarily represent those of their affiliated organizations, or those of the publisher, the editors and the reviewers. Any product that may be evaluated in this article, or claim that may be made by its manufacturer, is not guaranteed or endorsed by the publisher.

References

1. Bray F, Ferlay J, Soerjomataram I, Siegel RL, Torre LA, Jemal A. Global cancer statistics 2018: GLOBOCAN estimates of incidence and mortality worldwide for 36 cancers in 185 countries. *CA Cancer J Clin* (2018) 68(6):394–424. doi: 10.3322/caac.21492

2. Marrero JA, Kulik LM, Sirlin CB, Zhu AX, Finn RS, Abecassis MM, et al. Diagnosis, staging, and management of hepatocellular carcinoma: 2018 practice guidance by the American association for the study of liver diseases. *Hepatology* (2018) 68(2):723–50. doi: 10.1002/hep.29913

3. Pelizzaro F, Vitale A, Sartori A, Vieno A, Penzo B, Russo FP, et al. Surveillance as determinant of long-term survival in non-transplanted hepatocellular carcinoma patients. *Cancers (Basel)* (2021) 13(4):897. doi: 10.3390/cancers13040897

4. Forner A, Reig M, Bruix J. Hepatocellular carcinoma. *Lancet* (2018) 391 (10127):1301–14. doi: 10.1016/S0140-6736(18)30010-2

5. Galle PR, Foerster F, Kudo M, Chan SL, Llovet JM, Qin S, et al. Biology and significance of alpha-fetoprotein in hepatocellular carcinoma. *Liver Int* (2019) 39 (12):2214–29. doi: 10.1111/liv.14223

6. Bruix J, Sherman MAmerican Association for the Study of Liver D. Management of hepatocellular carcinoma: an update. *Hepatology* (2011) 53 (3):1020–2. doi: 10.1002/hep.24199

7. Khan IM, Gjuka D, Jiao J, Song X, Wang Y, Wang J, et al. A novel biomarker panel for the early detection and risk assessment of hepatocellular carcinoma in patients with cirrhosis. *Cancer Prev Res (Phila)* (2021) 14(6):667–74. doi: 10.1158/1940-6207.CAPR-20-0600

8. Zhao S, Long M, Zhang X, Lei S, Dou W, Hu J, et al. The diagnostic value of the combination of golgi protein 73, glypican-3 and alpha-fetoprotein in hepatocellular carcinoma: a diagnostic meta-analysis. *Ann Transl Med* (2020) 8 (8):536. doi: 10.21037/atm.2020.02.89

9. Gatselis NK, Tornai T, Shums Z, Zachou K, Saitis A, Gabeta S, et al. Golgi protein-73: A biomarker for assessing cirrhosis and prognosis of liver disease patients. *World J Gastroenterol* (2020) 26(34):5130–45. doi: 10.3748/wjg.v26.i34.5130

10. Russo FP, Imondi A, Lynch EN, Farinati F. When and how should we perform a biopsy for HCC in patients with liver cirrhosis in 2018? a review. *Dig Liver Dis* (2018) 50(7):640–6. doi: 10.1016/j.dld.2018.03.014

11. Li J, Han X, Yu X, Xu Z, Yang G, Liu B, et al. Clinical applications of liquid biopsy as prognostic and predictive biomarkers in hepatocellular carcinoma: circulating tumor cells and circulating tumor DNA. *J Exp Clin Cancer Res* (2018) 37(1):213. doi: 10.1186/s13046-018-0893-1

12. Yin CQ, Yuan CH, Qu Z, Guan Q, Chen H, Wang FB. Liquid biopsy of hepatocellular carcinoma: Circulating tumor-derived biomarkers. *Dis Markers* (2016) 2016:1427849. doi: 10.1155/2016/1427849

13. Chen J, Cao SW, Cai Z, Zheng L, Wang Q. Epithelial-mesenchymal transition phenotypes of circulating tumor cells correlate with the clinical stages

and cancer metastasis in hepatocellular carcinoma patients. *Cancer biomark* (2017) 20(4):487–98. doi: 10.3233/CBM-170315

14. Dirix L, Buys A, Oeyen S, Peeters D, Liegeois V, Prove A, et al. Circulating tumor cell detection: A prospective comparison between CellSearch(R) and RareCyte(R) platforms in patients with progressive metastatic breast cancer. *Breast Cancer Res Treat* (2022) 193(2):437–44. doi: 10.1007/s10549-022-06585-5

15. Tamminga M, de Wit S, van de Wauwer C, van den Bos H, Swennenhuis JF, Klinkenberg TJ, et al. Analysis of released circulating tumor cells during surgery for non-small cell lung cancer. *Clin Cancer Res* (2020) 26(7):1656–66. doi: 10.1158/1078-0432.CCR-19-2541

16. Riethdorf S, O'Flaherty L, Hille C, Pantel K. Clinical applications of the CellSearch platform in cancer patients. *Adv Drug Delivery Rev* (2018) 125:102–21. doi: 10.1016/j.addr.2018.01.011

17. Heidrich I, Ackar L, Mossahebi Mohammadi P, Pantel K. Liquid biopsies: Potential and challenges. *Int J Cancer* (2021) 148(3):528–45. doi: 10.1002/ijc.33217

18. Cui K, Ou Y, Shen Y, Li S, Sun Z. Clinical value of circulating tumor cells for the diagnosis and prognosis of hepatocellular carcinoma (HCC): A systematic review and meta-analysis. *Med (Baltimore)* (2020) 99(40):e22242. doi: 10.1097/MD.0000000000022242

19. Hurtado P, Martinez-Pena I, Pineiro R. Dangerous liaisons: Circulating tumor cells (CTCs) and cancer-associated fibroblasts (CAFs). *Cancers (Basel)* (2020) 12(10):2861. doi: 10.3390/cancers12102861

20. Agashe R, Kurzrock R. Circulating tumor cells: From the laboratory to the cancer clinic. *Cancers (Basel)* (2020) 12(9):2361. doi: 10.3390/cancers12092361

21. Massague J, Obenauf AC. Metastatic colonization by circulating tumour cells. *Nature* (2016) 529(7586):298–306. doi: 10.1038/nature17038

22. Wu S, Liu S, Liu Z, Huang J, Pu X, Li J, et al. Classification of circulating tumor cells by epithelial-mesenchymal transition markers. *PloS One* (2015) 10(4):e0123976. doi: 10.1371/journal.pone.0123976

23. Aceto N, Bardia A, Miyamoto DT, Donaldson MC, Wittner BS, Spencer JA, et al. Circulating tumor cell clusters are oligoclonal precursors of breast cancer metastasis. *Cell* (2014) 158(5):1110–22. doi: 10.1016/j.cell.2014.07.013

24. Gkountela S, Castro-Giner F, Szczerba BM, Vetter M, Landin J, Scherrer R, et al. Circulating tumor cell clustering shapes DNA methylation to enable metastasis seeding. *Cell* (2019) 176(1-2):98–112 e14. doi: 10.1016/j.cell.2018.11.046

25. Yu M, Bardia A, Wittner BS, Stott SL, Smas ME, Ting DT, et al. Circulating breast tumor cells exhibit dynamic changes in epithelial and mesenchymal composition. *Science* (2013) 339(6119):580–4. doi: 10.1126/science.1228522

26. Heeke S, Mograbi B, Alix-Panabieres C, Hofman P. Never travel alone: The crosstalk of circulating tumor cells and the blood microenvironment. *Cells* (2019) 8(7):714. doi: 10.3390/cells8070714

27. Hou HW, Warkiani ME, Khoo BL, Li ZR, Soo RA, Tan DS, et al. Isolation and retrieval of circulating tumor cells using centrifugal forces. *Sci Rep* (2013) 3:1259. doi: 10.1038/srep01259

28. Low WS, Wan Abas WA. Benchtop technologies for circulating tumor cells separation based on biophysical properties. *BioMed Res Int* (2015) 2015:239362. doi: 10.1155/2015/239362

29. Chen K, Amontree J, Varillas J, Zhang J, George TJ, Fan ZH. Incorporation of lateral microfiltration with immunoaffinity for enhancing the capture efficiency of rare cells. *Sci Rep* (2020) 10(1):14210. doi: 10.1038/s41598-020-71041-7

30. Wang L, Li Y, Xu J, Zhang A, Wang X, Tang R, et al. Quantified postsurgical small cell size CTCs and EpCAM(+) circulating tumor stem cells with cytogenetic abnormalities in hepatocellular carcinoma patients determine cancer relapse. *Cancer Lett* (2018) 412:99–107. doi: 10.1016/j.canlet.2017.10.004

31. Ito H, Yamaguchi N, Onimaru M, Kimura S, Ohmori T, Ishikawa F, et al. Change in number and size of circulating tumor cells with high telomerase activity during treatment of patients with gastric cancer. *Oncol Lett* (2016) 12(6):4720–6. doi: 10.3892/ol.2016.5239

32. Dolfus C, Piton N, Toure E, Sabourin JC. Circulating tumor cell isolation: the assets of filtration methods with polycarbonate track-etched filters. *Chin J Cancer Res* (2015) 27(5):479–87. doi: 10.3978/j.issn.1000-9604.2015.09.01

33. Russo GI, Musso N, Romano A, Caruso G, Petralia S, Lanzano L, et al. The role of dielectrophoresis for cancer diagnosis and prognosis. *Cancers (Basel)* (2021) 14(1):198. doi: 10.3390/cancers14010198

34. Renier C, Pao E, Che J, Liu HE, Lemaire CA, Matsumoto M, et al. Label-free isolation of prostate circulating tumor cells using vortex microfluidic technology. *NPJ Precis Oncol* (2017) 1(1):15. doi: 10.1038/s41698-017-0015-0

35. Undvall Anand E, Magnusson C, Lenshof A, Ceder Y, Lilja H, Laurell T. Two-step acoustophoresis separation of live tumor cells from whole blood. *Anal Chem* (2021) 93(51):17076–85. doi: 10.1021/acs.analchem.1c04050

36. Hoshino K, Huang YY, Lane N, Huebschman M, Uhr JW, Frenkel EP, et al. Microchip-based immunomagnetic detection of circulating tumor cells. *Lab Chip* (2011) 11(20):3449–57. doi: 10.1039/c1lc20270g

37. Kuai JH, Wang Q, Zhang AJ, Zhang JY, Chen ZF, Wu KK, et al. Epidermal growth factor receptor-targeted immune magnetic liposomes capture circulating colorectal tumor cells efficiently. *World J Gastroenterol* (2018) 24(3):351–9. doi: 10.3748/wjg.v24.i3.351

38. Schulze K, Gasch C, Staufer K, Nashan B, Lohse AW, Pantel K, et al. Presence of EpCAM-positive circulating tumor cells as biomarker for systemic disease strongly correlates to survival in patients with hepatocellular carcinoma. *Int J Cancer* (2013) 133(9):2165–71. doi: 10.1002/ijc.28230

39. Kelley RK, Magbanua MJ, Butler TM, Collisson EA, Hwang J, Sidiropoulos N, et al. Circulating tumor cells in hepatocellular carcinoma: a pilot study of detection, enumeration, and next-generation sequencing in cases and controls. *BMC Cancer* (2015) 15:206. doi: 10.1186/s12885-015-1195-z

40. von Felden J, Schulze K, Krech T, Ewald F, Nashan B, Pantel K, et al. Circulating tumor cells as liquid biomarker for high HCC recurrence risk after curative liver resection. *Oncotarget* (2017) 8(52):89978–87. doi: 10.18632/oncotarget.21208

41. Yu JJ, Xiao W, Dong SL, Liang HF, Zhang ZW, Zhang BX, et al. Effect of surgical liver resection on circulating tumor cells in patients with hepatocellular carcinoma. *BMC Cancer* (2018) 18(1):835. doi: 10.1186/s12885-018-4744-4

42. Zhou KQ, Sun YF, Cheng JW, Du M, Ji Y, Wang PX, et al. Effect of surgical margin on recurrence based on preoperative circulating tumor cell status in hepatocellular carcinoma. *EBioMedicine* (2020) 62:103107. doi: 10.1016/j.ebiom.2020.103107

43. Wang PX, Sun YF, Zhou KQ, Cheng JW, Hu B, Guo W, et al. Circulating tumor cells are an indicator for the administration of adjuvant transarterial chemoembolization in hepatocellular carcinoma: A single-center, retrospective, propensity-matched study. *Clin Transl Med* (2020) 10(3):e137. doi: 10.1002/ctm2.137

44. Sun YF, Wang PX, Cheng JW, Gong ZJ, Huang A, Zhou KQ, et al. Postoperative circulating tumor cells: An early predictor of extrahepatic metastases in patients with hepatocellular carcinoma undergoing curative surgical resection. *Cancer Cytopathol* (2020) 128(10):733–45. doi: 10.1002/cncy.22304

45. Lowes LE, Allan AL. Circulating tumor cells and implications of the epithelial-to-Mesenchymal transition. *Adv Clin Chem* (2018) 83:121–81. doi: 10.1016/bs.acc.2017.10.004

46. Joosse SA, Gorges TM, Pantel K. Biology, detection, and clinical implications of circulating tumor cells. *EMBO Mol Med* (2015) 7(1):1–11. doi: 10.15252/emmm.201303698

47. Liu HY, Qian HH, Zhang XF, Li J, Yang X, Sun B, et al. Improved method increases sensitivity for circulating hepatocellular carcinoma cells. *World J Gastroenterol* (2015) 21(10):2918–25. doi: 10.3748/wjg.v21.i10.2918

48. Li J, Shi L, Zhang X, Sun B, Yang Y, Ge N, et al. pERK/pAkt phenotyping in circulating tumor cells as a biomarker for sorafenib efficacy in patients with advanced hepatocellular carcinoma. *Oncotarget* (2016) 7(3):2646–59. doi: 10.18632/oncotarget.6104

49. Wang PX, Xu Y, Sun YF, Cheng JW, Zhou KQ, Wu SY, et al. Detection of circulating tumour cells enables early recurrence prediction in hepatocellular carcinoma patients undergoing liver transplantation. *Liver Int* (2021) 41(3):562–73. doi: 10.1111/liv.14734

50. Hamaoka M, Kobayashi T, Tanaka Y, Mashima H, Ohdan H. Clinical significance of glypican-3-positive circulating tumor cells of hepatocellular carcinoma patients: A prospective study. *PloS One* (2019) 14(5):e0217586. doi: 10.1371/journal.pone.0217586

51. Guo W, Yang XR, Sun YF, Shen MN, Ma XL, Wu J, et al. Clinical significance of EpCAM mRNA-positive circulating tumor cells in hepatocellular carcinoma by an optimized negative enrichment and qRT-PCR-based platform. *Clin Cancer Res* (2014) 20(18):4794–805. doi: 10.1158/1078-0432.CCR-14-0251

52. Zhang J, Peng H, Wang B, Luo L, Cheng Y, He G, et al. Efficacy of postoperative adjuvant transcatheter arterial chemoembolization in hepatocellular carcinoma patients with mesenchymal circulating tumor cell. *J Gastrointest Surg* (2021) 25(7):1770–8. doi: 10.1007/s11605-020-04755-8

53. Zhu L, Lin H, Wan S, Chen X, Wu L, Zhu Z, et al. Efficient isolation and phenotypic profiling of circulating hepatocellular carcinoma cells *via* a combinatorial-Antibody-Functionalized microfluidic synergetic-chip. *Anal Chem* (2020) 92(22):15229–35. doi: 10.1021/acs.analchem.0c03936

54. Lin Z, Luo G, Du W, Kong T, Liu C, Liu Z. Recent advances in microfluidic platforms applied in cancer metastasis: Circulating tumor cells' (CTCs) isolation and tumor-On-A-Chip. *Small* (2020) 16(9):e1903899. doi: 10.1002/smll.201903899

55. Zhong Y, Ma T, Qiao T, Hu H, Li Z, Luo K, et al. Role of phenotypes of circulating tumor cells in the diagnosis and treatment of colorectal cancer. *Cancer Manag Res* (2021) 13:7077–85. doi: 10.2147/CMAR.S316544

56. Liu YK, Hu BS, Li ZL, He X, Li Y, Lu LG. An improved strategy to detect the epithelial-mesenchymal transition process in circulating tumor cells in

hepatocellular carcinoma patients. *Hepatol Int* (2016) 10(4):640–6. doi: 10.1007/s12072-016-9732-7

57. Ou H, Huang Y, Xiang L, Chen Z, Fang Y, Lin Y, et al. Circulating tumor cell phenotype indicates poor survival and recurrence after surgery for hepatocellular carcinoma. *Dig Dis Sci* (2018) 63(9):2373–80. doi: 10.1007/s10620-018-5124-2

58. Yin LC, Luo ZC, Gao YX, Li Y, Peng Q, Gao Y. Twist expression in circulating hepatocellular carcinoma cells predicts metastasis and prognoses. *BioMed Res Int* (2018) 2018:3789613. doi: 10.1155/2018/3789613

59. Qi LN, Xiang BD, Wu FX, Ye JZ, Zhong JH, Wang YY, et al. Circulating tumor cells undergoing EMT provide a metric for diagnosis and prognosis of patients with hepatocellular carcinoma. *Cancer Res* (2018) 78(16):4731–44. doi: 10.1158/0008-5472.CAN-17-2459

60. Wang Z, Luo L, Cheng Y, He G, Peng B, Gao Y, et al. Correlation between postoperative early recurrence of hepatocellular carcinoma and mesenchymal circulating tumor cells in peripheral blood. *J Gastrointest Surg* (2018) 22(4):633–9. doi: 10.1007/s11605-017-3619-3

61. Cheng Y, Luo L, Zhang J, Zhou M, Tang Y, He G, et al. Diagnostic value of different phenotype circulating tumor cells in hepatocellular carcinoma. *J Gastrointest Surg* (2019) 23(12):2354–61. doi: 10.1007/s11605-018-04067-y

62. Meng J, Chen S, Han JX, Qian B, Wang XR, Zhong WL, et al. Twist1 regulates vimentin through Cul2 circular RNA to promote EMT in hepatocellular carcinoma. *Cancer Res* (2018) 78(15):4150–62. doi: 10.1158/0008-5472.CAN-17-3009

63. Pal M, Bhattacharya S, Kalyan G, Hazra S. Cadherin profiling for therapeutic interventions in epithelial mesenchymal transition (EMT) and tumorigenesis. *Exp Cell Res* (2018) 368(2):137–46. doi: 10.1016/j.yexcr.2018.04.014

64. Yang J, Antin P, Berx G, Blanpain C, Brabletz T, Bronner M, et al. Guidelines and definitions for research on epithelial-mesenchymal transition. *Nat Rev Mol Cell Biol* (2020) 21(6):341–52. doi: 10.1038/s41580-020-0237-9

65. Thiery JP. EMT: An update. *Methods Mol Biol* (2021) 2179:35–9. doi: 10.1007/978-1-0716-0779-4_6

66. Dongre A, Weinberg RA. New insights into the mechanisms of epithelial-mesenchymal transition and implications for cancer. *Nat Rev Mol Cell Biol* (2019) 20(2):69–84. doi: 10.1038/s41580-018-0080-4

67. Greaves D, Calle Y. Epithelial mesenchymal transition (EMT) and associated invasive adhesions in solid and haematological tumours. *Cells* (2022) 11(4):649. doi: 10.3390/cells11040649

68. Nieto MA, Huang RY, Jackson RA, Thiery JP. Emt: 2016. *Cell* (2016) 166 (1):21–45. doi: 10.1016/j.cell.2016.06.028

69. Scheau C, Badarau IA, Costache R, Caruntu C, Mihai GL, Didilescu AC, et al. The role of matrix metalloproteinases in the epithelial-mesenchymal transition of hepatocellular carcinoma. *Anal Cell Pathol (Amst)* (2019) 2019:9423907. doi: 10.1155/2019/9423907

70. Stavropoulou V, Kaspar S, Brault L, Sanders MA, Juge S, Morettini S, et al. MLL-AF9 expression in hematopoietic stem cells drives a highly invasive AML expressing EMT-related genes linked to poor outcome. *Cancer Cell* (2016) 30 (1):43–58. doi: 10.1016/j.ccell.2016.05.011

71. Beerling E, Seinstra D, de Wit E, Kester L, van der Velden D, Maynard C, et al. Plasticity between epithelial and mesenchymal states unlinks EMT from metastasis-enhancing stem cell capacity. *Cell Rep* (2016) 14(10):2281–8. doi: 10.1016/j.celrep.2016.02.034

72. Terry S, Savagner P, Ortiz-Cuaran S, Mahjoubi L, Saintigny P, Thiery JP, et al. New insights into the role of EMT in tumor immune escape. *Mol Oncol* (2017) 11(7):824–46. doi: 10.1002/1878-0261.12093

73. Yu X, Wang Q, Liu B, Zhang N, Cheng G. Vitamin d enhances radiosensitivity of colorectal cancer by reversing epithelial-mesenchymal transition. *Front Cell Dev Biol* (2021) 9:684855. doi: 10.3389/fcell.2021.684855

74. Zhang N, Ng AS, Cai S, Li Q, Yang L, Kerr D. Novel therapeutic strategies: targeting epithelial-mesenchymal transition in colorectal cancer. *Lancet Oncol* (2021) 22(8):e358–68. doi: 10.1016/S1470-2045(21)00343-0

75. Zhang B, Li Y, Wu Q, Xie L, Barwick B, Fu C, et al. Acetylation of KLF5 maintains EMT and tumorigenicity to cause chemoresistant bone metastasis in prostate cancer. *Nat Commun* (2021) 12(1):1714. doi: 10.1038/s41467-021-21976-w

76. Bakir B, Chiarella AM, Pitarresi JR, Rustgi AK. EMT, MET, plasticity, and tumor metastasis. *Trends Cell Biol* (2020) 30(10):764–76. doi: 10.1016/j.tcb.2020.07.003

77. Ocana OH, Corcoles R, Fabra A, Moreno-Bueno G, Acloque H, Vega S, et al. Metastatic colonization requires the repression of the epithelial-mesenchymal transition inducer Prrx1. *Cancer Cell* (2012) 22(6):709–24. doi: 10.1016/j.ccr.2012.10.012

78. Tsai JH, Donaher JL, Murphy DA, Chau S, Yang J. Spatiotemporal regulation of epithelial-mesenchymal transition is essential for squamous cell carcinoma metastasis. *Cancer Cell* (2012) 22(6):725–36. doi: 10.1016/j.ccr.2012.09.022

79. Pei D, Shu X, Gassama-Diagne A, Thiery JP. Mesenchymal-epithelial transition in development and reprogramming. *Nat Cell Biol* (2019) 21(1):44–53. doi: 10.1038/s41556-018-0195-z

80. Jolly MK, Ware KE, Gilja S, Somarelli JA, Levine H. Emt and Met: necessary or permissive for metastasis? Mol Oncol. (2017) 11(7):755–69. doi: 10.1002/1878-0261.12083

81. Fang ZT, Zhang W, Wang GZ, Zhou B, Yang GW, Qu XD, et al. Circulating tumor cells in the central and peripheral venous compartment - assessing hematogenous dissemination after transarterial chemoembolization of hepatocellular carcinoma. *Onco Targets Ther* (2014) 7:1311–8. doi: 10.2147/OTT.S62605

82. Li YM, Xu SC, Li J, Han KQ, Pi HF, Zheng L, et al. Epithelial-mesenchymal transition markers expressed in circulating tumor cells in hepatocellular carcinoma patients with different stages of disease. *Cell Death Dis* (2013) 4:e831. doi: 10.1038/cddis.2013.347

83. Sun YF, Guo W, Xu Y, Shi YH, Gong ZJ, Ji Y, et al. Circulating tumor cells from different vascular sites exhibit spatial heterogeneity in epithelial and mesenchymal composition and distinct clinical significance in hepatocellular carcinoma. *Clin Cancer Res* (2018) 24(3):547–59. doi: 10.1158/1078-0432.CCR-17-1063

84. Ha Y, Kim TH, Shim JE, Yoon S, Jun MJ, Cho YH, et al. Circulating tumor cells are associated with poor outcomes in early-stage hepatocellular carcinoma: a prospective study. *Hepatol Int* (2019) 13(6):726–35. doi: 10.1007/s12072-019-09994-9

85. Takahashi K, Ofuji K, Hiramatsu K, Nosaka T, Naito T, Matsuda H, et al. Circulating tumor cells detected with a microcavity array predict clinical outcome in hepatocellular carcinoma. *Cancer Med* (2021) 10(7):2300–9. doi: 10.1002/cam4.3790

86. Xu W, Cao L, Chen L, Li J, Zhang XF, Qian HH, et al. Isolation of circulating tumor cells in patients with hepatocellular carcinoma using a novel cell separation strategy. *Clin Cancer Res* (2011) 17(11):3783–93. doi: 10.1158/1078-0432.CCR-10-0498

87. Li J, Chen L, Zhang X, Zhang Y, Liu H, Sun B, et al. Detection of circulating tumor cells in hepatocellular carcinoma using antibodies against asialoglycoprotein receptor, carbamoyl phosphate synthetase 1 and pan-cytokeratin. *PloS One* (2014) 9(4):e96185. doi: 10.1371/journal.pone.0096185

88. Ogle LF, Orr JG, Willoughby CE, Hutton C, McPherson S, Plummer R, et al. Imagestream detection and characterisation of circulating tumour cells - a liquid biopsy for hepatocellular carcinoma? *J Hepatol* (2016) 65(2):305–13. doi: 10.1016/j.jhep.2016.04.014

89. Ye X, Li G, Han C, Han Q, Shang L, Su H, et al. Circulating tumor cells as a potential biomarker for postoperative clinical outcome in HBV-related hepatocellular carcinoma. *Cancer Manag Res* (2018) 10:5639–47. doi: 10.2147/CMAR.S175489

90. Pang Y, Wang C, Xiao R, Sun Z. Dual-selective and dual-enhanced SERS nanoprobes strategy for circulating hepatocellular carcinoma cells detection. *Chemistry* (2018) 24(27):7060–7. doi: 10.1002/chem.201801133

91. Fan ST, Yang ZF, Ho DW, Ng MN, Yu WC, Wong J. Prediction of posthepatectomy recurrence of hepatocellular carcinoma by circulating cancer stem cells: a prospective study. *Ann Surg* (2011) 254(4):569–76. doi: 10.1097/SLA.0b013e3182300a1d

92. Sun YF, Xu Y, Yang XR, Guo W, Zhang X, Qiu SJ, et al. Circulating stem cell-like epithelial cell adhesion molecule-positive tumor cells indicate poor prognosis of hepatocellular carcinoma after curative resection. *Hepatology* (2013) 57(4):1458–68. doi: 10.1002/hep.26151

93. Wan S, Kim TH, Smith KJ, Delaney R, Park GS, Guo H, et al. New labyrinth microfluidic device detects circulating tumor cells expressing cancer stem cell marker and circulating tumor microemboli in hepatocellular carcinoma. *Sci Rep* (2019) 9(1):18575. doi: 10.1038/s41598-019-54960-y

94. Winograd P, Hou S, Court CM, Lee YT, Chen PJ, Zhu Y, et al. Hepatocellular carcinoma-circulating tumor cells expressing PD-L1 are prognostic and potentially associated with response to checkpoint inhibitors. *Hepatol Commun* (2020) 4(10):1527–40. doi: 10.1002/hep4.1577

95. Nicolazzo C, Gradilone A, Loreni F, Raimondi C, Gazzaniga P. EpCAM (low) circulating tumor cells: Gold in the waste. *Dis Markers* (2019) 2019:1718920. doi: 10.1155/2019/1718920

96. Giannelli G, Koudelkova P, Dituri F, Mikulits W. Role of epithelial to mesenchymal transition in hepatocellular carcinoma. *J Hepatol* (2016) 65(4):798–808. doi: 10.1016/j.jhep.2016.05.007

97. Espejo-Cruz ML, Gonzalez-Rubio S, Zamora-Olaya J, Amado-Torres V, Alejandre R, Sanchez-Frias M, et al. Circulating tumor cells in hepatocellular carcinoma: A comprehensive review and critical appraisal. *Int J Mol Sci* (2021) 22 (23):13073. doi: 10.3390/ijms222313073

98. Chen F, Zhong Z, Tan HY, Wang N, Feng Y. The significance of circulating tumor cells in patients with hepatocellular carcinoma: Real-time monitoring and moving targets for cancer therapy. *Cancers (Basel)* (2020) 12(7):1734. doi: 10.3390/cancers12071734

99. Sberna AL, Bouillet B, Rouland A, Brindisi MC, Nguyen A, Mouillot T, et al. European Association for the study of the liver (EASL), European association for the study of diabetes (EASD) and European association for the study of obesity (EASO) clinical practice recommendations for the management of non-alcoholic fatty liver disease: evaluation of their application in people with type 2 diabetes. *Diabetes Med* (2018) 35(3):368–75. doi: 10.1111/dme.13565

100. Tzartzeva K, Obi J, Rich NE, Parikh ND, Marrero JA, Yopp A, et al. Surveillance imaging and alpha fetoprotein for early detection of hepatocellular carcinoma in patients with cirrhosis: A meta-analysis. *Gastroenterology* (2018) 154 (6):1706–1718 e1. doi: 10.1053/j.gastro.2018.01.064

101. Court CM, Hou S, Winograd P, Segel NH, Li QW, Zhu Y, et al. A novel multimarker assay for the phenotypic profiling of circulating tumor cells in hepatocellular carcinoma. *Liver Transpl* (2018) 24(7):946–60. doi: 10.1002/lt.25062

102. Lv D, Chen L, Du L, Zhou L, Tang H. Emerging regulatory mechanisms involved in liver cancer stem cell properties in hepatocellular carcinoma. *Front Cell Dev Biol* (2021) 9:691410. doi: 10.3389/fcell.2021.691410

103. Walcher L, Kistenmacher AK, Suo H, Kitte R, Dluczek S, Strauss A, et al. Cancer stem cells-origins and biomarkers: Perspectives for targeted personalized therapies. *Front Immunol* (2020) 11:1280. doi: 10.3389/fimmu.2020.01280

104. Holczbauer A, Factor VM, Andersen JB, Marquardt JU, Kleiner DE, Raggi C, et al. Modeling pathogenesis of primary liver cancer in lineage-specific mouse cell types. *Gastroenterology* (2013) 145(1):221–31. doi: 10.1053/j.gastro.2013.03.013

105. Mu X, Espanol-Suner R, Mederacke I, Affo S, Manco R, Sempoux C, et al. Hepatocellular carcinoma originates from hepatocytes and not from the progenitor/biliary compartment. *J Clin Invest* (2015) 125(10):3891–903. doi: 10.1172/JCI77995

106. Mishra L, Banker T, Murray J, Byers S, Thenappan A, He AR, et al. Liver stem cells and hepatocellular carcinoma. *Hepatology* (2009) 49(1):318–29. doi: 10.1002/hep.22704

107. Zahran AM, Abdel-Rahim MH, Refaat A, Sayed M, Othman MM, Khalak LMR, et al. Circulating hematopoietic stem cells, endothelial progenitor cells and cancer stem cells in hepatocellular carcinoma patients: contribution to diagnosis and prognosis. *Acta Oncol* (2020) 59(1):33–9. doi: 10.1080/0284186X.2019.1657940

108. Reig M, Forner A, Rimola J, Ferrer-Fabrega J, Burrel M, Garcia-Criado A, et al. BCLC strategy for prognosis prediction and treatment recommendation: The 2022 update. *J Hepatol* (2022) 76(3):681–93. doi: 10.1016/j.jhep.2021.11.018

109. Amin MB, Greene FL, Edge SB, Compton CC, Gershenwald JE, Brookland RK, et al. The eighth edition AJCC cancer staging manual: Continuing to build a bridge from a population-based to a more "personalized" approach to cancer staging. *CA Cancer J Clin* (2017) 67(2):93–9. doi: 10.3322/caac.21388

110. Kamarajah SK, Frankel TL, Sonnenday C, Cho CS, Nathan H. Critical evaluation of the American joint commission on cancer (AJCC) 8th edition staging system for patients with hepatocellular carcinoma (HCC): A surveillance, epidemiology, end results (SEER) analysis. *J Surg Oncol* (2018) 117(4):644–50. doi: 10.1002/jso.24908

111. Fan JL, Yang YF, Yuan CH, Chen H, Wang FB. Circulating tumor cells for predicting the prognostic of patients with hepatocellular carcinoma: A meta analysis. *Cell Physiol Biochem* (2015) 37(2):629–40. doi: 10.1159/000430382

112. Xing R, Gao J, Cui Q, Wang Q. Strategies to improve the antitumor effect of immunotherapy for hepatocellular carcinoma. *Front Immunol* (2021) 12:783236. doi: 10.3389/fimmu.2021.783236

113. Lang L. FDA Approves sorafenib for patients with inoperable liver cancer. *Gastroenterology* (2008) 134(2):379. doi: 10.1053/j.gastro.2007.12.037

114. Ma Y, Xu R, Liu X, Zhang Y, Song L, Cai S, et al. LY3214996 relieves acquired resistance to sorafenib in hepatocellular carcinoma cells. *Int J Med Sci* (2021) 18(6):1456–64. doi: 10.7150/ijms.51256

115. Qi F, Qin W, Zhang Y, Luo Y, Niu B, An Q, et al. Sulfarotene, a synthetic retinoid, overcomes stemness and sorafenib resistance of hepatocellular carcinoma *via* suppressing SOS2-RAS pathway. *J Exp Clin Cancer Res* (2021) 40(1):280. doi: 10.1186/s13046-021-02085-4

116. Liu H, Zhao L, Wang M, Yang K, Jin Z, Zhao C, et al. FNDC5 causes resistance to sorafenib by activating the PI3K/Akt/Nrf2 pathway in hepatocellular carcinoma cells. *Front Oncol* (2022) 12:852095. doi: 10.3389/fonc.2022.852095

117. Wang L, Zhan Y, Wu Z, Lin M, Jin X, Jiang L, et al. A novel multitarget kinase inhibitor BZG with potent anticancer activity *in vitro* and vivo enhances efficacy of sorafenib through PI3K pathways in hepatocellular carcinoma cells. *BioMed Pharmacother* (2020) 125:110033. doi: 10.1016/j.biopha.2020.110033

118. Ribas A, Wolchok JD. Cancer immunotherapy using checkpoint blockade. *Science* (2018) 359(6382):1350–5. doi: 10.1126/science.aar4060

119. Khattak MA, Reid A, Freeman J, Pereira M, McEvoy A, Lo J, et al. PD-L1 expression on circulating tumor cells may be predictive of response to pembrolizumab in advanced melanoma: Results from a pilot study. *Oncologist* (2019) 25(3):e520–27. doi: 10.1634/theoncologist.2019-0557

frontiers | Frontiers in Pharmacology

TYPE Original Research
PUBLISHED 25 August 2022
DOI 10.3389/fphar.2022.969422

Check for updates

OPEN ACCESS

EDITED BY
Weilong Zhong,
Tianjin Medical University General Hospital, China

REVIEWED BY
Yifei Gao,
Tsinghua University, China
Zhaowei Xu,
Binzhou Medical University, China
Xiaowei Guo,
Hunan Normal University, China

*CORRESPONDENCE
Yuan Qin,
qinyuan@zstu.edu.cn

†These authors have contributed equally to this work

SPECIALTY SECTION
This article was submitted to Pharmacology of Anti-Cancer Drugs, a section of the journal Frontiers in Pharmacology

RECEIVED 15 June 2022
ACCEPTED 25 July 2022
PUBLISHED 25 August 2022

CITATION
Chen X, Zhou Z, Zhang Z, Zhao C, Li J, Jiang J, Huang B and Qin Y (2022), Puerarin inhibits EMT induced by oxaliplatin via targeting carbonic anhydrase XII.
Front. Pharmacol. 13:969422.
doi: 10.3389/fphar.2022.969422

COPYRIGHT
© 2022 Chen, Zhou, Zhang, Zhao, Li, Jiang, Huang and Qin. This is an open-access article distributed under the terms of the Creative Commons Attribution License (CC BY). The use, distribution or reproduction in other forums is permitted, provided the original author(s) and the copyright owner(s) are credited and that the original publication in this journal is cited, in accordance with accepted academic practice. No use, distribution or reproduction is permitted which does not comply with these terms.

Puerarin inhibits EMT induced by oxaliplatin *via* targeting carbonic anhydrase XII

Xindong Chen[1†], Zhiruo Zhou[2,3†], Zhi Zhang[1], Chenhao Zhao[1], Jiayu Li[1], Jingwen Jiang[1], Biao Huang[1] and Yuan Qin[1*]

[1]College of Life Sciences and Medicine, Zhejiang Sci-Tech University, Hangzhou, China, [2]School of Environmental Science and Engineering, Zhejiang Gongshang University, Hangzhou, China, [3]Zhejiang Provincial Key Laboratory of Solid Waste Treatment and Recycling, Hangzhou, China

Puerarin is a flavonoid molecule that widely exists in various plants. Puerarin has been reported to exhibit anti-tumor effects in various cancers. However, its exact underlying pharmacological mechanism is unclear. This study evaluated the anticancer effect of puerarin combined with oxaliplatin (OXA) *in vitro* and *in vivo*. Our results indicated that puerarin can reverse platinum-based anti-cancer drug resistance, and enhance the OXA's anticancer effects on breast cancer. Furthermore, puerarin can inhibit migration and reverse the epithelial-mesenchymal transition (EMT) induced by low-dose OXA. Further studies showed that the carbonic anhydrase (CA) XII is a potential target of puerarin. In conclusion, puerarin is expected to become an adjuvant chemotherapy drug and potentially become one of the medicated foods for breast cancer patients.

KEYWORDS

puerarin, oxaliplatin, breast cancer, epithelial-mesenchymal transition, carbonic anhydrase XII

Introduction

Chemotherapy is used to treat cancer, prolong the life of cancer patients, and even cure cancer, however, sometimes it can stimulate cancer cells and cause metastasis (Wills et al., 2021; Dai et al., 2022). Therefore, continuous efforts have been made to find and develop new strategies for cancer therapy with lower side effects and better efficacy. For this, various researchers pay great attention to compounds from natural plants and their derivatives, which can be potential in the treatment of cancers (Chen et al., 2009; Shirode et al., 2015). These compounds are found in many diets and can be good options for adjuvant cancer treatment.

Flavonoids are a type of natural small molecules with anti-cancer, anti-inflammatory and antioxidant effects (Maleki et al., 2019; Bisol et al., 2020; Kopustinskiene et al., 2020; Liu et al., 2022). Puerarin is a typical flavonoid molecule and active ingredient extracted from leguminous plants of the genus *Pueraria*, an important medicinal plant known for its health and beauty benefits. In 1993, puerarin was approved for clinical use and was widely used in treating cardiovascular diseases (Ahmad et al., 2020). In addition, puerarin has two benzene rings (A ring and B ring) linked to each other through the central three carbon structure, and many evidences have proved that this structure has the ability to down-regulate mutant p53 protein, block cell cycle and inhibit Ras protein expression and anti-cancer

properties (Lamson and Brignall, 2000; Bisol et al., 2020). Various studies demonstrated that puerarin plays an anti-cancer role in several trials (Wang et al., 2013; Kang et al., 2017; Liu et al., 2017). Puerarin inhibits lymphatic carcinoma cell proliferation and reduces the levels of matrix metalloproteinase through reactive oxygen oxidative stress. In addition, through endogenous and exogenous mitochondrial pathways, puerarin induces tumor cells apoptosis (Chen et al., 2016; Hu et al., 2018). Puerarin selectively reduces tumor cells' proliferative capacity and extensively inhibits cancer cells signaling pathway transduction (Liu et al., 2017). Liu et al. showed that lipopolysaccharide (LPS) treatment increases the capacity to metastasize of breast cancer cells, while puerarin reduces the metastasis and invasion of LPS-induced breast cancer cells (Liu et al., 2017), suggesting that puerarin can potentially be used for anti-breast cancer.

Epithelial-mesenchymal transition (EMT) refers to how epithelial cells are depolarized and transformed into mesenchymal cells due to certain factors (Jiang et al., 2022). During the metastasis in epithelial tumors, the phenotype of tumor cells changes primarily caused by environmental stimuli that enable tumor cells to adapt to the various microenvironments they encounter (intercellular stroma, humoral components, or blood) (Park et al., 2020; Qiao et al., 2021). EMT regulates these phenotypic transformations. Therefore, to some extent, EMT promotes tumor metastasis (Pastushenko and Blanpain, 2019). Meanwhile, it has been reported that low-concentration chemotherapy drugs not only significantly inhibit tumor proliferation, but also induce EMT of tumor cells, thus promoting tumor metastasis (Middleton et al., 2018).

Therefore, this study aims to detect whether puerarin can enhance the effect of oxaliplatin (OXA), the third generation of platinum chemotherapy drugs, on breast cancer and inhibit metastasis of breast cancer cells.

Materials and methods

Chemicals and cell culture

Puerarin was purchased from Meilunbio (Dalian, China). E-cadherin antibody (ab40772) and vimentin antibody (BF8006) were purchased from Abcam and Affinity, respectively. Apoptosis Detection Kit was purchased from Beyotime (Shanghai, China). Crystal violet was purchased from Sigma-Aldrich Fluka (America). OXA was purchased from Meilunbio (Dalian, China), LTD. Cisplatin (DDP) was purchased from Sigma-Aldrich.

The MCF-7 (human breast cancer cell lines) and MCF-7/DDP (DDP-resistant cell lines), were from KeyGEN BioTECH (Nanjing, China). These cells were grown in DMEM containing penicillin, streptavidin, and 10% bovine serum at 5% CO_2, and 37°C.

Cell viability assay

The drug tolerance effects of puerarin were detected using the 3-(4,5-dimethyl-2-thiazolyl)-2,5-diphenyl-2-H-tetrazolium bromide (MTT) assay on MCF-7, MCF-7/DDP. The cells (5,000 cells/well) were added to 96-well plates cultured overnight. All assays were repeated three times. In each flask, MTT solution was added after 48 h of drug treatment. Incubation in dimethyl sulfoxide (DMSO) for 4 h dissolves the formazan crystals. OD_{590} value was detected with a microplate reader, and detected a 50% inhibitory concentration (IC_{50}) value. The synergistic effect was calculated using CompuSyn software.

Rh123 efflux assay

Cells (1×10^6) were cultured for 24 h in six-well plates. A variety of levels of puerarin were used for the pretreatment of MCF-7/DDP cells for 24 h [0 μM, 20 μM (L), 40 μM (H)]. After the pretreatment, cells were incubated with Rh123 (5 mg/mL) in a dark room. Then, Rh123-free medium was used to replace the above medium, and drained the remaining efflux intervals every hour. After incubation, PBS was used to wash cells twice. Then, 400 μL lysis buffer was used for lysing cells, and PBS with 10% FBS was used to maintain the cells. The flow cytometry was used to determine the green fluorescence of Rh123.

Wound-healing assay

A wound healing assay was performed to assess changes in cell motility and migration. Cells were grown to confluency at 5×10^5 cells per well in 48-well plates. Scratch the cell monolayer with an apipette tip and then rinse using phosphate buffer saline (PBS). After the treatment [Control, OXA (5 μM), puerarin (40 μM) + OXA (5 μM)], a Nikon microscope was used to take images 0, 24, and 48 h.

Transwell assays

The transwell assay is used to evaluate cell invasiveness. Three different concentrations of medium [Control, OXA (5 μM), puerarin (40 μM) + OXA (5 μM)] were used for the suspension of the cells below. The cells were then inoculated into an 8 μm polyethylene terephthalate filter membrane coated with matrix gel. In the lower chamber, about 500 mL of medium was placed. The cells were fixed for 30 min with paraformaldehyde (4%) and stained for 20 min with crystal violet (0.1%). A hundred-fold magnification inverted microscope was used to image the invaded cells, and the cell numbers were manually counted.

Immunofluorescence assays

Cells were treated [Control, OXA (5 μM), puerarin (40 μM) + OXA (5 μM)] and were cultured overnight. The cells were treated with methanol and Triton X-100. E-cadherin and vimentin (both 1:100) were used in an immunofluorescence experiment. After washing thrice for 20 min, Incubation of the cells with a secondary antibody (1:200) for 30 min. Following 4,6-diamino-2-phenyl indole (DAPI) staining for 10 min, and observed under a laser scanning confocal microscope.

Apoptosis assays

A 96-well plate was used to culture the cells. After drugs treatment, the culture solution was discarded. Then, Annexin V-FITC binding solution, Annexin V-FITC and propyl iodide solution were successively added and gently mixed all the solutions. In a dark room, plates were incubated for 20 min. The red and green fluorescence was detected by a fluorescence microscope.

Animal studies

In this section, BALB/c nude mice (5 weeks) were used. All mice were raised in sterile conditions. All procedures were approved according to the guidelines of the Animal Ethics Committee of the Zhejiang Sci-tech University. The MCF-7 cells were orthotopically implanted into the mice. Cells were grown until the logarithmic growth stage, centrifuged with PBS. 50% Matrigel mixture was resuspended in PBS, resulting in 2×10^7 cells/mL. The right flank of each mouse was injected 0.2 mL cell suspension. After 14 d of tumor transplantation, four groups of mice were divided: control group (saline given orally once daily), puerarin treated group (50 mg/kg), OXA treated group (5 mg/kg), and puerarin and OXA treated group (50 mg/kg + 5 mg/kg). After the tumor was transplanted, daily measurements were taken of its volume and weight. All mice were euthanized after 3 weeks. Tumors were resected and volumes were measured. $V = ab^2/2$ (a = length, b = width) was used to calculate tumor volumes. To measure their survival rates, another 40 mice were distributed into 4 groups (10 per group). The survival time of each mouse was monitored.

RNA sequencing data collection and procession

The RNA sequencing data for cancer tissues and adjacent tissues from patients with breast cancer were obtained from the Gene Expression Omnibus (GEO) database. The differentially expressed gene (DEG) was considered by four sample data, involving GSM2286198, GSM2286199, GSM2286316, and GSM2286317 with two drug treatment samples and two control samples.

Analysis of differentially expressed genes

In the R computing environment, with the Limma package, the corresponding fold change and p value for DEGs between different groups were compared using a volcano plot. Up- and down-regulated genes had $p \leq 0.05$, a fold change of more than 2.0, defined as $\log_2$ (fold change) > 1 or < - 1 for up- and down-regulated genes, respectively. For gene function enrichment analysis, gene ontology (GO) annotations of genes in R software were used. A maximum gene of 5,000 and a minimum gene of 5 was set ($p < 0.05$ and FDR <0.25).

Target prediction and molecular docking

To predict puerarin's targets, the simplified molecular input line entry system (SMILES) format of puerarin from PubChem and the similarity ensemble approach (SEA) website were used (Keiser et al., 2007). Molecular docking was performed with puerarin and carbonic anhydrase (CA) XII. An analysis of the complex between the ligand and protein was carried out by Pymol using the PDB format.

CA XII activity analysis

The CA XII activity in breast cancer cells was determined by extracellular pH analysis. Cells were treated with [20 μM (L) puerarin +500 nM U-104] and [40 μM (H) puerarin +200 nM U-104] for 3 h. The Wilbur-Anderson method was used to calculate CA XII activity (WAU/mg = 2× (T_0-T)/T*mg protein). To determine how long it will take to reduce the pH of an isotonic buffer from 8.00 to 6.60, using time (T) (T: catalyzed reaction and T0: unanalyzed reaction).

Data statistics

Data are analyzed as mean ± standard deviation (SD). The independent variance t-test were used to assess the differences between the two groups. The multiple comparisons test were compared using a one-way analysis of variance, followed by the least significance difference (LSD) post-hoc test (SPSS 23.0).

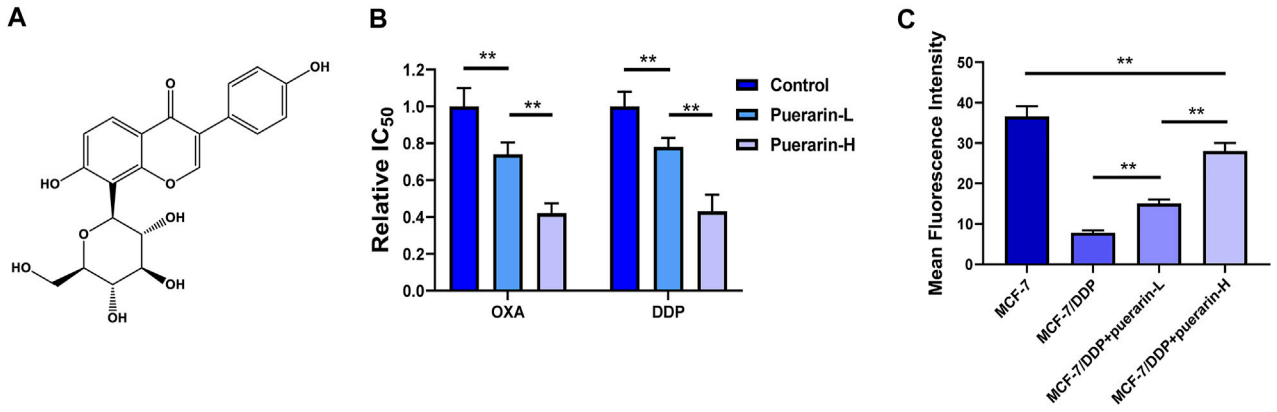

FIGURE 1
Puerarin reversed drug resistance of platinum-based anti-cancer drug. **(A)** The structural formulas of puerarin **(B)** The IC_{50} values of OXA and DDP on MCF-7 were detected. The cancer cells were treated with different concentrations of puerarin (Control: DMSO, puerarin-L: 20 μM, puerarin-H: 40 μM). **(C)** The fluorescence intensity of Rh123 in MCF-7/DDP was lower than the fluorescence intensity in MCF-7. Puerarin treatment reversed the change in a dose-dependent manner (*$p < 0.05$, **$p < 0.01$).

Results

Puerarin enhanced the effects of platinum-based anti-cancer drug and reversed drug-resistance

Figure 1A shows the structural formulas of puerarin. In order to detect the effect of puerarin in reversing drug resistance, OD_{590} was measured. In our results, drug resistance to DDP and OXA can be reversed by puerarin in MCF-7/DDP cells. In addition, there is a dose-effect relationship in the reverse effect of puerarin on MCF-7/DDP cells (Figure 1B). A study was carried out to evaluate the efflux of Rh123 from MCF-7/DDP cells. Figure 1C indicates that as compared to the other groups, the puerarin groups had a higher fluorescence intensity.

There is a synergistic effect of puerarin and OXA on tumor inhibition

In order to detect the synergistic effects of puerarin and OXA, the MTT assay was performed. As shown in Figures 2A,B, puerarin improves the inhibitory effect of OXA and DDP on cell proliferation. Furthermore, combining puerarin with platinum-based drugs resulted in a combination index (CI) value less than 1, thus indicating synergistic effects. The effect of co-treatment on MCF-7/DDP xenografts in nude mice BALB/c was evaluated. Mice in the combination treatment group gained weight compared to those in the OXA-treated group. Compared to the other groups, the tumor weight of co-treatment group is lowest (Figures 2C–E).

Each group of tumor cells was tested for apoptosis using the apoptosis detection kit. Annexin V was marked with green fluorescence indicating apoptotic cells and PI was marked with red fluorescence indicating necrotic cells. As shown in Figures 2F,G, puerarin improves the efficacy of OXA and a significant increase in apoptosis cells was observed in the co-treatment group. Moreover, compared to a single treatment, mice of co-treatment group had a higher survival rate (Figure 2H).

Puerarin inhibited migration and invasion and reversed EMT induced by low dose OXA

Morphological changes in the cancer cells in different treatment groups were observed by an optical microscope. As a result of low dose OXA, cancer cells developed pseudopodia and the co-treatment group displayed signs of apoptosis, such as rounded and shed cells, as shown in Figure 3A. The migration and invasion of co-treated cells was detected by wound-healing assay and transwell assay, and the results as shown in Figures 3B,D, the migration was highly enhanced in the OXA-treated group, whereas, it was significantly inhibited in the co-treatment group. Similarly, A combination of purarin and OXA inhibits the invasion of cancer cells by low-dose OXA (Figures 3C,E). Moreover, the expression of EMT biomarkers was detected using an immunofluorescence assay and it was found that vimentin levels of co-treatment group were lower than that of OXA group, whereas E-cadherin levels were higher, as shown in Figures 3F–H. Based on these results, the OXA-treated group promotes EMT, whereas puerarin inhibits the EMT process caused by OXA.

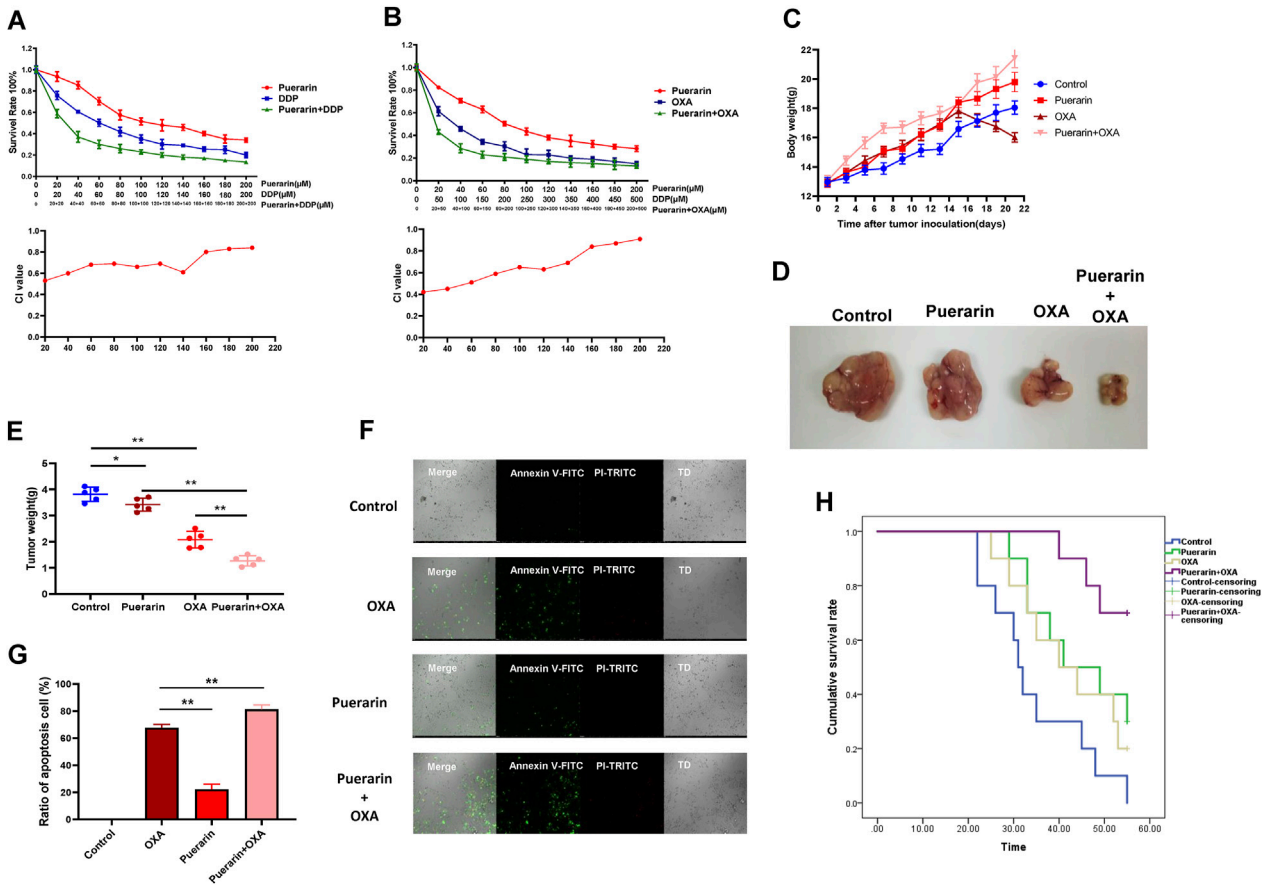

FIGURE 2
Puerarin enhanced the effects of OXA. **(A,B)** MTT assay was operated to detect the inhibition on MCF-7 cells. Puerarin enhances the inhibitory effect of OXA and DDP on cell proliferation **(C–E)** Mice in the combination treatment group gained weight compared to those in the OXA-treated group. Compared to the other groups, the tumor weight of co-treatment group is lowest. **(F,G)** Annexin V-FITC and PI-TRITC were used to detected the apoptosis cells. Puerarin improves the efficacy of OXA and a significant increase in apoptosis cells was observed in the co-treatment group **(H)** Mice of co-treatment group had a higher survival rate than the mice in other groups (*$p < 0.05$, **$p < 0.01$).

There is a widespread influence of puerarin in cancer cells

The RNA sequencing data (GSE85871) for cancer tissues and adjacent tissues of patients with breast cancer were got from GEO database. The graph was drawn with the $\log_2$ ratio and the $-\log_{10}$ (p) of each gene as shown in Figure 4A. Downregulated genes and upregulated genes are indicated by green and red, respectively. The hierarchical clustering was made using the differentially expressed genes, as shown in Figure 4B. The various interactions between the control group and puerarin treatment groups were recorded by the STRING database and visualized in Cytoscape, as shown in Figure 4C. Analysis with GO and the KEGG revealed that differentially expressed genes tended to be enriched for tumor metastasis and energy metabolism, as shown in Figures 4D–G.

CA XII is a potential drug target of puerarin

The SMILES format of puerarin from PubChem and the SEA website was used to predict puerarin's targets. CA VII and CA XII were the first two potential drug targets with the Max Tanimoto Coefficient (MaxTC) of 1.00, as shown in Figure 5A. The CA XII is more closely associated with cancer cells than with CA VII. The molecular docking results showed that there is a good combination between puerarin and CA XII, with the docking score -5.93, as shown in Figure 5B. CA XII catalyzes the hydration of carbon dioxide to H^+ and HCO_3^-, causing the acidic extracellular pH to decrease. The ability of puerarin to inhibit CA activity was determined by measuring extracellular pH. The results showed that puerarin could inhibit CA activity under a dose-effect relationship (Figure 5C). Low dose OXA treatment increased the

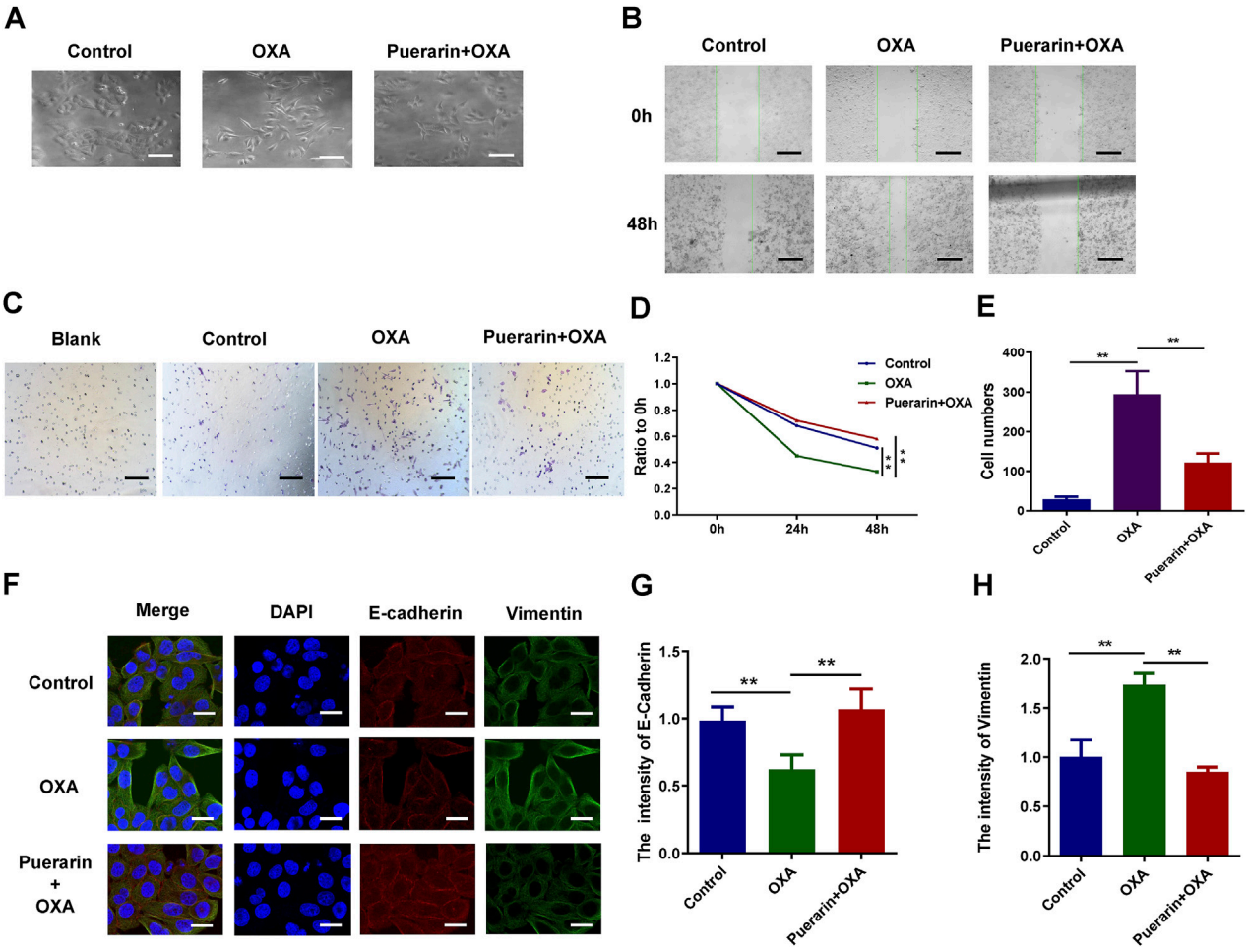

FIGURE 3
Puerarin inhibited migration and invasion and reversed EMT. **(A)** Morphological changes of the cancer cells in different treatment groups observed by a microscope **(B,D)** The results of wound-healing assay. **(C,E)** The results of transwell assay **(F–H)** The results of immunofluorescence (*$p < 0.05$, **$p < 0.01$).

extracellular pH compared to the control group, meanwhile, the puerarin inhibited this trend, thereby suggesting that puerarin inhibited CA activity, as shown in Figure 5D.

Discussion

Recently, for breast cancer, while significant progress has been made in diagnosis and treatment, the prognosis remains bleak (Zhao et al., 2017; Chen et al., 2022). It was reported that after OXA treatment, residual cancer cells revealed increased metastasis significantly. Our previous study and other research all showed that low-dose platinum-based anti-cancer drugs could induce EMT of cancer cells (Liu et al., 2015). EMT caused by chemotherapy is a significant determinant of drug resistance to chemotherapy and cancer metastasis.

New therapeutic options that safely enhance chemotherapy sensitivity significantly improve efficiency in cancer treatment (Luan et al., 2020; Zhang et al., 2020). In our study, the combination of puerarin and OXA can improve the sensitivity of OXA chemotherapy, thus, inhibiting the metastasis of breast cancer. In addition, puerarin can reverse OXA resistance in drug-resistant breast cancer. The combined administration of puerarin can also inhibit low-dose OXA-induced EMT as indicated in the results. Meanwhile, the co-treatment group inhibited tumor weight *in vivo* compared with the chemotherapy drug group alone. Therefore, puerarin can be used as a complementary medicine for OXA in enhancing the chemotherapy sensitivity and anti-cancer ability of OXA.

Multiple studies have shown that puerarin has good anticancer mechanisms against several cancer cells (Li et al., 2019; Aboushanab et al., 2021). However, the exact molecular

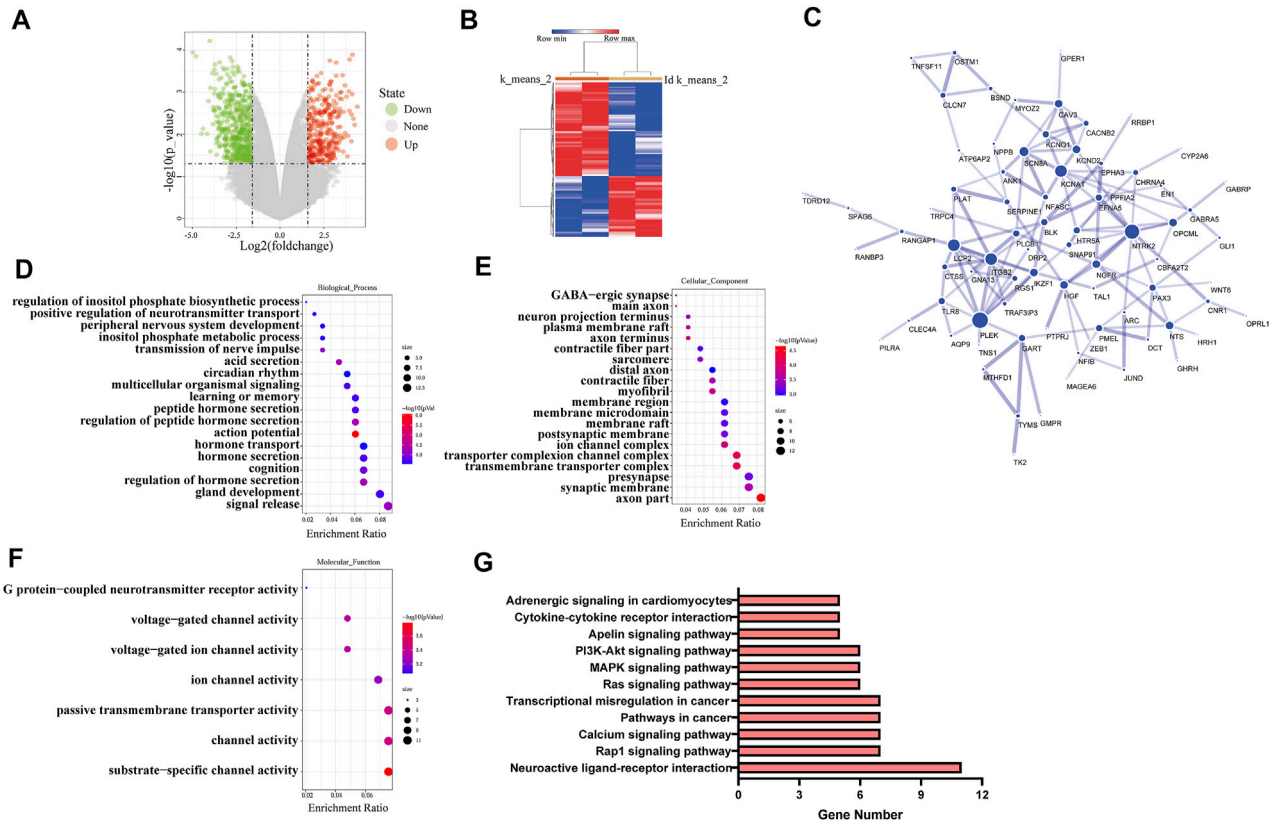

FIGURE 4
Puerarin effected multiple functions and signal pathways of cancer cells. **(A)** The volcano plot of differentially expressed genes **(B)** The hierarchical clustering of differentially expressed genes. **(C)** The protein-protein interaction network of differentially expressed genes **(D–F)** The GO analysis results of differentially expressed genes, **(D)** Biological process, **(E)** Cellular component, **(F)** Molecular fuction **(G)** The KEGG analysis results of differentially expressed genes.

mechanism and potential drug target of puerarin remain unknown (Wang et al., 2020). Natural small molecules from plants generally have an extensive range of pharmacological activities (Sun et al., 2017). Our results showed that puerarin has the potential to inhibit various functions and signaling pathways of breast cancer cells. Furthermore, it was found that the CA XII is the puerarin's potential target and puerarin inhibits the acid secretion mediated by the CA protein. The CA XII exists in various organsand plays a key role in life activities (Karhumaa et al., 2000; Parkkila et al., 2000; Liao et al., 2003). CA XII's expression can be detected in various types of tumor, including breast cancer and other cancer (Kivela et al., 2005; Hsieh et al., 2010; Ilie et al., 2011). Extensive evidences suggest that CA XII plays a key role in the migration, invasion and metastasis of cancer cells. Hsieh et al. demonstrated that silencing CA XII also reduces the migration and invasion of breast cancer cells, and that CA XII interacts with matrix metalloproteinases in proteolysis of ECM during migration and invasion of cancer cells (Hsieh et al., 2010). As another target protein in this study, CA VII is mainly related to the pathogenesis of neuromuscular disorders and has almost no correlation with cancer (Pastorekova et al., 2004; Viikilä et al., 2016), therefore we chose CA XII as our target protein. Recent studies have indicated that CA XII participates in chemotherapy drug resistance, hence, promoting the further development of tumors (Kobayashi et al., 2012; Kopecka et al., 2015). Our results showed that a low dose of OXA activates the CA XII's activity in breast cancer cells, which is detrimental to cancer treatment. Puerarin can inhibit the activity of CA XII, which can influence chemotherapy drugs to enhance the anticancer effect of chemotherapy drugs.

There are also some deficiencies in this study. In future research, in-depth studies on the mechanism of puerarin *in vivo* and systematic studies on the toxicity, side effects of puerarin could be done. In addition, the pharmacological activity of puerarin could be further enhanced by targeted modification of its structure through medicinal chemistry methods.

Our results demonstrated the anticancer effects of puerarin on tumor cells and models of xenograft mice. Puerarin targeted CA XII and affected multiple carcinogenic signaling networks. In

A

Target protein	P-value	MaxTC
Carbonic anhydrase VII	2.59e-07	1.00
Carbonic anhydrase XII	0.0001284	1.00
Type 1 fimbrin D-mannose specific adhesin	1.839e-74	0.32
Aldehyde dehydrogenase, mitochondrial	8.702e-71	0.54
Sodium/glucose cotransporter 2	4.823e-63	0.42

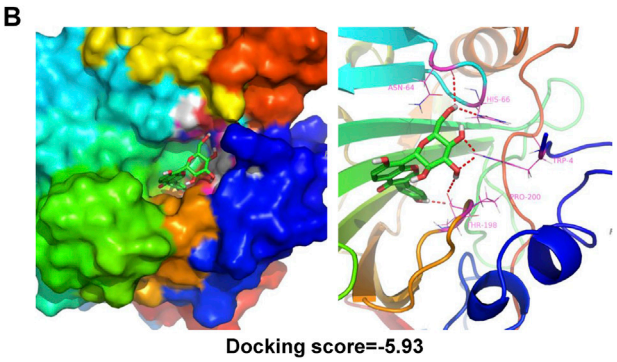

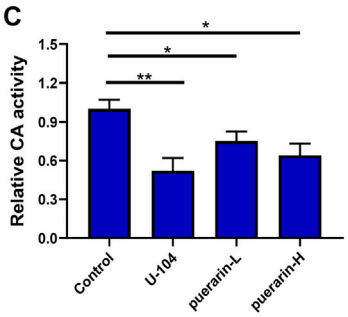

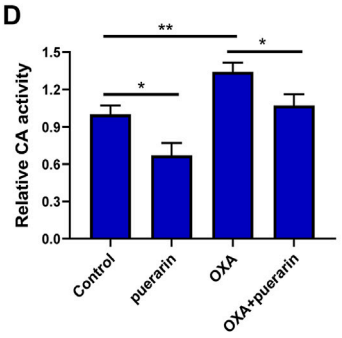

FIGURE 5
CA XII is a potential drug target of puerarin. **(A)** The predicted targets for puerarin **(B)** The molecular docking results showed that there is a good combination between puerarin and CA XII, with the docking score -5.93. **(C)** Puerarin could inhibit CA activity under a dose-effect relationship **(D)** Low dose OXA treatment increased the extracellular pH level compared with the control group, and puerarin inhibited this trend (*$p < 0.05$, **$p < 0.01$).

addition, puerarin significantly increased platinum sensitivity and inhibited platinum-induced EMT in breast cancer. There are some reasons why puerarin is expected to become an adjuvant chemotherapy drug and has the potential to become one of the medicated foods for breast cancer patients.

Data availability statement

The datasets presented in this study can be found in online repositories. The names of the repository/repositories and accession number(s) can be found in the article/Supplementary Material.

Ethics statement

The animal study was reviewed and approved by the Animal Ethics Committee of the Zhejiang Sci-tech University.

Author contributions

XC and ZZ wrote the main manuscript text and prepared all figures. ZZ and CZ did the data processing. JL, JJ, and BH offered their opinions on the paper. YQ provided the funds and supervised the project.

Funding

Scientific Research Foundation of Zhejiang Sci-Tech University (Project Number: 21042102-Y).

Conflict of interest

The authors declare that the research was conducted in the absence of any commercial or financial relationships that could be construed as a potential conflict of interest.

Publisher's note

All claims expressed in this article are solely those of the authors and do not necessarily represent those of their affiliated organizations, or those of the publisher, the editors and the reviewers. Any product that may be evaluated in this article, or claim that may be made by its manufacturer, is not guaranteed or endorsed by the publisher.

References

Aboushanab, S. A., Khedr, S. M., Gette, I. F., Danilova, I. G., Kolberg, N. A., Ravishankar, G. A., et al. (2021). Isoflavones derived from plant raw materials: Bioavailability, anti-cancer, anti-aging potentials, and microbiome modulation. *Crit. Rev. Food Sci. Nutr.* 6, 1–27. doi:10.1080/10408398.2021.1946006

Ahmad, B., Khan, S., Liu, Y., Xue, M., Nabi, G., Kumar, S., et al. (2020). Molecular mechanisms of anticancer activities of puerarin. *Cancer Manag. Res.* 12, 79–90. doi:10.2147/CMAR.S233567

Bisol, Â., de Campos, P. S., and Lamers, M. L. (2020). Flavonoids as anticancer therapies: A systematic review of clinical trials. *Phytother. Res.* 34 (3), 568–582. doi:10.1002/ptr.6551

Chen, H. M., Wu, Y. C., Chia, Y. C., Chang, F. R., Hsu, H. K., Hsieh, Y. C., et al. (2009). Gallic acid, a major component of Toona sinensis leaf extracts, contains a ROS-mediated anti-cancer activity in human prostate cancer cells. *Cancer Lett.* 286 (2), 161–171. doi:10.1016/j.canlet.2009.05.040

Chen, T., Chen, H., Wang, Y., and Zhang, J. (2016). *In vitro* and *in vivo* antitumour activities of puerarin 6″-O-xyloside on human lung carcinoma A549 cell line via the induction of the mitochondria-mediated apoptosis pathway. *Pharm. Biol.* 54 (9), 1793–1799. doi:10.3109/13880209.2015.1127980

Chen, X., Zhou, K., Xiang, Z., Zhou, X., Wang, Y., Hong, J., et al. (2022). Establishment and clinical application of time-resolved immunofluorescence assay of lipoprotein-associated phospholipase A2. *Anal. Biochem.* 648, 114674. doi:10.1016/j.ab.2022.114674

Dai, C. J., Cao, Y. T., Huang, F., and Wang, Y. G. (2022). Multiple roles of mothers against decapentaplegic homolog 4 in tumorigenesis, stem cells, drug resistance, and cancer therapy. *World J. Stem Cells* 14 (1), 41–53. doi:10.4252/wjsc.v14.i1.41

Hsieh, M. J., Chen, K. S., Chiou, H. L., and Hsieh, Y. S. (2010). Carbonic anhydrase XII promotes invasion and migration ability of MDA-MB-231 breast cancer cells through the p38 MAPK signaling pathway. *Eur. J. Cell Biol.* 89 (8), 598–606. doi:10.1016/j.ejcb.2010.03.004

Hu, Y., Li, X., Lin, L., Liang, S., and Yan, J. (2018). Puerarin inhibits non-small cell lung cancer cell growth via the induction of apoptosis. *Oncol. Rep.* 39 (4), 1731–1738. doi:10.3892/or.2018.6234

Ilie, M. I., Hofman, V., Ortholan, C., Ammadi, R. E., Bonnetaud, C., Havet, K., et al. (2011). Overexpression of carbonic anhydrase XII in tissues from resectable non-small cell lung cancers is a biomarker of good prognosis. *Int. J. Cancer* 128 (7), 1614–1623. doi:10.1002/ijc.25491

Jiang, J., Li, J., Zhou, X., Zhao, X., Huang, B., and Qin, Y. (2022). Exosomes regulate the epithelial-mesenchymal transition in cancer. *Front. Oncol.* 12, 864980. doi:10.3389/fonc.2022.864980

Kang, H., Zhang, J., Wang, B., Liu, M., Zhao, J., Yang, M., et al. (2017). Puerarin inhibits M2 polarization and metastasis of tumor-associated macrophages from NSCLC xenograft model via inactivating MEK/ERK 1/2 pathway. *Int. J. Oncol.* 50 (2), 545–554. doi:10.3892/ijo.2017.3841

Karhumaa, P., Parkkila, S., Tureci, O., Waheed, A., Grubb, J. H., Shah, G., et al. (2000). Identification of carbonic anhydrase XII as the membrane isozyme expressed in the normal human endometrial epithelium. *Mol. Hum. Reprod.* 6 (1), 68–74. doi:10.1093/molehr/6.1.68

Keiser, M. J., Roth, B. L., Armbruster, B. N., Ernsberger, P., Irwin, J. J., and Shoichet, B. K. (2007). Relating protein pharmacology by ligand chemistry. *Nat. Biotechnol.* 25 (2), 197–206. doi:10.1038/nbt1284

Kivela, A. J., Parkkila, S., Saarnio, J., Karttunen, T. J., Kivela, J., Parkkila, A. K., et al. (2005). Expression of von Hippel-Lindau tumor suppressor and tumor-associated carbonic anhydrases IX and XII in normal and neoplastic colorectal mucosa. *World J. Gastroenterol.* 11 (17), 2616–2625. doi:10.3748/wjg.v11.i17.2616

Kobayashi, M., Matsumoto, T., Ryuge, S., Yanagita, K., Nagashio, R., Kawakami, Y., et al. (2012). CAXII Is a sero-diagnostic marker for lung cancer. *PLoS One* 7 (3), e33952. doi:10.1371/journal.pone.0033952

Kopecka, J., Campia, I., Jacobs, A., Frei, A. P., Ghigo, D., Wollscheid, B., et al. (2015). Carbonic anhydrase XII is a new therapeutic target to overcome chemoresistance in cancer cells. *Oncotarget* 6 (9), 6776–6793. doi:10.18632/oncotarget.2882

Kopustinskiene, D. M., Jakstas, V., Savickas, A., and Bernatoniene, J. (2020). Flavonoids as anticancer agents. *Nutrients* 12 (2), E457. doi:10.3390/nu12020457

Lamson, D. W., and Brignall, M. S. (2000). Antioxidants and cancer, part 3: Quercetin. *Altern. Med. Rev.* 5 (3), 196–208.

Li, J., Guo, C., Lu, X., and Tan, W. (2019). Anti-colorectal cancer biotargets and biological mechanisms of puerarin: Study of molecular networks. *Eur. J. Pharmacol.* 858, 172483. doi:10.1016/j.ejphar.2019.172483

Liao, S. Y., Ivanov, S., Ivanova, A., Ghosh, S., Cote, M. A., Keefe, K., et al. (2003). Expression of cell surface transmembrane carbonic anhydrase genes CA9 and CA12 in the human eye: Overexpression of CA12 (CAXII) in glaucoma. *J. Med. Genet.* 40 (4), 257–261. doi:10.1136/jmg.40.4.257

Liu, F., Peng, Y., Qiao, Y., Huang, Y., Song, F., Zhang, M., et al. (2022). Consumption of flavonoids and risk of hormone-related cancers: A systematic review and meta-analysis of observational studies. *Nutr. J.* 21 (1), 27. doi:10.1186/s12937-022-00778-w

Liu, X., Zhao, W., Wang, W., Lin, S., and Yang, L. (2017). Puerarin suppresses LPS-induced breast cancer cell migration, invasion and adhesion by blockage NF-κB and Erk pathway. *Biomed. Pharmacother.* 92, 429–436. doi:10.1016/j.biopha.2017.05.102

Liu, Y. Q., Zhang, G. A., Zhang, B. C., Wang, Y., Liu, Z., Jiao, Y. L., et al. (2015). Short low concentration cisplatin treatment leads to an epithelial mesenchymal transition-like response in DU145 prostate cancer cells. *Asian pac. J. Cancer Prev.* 16 (3), 1025–1028. doi:10.7314/apjcp.2015.16.3.1025

Luan, J., Gao, X., Hu, F., Zhang, Y., and Gou, X. (2020). SLFN11 is a general target for enhancing the sensitivity of cancer to chemotherapy (DNA-damaging agents). *J. Drug Target.* 28 (1), 33–40. doi:10.1080/1061186X.2019.1616746

Maleki, S. J., Crespo, J. F., and Cabanillas, B. (2019). Anti-inflammatory effects of flavonoids. *Food Chem.* 299, 125124. doi:10.1016/j.foodchem.2019.125124

Middleton, J. D., Stover, D. G., and Hai, T. (2018). Chemotherapy-exacerbated breast cancer metastasis: A paradox explainable by dysregulated adaptive-response. *Int. J. Mol. Sci.* 19 (11), E3333. doi:10.3390/ijms19113333

Park, D. D., Phoomak, C., Xu, G., Olney, L. P., Tran, K. A., Park, S. S., et al. (2020). Metastasis of cholangiocarcinoma is promoted by extended high-mannose glycans. *Proc. Natl. Acad. Sci. U. S. A.* 117 (14), 7633–7644. doi:10.1073/pnas.1916498117

Parkkila, S., Parkkila, A. K., Saarnio, J., Kivela, J., Karttunen, T. J., Kaunisto, K., et al. (2000). Expression of the membrane-associated carbonic anhydrase isozyme XII in the human kidney and renal tumors. *J. Histochem. Cytochem.* 48 (12), 1601–1608. doi:10.1177/002215540004801203

Pastorekova, S., Parkkila, S., Pastorek, J., and Supuran, C. T. (2004). Carbonic anhydrases: Current state of the art, therapeutic applications and future prospects. *J. Enzyme Inhib. Med. Chem.* 19 (3), 199–229. doi:10.1080/14756360410001689540

Pastushenko, I., and Blanpain, C. (2019). EMT transition states during tumor progression and metastasis. *Trends Cell Biol.* 29 (3), 212–226. doi:10.1016/j.tcb.2018.12.001

Qiao, K., Chen, C., Liu, H., Qin, Y., and Liu, H. (2021). Pinin induces epithelial-to-mesenchymal transition in hepatocellular carcinoma by regulating m6A modification. *J. Oncol.* 2021, 7529164. doi:10.1155/2021/7529164

Shirode, A. B., Bharali, D. J., Nallanthighal, S., Coon, J. K., Mousa, S. A., and Reliene, R. (2015). Nanoencapsulation of pomegranate bioactive compounds for breast cancer chemoprevention. *Int. J. Nanomedicine* 10, 475–484. doi:10.2147/IJN.S65145

Sun, Y. F., Wang, Z. A., Han, R. L., Lu, H. F., Zhang, J. L., et al. (2017). Isaria cicadae conidia possess antiproliferative and inducing apoptosis properties in gynaecological carcinoma cells. *Mycology* 8 (4), 327–334. doi:10.1080/21501203.2017.1386243

Viikilä, P., Kivela, A. J., Mustonen, H., Koskensalo, S., Waheed, A., Sly, W. S., et al. (2016). Carbonic anhydrase enzymes II, VII, IX and XII in colorectal carcinomas. *World J. Gastroenterol.* 22 (36), 8168–8177. doi:10.3748/wjg.v22.i36.8168

Wang, S., Zhang, S., Gao, P., and Dai, L. (2020). A comprehensive review on Pueraria: Insights on its chemistry and medicinal value. *Biomed. Pharmacother.* 131, 110734. doi:10.1016/j.biopha.2020.110734

Wang, Y., Ma, Y., Zheng, Y., Song, J., Yang, X., Bi, C., et al. (2013). *In vitro* and *in vivo* anticancer activity of a novel puerarin nanosuspension against colon cancer, with high efficacy and low toxicity. *Int. J. Pharm.* 441 (1-2), 728–735. doi:10.1016/j.ijpharm.2012.10.021

Wills, C. A., Liu, X., Chen, L., Zhao, Y., Dower, C. M., Sundstrom, J., et al. (2021). Chemotherapy-induced upregulation of small extracellular vesicle-associated PTX3 accelerates breast cancer metastasis. *Cancer Res.* 81 (2), 452–463. doi:10.1158/0008-5472.CAN-20-1976

Zhang, X., Wu, L., Xu, Y., Yu, H., Chen, Y., Zhao, H., et al. (2020). Microbiota-derived SSL6 enhances the sensitivity of hepatocellular carcinoma to sorafenib by down-regulating glycolysis. *Cancer Lett.* 481, 32–44. doi:10.1016/j.canlet.2020.03.027

Zhao, M., Ding, X. F., Shen, J. Y., Zhang, X. P., Ding, X. W., and Xu, B. (2017). Use of liposomal doxorubicin for adjuvant chemotherapy of breast cancer in clinical practice. *J. Zhejiang Univ. Sci. B* 18 (1), 15–26. doi:10.1631/jzus.B1600303

frontiers | Frontiers in Oncology

TYPE Case Report
PUBLISHED 12 September 2022
DOI 10.3389/fonc.2022.972650

Check for updates

OPEN ACCESS

EDITED BY
Tao Sun,
Nankai University, China

REVIEWED BY
Jun Zhu,
Fudan University, China
Faten Limaiem,
Hôpital Mongi Slim, Tunisia

*CORRESPONDENCE
Yanrong Liu
liuyanrong1984@163.com
Ting Wang
jiningwangting@163.com

†These authors have contributed equally to this work

SPECIALTY SECTION
This article was submitted to Pharmacology of Anti-Cancer Drugs, a section of the journal Frontiers in Oncology

RECEIVED 18 June 2022
ACCEPTED 19 August 2022
PUBLISHED 12 September 2022

CITATION
Zhang M, Yang D, Li L, Liu L, Wang T, Liu T, Li L and Liu Y (2022) Case report: ZEB1 expression in three cases of hepatic carcinosarcoma. *Front. Oncol.* 12:972650. doi: 10.3389/fonc.2022.972650

COPYRIGHT
© 2022 Zhang, Yang, Li, Liu, Wang, Liu, Li and Liu. This is an open-access article distributed under the terms of the Creative Commons Attribution License (CC BY). The use, distribution or reproduction in other forums is permitted, provided the original author(s) and the copyright owner(s) are credited and that the original publication in this journal is cited, in accordance with accepted academic practice. No use, distribution or reproduction is permitted which does not comply with these terms.

Case report: ZEB1 expression in three cases of hepatic carcinosarcoma

Mingming Zhang[1,2†], Dongchang Yang[3†], Lu Li[1,2], Lin Liu[4], Ting Wang[1*], Tao Liu[3], Lei Li[1] and Yanrong Liu[1*]

[1]Department of Pathology, Affiliated Hospital of Jining Medical University, Jining Medical University, Jining, China, [2]School of Clinical Medicine, Jining Medical University, Jining, China, [3]Department of Surgery, Affiliated Hospital of Jining Medical University, Jining Medical University, Jining, China, [4]Health Management Center, Affiliated Hospital of Jining Medical University, Jining Medical University, Jining, China

Hepatic carcinosarcoma (HCS) is defined as a tumor that contains cancer from the epithelium and sarcoma from mesenchymal tissue. HCS has a low incidence rate and is composed of osteosarcoma, chondrosarcoma, or angiosarcoma. Though surgery is the main treatment for HCS, it has proven unsatisfactory, resulting in a very poor prognosis of HCS. Currently, the reports on HCS are mainly about the description of clinical pathological phenomena, imaging features, and mutation sites of related genes, the underlying molecular mechanism of HCS remains undefined. Through the dynamic process of epithelial-mesenchymal transition (EMT), cancer cells acquire a mesenchymal phenotype, simultaneously losing epithelial properties. Zinc finger E-box binding homeobox 1 (ZEB1) is an EMT-inducing transcription factor; its main regulatory target is E-cadherin in EMT process. Esophageal carcinosarcoma (ECS) is associated with EMT. The current study showed that EMT might promote the development of ECS and uterine carcinosarcoma (UCS), and ZEB1 was highly expressed in the sarcomatous components. In the current study, three cases were collected, and the clinicopathological features were compared with those of corresponding cases. The expression level, and subcellular localization of ZEB1 were detected using immunohistochemistry. The expression of the ZEB1 in the nucleus was found to be significantly higher in sarcomatous components than that in cancer components in all three cases, suggesting an association of HCS with EMT.

KEYWORDS

hepatic carcinosarcoma, EMT, ZEB1, liver, carcinosarcoma

Introduction

Hepatic carcinosarcoma (HCS), a rare malignant tumor, combines carcinomatous and sarcomatous elements (1). The tumor comprise spindles or polymorphous tumor cells with a mesenchymal character and polygonal cancer cells with epithelioid morphology (2). Usually manifesting in advanced stages, HCS demonstrates aggressive behavior and has a poor prognosis (3). Other than curative primary resection, no effective treatment options exist for HCS. Several studies have shown concordant genomic alterations in microdissected carcinomatous and sarcomatous components of HCS, strengthening the notion of a monoclonal origin of HCS (4). Current research on HCS remains predominantly limited to the description of clinicopathological phenomena, the molecular mechanism underlying HCS remains unclear.

Several studies have proved that in epithelial-mesenchymal transition (EMT), the histological change from epithelial elements to mesenchymal elements plays a vital role in the progression and metastasis of various cancers (5, 6). The hallmark of the EMT is the loss of epithelial surface markers, most remarkably E-cadherin (E-cad), and the acquisition of mesenchymal markers, including vimentin (Vim) and N-cadherin(N-cad) (7, 8). Carcinosarcoma (CS) possesses both epithelial and mesenchymal components and expresses several markers of EMT, including E-cad and Vim, suggesting HCS to be a prototype of EMT-related neoplasia. EMT is associated with the tumorigenesis of uterine carcinosarcoma (UCS) and esophageal carcinosarcoma (ECS) (9, 10). The association of HCS with EMT remains unclear.

In this study, three cases were collected, and the expression level of ZEB1 and its subcellular localization was detected by immunohistochemistry (IHC). The expression level of ZEB1 was found remarkably higher in the nucleus of the sarcomatous components than that in cancer components, suggesting the role of ZEB1 in regulating HCS *via* EMT.

Methods

Patients and data collection

Three cases were collected from the Affiliated Hospital of Jining Medical University from January 2013 through September 2021. The parameters of blood samples of each case were summarized, including serum levels of hepatitis B surface antigen (HBsAg), carcinoembryonic antigen (CEA), carbohydrate cancer antigen 19-9 (CA19-9), and alpha-fetoprotein (AFP). The HCS samples were biopsied, formalin-fixed, and paraffin-embedded. All the patients signed the prior informed consent. The Ethics Committee of the Affiliated Hospital of Jining Medical University granted the necessary ethical approval for this study.

Immunohistochemistry analysis

The tissues of the sample cases were deparaffinized with xylene and dehydrated with ethanol at decreasing concentrations. Endogenous peroxidase was blocked by incubating with 3% hydrogen peroxide for 15 min. After incubation with normal goat serum for 20 min at room temperature to block unspecific labeling, the tissues were incubated with primary antibodies (Table S1) in a humidified chamber overnight at 4°C. Diaminobenzidine was used for color development, and hematoxylin was used as a counterstain. The staining index of ZEB1 was evaluated. A staining index was used to interpret the results by analyzing both the staining intensity and the proportion of positive cells (11). The staining index (value, 0-12) was determined by multiplying the score for staining intensity with the score for the positive area. The staining index was evaluated by two pathologists. The ZEB1 staining index of the nucleus and cytoplasm was counted in 200× separately, and the average of five fields was determined. The ZEB1 staining index of the nucleus and cytoplasm in cancer cells and sarcomatous cells were respectively analyzed.

Statistical analysis

Statistical analyses were performed using GraphPad Prism (GraphPad Software, Inc., USA) and SPSS version 17.0 (SPSS Software, USA). Data from biological experiments were presented as mean ± standard deviation. Two-tailed unpaired Student's t-test was used to compare the data of the two groups. Differences were considered statistically significant when $P < 0.05$.

Results

Patient characteristics

Table 1 shows the characteristics of the patients with HCS. Case 1 was male, and cases 2 and 3 were female. The mean age was 64 years. The main symptoms reported were epigastric discomfort in all cases. All patients underwent computed tomography (CT) and radical surgery with complete tumor resection. During the operation, the tumor was found invading the right posterior diaphragm and perirenal fat sac in case 2. In case 3, the tumor had severe adhesion with the omentum and right colon, and the tumor ruptured during surgical resection.

CT images of the three patients are shown in Figure 1 and Supplementary Figure 1. HCS usually showed low density in non-enhanced CT, heterogeneous enhancement in the arterial phase, and gradually decreased enhancement in the portal vein phase and in the delayed phase. Tumor boundaries are usually clear after enhancement. Because of the lack of specific radiological features, sometimes distinguishing HCS from

10.3389/fonc.2022.972650

TABLE 1 Clinical characteristics of the three patients with HCS.

	Case 1	Case 2	Case 3
Gender	Male	Female	Female
Age	64	66	64
Early symptoms	Epigastric discomfort	Epigastric discomfort	Epigastric discomfort
Tumor examination	15x11cm	7x6.5cm	13x6.7cm
Location in the liver	Right	Right	Right
Serum AFP (normal < 20μg/l)	3.47	24.87	340.28
Serum CEA (normal < 10μg/l)	1.68	1.51	2.15
Serum CA19-9 (normal < 39μg/l)	6.00	119.86	6.35
Serum albumin (normal 34-48 g/l)	49.10	32.90	31.6
Serum A/G (normal 1.5-2.5)	1.00	1.40	1.5
Serum ALT (normal 0-41 U/l)	32.30	26	28
Serum AST (normal 0-37 U/l)	25	24	43
Bold HBsAg (normal; negative)	Positive	Negative	Positive
Cirrhosis	No	No	No
Surgical method	Right hepatic tumor resection	Right hepatic tumor resection	Right hepatic tumor resection
Clinical diagnosis	HCC	HCC	HCC

AFP, alpha-fetoprotein; A/G, specific value of albumin and globulin; ALT, alanine aminotransferase; AST, serum aspartate aminotransferase; CEA, carcinoembryonic antigen; CA19-9, cancer antigen 19-9; HBsAg, hepatitis B surface antigen; HCC, hepatocellular carcinoma.

hepatocellular carcinoma or hepatic abscess poses a challenge. In case 1, HCS showed a huge mixed-density space-occupying lesion in the right lobe of the liver. The tumor was unevenly enhanced in the arterial phase, and the enhancement degree in the portal vein phase and the delayed phase gradually decreased. In case 2, HCS showed an irregular mass with mixed cystic and solid components. Post enhancement, the solid components were enhanced unevenly and slightly in the arterial phase, though no obvious enhancement was found in the cystic area. The enhancement degree in the portal vein phase and delayed phase showed a gradual decrease. In case 3, the tumor showed a mixed density lesion in the right lobe, enhanced unevenly in the

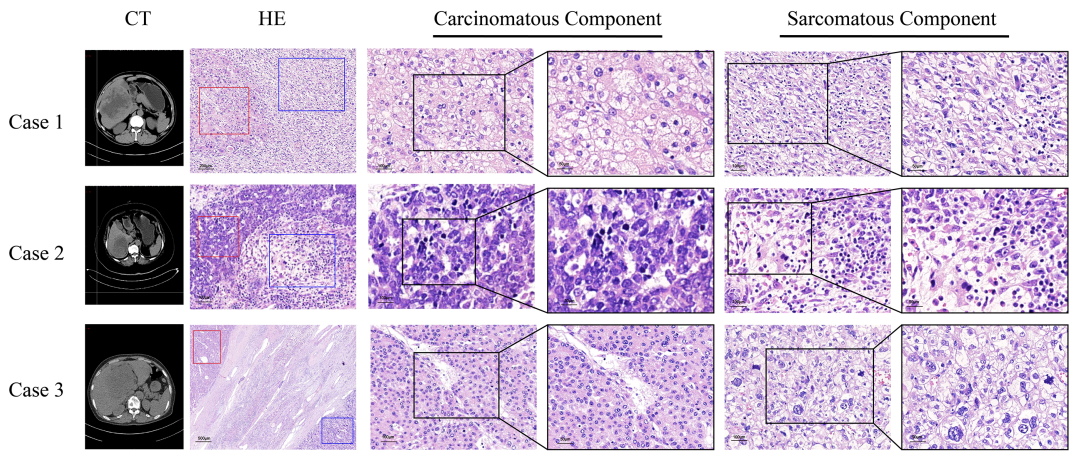

FIGURE 1
Computed tomography scans, the morphology of sarcomatous components and carcinomatous components in the tissues of three HCS cases. Red frames represent carcinomatous components and blue frames represent sarcomatous components.

arterial phase and portal phase, and the degree of enhancement got decreased in the delayed phase. No enlarged lymph nodes or distant metastases were observed in all cases.

Cases 1 and 3 were found positive for HBsAg. The serum tumor biomarkers CEA, the serum CA19–9, and the serum AFP were negative in case 1. However, the serum AFP was found elevated in cases 2 (24.87 μg/L) and 3 (340.28 μg/L); the serum CA19–9 was observed to be elevated in case 2 (119.86 μg/L). All three cases underwent partial excision of the right hepatic lobes (Table 1).

Pathological features

The tumor sizes of the three cases were 15.0 cm × 11.0 cm, 7.0 cm × 6.5 cm, and 13.0 cm × 6.4 cm, respectively. Histopathological findings indicated the existence of necrosis in the carcinomatous areas and sarcomatous areas in the three cases (Table 1). The sarcomatous cells exhibited spindle-shaped heterotypic cells with varying sizes of enlarged nuclei. The cancer cells showed polygonal epithelial phenotype. Both components were separate in certain areas and intermingled in other areas. In case 1, well-differentiated cancer cells were arranged in a trabecular pattern, the cytoplasm of cancer cells was eosinophilic, and some cells showed hyaline degeneration. In case 2, medium-differentiated cancer cells were arranged in the gland; a pseudo glandular structure was formed. In case 3, poorly differentiated cancer cells exhibited a nodular growth pattern. Numerous tumor giant cells and thick, irregular capillaries could be found in the sarcomatous areas. A clear boundary between the two components was observed. Besides, intravascular cancer emboli was noticed in case 3 (Figure 1).

Molecular markers of HCS

When the three cases of HCS were examined immunohistochemically (Figure 2), all sarcomatous components were found positive for Vim staining but negative for CK8/18 and Hep Par-1. In contrast, all cancer components were found positive for CK8/18 and Hep Par-1 but negative for Vim. In case 1, the sarcomatous component was positive for smooth muscle actin (SMA), indicating its origin from smooth muscle differentiation. In case 2, the sarcomatous component was found positive for myogenic differentiation 1 (MyoD1), indicating its origin from striated muscle differentiation. In case 3, the sarcomatous component was positive for FLI1, INI-1, and CD31, indicating that it was derived from angiogenic differentiation.

ZEB1 expression in HCS

Because the sarcomatous components were found positive for Vim, an EMT marker, we speculate the association of EMT with the tumorigenesis of HCS. Therefore, we evaluated the expression of ZEB1 by IHC, in the three cases of HCS (Figure 3A). In the carcinomatous components, the cytoplasmic staining index of ZEB1 was 8.200 ± 1.400 (mean ± SD; N=3); the nucleus staining

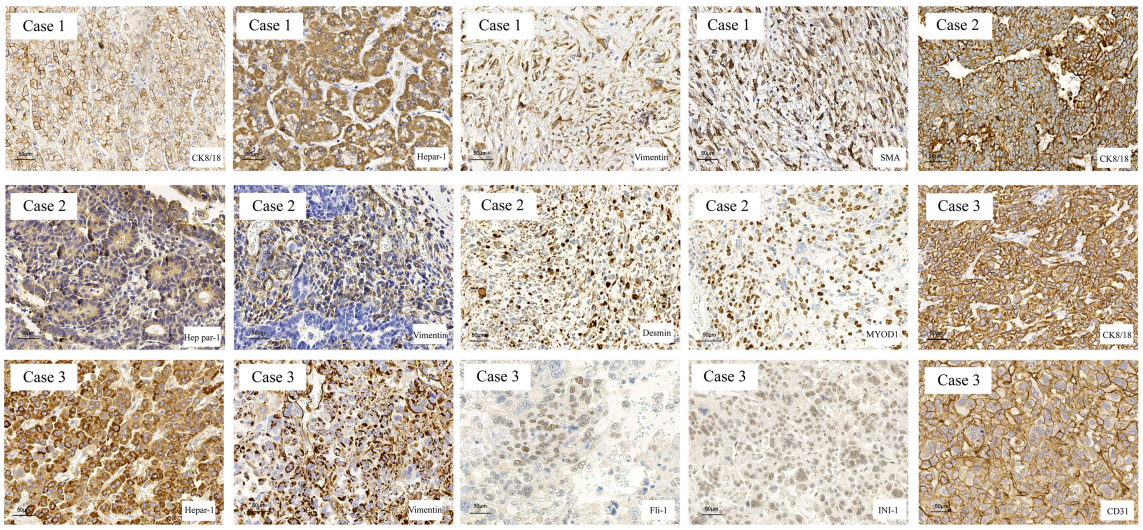

FIGURE 2
The markers of hepatocarcinoma and sarcoma were determined in HCS tissues by IHC. The hepatocarcinoma markers, including CK8/18 and Hep Par-1, were positive in the carcinomatous components, and the mesenchymal markers, including Vimentin, SMA, MYOD1, FLI-1, INI-1, and CD31, were used to determine the tissue source of the mesenchymal components.

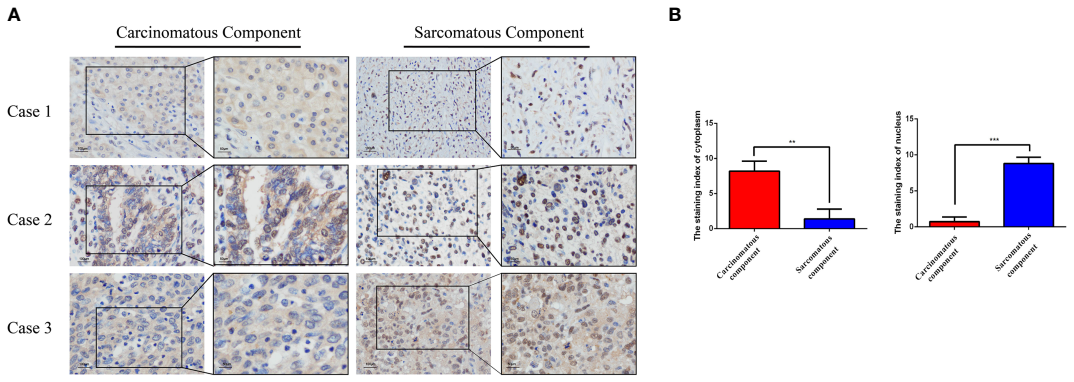

FIGURE 3
The expression of ZEB1 was examined in HCS tissues using IHC analysis. **(A)** Representative images of ZEB1 expression in the sarcomatous components and the carcinomatous components as detected by IHC analysis. **(B)** Statistical analysis of ZEB1 staining index in the sarcomatous components and the carcinomatous components of HCS tissues. ***P* < 0.01, ****P* < 0.001.

index of ZEB1 was 0.7333 ± 0.6429 (mean ± SD; N=3). In the sarcomatous components, the cytoplasmic staining index of ZEB1 was 1.400 ± 1.400 (mean ± SD; N=3), and the nucleus staining index of ZEB1 was 8.800 ± 0.8718 (mean ± SD; N=3). The expression of ZEB1 is higher in the nucleus of the sarcomatous cells than that in cancer cells ($P < 0.001$), In contrast, a decrease in ZEB1 expression could be observed in the cytoplasm of the sarcomatous cells ($P < 0.01$) (Figure 3B). ZEB1 was found mainly expressed in the cytoplasm of the cancer cells, though primarily located in the nucleus of the sarcomatous cells. An increasing expression of ZEB1 was noted in the nucleus of the sarcomatous cells, suggesting the role of ZEB1 as a transcription factor in the nucleus; it also suggests an association of tumorigenesis of HCS with EMT.

Discussion

CS is defined as having both definite cancer components and sarcoma components in the same tumor. The common incidence sites are lung, esophagus, breast, and so on. Primary carcinosarcoma of the liver is a rare occurrence. In 2010, World Health Organization (WHO) classified HCS as a type of mesenchymal tumor of the liver and defined it as a malignant tumor mixed with cancer-like components both hepatocyte-derived and cholangiocyte-derived and sarcoma-like components. In 2019, the WHO divided liver tumors into benign hepatocellular tumors, malignant hepatocellular tumors, and precancerous lesions. However, it does not include the classification of HCS. Currently, the main treatment interventions include surgical resection and postoperative chemotherapy. By using targeted next-generation sequencing, studies have revealed frequent oncogenic aberrations involving tumor protein p53 (TP53), NF1/2, and vascular endothelial growth factor A (VEGFA) in both tumor components, suggesting their correlation with HCS (4). The tumorigenesis of HCS remained poorly understood.

Most of the studies on CS focus on the description of clinical pathological phenomena though a few studies focus on the mechanism of tumorigenesis of CS. Sarcoma components may derive from EMT in CS (12). ALK-related signal cascades may participate in initial signaling for sarcomatous differentiation driven from carcinomatous components through the induction of the EMT process of UCS (13).

ZEB1, a crucial EMT transcription factor, is a member of the E-box binding zinc finger protein family of zinc finger structure transcription factors and is necessary for embryonic development. The zinc finger structure is a common DNA binding unit in eukaryotic cells. The ZEB family contains ZEB1 and ZEB2 protein transcription factors. ZEB1 gene expression is highest in the bladder and uterus in normal tissues and highest in the heart, lung, and thymus during embryonic development (14). A few studies have indicated that ZEB1 is closely related to tumorigenesis and tumor invasion (15, 16). A high level of ZEB1 expression is correlated with poor outcomes, including chemotherapy resistance (17). In ECS, ZEB1 has been suggested to play a critical role in the EMT process (10). A significantly higher expression of ZEB1 was observed in the sarcomatous components in UCS (18). However, the role of ZEB1 as a key transcription factor in HCS remains unclear.

The current study presents the clinicopathological and radiological features of HCS. Further, the ZEB1 staining index in the nucleus was found to increase in the sarcomatous components of HCS than that in the carcinomatous component. The study results revealed that ZEB1 is highly characteristic of sarcoma components of EMT, suggesting an association of tumorigenesis of HCS with EMT. Overall, more cases are still needed to verify the correlation between HCS and EMT.

Data availability statement

The original contributions presented in the study are included in the article/Supplementary Material. Further inquiries can be directed to the corresponding authors.

Ethics statement

Written informed consent was obtained from the individual(s) for the publication of any potentially identifiable images or data included in this article.

Author contributions

MZ and DY performed the experiments, DY performed data collection, and MZ performed data analysis. TL and LuL contributed to the collection of clinical data. YL and LeL reviewed the pathological sections. MZ wrote the manuscript; TW and YL designed the study. YL, TW and LiL revised the manuscript. All authors contributed to the article and approved the submitted version.

Funding

This work was supported by the National Natural Science Foundation of China (81972629), the Taishan Scholars Program of Shandong Province (tsqn201909193), Shandong Youth Innovation and Technology program (2020KJL003).

Conflict of interest

The authors declare that the research was conducted in the absence of any commercial or financial relationships that could be construed as a potential conflict of interest.

Publisher's note

All claims expressed in this article are solely those of the authors and do not necessarily represent those of their affiliated organizations, or those of the publisher, the editors and the reviewers. Any product that may be evaluated in this article, or claim that may be made by its manufacturer, is not guaranteed or endorsed by the publisher.

Supplementary material

The Supplementary Material for this article can be found online at: https://www.frontiersin.org/articles/10.3389/fonc.2022.972650/full#supplementary-material

References

1. Bosman FT, Carneiro F, Hruban RH, Theise ND. World health organization classification of tumours of the digestive system. (Lyons: International Agency for Research on Cancer) (2010) 1–155. Available at: https://www.scienceopen.com/document?vid=d5a5b818-fe34-44cb-8e60-0e10a70a6ba4 with our cited paper.

2. Fayyazi A, Nolte W, Oestmann JW, Sattler B, Ramadori G, Radzun HJ. Carcinosarcoma of the liver. *Histopathology* (1998) 32:385–7. doi: 10.1046/j.1365-2559.1998.0401j.x

3. Çelikbilek M, Deniz K, Torun E, Artış T, Özaslan E, Karahan Öİ, et al. Primary hepatic carcinosarcoma. *Hepatobiliary Pancreatic Dis Int* (2011) 10 (001):101–3. doi: 10.1016/S1499-3872(11)60015-5

4. Zhang X, Bai Q, Xu Y, Wang W, Chen L, Han J, et al. Molecular profiling of the biphasic components of hepatic carcinosarcoma by the use of targeted next-generation sequencing. *Histopathology* (2019) 74(6):944–58. doi: info:doi/10.1111/his.13822

5. Thiery JP, Acloque H, Huang R, Nieto MA. Epithelial-mesenchymal transitions in development and disease. *Cell* (2009) 139(5):871–90. doi: 10.3390/cimb43020064

6. Polyak K, Weinberg RA. Transitions between epithelial and mesenchymal states: Acquisition of malignant and stem cell traits. *Nat Rev Cancer* (2009) 9 (4):265–73. doi: 10.1038/nrc2620

7. Peinado H, Olmeda D, Cano A. Snail, zeb and bHLH factors in tumour progression: An alliance against the epithelial phenotype? *Nat Rev Cancer* (2007) 7 (6):415–28. doi: 10.1038/nrc2131

8. Nieto AM. The ins and outs of the epithelial to mesenchymal transition in health and disease. *Annu Rev Cell Dev Biol* (2011) 27(1):347–76. doi: 10.1146/annurev-cellbio-092910-154036

9. Tochimoto M, Oguri Y, Hashimura M, Konno R, Saegusa M. S100A4/non-muscle myosin II signaling regulates epithelial-mesenchymal transition and stemness in uterine carcinosarcoma. *Lab Invest* (2020) 100(5):682–95. doi: 10.1038/s41374-019-0359-x

10. Harada H, Hosoda K, Moriya H, Mieno H, Ema A, Washio M, et al. Carcinosarcoma of the esophagus: A report of 6 cases associated with zinc finger e–box –binding homeobox 1 expression. *Oncol Lett* (2019) 17:578–86. doi: 10.3892/ol.2018.9585

11. Liu Y, Ji R, Li J, Qiang G. Correlation effect of EGFR and CXCR4 and CCR7 chemokine receptors in predicting breast cancer metastasis and prognosis. *J Exp Clin Cancer Res* (2010) 29(1):16–6. doi: 10.1186/1756-9966-29-16

12. Pang A, Carbini M, Moreira AL, Maki RG. Carcinosarcomas and related cancers: Tumors caught in the act of epithelial-mesenchymal transition. *J Clin Oncol* (2017) 36(2):JCO.2017.74.952. doi: 10.1200/JCO.2017.74.9523

13. Inoue H, Hashimura M, Akiya M, Chiba R, Saegusa M. Functional role of ALK-related signal cascades on modulation of epithelial-mesenchymal transition and apoptosis in uterine carcinosarcoma. *Mol Cancer* (2017) 16(1):37. doi: 10.1186/s12943–017–0609–8

14. Hurt EM, Saykally JN, Anose BM, Kalli KR, Sanders MM. Expression of the ZEB1 (δEF1) transcription factor in human: additional insights. *Mol Cell Biochem* (2008) 318(1–2):89–99. doi: 10.1007/s11010-008-9860-z

15. He C, Wu T, Hao Y. Anlotinib induces hepatocellular carcinoma apoptosis and inhibits proliferation *via* erk and akt pathway. *Biochem Biophys Res Commun* (2018) 503(4):3093–9. doi: 10.1016/j.bbrc.2018.08.098

16. Caramel J, Ligier M, Puisieux A. Pleiotropic roles for ZEB1 in cancer. *Cancer Res* (2018) 78(1):30–5. doi: 10.1158/0008–5472.Can-17–2476

17. Perez-Oquendo M, Gibbons D. Regulation of ZEB1 function and molecular associations in tumor progression and metastasis. *Cancers* (2022) 14(8):1864. doi: 10.3390/cancers14081864

18. Osakabe M, Fukagawa D, Sato C, Sugimoto R, Uesugi N, Ishida K, et al. Immunohistochemical analysis of the epithelial to mesenchymal transition in uterine carcinosarcoma. *Int J Gynecological Cancer* (2019) 29(2):277–81. doi: 10.1136/ijgc-2018-000038

frontiers | Frontiers in Oncology

TYPE Original Research
PUBLISHED 15 September 2022
DOI 10.3389/fonc.2022.974614

Check for updates

OPEN ACCESS

EDITED BY
Tao Sun,
Nankai University, China

REVIEWED BY
Yiping Zou,
Tianjin Medical University Cancer Institute and Hospital, China
Liming Chen,
Nanjing Normal University, China
Chunlin Ou,
Xiangya Hospital, Central South University, China

*CORRESPONDENCE
Ying Xing
xingying@hrbmu.edu.cn
Li Cai
caili@ems.hrbmu.edu.cn

†These authors have contributed equally to this work

SPECIALTY SECTION
This article was submitted to Pharmacology of Anti-Cancer Drugs, a section of the journal Frontiers in Oncology

RECEIVED 21 June 2022
ACCEPTED 30 August 2022
PUBLISHED 15 September 2022

CITATION
Cui Y, Wang X, Zhang L, Liu W, Ning J, Gu R, Cui Y, Cai L and Xing Y (2022) A novel epithelial-mesenchymal transition (EMT)-related gene signature of predictive value for the survival outcomes in lung adenocarcinoma. *Front. Oncol.* 12:974614. doi: 10.3389/fonc.2022.974614

COPYRIGHT
© 2022 Cui, Wang, Zhang, Liu, Ning, Gu, Cui, Cai and Xing. This is an open-access article distributed under the terms of the Creative Commons Attribution License (CC BY). The use, distribution or reproduction in other forums is permitted, provided the original author(s) and the copyright owner(s) are credited and that the original publication in this journal is cited, in accordance with accepted academic practice. No use, distribution or reproduction is permitted which does not comply with these terms.

A novel epithelial-mesenchymal transition (EMT)-related gene signature of predictive value for the survival outcomes in lung adenocarcinoma

Yimeng Cui[1†], Xin Wang[1†], Lei Zhang[1†], Wei Liu[1], Jinfeng Ning[2], Ruixue Gu[1], Yaowen Cui[1], Li Cai[1*] and Ying Xing[1*]

[1]The Fourth Department of Medical Oncology, Harbin Medical University Cancer Hospital, Harbin, China, [2]Department of Thoracic Surgery, Harbin Medical University Cancer Hospital, Harbin, China

Lung adenocarcinoma (LUAD) is a remarkably heterogeneous and aggressive disease with dismal prognosis of patients. The identification of promising prognostic biomarkers might enable effective diagnosis and treatment of LUAD. Aberrant activation of epithelial-mesenchymal transition (EMT) is required for LUAD initiation, progression and metastasis. With the purpose of identifying a robust EMT-related gene signature (E-signature) to monitor the survival outcomes of LUAD patients. In The Cancer Genome Atlas (TCGA) database, least absolute shrinkage and selection operator (LASSO) analysis and cox regression analysis were conducted to acquire prognostic and EMT-related genes. A 4 EMT-related and prognostic gene signature, comprising dickkopf-like protein 1 (DKK1), lysyl oxidase-like 2 (LOXL2), matrix Gla protein (MGP) and slit guidance ligand 3 (SLIT3), was identified. By the usage of datum derived from TCGA database and Western blotting analysis, compared with adjacent tissue samples, DKK1 and LOXL2 protein expression in LUAD tissue samples were significantly higher, whereas the trend of MGP and SLIT3 expression were opposite. Concurrent with upregulation of epithelial markers and downregulation of mesenchymal markers, knockdown of DKK1 and LOXL2 impeded the migration and invasion of LUAD cells. Simultaneously, MGP and SLIT3 silencing promoted metastasis and induce EMT of LUAD cells. In the TCGA-LUAD set, receiver operating characteristic (ROC) analysis indicated that our risk model based on the identified E-signature was superior to those reported in literatures. Additionally, the E-signature carried robust prognostic significance. The validity of prediction in the E-signature was validated by the three independent datasets obtained from Gene Expression Omnibus (GEO) database. The probabilistic nomogram including the E-signature, pathological T stage and N stage was constructed and the nomogram demonstrated satisfactory discrimination and calibration. In LUAD patients, the E-signature risk score was associated with T stage, N stage, M stage and TNM stage. GSEA

(gene set enrichment analysis) analysis indicated that the E-signature might be linked to the pathways including GLYCOLYSIS, MYC TARGETS, DNA REPAIR and so on. In conclusion, our study explored an innovative EMT based prognostic signature that might serve as a potential target for personalized and precision medicine.

KEYWORDS

lung adenocarcinoma, EMT, signature, prognosis, nomogram

Introduction

Lung adenocarcinoma (LUAD), as the predominant histological type of lung cancer, has biological characteristics of strong aggressiveness and heterogeneity (1–3). In spite of optimized treatment methods including surgery, chemotherapy, radiotherapy, immunotherapy and targeted therapy, prognosis of LUAD patients remains dismal, because of cancer progression (4, 5). Collectively, it is imperative to distinguish populations at a high-risk of LUAD for early intervention and improving clinical outcome. At present, the combination of clinicopathological features and TNM staging system is the consensus criterion for determining treatment options and predicting relapse of LUAD, however this criterion restrains the provision of optimal clinical care to patients (6). Hence, identifying reliable biomarkers for optimizing the prognosis of LUAD is urgently needed.

Metastases are the primary cause of LUAD-associated mortality (7, 8). Migratory tumor cells escape from the primary site, remodel the basement membrane to engage with peritumoural stroma, undergo intravasation, endure shear stress in circulation and adapt to the tumor microenvironment of distant metastasis (9, 10). In total, the metastatic process generally involves three distinct phases: dissemination, dormancy and colonization (11). Epithelial mesenchymal transition (EMT) of cancer cells is a fundamental event during the multistep process participated in cancer metastasis (12, 13). Moreover, EMT activation confers on tumor cells to acquire plasticity with more aggressive phenotype, which exerts a decisive function on the malignant cancer progression (14, 15). Accumulating evidence has revealed that EMT process was closely implicated in tumorigenicity, angiogenesis and drug resistance (16–18). EMT results in a series of changes during epithelial tumor cells transforming into mesenchymal cells, including loss of tight junctions, cell polarity, cytoskeletal reorganization, and increase of cell viability (19). EMT is controlled or induced by a number of factors such as exosomal circRNAs, varied transcripts (Twist, Snail, ZEB1, et al.), microRNAs (miR212, mir200 family, et al.) and cellular oncogenic pathways (EGFR signaling pathway, et al.) (20–22). There is a significant link between the aberrant expression of genes related with EMT and poor clinical outcomes in LUAD patients (13, 23).

Since the advent of next generation sequencing, research on bioinformatic analysis has flourished (24; 25). For instance, The Cancer Genome Atlas (TCGA) database and Gene Expression Omnibus (GEO) database, such public databases are desirable to access transcriptomic information, that advances the efficient methods to select gene signatures (26–28). Numerous studies have attempted to construct the risk model to get biological characteristics or prognostic appraisal in malignant tumors, which had potential clinical impact (29–31). Interestingly, EMT-related gene signature (E-signature) could reveal the prognostic consequences in various types of cancer (32–34). Nevertheless, the existence of heterogeneity in samples among diversified studies on various tumours resulting in different risk models (35). Recently, some researchers reported the prognostic significance of E-signature, however they did not validate the biological functions of EMT-related genes with *in vitro* experiments in LUAD and their studies remains rudimentary to some extent (36–38).

In the current study, candidate genes involved in EMT process were identified based on TCGA-LUAD training dataset and validated using cell-based assays *in vitro* and clinical tissue samples. Then, the E-signature which can accurately predict the prognosis of LUAD patients was developed by us. Meanwhile, the nomogram affirmed the feasibility in clinical application of the E-signature. Subgroup analysis suggested that E-Signature could be conducive to identify patients with adverse events at high risk. The E-signature is closely related to multiple pathways associated with cancer progression, as well. In conclusion, the E-signature could be used as an inspiring molecular indicator for evaluation of clinical prognosis in LUAD patients.

Materials and methods

Data capturing and processing

Entire design attached to our research was presented in Figure 1. TCGA website (http://portal.gdc.cancer.gov) were used to obtain raw microarray data and matched clinical of LUAD patients. Expression profiles were processed with robust multiarray average (RMA) algorithm (29). Differential expression analysis was performed by "limma" package. GEO database(https://www.ncbi.nlm.nih.gov/geo/) (Table 1) were used as independent external verification sets, including GSE30219, GSE37745, GSE50081 and GSE8894 (https://www.ncbi.nlm.nih.gov/geo/) (Table 1). Besides, we retrieved "HALLMARK EPITHELIAL MESENCHYMAL TRANSITION" gene list encompassing 200 genes in the MsigDB (https://www.gsea-msigdb.org/gsea/msigdb/index.jsp).

LASSO Cox regression analysis

To yield the independent prognostic EMT factor, univariate analysis and multivariate analysis were showed with $P< 0.05$ as a threshold. least absolute shrinkage and selection operator (LASSO) analysis was capable for reducing the dimension (39). 80% TCGA samples after preprocessing were randomized to the training dataset. our prognostic model preserved the advantage of subset shrinkage and maintained a high accuracy rate based on the penalty parameter λ (40). Risk score was calculated from expression of related gene and associated coefficient. Analytical formula for risk score assessment was derived on the basis of the EMT related gene signature = $\sum_{i=1}^{n}$ (coef$i$ × Expr$i$), in this formula, $Expr_i$ represents gene expression of patient, and $coef_i$ represents the multivariate regression coefficient.

Survival analysis

According to median risk scores, all LUAD samples were divided into two groups, involving in high-risk and low-risk groups in different cohorts. Kaplan Meier (KM) curves were plotted to compare the prognostic difference (41). The area under the curve (AUC) which performed from receiver operating characteristic (ROC) curve analysis for overall

TABLE 1 Various clinicopathological characteristics of patients with LUAD in TCGA training cohort and GEO datasets.

Characteristics		TCGA Set (n = 490)	GSE30219 (n = 83)	GSE37745 (n = 105)	GSE50081 (n = 128)	GSE8894 (n = 63)
Age(years)	≤60	153	43	45	19	30
	>60	327	40	60	109	31
Survival status	Alive	312	40	29	76	–
	Dead	178	43	76	52	–
Recurrence	No	284	56	–	88	30
	Yes	206	27	–	37	29
Gender	Female	262	18	60	53	34
	Male	228	65	45	65	–
pT stage	T1	163	69	–	43	–
	T2	263	12	–	83	–
	T3	43	2	–	2	–
	T4	18	0	–	0	–
pN stage	N0	317	80	–	94	–
	N1	92	3	–	34	–
	N2	68	0	–	0	–
	N3/NX	12	0	–	0	–
pM stage	M0	324	83	–	128	–
	M1/MX	162	0	–	0	–
Tumor stage	Stage I	263	–	70	92	–
	Stage II	115	–	19	36	–
	Stage III	79	–	12	0	–
	Stage IV	25	–	4	0	–
Smoking	No	68	–	–	23	–
	Yes	408	–	–	92	–
EGFR	Wild type	186	–	–	–	–
	Mutant	79	–	–	–	–

survival (OS) was employed to designate the predictive efficiency (42).

Establishment and validation of the nomogram

The significant variables from the multivariate models were introduced to draw the graphical nomogram by utilizing "rms" and "nomogramEx" packages (43). The calibration curves for probability of OS showed that match condition between prediction by nomogram and actual observation (44). Decision curve analysis (DCA) was utilized to evaluate the ability of the predictive model in view of clinical applicability (44).

Gene set variation analysis (GSVA)

Single-sample gene set enrichment analysis (ssGSEA) scores were gained by "ClusterProfiler" and "GSVA" R package to recognize the correlation between risk scores and enriched biological processes (45). The results with a cut-off criterion of *P* value< 0.05 were statistical significance.

Collection of LUAD tissues and cell culture

Under the premise that ethical clearance and approval have been obtained, 5 pairs of fresh tumor samples and matched normal tumor-adjacent samples were dissected from 5 LUAD patients who underwent lobectomy but did not receive radiotherapy and chemotherapy at Harbin Medical University Cancer Hospital between May 2021 and June 2021.

Human LUAD cell lines (A549 and NCI-H1299) were cultured with RPMI-1640 including 10% fetal bovine serum (FBS) and 1% penicillin/streptomycin, and the culture environment needed to be maintained at 37°C and containing 5% carbon dioxide.

Small interfering RNA transfection

SiRNAs of dickkopf-like protein 1 (DKK1), lysyl oxidase-like 2 (LOXL2), matrix Gla protein (MGP) and slit guidance ligand 3 (SLIT3) were made by Hanyinbt (Shanghai, China), in addition, these target sequences were presented as: DKK1#1, 5'-GCUUCACACUUGUCAGAGAtt-3'; DKK1#2, 5'-GGCUCUCAUGGACUAGAAAtt-3'; LOXL2#1, 5'-CAUACAAUACCAAAGUGUAtt-3'; LOXL2#2, 5'-GGGUGGAGGUGUACUAUGAtt-3'; MGP#1, 5'-CCCUACUGCUGCUACACAATT-3'; MGP#2, 5'-GAUAAGUAAUGAAAGUGCATT-3'; SLIT3#1, 5'-CGCGAUUUGGAGAUCCUUAtt-3'; SLIT3#2, 5'-GUACAAAGAGCCAGGAAUATT-3'. All corresponding negative control siRNA sequences were completed by Hanyinbt Company.

When the density of A549 and H1299 cells reached 60-70% in 6-well dishes, the transfection mixture was prepared by fully mixing 120μL riboFECT^{TM}CP Buffer, 12μL riboFECT^{TM}CP Reagent and 5μL siRNA, and incubated at room temperature for 15min. Finally, 3mL RPMI-1640 containing 10% FBS was added into the 6-well dishes. Follow-up experiments were carried out after ensuring the efficiency of knockout.

Western blotting

Lysate of tissues or cells was centrifuged for 15 min (4°C, 14000rpm) and we measured protein concentrations using the BCA protein analysis kit. Electrophoretic separation and electro-transfer of protein samples with the comparable quality, membrane blocking and incubate overnight (primary antibody, 4°C). PVDF membranes containing proteins are incubated with secondary antibodies for 1 hour at room temperature. The bands on membrane were exposed by CL Xposure film (Thermo Fisher Scientific). Specific antibodies included: DKK1 (21112-1-AP, Proteintech Group Inc., Wuhan, China), LOXL2 (AB179810, Abcam), MGP (10734-1-AP, Proteintech Group Inc., Wuhan, China), SLIT3 (DF9909, Affinity Biosciences, Jiangsu, China), E-Cadherin (20874-1-AP, Proteintech Group Inc., Wuhan, China), N-Cadherin (22018-1-AP, Proteintech Group Inc., Wuhan, China), Vimentin (10366-1-AP, Proteintech Group Inc., Wuhan, China), β-actin (AF7018, Affinity Biosciences, Jiangsu, China).

Detection of cancer cell migration and invasion

Use the tip of a 10 μL pipette to form a scratch on a six-well plate covered with LUAD cells. By comparing the rate of wound healing and taking pictures under the microscope, the cell migration rate was finally counted. Transwell assay was conducted with the Corning Inc. transwell chamber. The invasion experiment required the participation of the matrigel matrix involved. Cell suspension arranged in the upper chamber contained $2x10^4$ cells, besides, ingredient of the lower chamber was 600μL RPMI-1640 complemented with 10% FBS. The fixation of methanol and staining of 0.1% crystal violet for observing the migration and invasion efficiency after 24h or 48h, respectively. Fields were randomly selected in each membrane for capturing.

Statistical methods

Data processing was focused on GraphPad Prism 8.0.2 software. Typicality of data in the study could be reflected with at least three independent experiments completed. Continuous data conforming to a normal distribution were analyzed by Student's t-test, and subgroup differences were counted using the $\chi 2$ test. All results are expressed as mean ± SEM (* $P< 0.05$, ** $P< 0.01$, *** $P< 0.001$).

Results

The identification and validation with *in vitro* experiments of 4 prognostic EMT-related genes comprising the E-signature

The 200 genes linked to EMT were acquired from the "HALLMARK_EPITHELIAL_MESENCHYMAL_TRANSITION" gene list in the MsigDB. Univariate Cox analyses systematically deduced 68 genes significantly relevant to prognosis based on TCGA-LUAD training cohort. To exploit an optimal model for testing risk, the LASSO analysis was used in its broadest sense to summary the results of each dimensionality reduction and count the occurrence frequency and standard deviation distribution of each probe. Standard deviation (SD) calculations may comprehensively describe the distribution characteristics of data, which is generally understood to measure the deviation degree (46). Four EMT-related genes, including dickkopf-like protein 1 (DKK1), lysyl oxidase-like 2 (LOXL2), matrix Gla protein (MGP) and slit guidance ligand 3 (SLIT3), were comprehensively screened depending on the following criteria (Figure 2A). SD of candidate mRNAs was greater than the median and frequency was well over 500 (Figure 2A). Patients with high DKK1 and LOXL2 expression had the shorter overall survival (OS) according to a Kaplan-Meier analysis, whereas ones with high expression of MGP or SLIT3 had longer OS (Figure 2B). Based on TCGA-LUAD transcriptome data, differential expression analysis showed that with the comparison of normal samples, DKK1 and LOXL2 expression were significantly increased in tumor tissues, whereas MGP and SLIT3 were markedly overexpressed in non-tumoral tissues (Figure 2C). The same results were achieved from the collected clinical tissue samples by western blotting (Figure 2D).

The functions and roles of these four genes in LUAD metastasis and EMT remain to be clarified (47–50). We used cell-based assays *in vitro* to examine the effect of these four genes on EMT and metastasis, respectively. In A549 and H1299 cells, Gene-specific siRNAs were used with three independent siRNAs for knockdown of each gene. Successful knockdown of these four genes was validated by Western blotting in A549 (Figure 3A) and NCI-H1299 cell lines (Figure S1A). Moreover, as illustrated in Figure 3A and Figure S1A, knockdown of DKK1 or si-LOXL2 enhanced the expression of E-cadherin and inhibited the mesenchymal markers' expression, including N-cadherin and Vimentin. MGP or SLIT3 knockdown led to downregulation of epithelium-derived markers and upregulation of mesenchymal markers (Figure 3A; Figure S1A). Furthermore, wound healing and Transwell assays revealed silencing of DKK1 and LOXL2 suppressed the ability of migration and invasion in LUAD cells, but silencing of MGP and SLIT3 had the opposite effect (Figures 3B, C; Figures S1B, C). Our experimental data indicated that the four EMT-related genes could regulate metastasis and EMT program.

Construction of the prognostic E-signature in LUAD

Based on multivariate Cox regression analysis, the independent prognostic signature still composed of four EMT genes was generated. Scoring formula as follows: Risk Score = $0.308\times\exp^{DKK1}+0.299\times\exp^{LOXL2}-0.084\times\exp^{MGP}-0.165\times\exp^{SLIT3}$ (Figure 4A). The statistical correlation between risk model and 4 genes expression was assessed by the Pearson correlation metric (Figure 4B). Risk score was converted into Z-score, taking 0 served as the optimal boundary value to divide the samples into two groups, in which z score of the high-risk subgroup was greater than 0, and the rest belonged to the low-risk subgroup. The permutation of risk scores, survival status and four genes expression levels were displayed (Figure 4C). These results demonstrated that the risk E-signature was a deleterious indicator of prognosis.

Furthermore, based on TCGA training dataset, the prognostic accuracy of E-signature was appraised by time-dependent ROC analysis, the AUC was 0.73 (1-year), 0.7 (2-year) and 0.69 (3-year), respectively (Figure 4D). Referring to the training set, in comparison with the high-risk group, the low-risk group revealed a significantly longer OS (Figure 4D). The ROC and KM curve also revealed that our model exhibited good sensitivity and specificity in predicting TCGA-LUAD recurrence free survival (RFS, Figure 4E). Compared with recently published lung cancer prognostic models in the literatures (Figure 4F) including Zhu (51), Ma (52), Zhang (53) and Zhang M (54), our E-signature had better specificity by ROC curve analysis especially at 1-year (Figure 4F). Similarly, the E-signature predicted OS better than either the known signatures alone, with a better calibration and classification accuracy (Figure 4G).

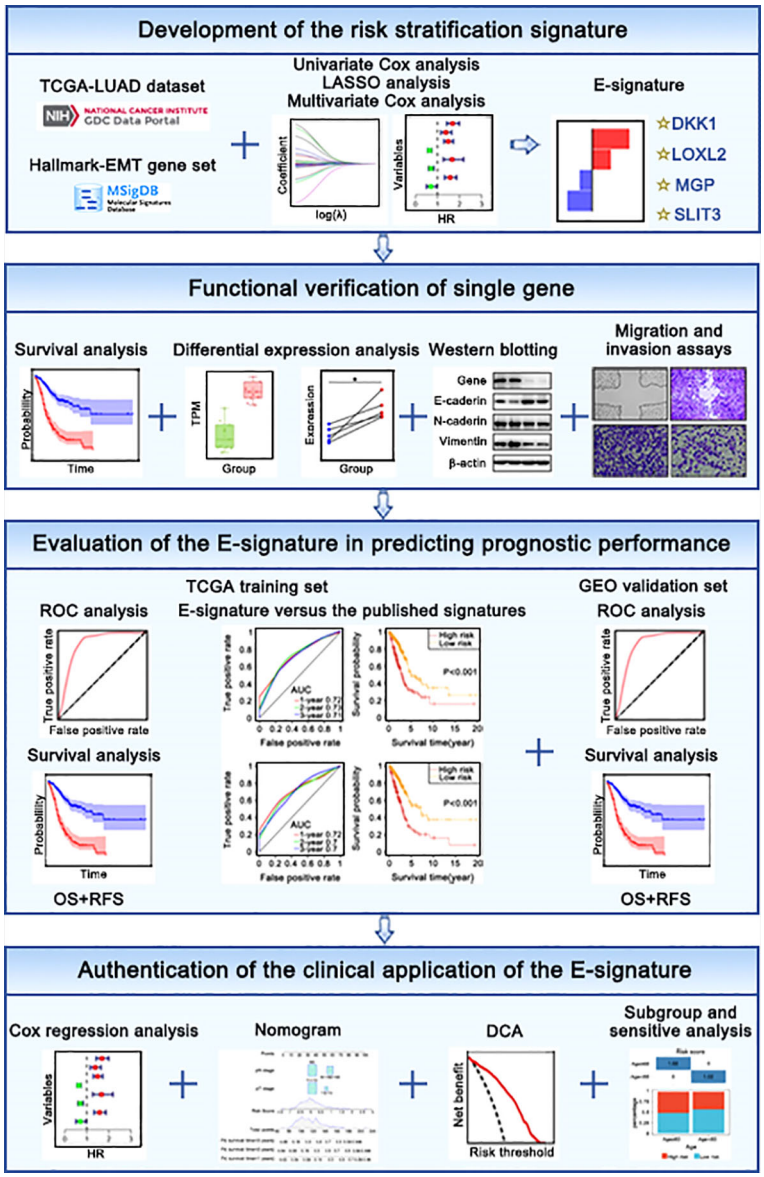

FIGURE 1
The flow chart in our study.

External validation of the prognostic E-signature

For further emphasizing the robustness of the constructed signature, GSE30219, GSE37745 and GSE50081 external validation sets were used for ROC analysis and KM analysis. In line with the training set, E-signature had strong predictive accuracy (GSE30219 [1-year: 0.74; 2-year: 0.69; 3-year: 0.73]; GSE37745 [1-year: 0.65; 2-year: 0.66; 3-year: 0.6]; GSE50081 [1-year: 0.72; 2-year: 0.68; 3-year: 0.68]) and patients in the group with high-risk showed a predominant association with frustrating OS (Figure S2A). Next, we opt GSE30219, GSE50081 and GSE8894 datasets and executed the identical methods to validate the prognostic potential of E-signature in RFS. Likewise, the E-signature maintained ideal sensitivity and specificity as a prognostic indicator (GSE30219 [1-year: 0.87; 2-year: 0.76; 3-year: 0.80]; GSE50081 [1-year: 0.67; 2-year: 0.68; 3-year: 0.68]; GSE8894 [1-year: 0.71; 2-year: 0.68; 3-year: 0.68]) and high-risk patients had significantly worse RFS relative to the group at low risk (Figure S2B).

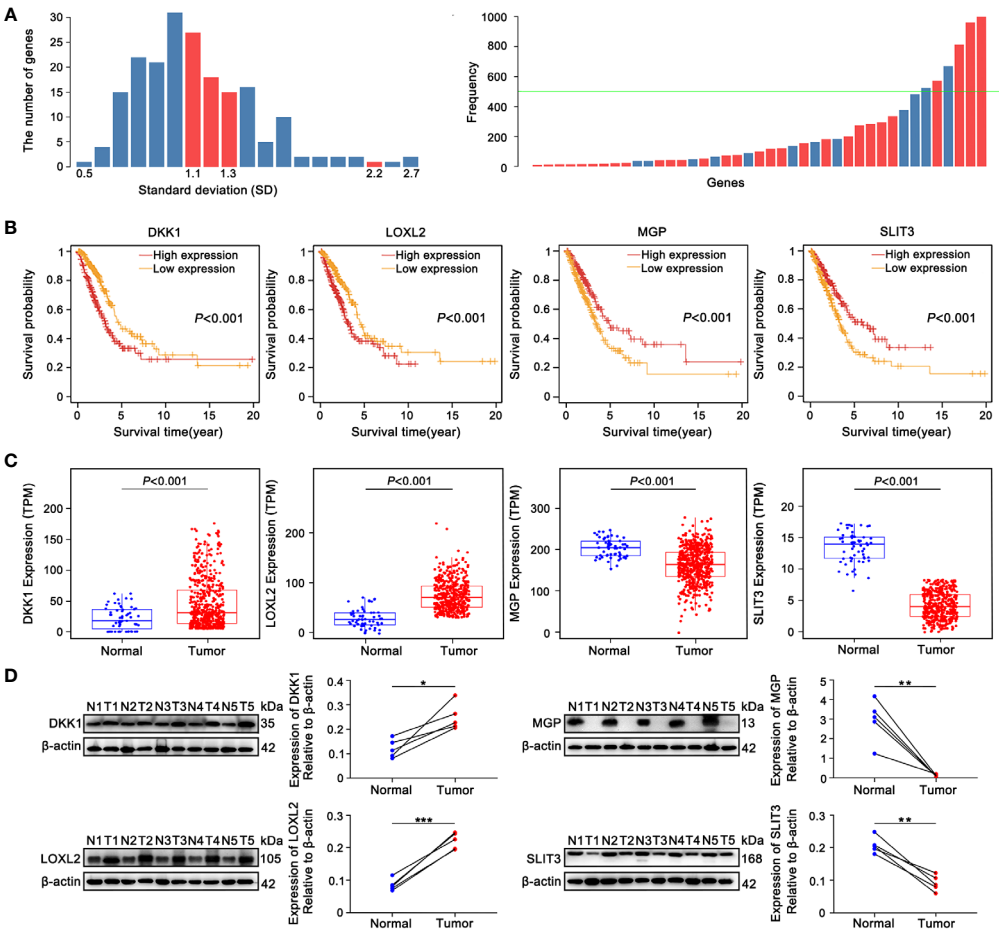

FIGURE 2
The identification 4 prognostic EMT-related genes comprising the E-signature. **(A)** The standard deviation distribution of all mRNAs. In the left panel, location corresponding to the red columns were standard deviation (SD) of genes with frequency greater than 500, where SD was used as the abscissa and the vertical axis represented the number of genes. The right panel showed that the gene frequency distribution chart obtained by LASSO analysis. The green baseline meant that frequency was equal to 500, the part exceeded the green line was genes with frequency greater than 500. **(B)** KM curves showed the overall survival (OS) of patients grouped according to expression patterns of 4 prognostic EMT-related genes comprising the E-signature in TCGA-LUAD datasets. **(C)** Differential expression analysis of DKK1, LOXL2, MGP and SLIT3 originated from TCGA-LUAD dataset. **(D)** The expression of 4 genes in fresh LUAD tumor samples (T) and adjacent normal-frozen tissues (N) detected by Western blot (*P< 0.05, **P< 0.01, ***P< 0.001).

Establishment of a nomogram based on the E-signature

clinicopathological characteristics, such as T stage, N stage, M stage, TNM stage, age, gender, and smoking history, and risk score were incorporated as covariates into univariate and multivariate Cox regression analyses. Risk score, T stage and N stage were demonstrated the independent prognostic factors by forest plot for OS (Figures 5A).

The nomogram could intuitively and effectively display the influence of the risk model on the prognostic outcome (55). A multi-scale nomogram was constructed on account of independent prognostic factors, which effectively predicted 1-year, 2-year and 3-year OS probabilities of LUAD patients. The scores corresponding to the parameters were calculated to obtain the total points. Thus, high total score was significantly correlated to worse outcome (Figure 5B). Furthermore, calibration curve implied well performance of the nomogram at predicting survival capacity in LUAD patients (Figure 5C). ROC curve analysis and Decision Curve Analysis (DCA) showed that, compared with other independent variables, the nomogram model classifier had the distinctly superior accuracy and net benefit rate (Figures 5D, E).

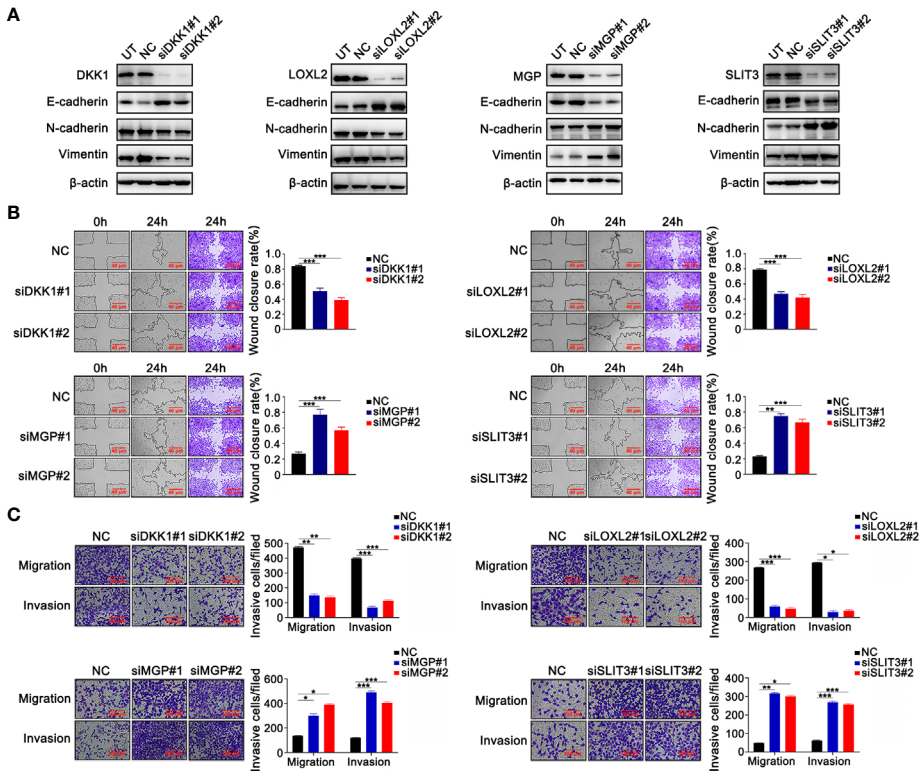

FIGURE 3
The validation experiments of 4 prognostic EMT-related genes comprising the E-signature *in vitro*. **(A)** Western blotting confirmed that silencing 4 genes respectively caused alterations of EMT-related protein expression in H1299 cells. **(B)** The effect of silencing four genes on H1299 cell migration confirmed by wound-healing assays. **(C)** Transferability and invasiveness of H1299 cells were evaluated. *P < 0.05; **P < 0.01; ***P < 0.001. Data wereobtained from three independent experiments.

Correlation between the prognostic model and clinicopathologic features

To further clarify the clinical implication of the EMT signature, we tested the relationship between risk score and clinicopathologic variables by the Chi-square test. LUAD patients were classified into different subgroups under diverse clinical properties, including T stage, N stage, M stage, tumor stage, gender, age, smoking history, status of EGFR. Notably, there was a gradual upward trend in the proportion of high-risk score patients with increase of malignant grade of pathological T stage, pathological N stage, pathological M stage and tumor stage. Regrettably, other clinicopathological characteristics showed no obvious difference in the distribution (Figure 6A). Subsequently, the risk model was also applied to each subgroup for KM survival analysis. We observed that subgroup with high-risk presented dramatically worse OS, suggesting that our specific signature had a precise predictive value (Figure 6B).

Functional annotation and enrichment analysis of the E-signature

The association between risk score and EMT biomarkers was assessed based on the TCGA database (Figure 7A). In order to further observe biological functions of the risk model, ssGSEA method was applied to derive scores of multifarious molecular pathways. The heatmap of hierarchical cluster analysis showed E-signature was enriched in "EPITHELIAL MESENCHYMAL TRANSITION" and other carcinogenic pathways, while metabolic-related pathways such as" HEME METABOLISM" and "BILE ACID METABOLISM" were inversely regulated by our signature (Figure 7B). Moreover, the correlation map visualized the KEGG pathways extracted by correlation coefficient > 0.3 statistically significant associated with the E-signature (Figure 7C). Taken together, the constructed specific signature played a compelling role in promoting tumor development.

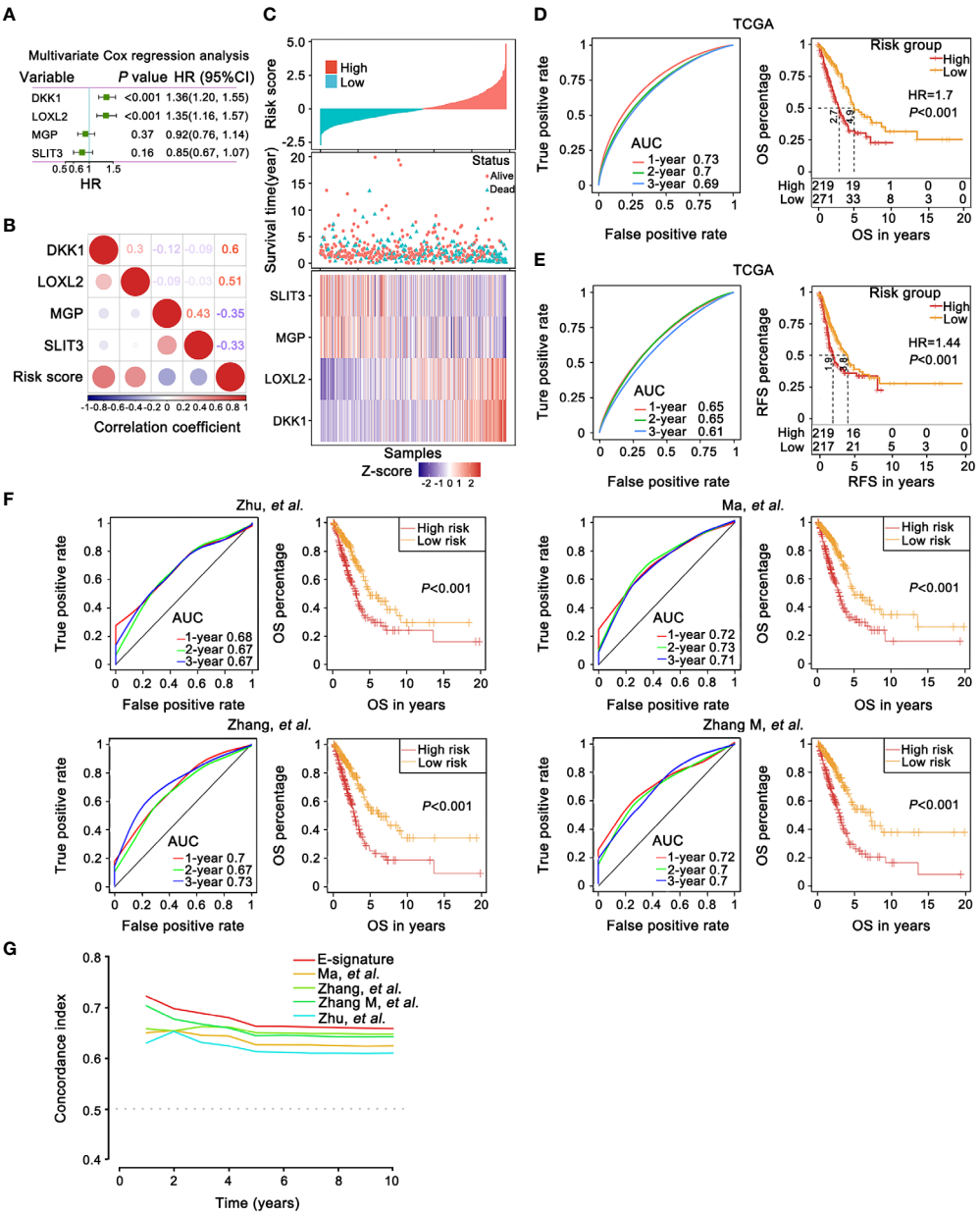

FIGURE 4
The prognostic robustness and clinical usefulness of the E-signature in the internal training set. **(A)** Evaluating the impact of 4 EMT-related genes on OS by means of forest plot. **(B)** Relatedness plot reported Pearson correlation values of each comparison. The bar color indicated Pearson corr. Values below the map calculated between risk score and genes in the matrix. **(C)** The risk score, survival time and status of each sample in TCGA-LUAD cohorts. The heatmap listed expression status of each gene involved in the signature. **(D, E)** The time-dependent receiver operating characteristic (ROC) curves for the 1-, 2- and 3-year OS **(D)** and relapse free survival (RFS) prediction **(E)** by the E-signature. Significant survival difference between high- and low-threshold group. **(F)** A comparison with previously reported E-signature models by KM survival analysis and ROC curve. **(G)** The E-signature had the highest concordance index (C-index) as opposed to other reported models, which proved that it could accurately predict prognosis.

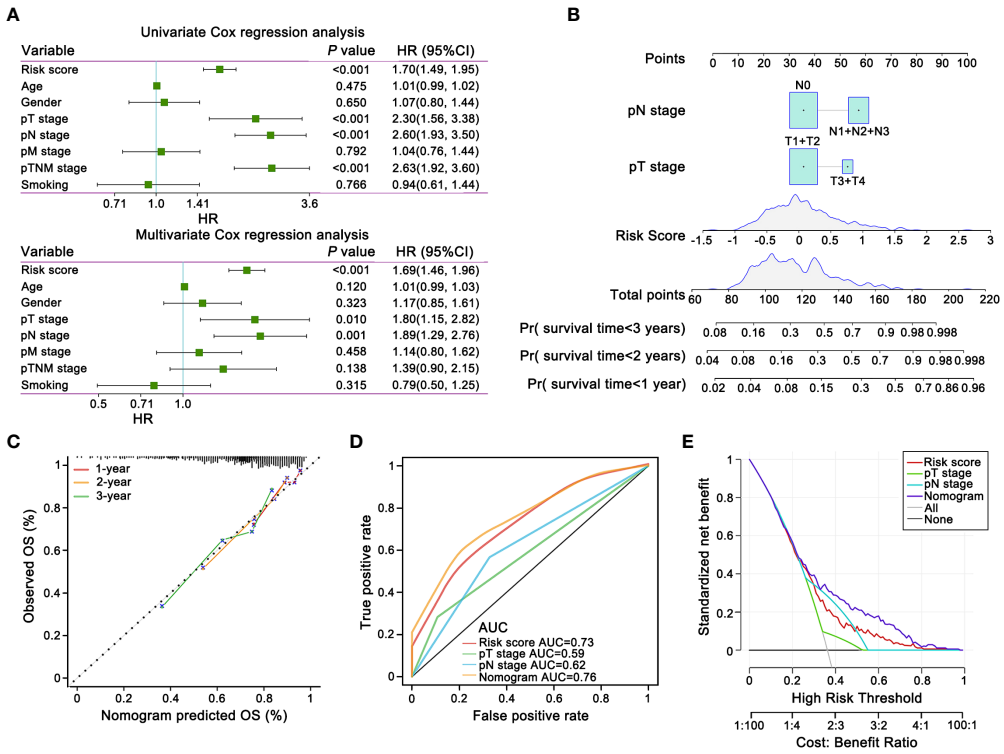

FIGURE 5
The prognostic nomogram and decision curve analysis (DCA) of the risk score based on E-signature. **(A)** The forest plot showed that the signature was independent from other risk factors for prognostic prediction. **(B)** Nomogram predicted risk of secondary progression. Each variable axis, containing T stage, N stage and risk score, corresponded to the characteristic attribute score of single sample. The final score was summarized on the total score axis and the likelihood of 1-, 2-, and 3 years OS is determined on the survival axis. **(C)** The nomogram yielded an accurate predictive capability that was extremely close to actual survival was presented by the calibration plots. X-axis represented the predicted value of survival probability and y-axis represented actual survival possibility. **(D)** ROC curves represented that the E-signature ranked first among all the parameters. **(E)** DCA curves graphically verified the E-signature brought more net benefit of survival than other clinical indexes. Solid lines indicated net benefit of the predictive model within the threshold probabilities range. The black and grey line respectively represented the hypothesis that none or all patients would experience.

Discussion

LUAD is the accepted common classification of lung cancer, accompanied by high prevalence and fatality (2, 56). In cancer patients, metastasis is primary cause of shorten survival and high mortality, and often has already occurred at the time of diagnosis (57, 58). During the procedure of the classical invasion-metastasis cascade, transformation from tumor epithelial cells to mesenchymal cells with the invasion and migration capacity (59). Subsequently, mesenchymal cells locally invade the surrounding matrix and extracellular matrix (ECM), transport and stay in distant organ tissues, eventually extravasate and proliferate to form metastasis (60). The induction and ultimate success of this process depends on EMT and its key regulators (59). Regulation of EMT markers expression, for instance, N-cadherin, Vimentin and E-cadherin, ultimately affects tumor progression, metastasis and drug resistance (61, 62). To date, considerable studies have shown that the marked association of sophisticated regulation of EMT with poor prognosis of lung cancer patients (63, 64). To break down this barrier in clinical settings, molecular biological characteristics should be adequately considered, and circulating tumor markers, TNM staging and other indicators are not accurate enough in predicting the survival of LUAD patients (65, 66). Similarly, single-gene biomarkers are unable to achieve a satisfying prediction result (67). Therefore, a multigene panel might be a promising and reliable method for precision and individualized treatment of LUAD patients.

With rapid advancements in high-throughput sequencing, abundant studies have used data from large communal databases, for example, TCGA and GEO databases, to construct the prognostic signatures for identification of patient risk stratification, guidance of treatment regimens, precise prognostic assessment, and improvement of clinical efficacy (68, 69). Previous studies have reported risk-prediction models based on EMT in LUAD (37, 38). Although the conventional analytical methods used were similar, the genes required for construction of the

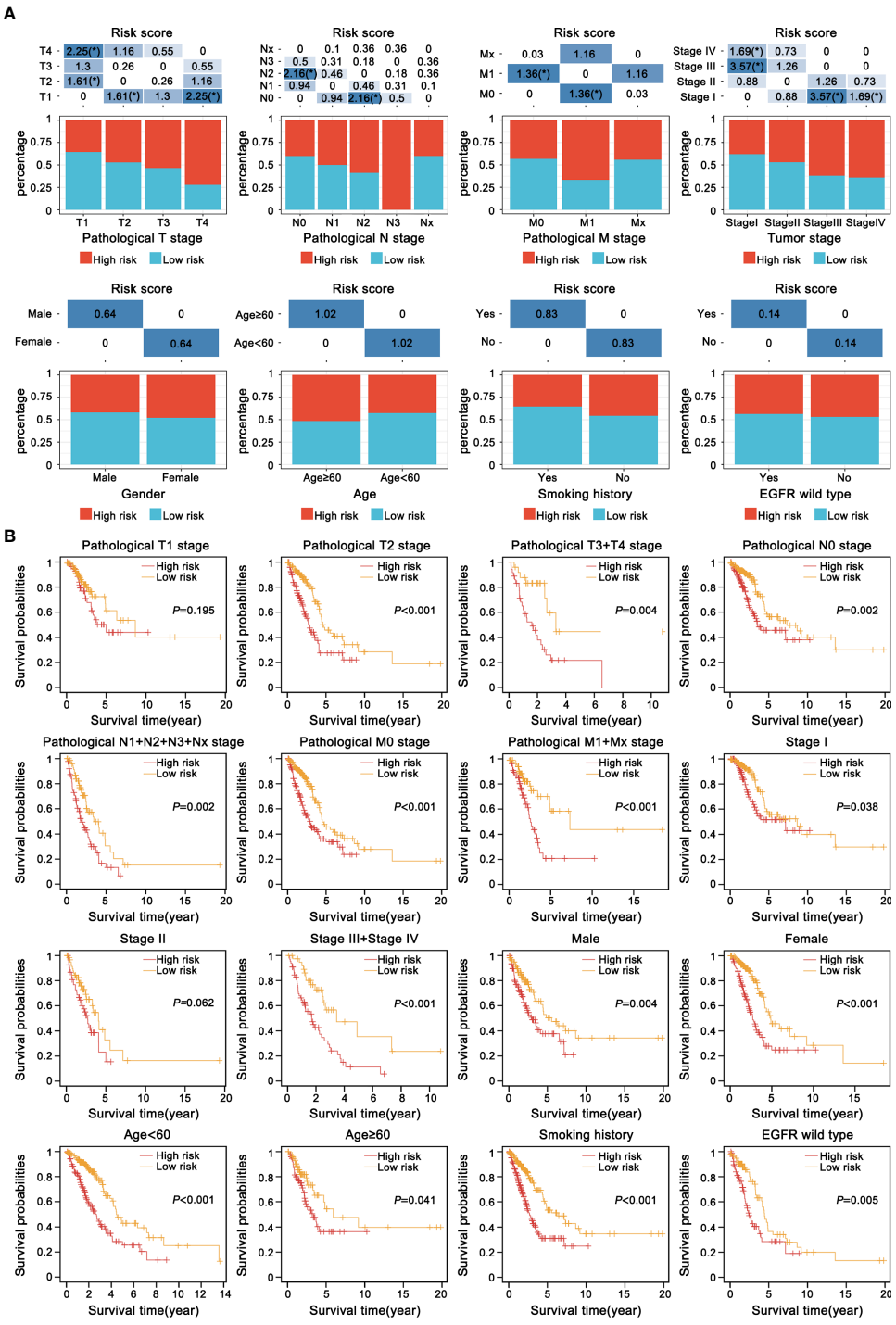

FIGURE 6
Correlation between the current prognostic E-signature and clinicopathologic attributes. **(A)** The distribution of samples with different risk scores classified by clinicopathologic traits, including T stage, N stage, M stage, tumour stage, gender, age, smoking history and EGFR mutation. *P < 0.05. **(B)** KM analysis of each subgroup was stratified by the E-signature to visualize the prognostic value of clinical parameters classification.

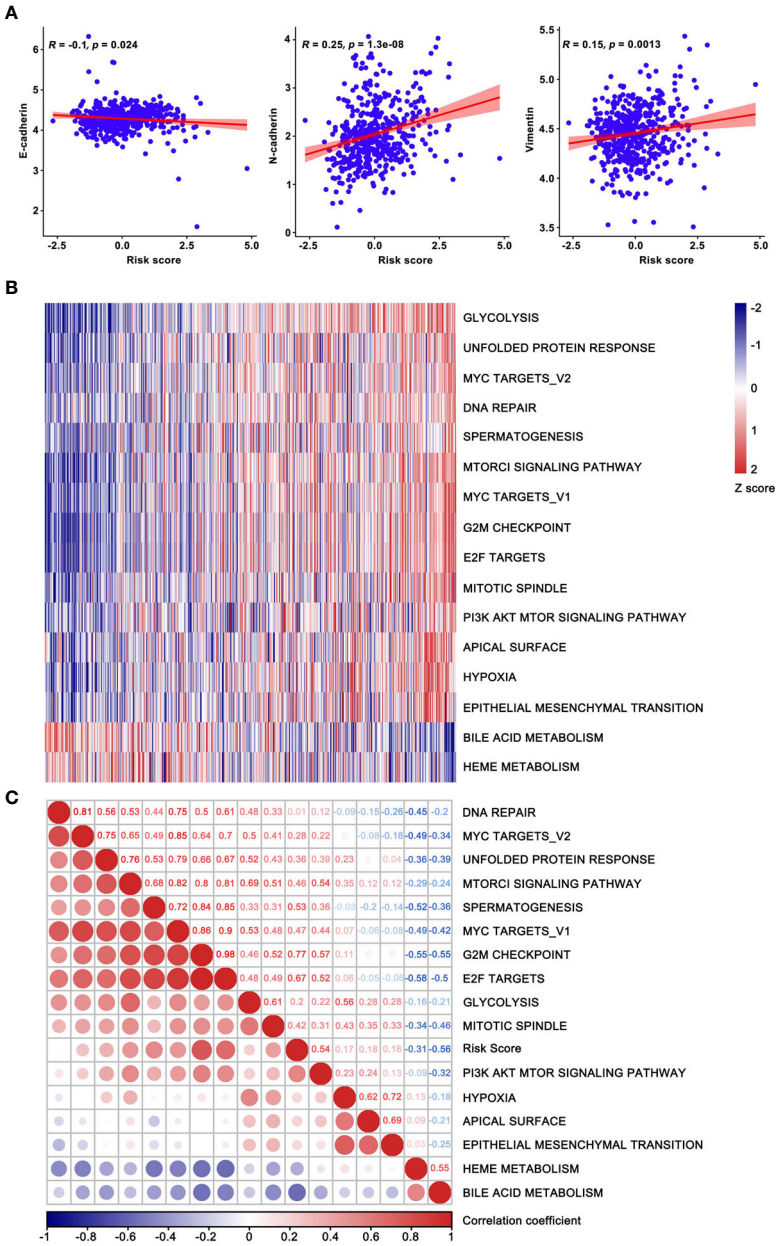

FIGURE 7
Functional enrichment analysis based on the current prognostic model. **(A)** The correlation between risk score and EMT biomarkers. **(B)** Hierarchical clustering analysis was used for heatmap plotting, showing KEGG pathways correlated with the model and coefficients were greater than 0.3. **(C)** The correlation map confirmed the high-risk group retained the oncogenic pathways. The risk score increased successively from left to right, where the enriched pathways and risk score were used as the abscissa.

signatures were fundamentally different, mainly due to the different databases and screening processes. In terms of bioinformatics analysis, our study not only plotted KM curves, ROC curves and nomogram to improve the accuracy and specificity of prognosis prediction, but also generated calibration curves for the nomogram to further prove effective clinical utility of E-signature. Secondly, the DCA (decision curve) was drawn for clarifying clinical feasibility of the risk model and prognostic significance of our signature was emphasized by comparing with known prognostic models (51–53). In addition, compared with the previously reported EMT models, we conducted *in vitro* experiments in-depth to verify a dramatically correlation between our signature and EMT procedure. Collectively, the specific E-signature we developed could predict the cancer process more

comprehensively and accurately, with more stable and robust predictive performance and superior clinical practice (37, 38).

In this study, the E-signature was found to be composed of DKK1, LOXL2, MGP and SLIT3. It is reported that DKK1 (a secreted protein) contains the cysteine-rich domain and is a member of the family of Dickkopf, (70). DKK1 has emerged as an indispensable regulatory factor in multiple cancers and commonly existed as an inhibitor of the Wnt pathway (71–73). Nevertheless, DKK1 acting as a tumor promoter, which played a critical role in the cancer progression (74–76). LOXL2 belonging to the LOX family, has the typical function of catalyzing the cross-link of elastin and collagen in the ECM and has attracted much attention in cancer biology (48). Plenty of studies have revealed that LOXL2 participated in tumor progression, metastasis, poor prognosis and chemoradiotherapy resistance in varied cancers, e.g., lung cancer, breast cancer, pancreatic cancer and colorectal cancer (77–80). MGP, an extracellular matrix protein, whose well-defined function is still unknown, and currently acts as a double-edged sword in cancers (49, 81–84). Upregulation of MGP promoted cancer proliferation, migration and invasion, that was linked with unfavorable prognosis (49, 81–83). Whereas, MGP reversed chemotherapy resistance and received favorable survival outcomes in estrogen receptor positive breast cancer (84). SLIT3, a secreted protein, is widely distributed in normal tissues and mainly participates in the Slit/Robo pathway (85). SLIT3 has rarely been reported in human cancers, which could inhibit the progression of thyroid cancer (86).

Conclusion

In summary, we developed and validated a trustworthy and powerful signature, which could serve as an independent and promising biomarker to optimize prognosis and surveillance protocols for individual LUAD patients.

Data availability statement

The datasets presented in this study can be found in online repositories. The names of the repository/repositories and accession number(s) can be found in the article/Supplementary Material.

Ethics statement

The study conducted in accordance with the guidelines of the Declaration of Helsinki, and was reviewed and approved by the Ethics Committee of Harbin Medical University. The need for written informed consent for participation was not required for this study in accordance with the national legislation and institutional requirements.

Author contributions

LC and YX designed and supervised the research. YMC completed the first draft of manuscript. XW and JN collected pathological information of LUAD patients. YWC provided technical support for bioinformatics and RG carried out experiments, besides, WL offered auxiliary services. LZ performed statistical analysis and conducted the figures. YMC revised the manuscript and figures. All authors contributed to the article and approved the submitted version.

Conflict of interest

The authors declare that the research was conducted in the absence of any commercial or financial relationships that could be construed as a potential conflict of interest.

Publisher's note

All claims expressed in this article are solely those of the authors and do not necessarily represent those of their affiliated organizations, or those of the publisher, the editors and the reviewers. Any product that may be evaluated in this article, or claim that may be made by its manufacturer, is not guaranteed or endorsed by the publisher.

Supplementary material

The Supplementary Material for this article can be found online at: https://www.frontiersin.org/articles/10.3389/fonc.2022.974614/full#supplementary-material

References

1. Siegel RL, Miller KD, Fuchs HE, Jemal A. Cancer statistics 2022. *CA Cancer J Clin* (2022) 72(1):7–33. doi: 10.3322/caac.21708

2. Sung H, Ferlay J, Siegel RL, Laversanne M, Soerjomataram I, Jemal A, et al. Global cancer statistics 2020: Globocan estimates of incidence and mortality worldwide for 36 cancers in 185 countries. *CA Cancer J Clin* (2021) 71(3):209–49. doi: 10.3322/caac.21660

3. Jang HR, Shin SB, Kim CH, Won JY, Xu R, Kim DE, et al. Plk1/Vimentin signaling facilitates immune escape by recruiting Smad2/3 to pd-L1 promoter in metastatic lung adenocarcinoma. *Cell Death Differ* (2021) 28(9):2745–64. doi: 10.1038/s41418-021-00781-4

4. Stinchcombe TE, Bradley JD. Thoracic oncology: Current standard therapy and future developments. *J Clin Oncol* (2022) 40(6):527–9. doi: 10.1200/JCO.21.02396

5. Liang W, Liu J, He J. Driving the improvement of lung cancer prognosis. *Cancer Cell* (2020) 38(4):449–51. doi: 10.1016/j.ccell.2020.09.008

6. Fujikawa R, Muraoka Y, Kashima J, Yoshida Y, Ito K, Watanabe H, et al. Clinicopathologic and genotypic features of lung adenocarcinoma characterized by the international association for the study of lung cancer grading system. *J Thorac Oncol* (2022) 17(5):700–7. doi: 10.1016/j.jtho.2022.02.005

7. Ganesh K, Massague J. Targeting metastatic cancer. *Nat Med* (2021) 27 (1):34–44. doi: 10.1038/s41591-020-01195-4

8. Cheng WC, Chang CY, Lo CC, Hsieh CY, Kuo TT, Tseng GC, et al. Identification of theranostic factors for patients developing metastasis after surgery for early-stage lung adenocarcinoma. *Theranostics* (2021) 11(8):3661–75. doi: 10.7150/thno.53176

9. Han Y, Wang D, Peng L, Huang T, He X, Wang J, et al. Single-cell sequencing: A promising approach for uncovering the mechanisms of tumor metastasis. *J Hematol Oncol* (2022) 15(1):59. doi: 10.1186/s13045-022-01280-w

10. Weiss F, Lauffenburger D, Friedl P. Towards targeting of shared mechanisms of cancer metastasis and therapy resistance. *Nat Rev Cancer* (2022) 22(3):157–73. doi: 10.1038/s41568-021-00427-0

11. Massague J, Ganesh K. Metastasis-initiating cells and ecosystems. *Cancer Discovery* (2021) 11(4):971–94. doi: 10.1158/2159-8290.CD-21-0010

12. Vieugue P, Blanpain C. Recording emt activity by lineage tracing during metastasis. *Dev Cell* (2020) 54(5):567–9. doi: 10.1016/j.devcel.2020.07.011

13. Yang J, Antin P, Berx G, Blanpain C, Brabletz T, Bronner M, et al. Guidelines and definitions for research on epithelial-mesenchymal transition. *Nat Rev Mol Cell Biol* (2020) 21(6):341–52. doi: 10.1038/s41580-020-0237-9

14. Dongre A, Weinberg RA. New insights into the mechanisms of epithelial-mesenchymal transition and implications for cancer. *Nat Rev Mol Cell Biol* (2019) 20(2):69–84. doi: 10.1038/s41580-018-0080-4

15. Lambert AW, Weinberg RA. Linking emt programmes to normal and neoplastic epithelial stem cells. *Nat Rev Cancer* (2021) 21(5):325–38. doi: 10.1038/s41568-021-00332-6

16. Liang H, Yu T, Han Y, Jiang H, Wang C, You T, et al. Lncrna ptar promotes emt and invasion-metastasis in serous ovarian cancer by competitively binding mir-101-3p to regulate Zeb1 expression. *Mol Cancer* (2018) 17(1):119. doi: 10.1186/s12943-018-0870-5

17. Lourenco AR, Ban Y, Crowley MJ, Lee SB, Ramchandani D, Du W, et al. Differential contributions of pre- and post-emt tumor cells in breast cancer metastasis. *Cancer Res* (2020) 80(2):163–9. doi: 10.1158/0008-5472.CAN-19-1427

18. Huang T, Song X, Xu D, Tiek D, Goenka A, Wu B, et al. Stem cell programs in cancer initiation, progression, and therapy resistance. *Theranostics* (2020) 10 (19):8721–43. doi: 10.7150/thno.41648

19. Gu Y, Zhang J, Zhou Z, Liu D, Zhu H, Wen J, et al. Metastasis patterns and prognosis of octogenarians with nsclc: A population-based study. *Aging Dis* (2020) 11(1):82–92. doi: 10.14336/AD.2019.0414

20. Singh M, Yelle N, Venugopal C, Singh SK. Emt: Mechanisms and therapeutic implications. *Pharmacol Ther* (2018) 182:80–94. doi: 10.1016/j.pharmthera.2017.08.009

21. Nieto MA, Huang RY, Jackson RA, Thiery JP. Emt: 2016. *Cell* (2016) 166 (1):21–45. doi: 10.1016/j.cell.2016.06.028

22. Lamouille S, Xu J, Derynck R. Molecular mechanisms of epithelial-mesenchymal transition. *Nat Rev Mol Cell Biol* (2014) 15(3):178–96. doi: 10.1038/nrm3758

23. Hu Z, Cunnea P, Zhong Z, Lu H, Osagie OI, Campo L, et al. The Oxford classic links epithelial-to-Mesenchymal transition to immunosuppression in poor prognosis ovarian cancers. *Clin Cancer Res* (2021) 27(5):1570–9. doi: 10.1158/1078-0432.CCR-20-2782

24. Consortium ITP-CAoWG. Pan-cancer analysis of whole genomes. *Nature* (2020) 578(7793):82–93. doi: 10.1038/s41586-020-1969-6

25. Liu J, Lichtenberg T, Hoadley KA, Poisson LM, Lazar AJ, Cherniack AD, et al. An integrated tcga pan-cancer clinical data resource to drive high-quality survival outcome analytics. *Cell* (2018) 173(2):400–16 e11. doi: 10.1016/j.cell.2018.02.052

26. Chang JT, Lee YM, Huang RS. The impact of the cancer genome atlas on lung cancer. *Transl Res* (2015) 166(6):568–85. doi: 10.1016/j.trsl.2015.08.001

27. Hutter C, Zenklusen JC. The cancer genome atlas: Creating lasting value beyond its data. *Cell* (2018) 173(2):283–5. doi: 10.1016/j.cell.2018.03.042

28. Yan S, Wong KC. Gesgnext: Gene expression signature extraction and meta-analysis on gene expression omnibus. *IEEE J BioMed Health Inform* (2020) 24 (1):311–8. doi: 10.1109/JBHI.2019.2896144

29. Wang S, Xiong Y, Zhang Q, Su D, Yu C, Cao Y, et al. Clinical significance and immunogenomic landscape analyses of the immune cell signature based prognostic model for patients with breast cancer. *Brief Bioinform* (2021) 22 (4):1093–107. doi: 10.1093/bib/bbaa311

30. Chen R, Goodison S, Sun Y. Molecular profiles of matched primary and metastatic tumor samples support a linear evolutionary model of breast cancer. *Cancer Res* (2020) 80(2):170–4. doi: 10.1158/0008-5472.CAN-19-2296

31. Liu M, Tong L, Liang B, Song X, Xie L, Peng H, et al. A 15-gene signature and prognostic nomogram for predicting overall survival in non-distant metastatic oral tongue squamous cell carcinoma. *Front Oncol* (2021) 11:587548. doi: 10.3389/fonc.2021.587548

32. Feng C, Liu S, Shang Z. Identification and validation of an emt-related lncrna signature for hnscc to predict survival and immune landscapes. *Front Cell Dev Biol* (2021) 9:798898. doi: 10.3389/fcell.2021.798898

33. Yu H, Gu D, Yue C, Xu J, Yan F, He X. An immune cell-based signature associating with emt phenotype predicts postoperative overall survival of escc. *Front Oncol* (2021) 11:636479. doi: 10.3389/fonc.2021.636479

34. Du Y, Wang B, Jiang X, Cao J, Yu J, Wang Y, et al. Identification and validation of a stromal emt related lncrna signature as a potential marker to predict bladder cancer outcome. *Front Oncol* (2021) 11:620674. doi: 10.3389/fonc.2021.620674

35. Lin WP, Xing KL, Fu JC, Ling YH, Li SH, Yu WS, et al. Development and validation of a model including distinct vascular patterns to estimate survival in hepatocellular carcinoma. *JAMA Netw Open* (2021) 4(9):e2125055. doi: 10.1001/jamanetworkopen.2021.25055

36. Han Y, Wong FC, Wang D, Kahlert C. An *in silico* analysis reveals an emt-associated gene signature for predicting recurrence of early-stage lung adenocarcinoma. *Cancer Inform* (2022) 21:11769351221100727. doi: 10.1177/11769351221100727

37. Tang Y, Jiang Y, Qing C, Wang J, Zeng Z. Systematic construction and validation of an epithelial-mesenchymal transition risk model to predict prognosis of lung adenocarcinoma. *Aging (Albany NY)* (2020) 13(1):794–812. doi: 10.18632/aging.202186

38. Shi J, Wang Z, Guo J, Chen Y, Tong C, Tong J, et al. Identification of a three-gene signature based on epithelial-mesenchymal transition of lung adenocarcinoma through construction and validation of a risk-prediction model. *Front Oncol* (2021) 11:726834. doi: 10.3389/fonc.2021.726834

39. Blanco JL, Porto-Pazos AB, Pazos A, Fernandez-Lozano C. Prediction of high anti-angiogenic activity peptides *in silico* using a generalized linear model and feature selection. *Sci Rep* (2018) 8(1):15688. doi: 10.1038/s41598-018-33911-z

40. Wysocki AC, Rhemtulla M. On penalty parameter selection for estimating network models. *Multivar Behav Res* (2021) 56(2):288–302. doi: 10.1080/00273171.2019.1672516

41. Zhang JH, Hou R, Pan Y, Gao Y, Yang Y, Tian W, et al. A five-microrna signature for individualized prognosis evaluation and radiotherapy guidance in patients with diffuse lower-grade glioma. *J Cell Mol Med* (2020) 24(13):7504–14. doi: 10.1111/jcmm.15377

42. Wang Q, Wang Z, Li G, Zhang C, Bao Z, Wang Z, et al. Identification of idh-mutant gliomas by a prognostic signature according to gene expression profiling. *Aging (Albany NY)* (2018) 10(8):1977–88. doi: 10.18632/aging.101521

43. Balachandran VP, Gonen M, Smith JJ, DeMatteo RP. Nomograms in oncology: More than meets the eye. *Lancet Oncol* (2015) 16(4):e173–80. doi: 10.1016/S1470-2045(14)71116-7

44. Mo S, Cai X, Zhou Z, Li Y, Hu X, Ma X, et al. Nomograms for predicting specific distant metastatic sites and overall survival of colorectal cancer patients: A Large population-based real-world study. *Clin Transl Med* (2020) 10(1):169–81. doi: 10.1002/ctm2.20

45. Yu J, Liu TT, Liang LL, Liu J, Cai HQ, Zeng J, et al. Identification and validation of a novel glycolysis-related gene signature for predicting the prognosis in ovarian cancer. *Cancer Cell Int* (2021) 21(1):353. doi: 10.1186/s12935-021-02045-0

46. Macaskill P. Standard deviation and standard error: Interpretation, usage and reporting. *Med J Aust* (2018) 208(2):63–4. doi: 10.5694/mja17.00633

47. Qi L, Sun B, Liu Z, Li H, Gao J, Leng X. Dickkopf-1 inhibits epithelial-mesenchymal transition of colon cancer cells and contributes to colon cancer suppression. *Cancer Sci* (2012) 103(4):828–35. doi: 10.1111/j.1349-7006.2012.02222.x

48. Wen B, Xu LY, Li EM. Loxl2 in cancer: Regulation, downstream effectors and novel roles. *Biochim Biophys Acta Rev Cancer* (2020) 1874(2):188435. doi: 10.1016/j.bbcan.2020.188435

49. Gong C, Zou J, Zhang M, Zhang J, Xu S, Zhu S, et al. Upregulation of mgp by Hoxc8 promotes the proliferation, migration, and emt processes of triple-negative breast cancer. *Mol Carcinog* (2019) 58(10):1863–75. doi: 10.1002/mc.23079

50. Zhang C, Guo H, Li B, Sui C, Zhang Y, Xia X, et al. Effects of Slit3 silencing on the invasive ability of lung carcinoma A549 cells. *Oncol Rep* (2015) 34(2):952–60. doi: 10.3892/or.2015.4031

51. Zhu J, Wang M, Hu D. Development of an autophagy-related gene prognostic signature in lung adenocarcinoma and lung squamous cell carcinoma. *PeerJ* (2020) 8:e8288. doi: 10.7717/peerj.8288

52. Ma B, Geng Y, Meng F, Yan G, Song F. Identification of a sixteen-gene prognostic biomarker for lung adenocarcinoma using a machine learning method. *J Cancer* (2020) 11(5):1288–98. doi: 10.7150/jca.34585

53. Zhang L, Zhang Z, Yu Z. Identification of a novel glycolysis-related gene signature for predicting metastasis and survival in patients with lung adenocarcinoma. *J Transl Med* (2019) 17(1):423. doi: 10.1186/s12967-019-02173-2

54. Zhang M, Zhu K, Pu H, Wang Z, Zhao H, Zhang J, et al. An immune-related signature predicts survival in patients with lung adenocarcinoma. *Front Oncol* (2019) 9:1314. doi: 10.3389/fonc.2019.01314

55. Tian S, Li Q, Li R, Chen X, Tao Z, Gong H, et al. Development and validation of a prognostic nomogram for hypopharyngeal carcinoma. *Front Oncol* (2021) 11:696952. doi: 10.3389/fonc.2021.696952

56. Adib E, Nassar AH, Abou Alaiwi S, Groha S, Akl EW, Sholl LM, et al. Variation in targetable genomic alterations in non-small cell lung cancer by genetic ancestry, sex, smoking history, and histology. *Genome Med* (2022) 14(1):39. doi: 10.1186/s13073-022-01041-x

57. Klein CA. Cancer progression and the invisible phase of metastatic colonization. *Nat Rev Cancer* (2020) 20(11):681–94. doi: 10.1038/s41568-020-00300-6

58. Jiang C, Zhang N, Hu X, Wang H. Tumor-associated exosomes promote lung cancer metastasis through multiple mechanisms. *Mol Cancer* (2021) 20 (1):117. doi: 10.1186/s12943-021-01411-w

59. Yeung KT, Yang J. Epithelial-mesenchymal transition in tumor metastasis. *Mol Oncol* (2017) 11(1):28–39. doi: 10.1002/1878-0261.12017

60. Lu J. The warburg metabolism fuels tumor metastasis. *Cancer Metastasis Rev* (2019) 38(1-2):157–64. doi: 10.1007/s10555-019-09794-5

61. Zhang N, Ng AS, Cai S, Li Q, Yang L, Kerr D. Novel therapeutic strategies: Targeting epithelial-mesenchymal transition in colorectal cancer. *Lancet Oncol* (2021) 22(8):e358–e68. doi: 10.1016/S1470-2045(21)00343-0

62. Wu J, He Z, Yang XM, Li KL, Wang DL, Sun FL. Rccd1 depletion attenuates tgf-Beta-Induced emt and cell migration by stabilizing cytoskeletal microtubules in nsclc cells. *Cancer Lett* (2017) 400:18–29. doi: 10.1016/j.canlet.2017.04.021

63. Pan Z, Cai J, Lin J, Zhou H, Peng J, Liang J, et al. A novel protein encoded by Circfndc3b inhibits tumor progression and emt through regulating snail in colon cancer. *Mol Cancer* (2020) 19(1):71. doi: 10.1186/s12943-020-01179-5

64. Yang S, Liu Y, Li MY, Ng CSH, Yang SL, Wang S, et al. Foxp3 promotes tumor growth and metastasis by activating Wnt/Beta-catenin signaling pathway and emt in non-small cell lung cancer. *Mol Cancer* (2017) 16(1):124. doi: 10.1186/s12943-017-0700-1

65. Zhang Z, Chen J, Zhu S, Zhu D, Xu J, He G. Construction and validation of a cell cycle-related robust prognostic signature in colon cancer. *Front Cell Dev Biol* (2020) 8:611222. doi: 10.3389/fcell.2020.611222

66. Mo S, Dai W, Zhou Z, Gu R, Li Y, Xiang W, et al. Comprehensive transcriptomic analysis reveals prognostic value of an emt-related gene signature in colorectal cancer. *Front Cell Dev Biol* (2021) 9:681431. doi: 10.3389/fcell.2021.681431

67. Nguyen LC, Naulaerts S, Bruna A, Ghislat G, Ballester PJ. Predicting cancer drug response *in vivo* by learning an optimal feature selection of tumour molecular profiles. *Biomedicines* (2021) 9(10):1319–43. doi: 10.3390/biomedicines9101319

68. Qi L, Li T, Shi G, Wang J, Li X, Zhang S, et al. An individualized gene expression signature for prediction of lung adenocarcinoma metastases. *Mol Oncol* (2017) 11(11):1630–45. doi: 10.1002/1878-0261.12137

69. Qi L, Li Y, Qin Y, Shi G, Li T, Wang J, et al. An individualised signature for predicting response with concordant survival benefit for lung adenocarcinoma patients receiving platinum-based chemotherapy. *Br J Cancer* (2016) 115 (12):1513–9. doi: 10.1038/bjc.2016.370

70. D'Amico L, Mahajan S, Capietto AH, Yang Z, Zamani A, Ricci B, et al. Dickkopf-related protein 1 (Dkk1) regulates the accumulation and function of myeloid derived suppressor cells in cancer. *J Exp Med* (2016) 213(5):827–40. doi: 10.1084/jem.20150950

71. Jiang J, Li J, Yao W, Wang W, Shi B, Yuan F, et al. Foxc1 negatively regulates Dkk1 expression to promote gastric cancer cell proliferation through activation of wnt signaling pathway. *Front Cell Dev Biol* (2021) 9:662624. doi: 10.3389/fcell.2021.662624

72. Zhuang X, Zhang H, Li X, Li X, Cong M, Peng F, et al. Differential effects on lung and bone metastasis of breast cancer by wnt signalling inhibitor Dkk1. *Nat Cell Biol* (2017) 19(10):1274–85. doi: 10.1038/ncb3613

73. Niu J, Li XM, Wang X, Liang C, Zhang YD, Li HY, et al. Dkk1 inhibits breast cancer cell migration and invasion through suppression of beta-Catenin/Mmp7 signaling pathway. *Cancer Cell Int* (2019) 19:168. doi: 10.1186/s12935-019-0883-1

74. Lyros O, Lamprecht AK, Nie L, Thieme R, Gotzel K, Gasparri M, et al. Dickkopf-1 (Dkk1) promotes tumor growth *Via* akt-phosphorylation and independently of wnt-axis in barrett's associated esophageal adenocarcinoma. *Am J Cancer Res* (2019) 9(2):330–46.

75. Feng Y, Zhang Y, Wei X, Zhang Q. Correlations of Dkk1 with pathogenesis and prognosis of human multiple myeloma. *Cancer biomark* (2019) 24(2):195–201. doi: 10.3233/CBM-181909

76. Shen Q, Yang XR, Tan Y, You H, Xu Y, Chu W, et al. High level of serum protein Dkk1 predicts poor prognosis for patients with hepatocellular carcinoma after hepatectomy. *Hepat Oncol* (2015) 2(3):231–44. doi: 10.2217/hep.15.12

77. Ferreira S, Saraiva N, Rijo P, Fernandes AS. Loxl2 inhibitors and breast cancer progression. *Antioxid (Basel)* (2021) 10(2):312–27. doi: 10.3390/antiox10020312

78. Li R, Li H, Zhu L, Zhang X, Liu D, Li Q, et al. Reciprocal regulation of Loxl2 and Hif1alpha drives the warburg effect to support pancreatic cancer aggressiveness. *Cell Death Dis* (2021) 12(12):1106. doi: 10.1038/s41419-021-04391-3

79. Peng DH, Ungewiss C, Tong P, Byers LA, Wang J, Canales JR, et al. Zeb1 induces Loxl2-mediated collagen stabilization and deposition in the extracellular matrix to drive lung cancer invasion and metastasis. *Oncogene* (2017) 36(14):1925–38. doi: 10.1038/onc.2016.358

80. Zheng GL, Liu YL, Yan ZX, Xie XY, Xiang Z, Yin L, et al. Elevated Loxl2 expression by Linc01347/Mir-328-5p axis contributes to 5-fu chemotherapy resistance of colorectal cancer. *Am J Cancer Res* (2021) 11(4):1572–85.

81. Sterzynska K, Klejewski A, Wojtowicz K, Swierczewska M, Andrzejewska M, Rusek D, et al. The role of matrix gla protein (Mgp) expression in paclitaxel and topotecan resistant ovarian cancer cell lines. *Int J Mol Sci* (2018) 19(10):2901–17. doi: 10.3390/ijms19102901

82. Huang C, Wang M, Wang J, Wu D, Gao Y, Huang K, et al. Suppression mgp inhibits tumor proliferation and reverses oxaliplatin resistance in colorectal cancer. *Biochem Pharmacol* (2021) 189:114390. doi: 10.1016/j.bcp.2020.114390

83. Li X, Wei R, Wang M, Ma L, Zhang Z, Chen L, et al. Mgp promotes colon cancer proliferation by activating the nf-kappab pathway through upregulation of the calcium signaling pathway. *Mol Ther Oncol* (2020) 17:371–83. doi: 10.1016/j.omto.2020.04.005

84. Tuo YL, Ye YF. Mgp is downregulated due to promoter methylation in chemoresistant er+ breast cancer and high mgp expression predicts better survival outcomes. *Eur Rev Med Pharmacol Sci* (2017) 21(17):3871–8.

85. Ni W, Liu T, Wang HY, Liu LH, Chen GX. [Expression of Slit3/Robo signal pathway in mouse aortic smooth muscle cell and its impact on proliferation and migration]. *Zhonghua Xin Xue Guan Bing Za Zhi* (2016) 44(6):542–7. doi: 10.3760/cma.j.issn.0253-3758.2016.06.016

86. Guan H, Wei G, Wu J, Fang D, Liao Z, Xiao H, et al. Down-regulation of mir-218-2 and its host gene Slit3 cooperate to promote invasion and progression of thyroid cancer. *J Clin Endocrinol Metab* (2013) 98(8):E1334–44. doi: 10.1210/jc.2013-1053

frontiers | Frontiers in Oncology

TYPE Original Research
PUBLISHED 29 September 2022
DOI 10.3389/fonc.2022.926025

Check for updates

OPEN ACCESS

EDITED BY
Tao Sun,
Nankai University, China

REVIEWED BY
Maysam Pedram,
Yale University, United States
Qiang Huang,
Second Affiliated Hospital of Soochow University, China

*CORRESPONDENCE
Hua Yan
yanhua20042007@sina.com
Hongguang Wang
luckywhg@163.com
Xiaoguang Tong
hongwu1984teda@126.com

†These authors have contributed equally to this work and share first authorship

SPECIALTY SECTION
This article was submitted to Pharmacology of Anti-Cancer Drugs, a section of the journal Frontiers in Oncology

RECEIVED 22 April 2022
ACCEPTED 05 September 2022
PUBLISHED 29 September 2022

CITATION
Song S, Wu H, Wang F, Jiao J, Xu L, Wang H, Tong X and Yan H (2022) Global research trends and hotspots on glioma stem cells.
Front. Oncol. 12:926025.
doi: 10.3389/fonc.2022.926025

COPYRIGHT
© 2022 Song, Wu, Wang, Jiao, Xu, Wang, Tong and Yan. This is an open-access article distributed under the terms of the Creative Commons Attribution License (CC BY). The use, distribution or reproduction in other forums is permitted, provided the original author(s) and the copyright owner(s) are credited and that the original publication in this journal is cited, in accordance with accepted academic practice. No use, distribution or reproduction is permitted which does not comply with these terms.

Global research trends and hotspots on glioma stem cells

Sirong Song[1†], Haiyang Wu[1†], Fanchen Wang[1], Jiji Jiao[1], Lixia Xu[2], Hongguang Wang[2,3*], Xiaoguang Tong[2,3*] and Hua Yan[2,3*]

[1]Clinical College of Neurology, Neurosurgery and Neurorehabilitation, Tianjin Medical University, Tianjin, China, [2]Tianjin Neurosurgical Institute, Tianjin Key Laboratory of Cerebrovascular and Neurodegenerative Diseases, Tianjin Huanhu Hospital, Tianjin, China, [3]Department of Neurology, Tianjin Huanhu Hospital, Tianjin, China

Background: Glioma stem cells (GSCs) are a sub-population of cancer stem cells with capacity of self-renewal and differentiation. Accumulated evidence has revealed that GSCs were shown to contribute to gliomagenesis, distant metastasis as well as the resistance to radiotherapy and chemotherapy. As a result, GSCs were regarded as a promising therapeutic target in human glioma. The purpose of our study is to identify current state and hotspots of GSCs research by analyzing scientific publications through bibliometric methods.

Methods: All relevant publications on GSCs during 2003-2021 were extracted from the Science Citation Index Expanded of Web of Science Core Collection (WoSCC), and related information was collected and analyzed using Microsoft Excel 2016, GraphPad Prism 8 and VOSviewer software.

Results: A total of 4990 papers were included. The United States accounted for the largest number of publications (1852), the second average citations per item (ACI) value (67.54) as well as the highest H-index (157). *Cancer Research* was the most influential journal in this field. The most contributive institution was League of European Research Universities. RICH JN was the author with the most publications (109) and the highest H-index (59). All studies were clustered into 3 groups: "glioma stem cell properties", "cell biological properties" and "oncology therapy". The keywords "identification", "CD133" and "side population" appeared earlier with the smaller average appearing years (AAY), and the keywords"radiotherapy" and "chemotherapy" had the latest AAY. The analysis of top cited articles showed that "temozolomide", "epithelial-mesenchymal transition", and "immunotherapy" emerged as new focused issues.

Conclusion: There has been a growing number of researches on GSCs. The United States has always been a leading player in this domain. In general, the research focus has gradually shifted from basic cellular biology to the solutions of clinical concerns. "Temozolomide resistance", "epithelial-mesenchymal transition", and "immunotherapy" should be given more attention in the future.

KEYWORDS

glioma stem cell (GSC), chemotherapy resistance, EMT - epithelial to mesenchymal transformation, hotpots, bibliometric analysis

Background

Glioma is one of the most common primary malignant tumors of the central nervous system, accounting for 45%-60% of adult intracranial tumors, with a 5-year survival rate of less than 10% (1, 2). Glioma stem cells (GSCs) are a particular group of cells within the glioma mass, which also were known as glioma-initiating cells (3, 4). Previous reports have demonstrated that GSCs share fundamental stem cell properties of self-proliferation and multi-lineage differentiation. Emerging evidence suggests that GSCs to a large extent contribute to glioma recurrence and therapy resistance (5, 6). For example, radiotherapy is particularly effective against rapidly proliferating tumors cells, while GSCs are mainly quiescent in the G0 state, and therefore allows them to exhibit high resistance to radiotherapy. In addition, GSCs are able to expel antineoplastic drugs to the extracellular medium by using multidrug resistance-associated protein transporter (7, 8). In view of this, GSCs are considered to be critical therapeutic targets for glioma relapse and drug resistance (9).

Appropriate epistasis regulation is vital for the maintenance of GSCs. Temozolomide (TMZ) is the first-line chemotherapeutic agent for glioma, and main mechanism of action of this drug is to promote methylation of guanine in DNA, leading to glioma cell cycle arrest (10). In contrast, O-6-Methylguanine-DNA methyltransferase (MGMT) is a key enzyme for DNA repair (9, 11), which functions as removing alkyl groups from guanine residues, thereby counteracting TMZ-induced DNA damage, an important mechanism in the resistance of glioma cells to TMZ treatment. Multiple studies have shown that miRNA and LncRNA could reduce MGMT activity levels to improve TMZ sensitivity (12, 13). And they could regulate the growth pathway of GSCs, promote apoptosis and inhibit cell proliferation. Additionally, some miRNAs were confirmed to be closely associated with glioma prognosis and can also be used as prognostic predictors (14).

Meanwhile, GSCs have been isolated mainly from glioma cell lines cultured *in vitro* or human brain tumors. Most GSCs' markers are derived from normal stem cells, including SOX2, NANOG, OLOG 2, MYC, BMI1 and differentiation inhibitor protein 1 (ID1), as well as surface markers CD133, CD24, CD44 and Nestin (3, 15). These markers can be used as an indicator for GSCs identification and also for cell sorting (16). However, GSCs cultured *in vitro* may not accurately reflect their physiological status as they showed *in vivo*, even though the glioma cells were derived from patients. As GSCs *in vivo* are exposed to the presence of large numbers of immune cells, complex regulation of substance metabolism and growth regulation, it is difficult to recreate the real context, even with three-dimensional (3D) cell cultures and organ models (17, 18).

Given the importance of GSCs in tumor progression and therapeutic resistance, an increasing amount of GSCs research has been carried out in recent years. However, few attempts have been undertaken to analyze the quantity and quality of publications in this field from a global perspective. Most of the studies focus only on one or some particular areas of GSCs research. Therefore, it is necessary to adopt appropriate statistical methods to reveal the overall knowledge framework, research hotspots, and future directions of this field.

Bibliometrics is a scientific discipline employing mathematical, statistical and other econometric methods to explore the nature of scientific activities (19, 20). This method could quantitatively reveal the development history, research focus and future research direction of the scientific field. Bibliometric analysis is now widely used in various fields, including mathematics (21), physics (22), forestry (23), agronomy (24) and medicine (25). However, to the best of our knowledge, no studies involving the bibliometric analysis of GSCs had been conducted. Thus, in the present study, we performed a bibliometric analysis through collecting publications related to GSCs research, and further using VOS viewer software, a widely used bibliometric software to estimate the contribution of countries/institutions/authors, and to identify research trends and hotspots in this field.

Materials and methods

Data sources and search strategies

Web of Science (WoS) is one of the most authoritative and well-known citation databases, currently covering more than 18000 journals and 256 subject categories. To date, there has been general agreement that the Science Citation Index-Expanded (SCI-EXPANDED) of Thomson Reuters' WoS Core Collection (WoSCC) is the most appropriate database for conducting bibliometric analysis (19, 20, 25). In this bibliometric research, data were retrieved and downloaded from SCI-EXPANDED (1998-present) of WoSCC. All the search works were completed within the same day in order to avoid the possible bias caused by the daily updating on WoSCC database. Since all data in this study were obtained from public databases and did not require any interactions with human or animal subjects, ethical consent was not applicable. We performed a visualization analysis on the number of publications, citations, and research trends by country, author, and institution using VOSviewer and other software to predict future research hotspots in this field (Figure 1).

Abbreviations: GSC, Glioma stem cell; ACI, Average citations per item; TLS, Total link strength; SOTC, Sum of the times cited; TMZ, Temozolomide; MGMT, O-6-Methylguanine-DNA methyltransferase; SCI-EXPANDED, Science Citation Index-Expanded; WoSCC, Thomson Reuters' WoS Core Collection; WoS, Web of Science; AAY, Average appearing year; EMT, Epithelial-to-mesenchymal transition.

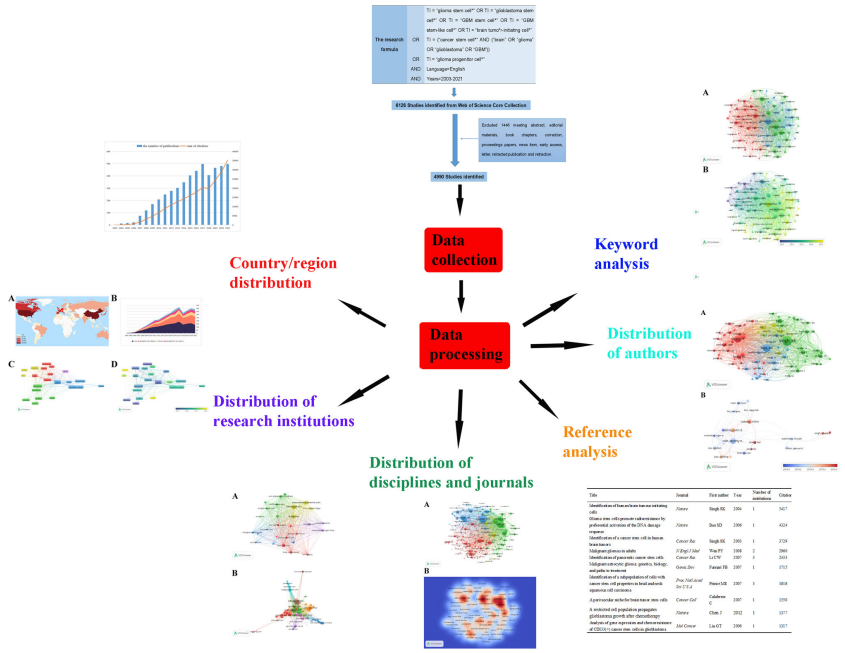

FIGURE 1
We searched the Web of Science Core Collection (WoSCC) on GSCs and performed a visualization analysis from the perspectives of countries, institutions, disciplines, journals, authors, references and keywords to predict future research hotspots in this field.

The search formula was set to TI = "glioma stem cell*" OR TI = "glioblastoma stem cell*" OR TI = "GBM stem cell*" OR TI = "GBM stem-like cell*" OR TI = "brain tumor-initiating cell*" OR TI = ("cancer stem cell*" AND ("brain" OR "glioma" OR "glioblastoma" OR "GBM")) OR TI = "glioma progenitor cell*" AND language=English. The retrieval time span was limited to 2003-2021 (Figure 2). There were 3905 original articles, which accounted for 63.75% of the total number of records, making articles the most frequent document type. Review articles ranked second with 1085 records, comprised 17.71% of the total.

Data collection

To optimize data analysis, only original articles and reviews were included in the final bibliometric analysis based on previous studies. All retrieved records were assessed and reviewed independently by two investigators (SSR, WHY). The exported data included the number of publications, citation frequency, active countries/regions and institutions, influential authors and journals, disciplines, H-index, average citations per item (ACI) and sum of the times cited (SOTC). Then the data were inputted into Microsoft Excel 2016 and GraphPad Prism 8 and analysed both quantitatively and qualitatively by descriptive analysis.

Bibliometric analysis

Microsoft Excel 2016 was applied to generate a prediction model: f(x) = ((number of publications in the last year ÷ number of publications in the first year)1/(last year - first year)- 1) × 100, in which we analyzed the time trend of the publications as well as the future change tendency based on the cumulative number of publications (20). The index of H means that a scholar/country has published H papers and that each of them has been cited at least H times by other publications. It is widely accepted that H-index could quantify both the scientific impact and research output of a scholar or a country (21, 22). In addition, a citation is a sign that one's research has recognized by other researchers and also a way for other scholars to draw on or directly prove their point. Usually speaking, the higher the number of citations, the more attention the result has received and the higher its academic value. Therefore, SOTC and AIC are the frequently used indicators to assess the scientific performance and contribution a scholar or a country (25, 26).

Bibliometric analysis, which takes advantage of mathematical and statistical approaches, is a comprehensive analytical method first defined by Pritchard in 1969. It is regards as one of the optimal methods for quantifying the content of literature and analyzing the correlation of highly cited references with productive authors. The java program VOS viewer (version 1.6.16, Leiden University, The Netherlands,

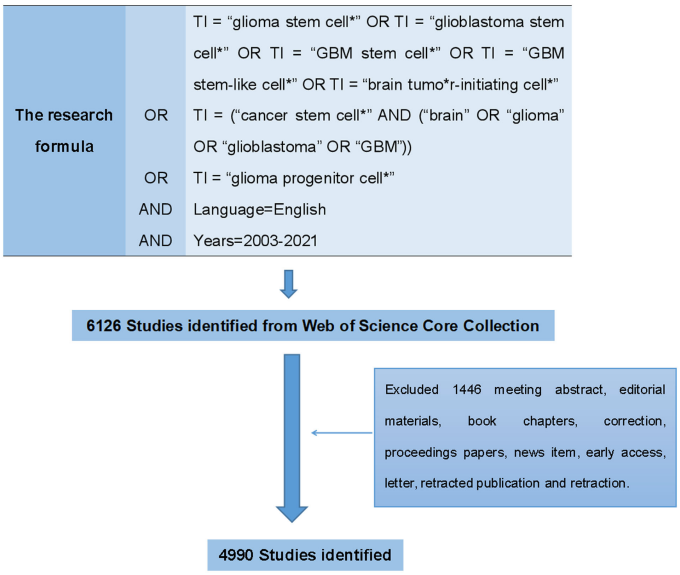

FIGURE 2
The flowchart of data collection about GSCs on WoSCC.

downloadable at www.Vosviewer.com) is one of the most popular bibliometric software tools used for constructing and visualizing the network of authors, country, institution, journal, and keywords. VOS viewer could provide three types of visualizations map including the network visualization map, the overlay visualization map, and the density visualization map (27). Take network visualization map as an example, items are represented by their label and the size of the label is determined by the weight of the item. The links between items indicate the correlation between parameters and the thickness of the link represents the strength of the link. Total Link Strength (TLS) which means the weighed links of the selected nodes is often used to quantitatively evaluate the total links (25, 26). In addition, VOS viewer could classify countries, journals, institutions, and keywords into different clusters based on co-authorship, citation, co-citation, as well as co-occurrence analysis. A detailed explanation for these maps is available in a handbook which could be downloaded from the following Web site: https://www.vosviewer.com/documentation/Manual_VOSviewer_1.6.16.pdf.

Result

Temporal distribution map of the scientific literature

Already in 2003, *Cancer Research* published an article by Canadian scholar Singh et al, entitled "Identification of a cancer stem cell in human brain tumors", which defined a class of brain tumor stem cell for the first time. Starting in 2007, the annual volume of publications related to GSCs has increased steadily, reaching a peak in 2017 (498), accounting for 9.98% of total publications, subsequently with a minor fluctuation in the literature published in 2018 (406) and a rebound in 2019. The annual growth rate from 2007 to 2021 was 14.56%, representing 98.98% of all papers meeting the criteria (4939/4990). In addition, as also can be seen from Figure 3, the annual number of citations showed an overall increasing trend, which was similar with the growth pattern of annual number of publications.

Country/region distribution

Of these 4990 articles and reviews, 85 countries are involved in GSCs research. From Figure 4A and Table 1, it can be seen that the United States was the most prolific country with 1852 (37.11%) publications, followed by China (1133, 22.71%) and Italy (469, 9.40%). In terms of the H-index, the United States also ranked first. Figure 4B presents the number of papers published per year in the top 5 countries during the period 2003-2021. There has been a consistent growth in annual number of studies on GSCs in the United States since 2004, and culminated in 2017 (186). China has made great progress in this field since the 2010s, but the number of research publications was still lower than the United States.

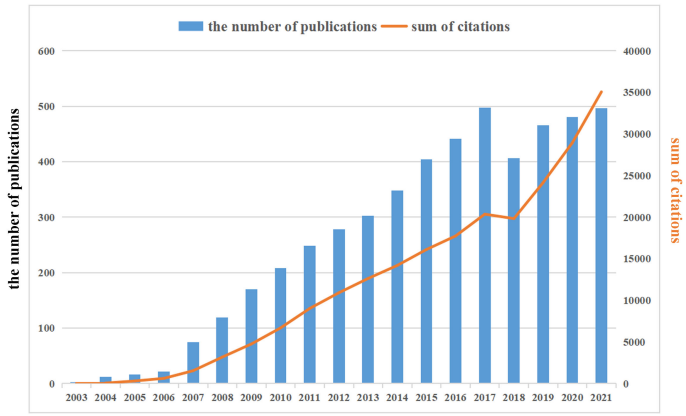

FIGURE 3
The annual publications and citations annual number of publications and citations in the field of glioma stem cells (GSCs) from 2003 to 2021. There is an increasing trend in GSCs.

Figure 4C illustrates the country co-authorship network visualization map. A total of 22 countries with the minimum number of 50 publications were selected. Each colored node represents a country, and nodes with the same color are grouped into the same cluster. Particularly, the thicker the line between two nodes indicates the closer cooperation between countries. As evident from Figure 4C, global country cooperation is broadly divided into five main clusters. The United States has a central position in collaboration with other countries, and collaborated most closely with China, Italy, and England. Figure 4D shows the country co-authorship overlay visualization map. The color of each node indicates the average appearing year (AAY) of each country according to the color gradient presented in the lower right corner. From this figure, we can find that the countries of Russia, Poland and Iran were the relatively new entrants in this field. And as one of the early

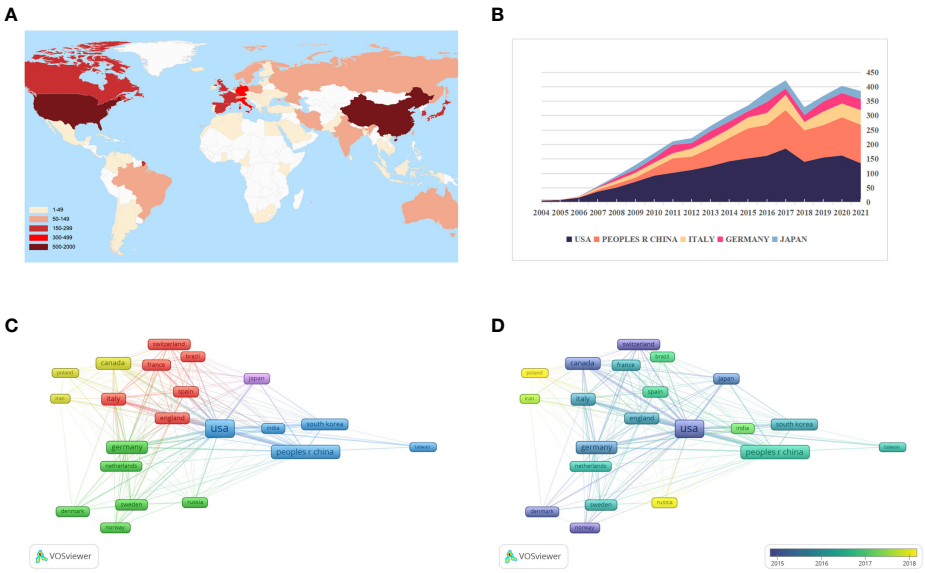

FIGURE 4
(A) The global distribution of different countries involved in glioma stem cells (GSCs) research based on their number of publications. The United State pays the most attention to GSCs, followed by China and Italy. **(B)** The growth trends of annual number of publications in the top 5 prolific countries during the period 2003-2021. The network visualization map **(C)** and overlay visualization map **(D)** of country co-authorship analysis generated by VOS viewer. Countries with the minimum number of 50 publications were assigned into five clusters.

TABLE 1 The top 10 countries in research scope of glioma stem cells.

Country	Quantity	% of 4990	H-index	ACI	TLS
USA	1852	37.114	157	67.54	739
Peoples R China	1133	22.705	81	31.33	301
Italy	469	9.399	68	43.84	184
Germany	355	7.114	66	52.19	201
Japan	299	5.992	60	40.51	89
South Korea	289	5.792	48	30.39	93
Canada	281	5.631	62	85.98	147
France	216	4.329	45	30.08	84
England	201	4.028	51	42.52	114
Spain	157	3.146	32	29.52	65

ACI, average citations per item.
TLS, Total link strength.

pioneers to focus on GSCs, although Canada is ranked only seventh in terms of total publications, its average number of citations is the highest (85.98).

Distribution of research institutions

The top 10 institutions in terms of publication on GSCs research were shown in Table 2. Of these, there were 7 American institutions, 2 French institutions, and 1 European institution. The League of European Research Universities holds the largest number of publications (289, 5.792%), citations (17623), and the highest value of H-index (66). The citation analysis between institutions is illustrated in Figure 5A, the size of the node indicates the centrality, that is TLS. From this figure, it can be seen that Cleveland Medical Center, Case Western Reserve University, Duke university, and University of Toronto occupied the center location of citation. While in terms of ACI, University of Toronto ranks first with 126.38 times, followed by Cleveland Medical Center (84.48) and Harvard University (80.98). Additionally, an institution co-authorship network map with 120 nodes and 1196 links was also generated (Figure 5B). Institutions with more than 20 documents were analyzed and the top 3 institutions with the largest TLS were Cleveland Medical Center (134 times), Case Western Reserve University (101) and University of Toronto (88).

Distribution of disciplines and journals

Of the 4990 included documents, 18 subject categories were identified. Table 3 lists the top 20 disciplines of GSCs based on the number of publications. It can be seen that the subject categories receiving the most interest were oncology (42.645%), cell biology (22.926%), biochemistry molecular biology (13.607%) and medicine research experimental (8.236%). Also, the literature in this field was also within the subject areas of pharmacology, genetic inheritance, materials science, and immunology.

A total of 921 journals have published related articles in this field. Table 4 shows the distribution of the top 10 productive

TABLE 2 The top 10 research institutions in regard to the research on glioma stem cells.

Institute	Quantity	% of 4990	Country	H-index	ACI	SOTC
League of European Research Universities	289	5.792	European	66	60.98	17623
University of California system	205	4.108	USA	58	67.03	13741
University of Texas system	198	3.968	USA	55	70.9	14038
Harvard University	193	3.868	USA	55	80.98	15629
Cleveland Clinic Foundation	168	3.367	USA	65	84.46	14189
Institut National de la Sante et de la Recherche Medicale	148	2.966	France	40	29.22	4325
UTMD Anderson Cancer Center	140	2.806	USA	49	59.64	8350
University of Toronto	136	2.725	USA	46	126.38	17188
Case Western reserve university	124	2.485	USA	49	66.4	8234
Centre national de la recherche scientifique cnrs	112	2.244	France	31	22.64	2536

ACI, average citations per item.
SOTC, sum of the times cited.

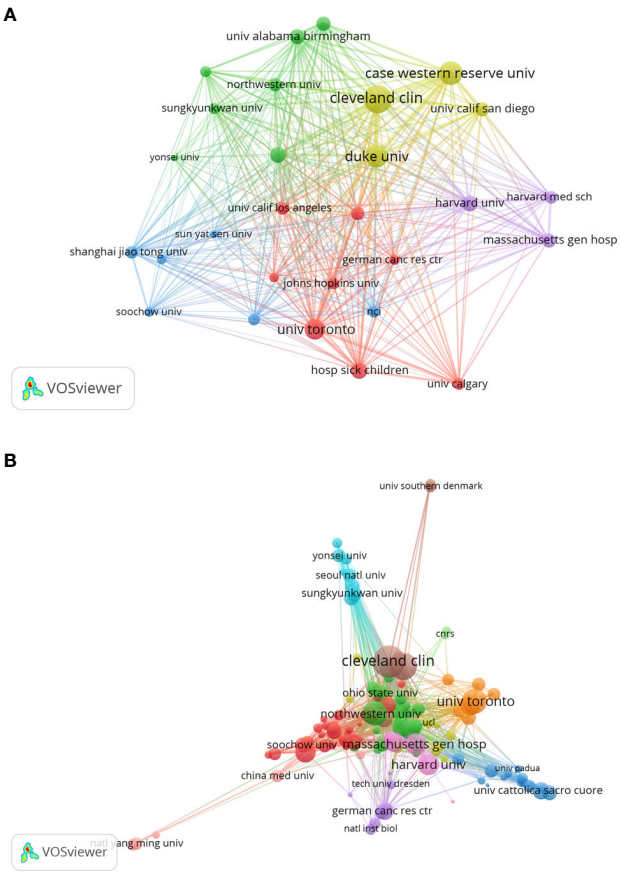

FIGURE 5
Institution citation map **(A)** and co-authorship network map **(B)** in regard to the research on glioma stem cells research. The connection between the nodes represents a co-citation relationship. Thickness of the line reflects the frequency of the cooperation. And the thicker the line, the stronger the cooperation.

journals in this area. *Oncotarget*, *Plos One* and *Cancers* are the top 3 contributors with 202, 158 and 132 papers, respectively. *Cancer Research* has the largest H-index of 61, followed by *Stem Cells* (45) and *Oncotarget* (45). As for ACI, *Cancer Research* is the top-ranked with 148.62 times, much higher than other journals. A co-citation analysis was also performed to evaluate the connection among different journals. As shown in the journal co-citation network visualization map (Figure 6A), the size of the node indicates the centrality, which is proportional to the number of citation times. There were 239 nodes and 28438 links and only journals with a minimum of 200 citations were included. The top 3 journals with the largest TLS were *Cancer Research* (17593), *Nature* (13624), and *Proc Natl Acad Sci U S A* (9388). A density visualization map of journal co-citation analysis was also provided in Figure 6B.

Distribution of authors

The top 20 productive authors published 937 papers on GSCs, accounting for 18.78% of all 4990 publications. The details of the top 20 authors published papers are shown in Table 5. RICH JN from the University of California, Santiago is the author with the most publications (109), comprised 2.18% of total, and the highest H-index (59), followed by LATHIA JD from Case Western Reserve University (71, 1.42%), and NAKANO I from the University of Alabama, Birmingham (67, 1.34%). Besides, of these top 20 scholars, the United States has the most authors with seven, followed by China (five authors), Korea (three authors), Italy (two authors), and Canada (two author). Notably, Dirks PB from University of Toronto is the author with the highest ACI (357.41 citations per publication), although he has published only 32 papers. The author co-citation network map in Figure 7A has also confirmed that SINGH SK was the author with the highest centrality (TLS=2969.37), followed by BAO SD (TLS=1995.09) and Stupp R (TLS=1782.19). As for author co-authorship analysis, a total of 37 authors with more than 20 documents were analyzed using the VOS viewer software (Figure 7B). The top 3 authors with the largest TLS were RICH JN, WU QL, and Bao SD. In addition, the authors of Jiang T, Zhang W and Singh Sk

TABLE 3 The top 20 disciplines on glioma stem cells.

Disciplines	Quantity	% of 4990
Oncology	2128	42.645
Cell Biology	1144	22.926
Biochemistry Molecular Biology	679	13.607
Medicine Research Experimental	411	8.236
Clinical Neurology	394	7.896
Neurosciences	360	7.214
Multidisciplinary Sciences	347	6.954
Pharmacology Pharmacy	319	6.393
Cell Tissue Engineering	227	4.549
Genetics Heredity	209	4.188
Biotechnology Applied Microbiology	199	3.988
Pathology	172	3.447
Chemistry Multidisciplinary	171	3.427
Hematology	115	2.305
Biophysics	106	2.124
Chemistry Medicinal	102	2.044
Surgery	102	2.044
Immunology	97	1.944
Nanoscience Nanotechnology	72	1.443
Materials Science Biomaterials	59	1.182

showed a relatively latest AAY of 2017.25, 2016.88, and 2015.83, respectively, which indicates that they are more active researchers in this field recently.

Reference analysis

Table 6 demonstrates the top 10 most frequently cited papers. Among them, 80% were based on original research, and 9 studies were published prior to 2010. All these studies were published in top-rank journals including 3 in *Nature*, 2 in *Cancer Research*, and so on. And all of them were co-cited more than 1300 times. The article by SINGH et al. published in 2004 was the most cited (5417 citations) paper, and the article is entitled "Identification of human brain tumor initiating cells". At the same time, the article by Bao et al. entitled "Glioma stem cells promote radio resistance by preferential activation of the DNA damage response" and the article by SINGH et al. entitled "Identification of a cancer stem cell in human brain tumors" also received enormous attention and each of them acquired more than 3000 citations.

Keyword analysis

The goal of keywords co-occurrence analysis is to trace scientific development and identify potential hot topics of a certain field. By applying VOS viewer, we extracted 41 keywords that appeared more than 200 times, of which 39remained after manually removing the duplicates. As shown in the Figure 8A, all the identified keywords were classified into 3 main clusters: "glioma stem cell properties" (red nodes), "cell biological properties" (green nodes) and "oncology therapy" (blue nodes). The keyword "glioblastoma" appeared most frequently, with 1690 occurrences, followed by expression (1251), caner stem cells (1014). In the cluster of "glioma stem cell characteristics", the prominent keywords were self-renewal (565), brain tumors (403), and gene expression (377). As for the cluster of "cell biology", expression (1278), glioma (903), identification (887) and growth (742) were the most frequently appearing words. In the third keyword cluster of "oncology therapy", studies on temozolomide (437), survival (397), stem cell (394) and resistance (386) are common.

As shown in the keywords overlay visualization map (Figure 8B), the keywords "progenitor cell", "CD133" and "identification" appeared earlier with the smaller AAY, which revealed that numbers of studies were focused on the identification and characterization of GSCs in the early stages of glioma stem cell research. While since 2016, research focus has shifted to "growth", "proliferation", "invasion", "apoptosis",

TABLE 4 The top 10 journals with the most attention to glioma stem cells.

Journal	Quantity	% of 4990	H-index	ACI
Oncotarget	202	4.048	45	35.45
Plos One	158	3.166	43	39.54
Cancers	132	2.645	24	14.8
Cancer ResearchA	123	2.465	61	148.62
Neuro Oncology	122	2.445	42	44.75
International Journal of Molecular Sciences	88	1.764	17	10.89
Oncogene	84	1.683	38	81.06
Stem Cells	80	1.603	45	80.36
Cancer Letters	75	1.503	34	48.4
Scientific Reports	73	1.463	22	21.53

ACI, average citations per item.

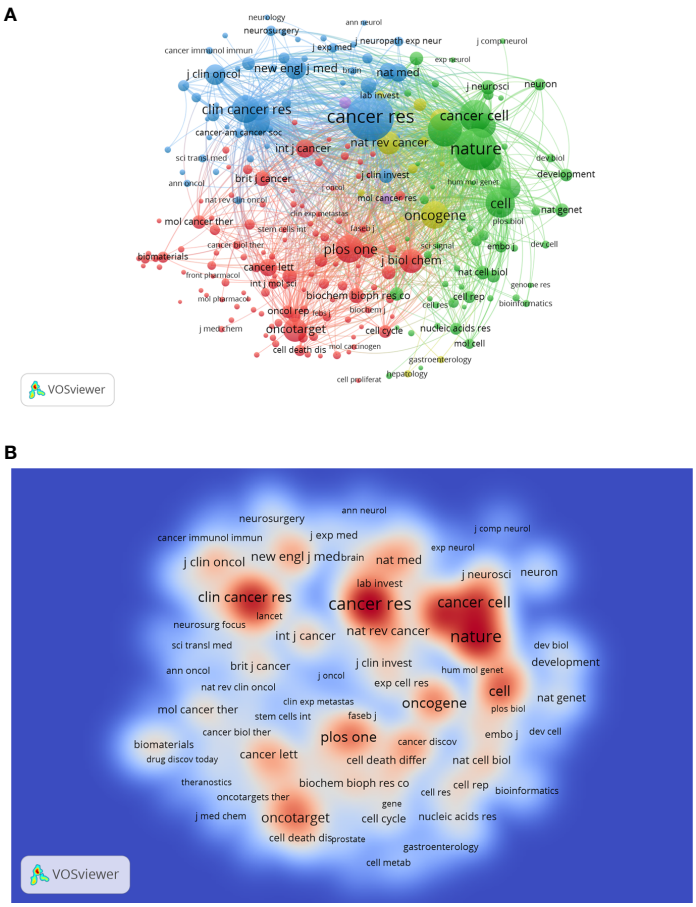

FIGURE 6
The network visualization map **(A)** and density visualization map **(B)** of journal co-citation analysis. In the visualization map, each node represents a journal and its size is proportional to the number of publications. The deeper the color of a node, the more frequently of keywords appears.

that is the biological characterization of glioma. Further, the emergence of keywords "radiotherapy" and "chemotherapy", which has the latest AAY, are seen as a shift in focus from basic cellular biology to clinical problem solving.

In order to validate this conclusion, we further analyzed the most cited papers between 2012-2016, as well as 2017-2021. As displayed in Supplement Table 1, the most cited articles between 2012-2016 was mainly about the topics of glioma stem cells, tumor microenvironment, and chemoresistance. While the analysis of the top 10 most cited articles from 2017 to 2021 showed that Temozolomide and epithelial-mesenchymal transition emerged as new issues for scholars and immunotherapy with glioma stem cells has also attracted great attention from researchers in this field (Supplement Table 2). Therefore, the above result could lead to the conclusion that cancer therapy resistance and immunotherapy with glioma stem cells will be the potential research hotspots in the near future.

Discussion

Unlike systematic reviews, bibliometrics is a type of document analysis method that integrates mathematics, statistics, philology, and other disciplines (20, 23), and can be employed to assess the scientific output in a certain field. In this study, we chose the WOS database as the main source of data (19) and then VOS viewer software (28) was used to visualize bibliometric networks of literature information related to GSCs research from 2003 to 2021.

To the search date, a total of 4990 publications with 226043 cited times were identified, and the annual volume of publications on GSCs showed an increasing trend from 2003 to 2021. Among 85 countries participated in the publication of this domain, the United States was the most prolific country accounting for more than one third of the global total publications, followed by China and Italy. As can be seen from the annual number of publications in the top five prolific

TABLE 5 The top 20 authors contributing the greatest amount to glioma stem cells.

Authors	Quantity	% of 4990	H-index	ACI	Country	Institute
Rich JN	109	2.184	59	163.37	USA	University of California San Diego
Lathia JD	71	1.423	38	91.03	USA	Case Western reserve university
Nakano I	67	1.343	33	54	USA	University of Alabama Birmingham
Wu QL	53	1.062	39	185.83	USA	Case Western reserve university
Kim SH	50	1.002	26	51.48	South Korea	Chonnam National University
Kim H	47	0.942	20	30.74	South Korea	Chonnam National University
Singh SK	46	0.922	23	237.83	Canada	McMaster University
Bao SD	41	0.822	33	200.73	USA	Cleveland Clinic Foundation
Zhang W	41	0.822	20	38.2	Peoples R China	Beijing Neurosurgical Institute
Zhang Y	41	0.822	21	41.17	Peoples R China	Shanxi Medical University
Liu Y	40	0.802	17	31.65	Peoples R China	Anhui University of Science and Technology
Hjelmeland AB	39	0.782	28	254.31	USA	University of Alabama Birmingham
Bian XW	38	0.762	28	54.24	Peoples R China	Third Military Medical University
Pallini R	38	0.762	18	64.34	Italy	Catholic University of the Sacred Heart
Ricci-vitiani L	38	0.762	19	67.76	Italy	Istituto Superiore di Sanita
Taylor MD	38	0.762	21	62.53	Canada	University of Toronto
Nam DH	37	0.741	25	59.76	South Korea	Sungkyunkwan University
Wakimoto H	37	0.741	24	58.7	USA	Harvard University
Wang Y	34	0.681	18	42.06	Peoples R China	Third Military Medical University
Dirks PB	32	0.641	24	357.41	Canada	University of Toronto

countries, the United States consistently maintains its leading position in this field during the period 2003-2021. Similarly, there has been an upward trend on the whole in annual number of publications in China and the gap with the United States gradually narrowed. This finding indicates that the studies of GSCs have attracted the interest of many Chinese scholars. It's quite predictable that the investment to GSCs research will be further strengthened globally, especially in the United States and China.

H-index is often used to measure both the productivity and academic impact of a scholar, institution or country. Specifically, if a scientist has n articles cited more than n times, then his/her H-index is n (27, 28). Moreover, ACI and SOTC are the additional indicators that widely used to describe academic contributions (20, 25). Our results suggest that the United States had the highest H-index (157) and the second largest AIC (67.54), which indicates that the United States not only published a large number of publications, but the quality of the publications was also highly valuable and informative in academic terms. Besides, the United States accounted for 70% of the top 10 productive institutions on GSCs research. University of California System in the United States had the large number of publications (205) and the high SOTC (13741). This may be an important reason why the United States has an irreplaceable position in the field of GSCs research.

Also, although the overall number of publications and H-index from China in this field ranked the second to the United States, the AIC was only 31.33 times. Therefore, except for increasing production, China also needs to enhance the innovativeness and depth of related research. Importantly, Zhang Y in Shanxi Medical and Zhang W in University Beijing Neurosurgical Institute both have the largest quantity of publications (41), indicating they pay plenty of attention in this field. Wang Y of Third Military Medical University obtains a large number of high-quality research results with the greatest AIC of 42.06. They are more likely to be funded and change the current largely homogeneous state of affairs.

In addition, as one of the early pioneers to focus on GSCs, although Canada ranked seventh in terms of publication quantity, its ACI is the highest (85.98). The University of Toronto was the first institution to study GSCs with an ACI of 126.38, much higher than other institutions. Already in 2003, *Cancer Research* published an article by Canadian scholar Singh et al, entitled "Identification of a cancer stem cell in human brain tumors" (29). CD133, a widely known transmembrane protein expressed on the surface of hematopoietic stem cells, is the first-reported CSC marker of leukemia (30, 31). Nevertheless, this study proposed that CD133 could mark GSCs and be used for identifying and sorting GSCs, making a tremendous advance to GSCs research. Then, in 2004, Singh et al, further demonstrated in "Identification of human brain tumor initiating cells" published in *Nature* that CD133+ GSCs spheres could initiate gliomagenesis and have the potential to differentiate into normal tumor cells (32).

Co-citation analysis is a method for measuring the degree of relationship between documents. It refers to when two documents are cited by a third document at the same time, and the two

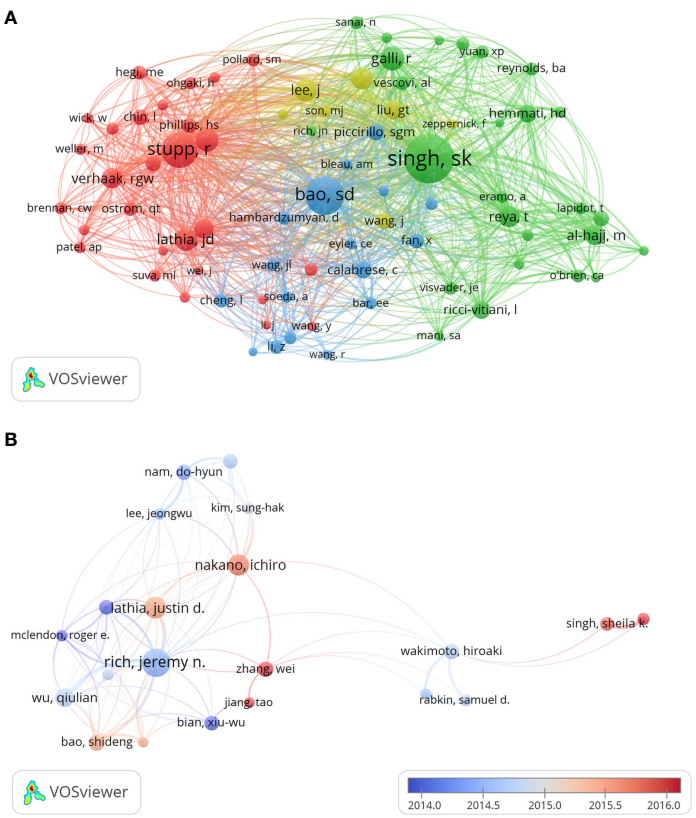

FIGURE 7
The author co-citation network map **(A)** and co-authorship overlay map **(B)** generated by VOS viewer. Each node represents an author, and node size indicates the number of publications. The purple nodes represent the author appear earlier, whereas the red nodes reflect the recent occurrence.

TABLE 6 The 10 most cited papers of research on glioma stem cells from 2003 to 2021.

Title	Journal	First author	Year	Number of institutions	Citation	Document type
Identification of human brain tumour initiating cells	*Nature*	Singh SK	2004	1	5417	Article
Glioma stem cells promote radioresistance by preferential activation of the DNA damage response	*Nature*	Bao SD	2006	1	4324	Article
Identification of a cancer stem cell in human brain tumors	*Cancer Res*	Singh SK	2003	1	3729	Article
Malignant gliomas in adults	*N Engl J Med*	Wen PY	2008	2	2960	Review
Identification of pancreatic cancer stem cells	*Cancer Res*	Li CW	2007	3	2433	Article
Malignant astrocytic glioma: genetics, biology, and paths to treatment	*Genes Dev*	Furnari FB	2007	1	1715	Review
Identification of a subpopulation of cells with cancer stem cell properties in head and neck squamous cell carcinoma	*Proc Natl Acad Sci U S A*	Prince ME	2007	3	1616	Article
A perivascular niche for brain tumor stem cells	*Cancer Cell*	Calabrese C	2007	1	1550	Article
A restricted cell population propagates glioblastoma growth after chemotherapy	*Nature*	Chen J	2012	1	1377	Article
Analysis of gene expression and chemoresistance of CDI33(+) cancer stem cells in glioblastoma	*Mol Cancer*	Liu GT	2006	1	1317	Article

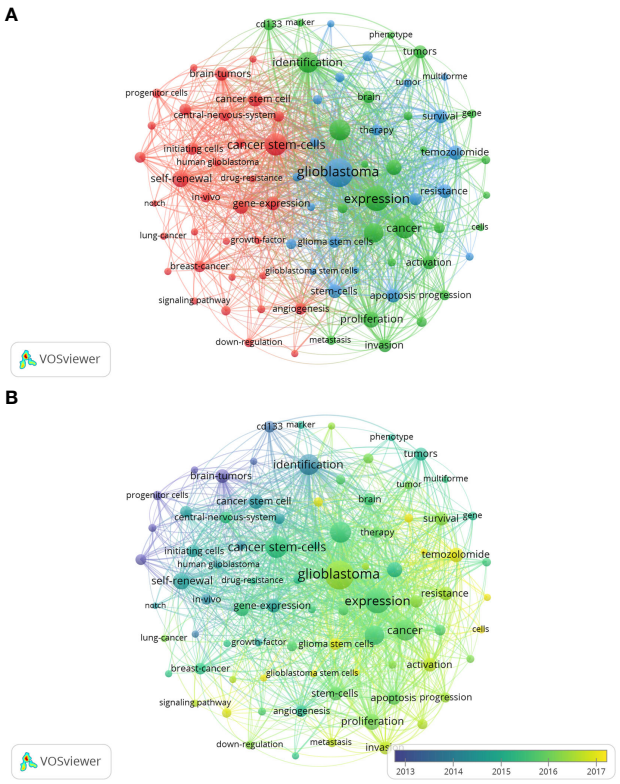

FIGURE 8
The network visualization map **(A)** and overlay visualization map **(B)** of keywords co-occurrence analysis on glioma stem cells research. Keywords with similar categories are gathered in a cluster. There are three clusters, including glioma stem cell properties" (red nodes), "cell biological properties" (green nodes) and "oncology therapy" (blue nodes).

documents can be considered to form a co-citation relationship. The higher the frequency of citations, the closer the academic relationship between the two documents. TLS is an important quantitative indicator to the strength of links between them and is positively correlated with the number of citations. The results of the journal co-citation analysis showed that the top three journals with the largest TLS were *Cancer Research*, *Nature*, and *Proc Natl Acad Sci U S A*. Beyond this, the top three H-index journals were *Cancer Research*, *Stem Cells* and *Oncotarget*. This indicates that some literature published in the above-mentioned journals may have significant academic impact and marvelous reference value for research in the field. Additionally, these results could also provide directions for scholars to submit related manuscripts. Moreover, authors were classified into four categories based on author co-citation analysis. The top three authors with the largest TLS were Singh Sk, BAO SD, and Stupp R. The authors of Jiang T, Zhang W and Singh Sk showed a relatively latest AAY of 2017.25, 2016.88, and 2015.83, respectively, which indicates that they are more active researchers in this field recently. However, none of these scholars have enormous cited times, which may be caused by the short time of publication.

The 10 top most frequently cited articles were distributed between 2003 and 2012. Of these 10 articles, there were 4 articles about identification of GSCs from 2003 to 2007, and 3 articles on the radiotherapy resistance of GSCs, suggesting GSCs may be considered as potential therapeutic targets in glioma. The most cited article titled "Identification of human brain tumor initiating cells" was published in *Nature* in 2004, which proposed that CD133 was a surface marker of GSCs and thus could be used for the identification and sorting of GSCs (32). Furthermore, it was demonstrated that GSCs have differentiation potential. Then, Prince ME proposed that CD44 was a surface marker in the study titled "Identification of a subpopulation of cells with cancer stem cell properties in head and neck squamous cell carcinoma" in 2007 (33). However, studies show that unlike normal stem cells, GSCs may respond to differentiation but fail to fully lose their stemness. Helena C found that GSCs-derived cells didn't undergo terminal cell cycle arrest and remain vulnerable to de-differentiation. When differentiation stimulation being withdrawn, they may return to GSC-like cells with proliferative potential (34–36).

GSCs received a lot of attention from 2010 to 2015 as a therapeutic target for glioma because of their association with oncologic therapy resistance (37, 38) and angiogenesis (39, 40). In the last five years, the research focus was mainly on the regulation of the immune microenvironment of GSCs (41, 42), including macrophages, neutrophils, and lymphocytes. A novel approach for glioma therapy is to promote apoptosis of GSCs (5), reduce immunosuppression and suppress metastasis by regulating immune cells (43, 44).

The purpose of keyword co-occurrence analysis was to track scientific developments and to identify prospective hot topics in a domain. All the identified keywords were classified into three main clusters: "glioma stem cell properties", "cell biological properties" and "oncology therapy". In the keywords overlay visualization map, keywords related to stem cells property such as "identification", "CD133" and "marker", occurred extremely frequently and appeared quite early, indicating early studies were mainly devoted to the identification of GSCs (29, 32, 33). Then, the keywords "apoptosis", "proliferation" and "invasion" appeared which were about cell biological properties (45, 46). After GSCs were marked and sorted, researchers began to use tools to regulate GSCs' growth, such as LncRNA or miRNA to alter cellular gene expression (12–14). These basic researches have provided new insights into the glioma treatment. In 2015, the terms of clinical relevance "angiogenesis" and "resistant" emerged frequently. The research task of many research teams during this period is mainly to find mechanisms of clinical symptoms on the cellular and genetic level (47). It is not hard to see that research hotspot is beginning to move from basic cellular studies to the solution of clinical problems.

Recently, keywords that appeared at a high frequency including "temozolomide" and "epithelial-mesenchymal transition" suggests that chemotherapy resistance in gliomas is currently the hot topic of GSCs research. TMZ is the first-line chemotherapy drug for glioma. A multitude of clinical studies showed that there was a significant decrease in the treatment effect in a subset of patients when TMZ treatment was repeated (13, 48). Currently, GSCs are considered as the main cause of the TMZ tolerance to glioma. TMZ prevents DNA replication by guanine methylation of DNA, causing cells to arrest in M phase. Target cells of TMZ are tumor cells with robust growth and metabolism instead of silent GSCs in quiet G0 phase (10). Therefore, most normal gliomas cells are killed and chemotherapy-insensitive GSCs are preserved following the first exposure to TMZ treatment. However, when TMZ treatment is repeated, the tumor cell killer effect of oncology therapy is strongly reduced. MGMT is mainly involved in DNA methylation repair and highly expressed in GSCs (9, 11). It is reported that there was a strong positive correlation between MGMT activity and TMZ tolerance of tumors in gliomas. It is a decent therapeutic approach to reduce TMZ resistance and improve the effect of TMZ by inhibiting MGMT activity and decreasing its expression. In addition, GSCs highly expresses the anti-apoptotic gene Bcl-2 (49) and ATP-binding cassette transporter (50) to pump drugs out of the cell and protect the tumor cell from oncology therapy. GSCs release extracellular vesicles, which is involved in therapeutic resistance. At the present time, studies are mainly aimed at promoting GSCs apoptosis and inhibiting GSCs proliferation. For example, LncRNA or miRNA promote GSCs apoptosis and autophagy (12, 13, 47). Generally, treatment combinations have a stronger effort against TMZ tolerance. Combinated treatment of photodynamic therapy or sonodynamic therapy with TMZ could kill tumor stem cells (38, 51). Recently, tumor treating fields (TTFields) is a novel tumor treatment. Paul C et al. demonstrated that TTFields with TMZ inhibited GSCs proliferation and tumor sphere formation (52). Theoretically, it is a potential treatment to promote GSC differentiating and escaping from quiescence for enhancing therapeutic sensitivity (53–55). Whereas, there are few reported clinical application about GSCs.

Epithelial-to-mesenchymal transition (EMT) is a cellular mechanism which is known to promote normal embryonic development (56, 57). EMT is a transcriptional process in which epithelial cells take on mesenchymal properties through loss of cell-to-cell adhesion, acquisition of migration and invasiveness, and loss of cell polarity (58). In general, EMT contributes to tumorigenesis, invasion, distant metastasis, and resistance to chemotherapy and/or radiotherapy in tumors. Significantly, in cancer, EMT is a dynamic process of mutual transformation of epithelial cells to mesenchymal cells. To some extent, tumor cells acquire stem cell-like properties, increased motility and invasive capacity through EMT (59). It also promotes glioma immune evasion and immunosuppression and enhances resistance to current oncology therapy. There are important pathways involved in epithelial mesenchymal transition that also maintain the stemness of GSCs such as Wnt/β-catenin pathway, SHH pathway and NOCTH pathway (60). The Wnt/β-catenin pathway combined with TGF-β signaling induces EMT through high expression of HIF-α (40). Critically, Frizzled-related protein (sFRP4), as a Wnt pathway antagonist, reverses EMT and reduces drug resistance. It is known that activation of receptor tyrosine kinases (RTK), such as epidermal growth factor and FGF, can induce EMT by activating the classical PI3K/AKT and RAS/MAPK pathways (61). Clinical trials have been conducted with STAT3 inhibitors for the treatment of cholangiocarcinoma, breast and ovarian cancers.

The neoplasm is surrounded by a multitude of non-tumor cells that constitute a complex tumor immune

microenvironment, including dendritic cells, microglia, lymphocytes, tumor-associated macrophages, and endothelial cells (42, 62). GSCs recruit monocytes by secreting CSF-1 and CCL2 (63), upregulate STAT3 expression, and promote the conversion of monocytes to M2 tumor-associated macrophages, which contribute to angiogenesis and tumor metastasis (42). In addition, M2 tumor-associated macrophages can contribute to GSCs immunosuppression through the secretion of immunosuppressive factors such as IL-10 and TGF-b1 (64). Therefore, M2 tumor-associated macrophage is a potential immunotherapeutic target for glioma stem cells (65). Besides, attracted oligodendrocytes and macrophages/microglia provide advantages for GBM in the development of the GSC niche in proliferation, migration, and stemness (66). In addition, tumor-associated macrophages expressed CD204 specifically engulf GSC-derived necrotic particles, and then upregulated the expression of IL-12 which enhance the sphere-forming activity of GBM patient-derived cells (67). Therefore, tumor-associated macrophages hold great promise to eliminate glioma. Glioma cells invade along some vital anatomical structures, including the white matters. Jun W et al. demonstrated that CD133+ GSCs are more likely to locate on the jagged1+ (a Notch ligand) nerve fibers. Importantly, a Notch1-Sox9-Sox2 positive feedback loop enhance the ability of GSCs to survive in WM tracts by enhancing stemness, thereby promoting invasive growth (68). When tumor invasion into the white matters induces an injury-like microenvironment, the white matter suppresses malignancy by directing GSC differentiation towards pre-oligodendrocyte fate. But once removed from white matter, GSC-derived oligodendrocytes reverse a GSC state. Continuous exposure to white matter is a condition of GSCs differentiation (69). Brain tumor metastasis is usually accompanied with destruction of blood vessels and blood brain barrier. Endothelial cells prompt GSCs self-renewal through activating Notch and Hedgehog pathway (70, 71). Hypoxic environment prompt GSCs stemness maintenance. In peri-hypoxic niches, hypoxia-induced factors are important in the regulation of stemness (72). Hypoxic environment modification probably is perpetual topic on tumor treatment.

Strengths and limitations

There are many systematic reviews but no bibliometric studies on GSCs. Our study is the first bibliometric study on GSCs. Bibliometric analysis combined with visualized maps can provide systematic information about GSC-related studies. There are several important advantages of our study. First, the visualized map can help readers to learn about the evolution of GSCs research and current research hotspots relatively easily. Second, keyword analysis makes it easy for researchers to capture potential research targets. Finally, co-author analysis and co-citation analysis in terms of country, institution and author could provide references for scientists and funding agencies.

However, this study still has several limitations. Because the language of the included studies was limited to English, it may have overlooked several important studies published in other languages. There are inconsistencies between the results of the bibliometric analysis and the status of the actual studies. This is due to the fact that the database on which this study is based stays open and updated. In addition, the growing trend in the number of published papers may last longer than predicted.

Conclusions

This study summarizes the current state and global trends in GSCs research. There is an increasing trend in the number of publications and the United States is in a leading position of this domain. The Cleveland Medical Center holds the largest number of publications, citations, and the highest value of H-index. RICH JN and SINGH SK were the key authors. According to keyword co-occurrence analysis, all the identified keywords were classified into three main clusters: “glioma stem cell properties”, ”cell biological properties” and “oncology therapy”. In particular, the research focus is gradually shifting from “glioma stem cell properties” to “oncology therapy”. Based on the analysis of top cited articles, research on “immunothreapy”, “epithelial-mesenchymal transition”, and “temozolomide resistance” will be the next potential research hotspots and may create new therapeutic strategies for GSCs.

Data availability statement

The raw data supporting the conclusions of this article will be made available by the authors, without undue reservation.

Author contributions

In review, HY and XGT designed the study. SRS and HYW collected the data. SRS, HYW, FCW, JJJ, LXX, HGW, XGT and HY analyzed the data and drafted the manuscript. HY, HGW and XGT revised and approved the final version of the manuscript. All authors contributed to the article andapproved the submitted version.

Funding

This research was supported by the grants awarded by Natural Science Foundation of Tianjin Municipal Science and Technology Commission (20JCQNJC00410).

Acknowledgments

The authors thank Dr. Jiao Dian and Dr. Duan Chenyang for their help in language polishing.

Conflict of interest

The authors declare that the research was conducted in the absence of any commercial or financial relationships that could be construed as a potential conflict of interest.

Publisher's note

All claims expressed in this article are solely those of the authors and do not necessarily represent those of their affiliated organizations, or those of the publisher, the editors and the reviewers. Any product that may be evaluated in this article, or claim that may be made by its manufacturer, is not guaranteed or endorsed by the publisher.

Supplementary material

The Supplementary Material for this article can be found online at: https://www.frontiersin.org/articles/10.3389/fonc.2022.926025/full#supplementary-material

References

1. Tan AC, Ashley DM, Lopez GY, Malinzak M, Friedman HS, Khasraw M. Management of glioblastoma: State of the art and future directions. *CA Cancer J Clin* (2020) 70:299–312. doi: 10.3322/caac.21613

2. Weller ,M, Wick W, Aldape K, Brada M, Berger M, Pfister SM, et al. Glioma. *Nat Rev Dis Primers* (2015) 1;15017. doi: 10.1038/nrdp.2015.17

3. Gimple RC, Bhargava S, Dixit D, Rich JN. Glioblastoma stem cells: lessons from the tumor hierarchy in a lethal cancer. *Genes Dev* (2019) 33:591–609. doi: 10.1101/gad.324301.119

4. Suva ML, Tirosh I. The glioma stem cell model in the era of single-cell genomics. *Cancer Cell* (2020) 37:630–6. doi: 10.1016/j.ccell.2020.04.001

5. Hombach-Klonisch S, Mehrpour M, Shojaei S, Harlos C, Pitz M, Hamai A, et al. Glioblastoma and chemoresistance to alkylating agents: Involvement of apoptosis, autophagy, and unfolded protein response. *Pharmacol Ther* (2018) 184:13–41. doi: 10.1016/j.pharmthera.2017.10.017

6. Osuka S, Van Meir EG. Overcoming therapeutic resistance in glioblastoma: the way forward. *J Clin Invest* (2017) 127:415–26. doi: 10.1172/JCI89587

7. Bleau AM, Hambardzumyan D, Ozawa T, Fomchenko EI, Huse JT, Brennan CW, et al. PTEN/PI3K/Akt pathway regulates the side population phenotype and ABCG2 activity in glioma tumor stem-like cells. *Cell Stem Cell* (2009) 4:226–35. doi: 10.1016/j.stem.2009.01.007

8. Lee CAA, Banerjee P, Wilson BJ, Wu S, Guo Q, Berg G, et al. Targeting the ABC transporter ABCB5 sensitizes glioblastoma to temozolomide-induced apoptosis through a cell-cycle checkpoint regulation mechanism. *J Biol Chem* (2020) 295:7774–88. doi: 10.1074/jbc.RA120.013778

9. Auffinger B, Tobias AL, Han Y, Lee G, Guo D, Dey M, et al. Conversion of differentiated cancer cells into cancer stem-like cells in a glioblastoma model after primary chemotherapy. *Cell Death Differ* (2014) 21:1119–31. doi: 10.1038/cdd.2014.31

10. D'Alessandris QG, Biffoni M, Martini M, Runci D, Buccarelli M, Cenci T, et al. The clinical value of patient-derived glioblastoma tumorspheres in predicting treatment response. *Neuro Oncol* (2017) 19:1097–108. doi: 10.1093/neuonc/now304

11. Tso JL, Yang S, Menjivar JC, Yamada K, Zhang Y, Hong I, et al. Bone morphogenetic protein 7 sensitizes O6-methylguanine methyltransferase expressing-glioblastoma stem cells to clinically relevant dose of temozolomide. *Mol Cancer* (2015) 14:189. doi: 10.1186/s12943-015-0459-1

12. Huang W, Zhong Z, Luo C, Xiao Y, Li L, Zhang X, et al. The miR-26a/AP-2alpha/Nanog signaling axis mediates stem cell self-renewal and temozolomide resistance in glioma. *Theranostics* (2019) 9:5497–516. doi: 10.7150/thno.33800

13. Wu P, Cai J, Chen Q, Han B, Meng X, Li Y, et al. Lnc-TALC promotes O(6)-methylguanine-DNA methyltransferase expression *via* regulating the c-met pathway by competitively binding with miR-20b-3p. *Nat Commun* (2019) 10:2045. doi: 10.1038/s41467-019-10025-2

14. Rouge JL, Sita TL, Hao L, Kouri FM, Briley WE, Stegh AH, et al. Ribozyme-spherical nucleic acids. *J Am Chem Soc* (2015) 137:10528–31. doi: 10.1021/jacs.5b07104

15. Lathia JD, Mack SC, Mulkearns-Hubert EE, Valentim CL, Rich JN. Cancer stem cells in glioblastoma. *Genes Dev* (2015) 29:1203–17. doi: 10.1101/gad.261982.115

16. Balca-Silva J, Matias D, Carmo AD, Sarmento-Ribeiro AB, Lopes MC, Moura-Neto V. Cellular and molecular mechanisms of glioblastoma malignancy: Implications in resistance and therapeutic strategies. *Semin Cancer Biol* (2019) 58:130–41. doi: 10.1016/j.semcancer.2018.09.007

17. Chiblak S, Tang Z, Campos B, Gal Z, Unterberg A, Debus J, et al. Radiosensitivity of patient-derived glioma stem cell 3-dimensional cultures to photon, proton, and carbon irradiation. *Int J Radiat Oncol Biol Phys* (2016) 95:112–9. doi: 10.1016/j.ijrobp.2015.06.015

18. Wang K, Kievit FM, Erickson AE, Silber JR, Ellenbogen RG, Zhang M. Culture on 3D chitosan-hyaluronic acid scaffolds enhances stem cell marker expression and drug resistance in human glioblastoma cancer stem cells. *Adv Healthc Mater* (2016) 5:3173–81. doi: 10.1002/adhm.201600684

19. Ale Ebrahim S, Ashtari A, Zamani Pedram M, Ale Ebrahim N, Sanati-Nezhad A. Publication trends in exosomes nanoparticles for cancer detection. *Int J Nanomed* (2020) 15:4453–70. doi: 10.2147/IJN.S247210

20. Yao RQ, Ren C, Wang JN, Wu GS, Zhu XM, Xia ZF, et al. Publication trends of research on sepsis and host immune response during 1999-2019: A 20-year bibliometric analysis. *Int J Biol Sci* (2020) 16:27–37. doi: 10.7150/ijbs.37496

21. Wang MH, Ho YS, Fu HZ. Global performance and development on sustainable city based on natural science and social science research: A bibliometric analysis. *Sci Total Environ* (2019) 666:1245–54. doi: 10.1016/j.scitotenv.2019.02.139

22. Zhang L, Geng Y, Zhong Y, Dong H, Liu Z. A bibliometric analysis on waste electrical and electronic equipment research. *Environ Sci pollut Res Int* (2019) 26:21098–108. doi: 10.1007/s11356-019-05409-2

23. Jiang M, Huo Y, Huang K, Li M. Way forward for straw burning pollution research: a bibliometric analysis during 1972-2016. *Environ Sci pollut Res Int* (2019) 26:13948–62. doi: 10.1007/s11356-019-04768-0

24. Bezak N, Mikos M, Borrelli P, Alewell C, Alvarez P, Anache JAA, et al. Soil erosion modelling: A bibliometric analysis. *Environ Res* (2021) 197:111087. doi: 10.1016/j.envres.2021.111087

25. Chen C, Lou Y, Li XY, Lv ZT, Zhang LQ, Mao W. Mapping current research and identifying hotspots on mesenchymal stem cells in cardiovascular disease. stem. *Cell Res Ther* (2020) 11:498. doi: 10.1186/s13287-020-02009-7

26. Wu H, Li Y, Tong L, Wang Y, Sun Z. Worldwide research tendency and hotspots on hip fracture: A 20-year bibliometric analysis. *Arch Osteoporos* (2021) 16:73. doi: 10.1007/s11657-021-00929-2

27. Wu H, Tong L, Wang Y, Yan H, Sun Z. Bibliometric analysis of global research trends on ultrasound microbubble: A quickly developing field. *Front Pharmacol* (2021) 12:646626. doi: 10.3389/fphar.2021.646626

28. Wang YX, Zhao N, Zhang XW, Li ZH, Liang Z, Yang JR, et al. Bibliometrics analysis of butyrophilins as immune regulators [1992-2019] and implications for cancer prognosis. *Front Immunol* (2020) 11. doi: 10.3389/fimmu.2020.01187

29. Singh SK, Clarke ID, Terasaki M, Bonn VE, Hawkins C, Squire J, et al. Identification of a cancer stem cell in human brain tumors. *Cancer Res* (2003) 63:5821–8.

30. Godfrey L, Crump NT, O'Byrne S, Lau IJ, Rice S, Harman JR, et al. H3K79me2/3 controls enhancer-promoter interactions and activation of the pan-cancer stem cell marker PROM1/CD133 in MLL-AF4 leukemia cells. *Leukemia* (2021) 35:90–106. doi: 10.1038/s41375-020-0808-y

31. Trendowski M, Wong V, Zoino JN, Christen TD, Gadeberg L, Sansky M, et al. Preferential enlargement of leukemia cells using cytoskeletal-directed agents and cell cycle growth control parameters to induce sensitivity to low frequency ultrasound. *Cancer Lett* (2015) 360:160–70. doi: 10.1016/j.canlet.2015.02.001

32. Singh SK, Hawkins C, Clarke ID, Squire JA, Bayani J, Hide T, et al. Identification of human brain tumour initiating cells. *Nature* (2004) 432:396–401. doi: 10.1038/nature03128

33. Prince ,ME, Sivanandan R, Kaczorowski A, Wolf GT, Kaplan MJ, Dalerba P, et al. Identification of a subpopulation of cells with cancer stem cell properties in head and neck squamous cell carcinoma. *Proc Natl Acad Sci U.S.A.* (2007) 104:973–8. doi: 10.1073/pnas.0610117104

34. Balasubramaniyan V, Vaillant B, Wang S, Gumin J, Butalid ME, Sai K, et al. Aberrant mesenchymal differentiation of glioma stem-like cells: implications for therapeutic targeting. *Oncotarget* (2015) 6:31007–17. doi: 10.18632/oncotarget.5219

35. Caren H, Stricker SH, Bulstrode H, Gagrica S, Johnstone E, Bartlett TE, et al. Glioblastoma stem cells respond to differentiation cues but fail to undergo commitment and terminal cell-cycle arrest. *Stem Cell Rep* (2015) 5:829–42. doi: 10.1016/j.stemcr.2015.09.014

36. Chen Z, Zhong Y, Chen J, Sun S, Liu W, Han Y, et al. Disruption of beta-catenin-mediated negative feedback reinforces cAMP-induced neuronal differentiation in glioma stem cells. *Cell Death Dis* (2022) 13:493. doi: 10.1038/s41419-022-04957-9

37. Moreno M, Pedrosa L, Pare L, Pineda E, Bejarano L, Martinez J, et al. GPR56/ADGRG1 inhibits mesenchymal differentiation and radioresistance in glioblastoma. *Cell Rep* (2017) 21:2183–97. doi: 10.1016/j.celrep.2017.10.083

38. Sharifzad F, Ghavami S, Verdi J, Mardpour S, Mollapour Sisakht M, Azizi Z, et al. Glioblastoma cancer stem cell biology: Potential theranostic targets. *Drug Resist Update* (2019) 42:35–45. doi: 10.1016/j.drup.2018.03.003

39. Griveau A, Seano G, Shelton SJ, Kupp R, Jahangiri A, Obernier K, et al. A glial signature and Wnt7 signaling regulate glioma-vascular interactions and tumor microenvironment. *Cancer Cell* (2018) 33:874–889 e877. doi: 10.1016/j.ccell.2018.03.020

40. Li Z, Bao S, Wu Q, Wang H, Eyler C, Sathornsumetee S, et al. Hypoxia-inducible factors regulate tumorigenic capacity of glioma stem cells. *Cancer Cell* (2009) 15:501–13. doi: 10.1016/j.ccr.2009.03.018

41. Jackson CM, Choi J, Lim M. Mechanisms of immunotherapy resistance: Lessons from glioblastoma. *Nat Immunol* (2019) 20:1100–9. doi: 10.1038/s41590-019-0433-y

42. Lim M, Xia Y, Bettegowda C, Weller M. Current state of immunotherapy for glioblastoma. *Nat Rev Clin Oncol* (2018) 15:422–42. doi: 10.1038/s41571-018-0003-5

43. Wang X, Guo G, Guan H, Yu Y, Lu J, Yu J. Challenges and potential of PD-1/PD-L1 checkpoint blockade immunotherapy for glioblastoma. *J Exp Clin Cancer Res* (2019) 38(1):87. doi: 10.1186/s13046-019-1085-3

44. Xue S, Hu M, Iyer V, Yu J. Blocking the PD-1/PD-L1 pathway in glioma: A potential new treatment strategy. *J Hematol Oncol* (2017) 10:81. doi: 10.1186/s13045-017-0455-6

45. Fan X. Gamma-secretase inhibitor-resistant glioblastoma stem cells require RBPJ to propagate. *J Clin Invest* (2016) 126:2415–8. doi: 10.1172/JCI88619

46. Michelakis ED, Sutendra G, Dromparis P, Webster L, Haromy A, Niven E, et al. Metabolic modulation of glioblastoma with dichloroacetate. *Sci Transl Med* (2010) 2:31ra34. doi: 10.1126/scitranslmed.3000677

47. Peng ZX, Liu CH, Wu MH. New insights into long noncoding RNAs and their roles in glioma. *Mol Cancer* (2018) 17(1):61. doi: 10.1186/s12943-018-0812-2

48. Meng X, Zhao Y, Han B, Zha C, Zhang Y, Li Z, et al. Dual functionalized brain-targeting nanoinhibitors restrain temozolomide-resistant glioma *via* attenuating EGFR and MET signaling pathways. *Nat Commun* (2020) 11:594. doi: 10.1038/s41467-019-14036-x

49. Qiu B, Wang Y, Tao J, Wang Y. Expression and correlation of bcl-2 with pathological grades in human glioma stem cells. *Oncol Rep* (2012) 28:155–60. doi: 10.3892/or.2012.1800

50. Uribe D, Torres A, Rocha JD, Niechi I, Oyarzun C, Sobrevia L, et al. Multidrug resistance in glioblastoma stem-like cells: Role of the hypoxic microenvironment and adenosine signaling. *Mol Aspects Med* (2017) 55:140–51. doi: 10.1016/j.mam.2017.01.009

51. Schimanski A, Ebbert L, Sabel MC, Finocchiaro G, Lamszus K, Ewelt C, et al. Human glioblastoma stem-like cells accumulate protoporphyrin IX when subjected to exogenous 5-aminolaevulinic acid, rendering them sensitive to photodynamic treatment. *J Photoch Photobio B* (2016) 163:203–10. doi: 10.1016/j.jphotobiol.2016.08.043

52. Clark PA, Gaal JT, Strebe JK, Pasch CA, Deming DA, Kuo JS, et al. The effects of tumor treating fields and temozolomide in MGMT expressing and non-expressing patient-derived glioblastoma cells. *J Clin Neurosci* (2017) 36:120–4. doi: 10.1016/j.jocn.2016.10.042

53. Fang X, Huang Z, Zhai K, Huang Q, Tao W, Kim L, et al. Inhibiting DNA-PK induces glioma stem cell differentiation and sensitizes glioblastoma to radiation in mice. *Sci Transl Med* (2021) 13(600). doi: 10.1126/scitranslmed.abc7275

54. Song S, Ma D, Xu L, Wang Q, Liu L, Tong X, et al. Low-intensity pulsed ultrasound-generated singlet oxygen induces telomere damage leading to glioma stem cell awakening from quiescence. *iScience* (2022) 25:10.1016/j.isci.2021.103558:103558. doi: 10.1016/j.isci.2021.103558

55. Zhu TZ, Li XM, Luo LH, Song ZQ, Gao X, Li ZQ, et al. Beta-elemene inhibits stemness, promotes differentiation and impairs chemoresistance to temozolomide in glioblastoma stem-like cells. *Int J Oncol* (2014) 45:699–709. doi: 10.3892/ijo.2014.2448

56. Cheng F, Guo D. MET in glioma: signaling pathways and targeted therapies. *J Exp Clin Cancer Res* (2019) 38:270. doi: 10.1186/s13046-019-1269-x

57. Meel MH, Schaper SA, Kaspers GJL, Hulleman E. Signaling pathways and mesenchymal transition in pediatric high-grade glioma. *Cell Mol Life Sci* (2018) 75:871–87. doi: 10.1007/s00018-017-2714-7

58. Lah TT, Novak M, Breznik B. Brain malignancies: Glioblastoma and brain metastases. *Semin Cancer Biol* (2020) 60:262–73. doi: 10.1016/j.semcancer.2019.10.010

59. Weidenfeld K, Barkan ,D. EMT and stemness in tumor dormancy and outgrowth: Are they intertwined processes? *Front Oncol* (2018) 8. doi: 10.3389/fonc.2018.00381

60. Kievit FM, Florczyk SJ, Leung MC, Wang K, Wu JD, Silber JR, et al. Proliferation and enrichment of CD133(+) glioblastoma cancer stem cells on 3D chitosan-alginate scaffolds. *Biomaterials* (2014) 35:9137–43. doi: 10.1016/j.biomaterials.2014.07.037

61. Kaushik NK, Kaushik N, Yoo KC, Uddin N, Kim JS, Lee SJ, et al. Low doses of PEG-coated gold nanoparticles sensitize solid tumors to cold plasma by blocking the PI3K/AKT-driven signaling axis to suppress cellular transformation by inhibiting growth and EMT. *Biomaterials* (2016) 87:118–30. doi: 10.1016/j.biomaterials.2016.02.014

62. Quail DF, Joyce JA. The microenvironmental landscape of brain tumors. *Cancer Cell* (2017) 31:326–41. doi: 10.1016/j.ccell.2017.02.009

63. Chang AL, Miska J, Wainwright DA, Dey M, Rivetta CV, Yu D, et al. CCL2 produced by the glioma microenvironment is essential for the recruitment of regulatory T cells and myeloid-derived suppressor cells. *Cancer Res* (2016) 76:5671–82. doi: 10.1158/0008-5472.CAN-16-0144

64. Dziurzynski K, Wei J, Qiao W, Hatiboglu MA, Kong LY, Wu A, et al. Glioma-associated cytomegalovirus mediates subversion of the monocyte lineage to a tumor propagating phenotype. *Clin Cancer Res* (2011) 17:4642–9. doi: 10.1158/1078-0432.CCR-11-0414

65. Nusblat LM, Carroll MJ, Roth CM. Crosstalk between M2 macrophages and glioma stem cells. *Cell Oncol (Dordr)* (2017) 40:471–82. doi: 10.1007/s13402-017-0337-5

66. Hide T, Komohara Y, Miyasato Y, Nakamura H, Makino K, Takeya M, et al. Oligodendrocyte progenitor cells and Macrophages/Microglia produce glioma

stem cell niches at the tumor border. *EBioMedicine* (2018) 30:94–104. doi: 10.1016/j.ebiom.2018.02.024

67. Taga T, Tabu K. Glioma progression and recurrence involving maintenance and expansion strategies of glioma stem cells by organizing self-advantageous niche microenvironments. *Inflammation Regener* (2020) 40:33. doi: 10.1186/s41232-020-00142-7

68. Wang J, Xu SL, Duan JJ, Yi L, Guo YF, Shi Y, et al. Invasion of white matter tracts by glioma stem cells is regulated by a NOTCH1-SOX2 positive-feedback loop. *Nat Neurosci* (2019) 22:91–105. doi: 10.1038/s41593-018-0285-z

69. Brooks LJ, Clements MP, Burden JJ, Kocher D, Richards L, Devesa SC, et al. The white matter is a pro-differentiative niche for glioblastoma. *Nat Commun* (2021) 12:2184. doi: 10.1038/s41467-021-22225-w

70. Yan GN, Yang L, Lv YF, Shi Y, Shen LL, Yao XH, et al. Endothelial cells promote stem-like phenotype of glioma cells through activating the hedgehog pathway. *J Pathol* (2014) 234:11–22. doi: 10.1002/path.4349

71. Zhu TS, Costello MA, Talsma CE, Flack CG, Crowley JG, Hamm LL, et al. Endothelial cells create a stem cell niche in glioblastoma by providing NOTCH ligands that nurture self-renewal of cancer stem-like cells. *Cancer Res* (2011) 71:6061–72. doi: 10.1158/0008-5472.CAN-10-4269

72. Mannino M, Chalmers AJ. Radioresistance of glioma stem cells: intrinsic characteristic or property of the 'microenvironment-stem cell unit'? *Mol Oncol* (2011) 5:374–86. doi: 10.1016/j.molonc.2011.05.001

Frontiers in Oncology

Advances knowledge of carcinogenesis and tumor progression for better treatment and management

The third most-cited oncology journal, which highlights research in carcinogenesis and tumor progression, bridging the gap between basic research and applications to imrpove diagnosis, therapeutics and management strategies.

Discover the latest Research Topics

See more →

Frontiers

Avenue du Tribunal-Fédéral 34
1005 Lausanne, Switzerland
frontiersin.org

Contact us

+41 (0)21 510 17 00
frontiersin.org/about/contact